PREDICTING SPAWNING HABITAT FOR COHO SALMON (*ONCORHYNCHUS KISUTCH*), CHINOOK SALMON (*ONCORHYNCHUS TSHAWYTSCHA*), AND STEELHEAD (*ONCORHYNCHUS MYKISS*) USING GEOSPATIALLY CONSTRUCTED STREAM MORPHOLOGY FROM HIGH-RESOLUTION LIDAR-DERIVED DIGITAL ELEVATION MODEL AND FIELD SURVEY DATA IN THE INDIAN CREEK WATERSHED, MENDOCINO COUNTY, CALIFORNIA

By

Justin P. Bissell

A Thesis Presented to

The Faculty of Humboldt State University

In Partial Fulfillment of the Requirements for the Degree

Master of Science in Natural Resources: Environmental and Natural Resource Sciences

Committee Membership

Dr. David Gwenzi, Committee Chair

Dr. Amy Rock, Committee Member

Dr. Darren Ward, Committee Member

Thomas Leroy, California Certified Engineering Geologist #2593, Committee Member

Dr. Andrew Stubblefield, Graduate Coordinator

May 2019

ABSTRACT

PREDICTING SPAWNING HABITAT FOR COHO SALMON (*ONCORHYNCHUS KISUTCH*), CHINOOK SALMON (*ONCORHYNCHUS TSHAWYTSCHA*), AND STEELHEAD (*ONCORHYNCHUS MYKISS*) USING GEOSPATIALLY CONSTRUCTED STREAM MORPHOLOGY DERIVED FROM HIGH-RESOLUTION LIDAR-DERIVED DIGITAL ELEVATION MODEL AND FIELD SURVEY DATA IN THE INDIAN CREEK WATERSHED, MENDOCINO COUNTY, CALIFORNIA

Justin P. Bissell

Restoration of anadromous salmonid habitat is of primary importance to the economic, historical, and cultural geography of the Pacific Northwest. Derivation and use of geospatial habitat models as guides to pinpoint key areas where limited restoration funding can be cost-effectively employed is of great importance. To this purpose, 1 meter resolution lidar-derived Digital Elevation Model data was acquired for the Indian Creek and neighboring watersheds in Mendocino County, California, and used together with field-acquired geomorphic stream data to geospatially model stream widths, depths, and streambank morphology. These geospatial covariates were field-verified in selected locations and then used in conjunction with field surveyed habitat presence data and substrate data to model potential anadromous salmonid species spawning habitat. Probability surfaces, each comprising the areal extent of the Indian Creek stream system and representing the probability for spawning habitat occurrence, were developed for each of the species of interest. The mean area under the curve (AUC) for 100 model replications for Chinook, Coho, and Steelhead were 0.954, 0.951, and 0.958, with

standard deviations of 0.036, 0.034, and 0.036, respectively. In contrast to other models that solely use linear lengths of stream, the models developed in this work incorporate modeled stream bankfull widths and modeled stream corridor morphology, thus allowing additional interpretation and prediction involving the amount of species' use of specific streams and watersheds. Models were field-verified by California Department of Fish and Wildlife fisheries biologist staff and Pacific Watershed Associates engineering geologists and field scientist staff as being representative of actual field conditions, thus assuring the value of modeling results and methodology in future projects and research.

ACKNOWLEDGEMENTS

I would like to express my deepest appreciation to my committee chair, Dr. David Gwenzi, and my committee members, Dr. Amy Rock, Dr. Darren Ward, and Thomas Leroy. I would like to thank my wife and family for their input, encouragement and support. I would also like to thank the rest of the faculty and staff of the Natural Resources and Geography Departments of Humboldt State University, particularly Dr. Nicolas Perdue and Dr. Rosemary Sherriff as well as Laurie Takao, Cassandra Tex, and Kyle Morgan for their kind advice and assistance. I would like to express my thanks to my colleagues and coworkers at Pacific Watershed Associates for their support and California Department of Fish and Wildlife biologists Seth Ricker and Allen Renger, members of the Redwood Forest Foundation, Inc., and the Lost Coast Forestlands LLC all for their advice and the use of their critically important data. None of this would have been possible without those I have mentioned here.

DOCUMENT ACCESSIBILITY

As part of Humboldt State University's commitment to providing equal accessibility to published research, additional resources for this document have been provided. Selected figures, as noted in the alternative text, have had specific contents of geospatially represented data made available for download and display for additional representation as needed.

TABLE OF CONTENTS

LIST OF TABLES

LIST OF FIGURES

LIST OF APPENDICES

1. INTRODUCTION

Salmonid species whose spawning habitat primarily resides in rivers and streams connected to the coastal regions of California, Oregon, Washington, and Canada have great importance in the historic and present day cultural and economic geography of those areas (Breslow, 2014; Bi et al., 2007; Bi et al. 2011). Nearly a century of poor land management and other negative anthropogenic influences have resulted in the salmonid species resident to the North Coast listed as threatened under the Endangered Species Act (ESA) (NOAA, 2017). Since that listing, major recovery efforts have taken place throughout areas that have historically been known to host salmonid spawning habitat. A major premise of ongoing anadromous salmonid species recovery efforts is that there is a high correlation between the presence, availability, and access to freshwater habitat and the overall numerical abundance of those species (NOAA, 2017). Restoration projects involving the rehabilitation or decommission of roads (thus limiting pollution of streams by fine-grained sediment), restoring stream access to migrating species (Null et al., 2014, Beechie et al., 2013), and reconstruction and rehabilitation of stream habitat via emplacement of large woody debris and removal of negative anthropogenic disturbance (Smith, 2008) are highly ranked candidates for restoration funding. Stream reaches that have been found to host salmonid spawning habitat generally contain high amounts of spawning gravels, appropriate seasonally-available stream depths and flows, as well as complex refuge habitats (Anlauf-Dunn et al., 2014, Mull and Wilzbach, 2007, Simenstad, 2000, McGlauflin, 2011).

The Pacific Northwest has numerous native anadromous salmonid species, three of which are the focus of this research: Southern Oregon/Northern California Coast Coho Salmon (*Oncorhynchus kisutch*), California Coastal Chinook salmon (*Oncorhynchus tshawytscha*), and Northern California steelhead (*Oncorhynchus mykiss*). These three species are listed as threatened under the Environmental Species Act of 1976, with listing dates of 1997, 1999, and 2000 respectively (NOAA, 2017). Work focused on restoration of anadromous salmonid habitat is key to preserving the economic, historical, and cultural geography of the Pacific Northwest.

The historical importance of salmonid species to indigenous peoples of the Pacific Northwest cannot be overstated, as many indigenous tribal members see salmon as part of their spiritual and cultural identity. Salmon served as a primary food source for native peoples long before European contact. The annual migration of salmonid species is subject of traditional celebration, and the salmon harvest is used as a time to transfer cultural values, knowledge, and identity between generations:

> "My strength is from the fish; my blood is from the fish, from the roots and berries. The fish and game are the essence of my life. I was not brought from a foreign country and did not come here. I was put here by the Creator."
>
> (*Chief Weninock, Yakama Indian Nation, 1915)*

Today, salmonid species hold equal importance – fishing as an occupation and recreation is an activity of preference for many, both tribal members and otherwise. Salmon is a popular staple throughout the world and increasing the productivity of the species can have immediately applicable economic benefits for the entire Pacific

Northwest. Though the necessity of restoring spawning habitat is acknowledged, care must be taken in judicious selection of targeted areas designated for restoration work. Limited funding and practicality preclude comprehensive restoration of all historic habitat, so available funds must be utilized in a cost-effective manner. Accurate habitat suitability modeling aids this process, allowing restorationists additional insight into the physical geography of potential restoration locations and helping pinpoint key locations and create planning strategies where funds can best be utilized.

The primary objective of this research was to predict spawning habitat suitability for the above-mentioned anadromous species in Indian Creek, a tributary to the South Fork Eel River, in Mendocino County, California (Figure 1, 2 and 3). The Eel River and its tributaries are denoted as key restoration areas by the National Oceanic and Atmospheric Administration (NOAA) and the California Department of Fish and Wildlife. Restoration projects whose target areas lie within the Eel River watershed have received millions of dollars in restoration grant funding in the last two decades.

Figure 1. Location of the Indian Creek watershed, Humboldt and Mendocino Counties, California.

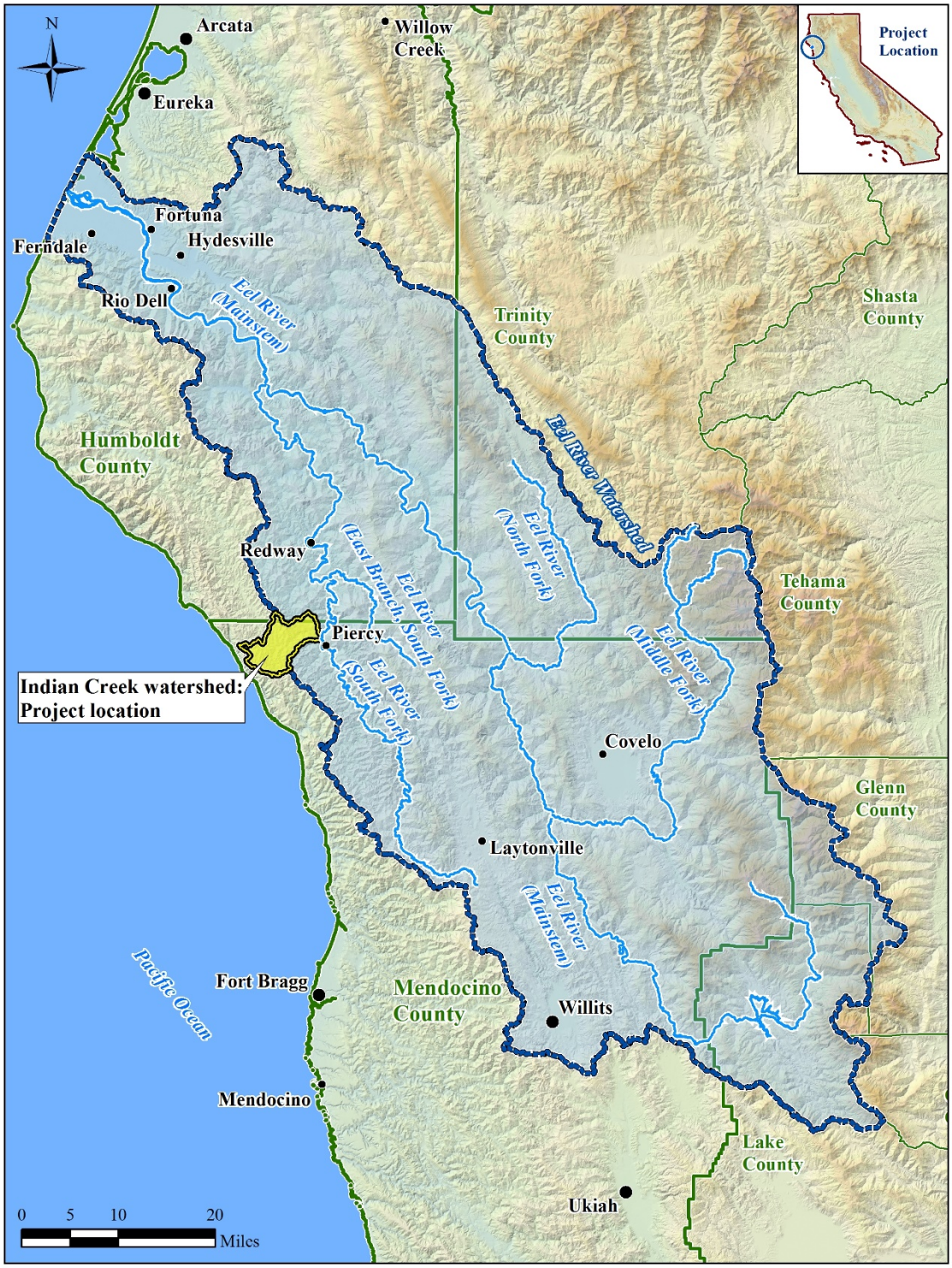

Figure 2. Selected tributaries of the Eel River in relation to project area.

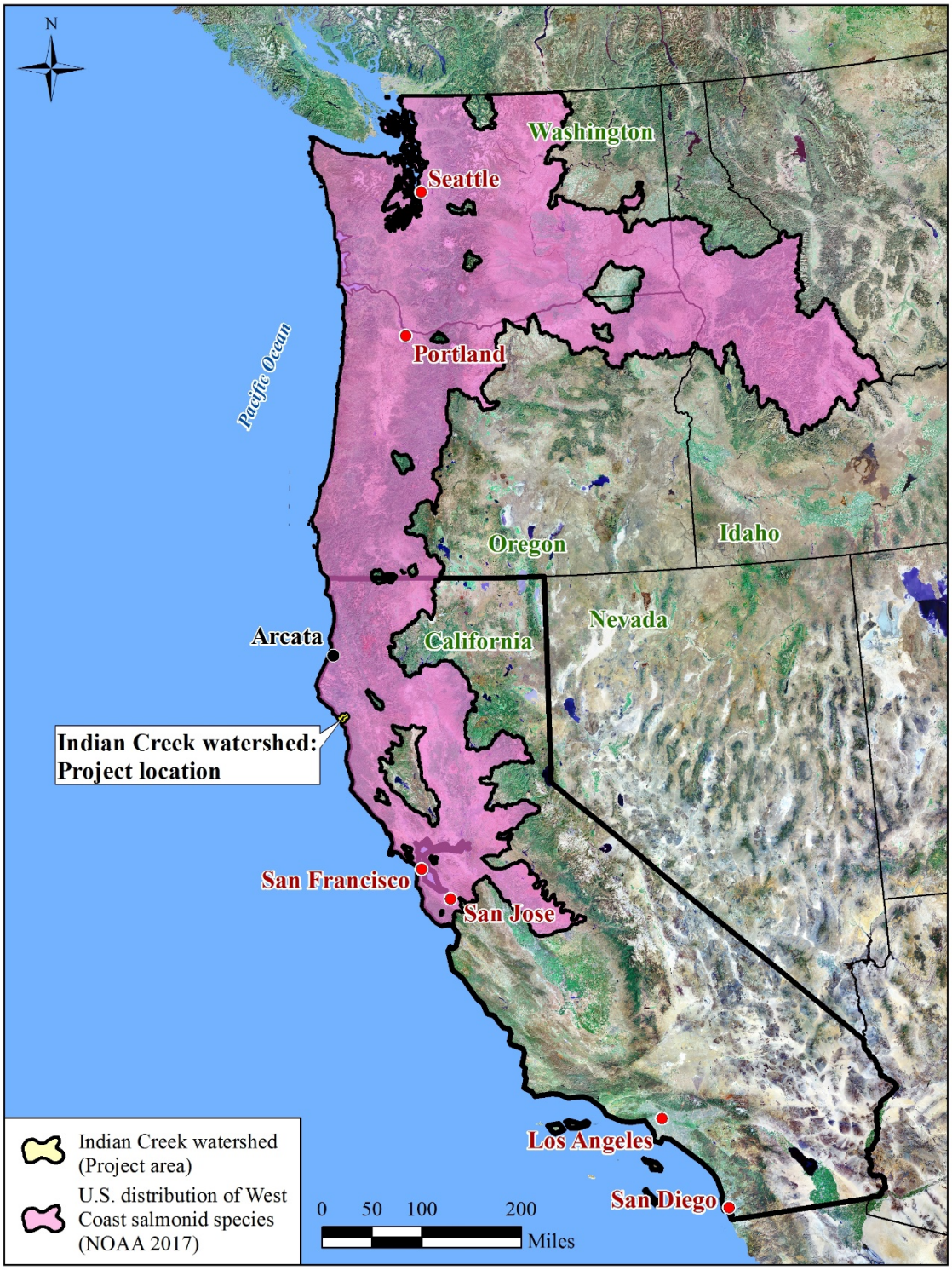

Figure 3. Project location in relation to distribution of West Coast salmonid species (Data extent: NOAA, 2017).

In this research, the applicability and use of high resolution (1 m) LIght Detection And Ranging (lidar)-derived Digital Elevation Model (DEM) data, field-acquired salmonid spawning habitat survey data, and field-acquired stream geomorphic survey data were tested in their ability to predict areas of salmonid spawning habitat for the three anadromous species of interest by developing a predictive probability surface using the geospatial covariates and examining the statistical ability of that surface to predict spawning habitat presence. These geospatial modeling products will be used as tools to better support intelligent decision making when selecting areas to concentrate long-term restoration efforts and make more effective use of time and funding devoted to habitat rehabilitation and water quality maintenance. Key to that endeavor was the preliminary identification of potential habitat that may have served the species as spawning grounds historically but may no longer be accessible due to anthropogenic influences. Further, there is equal importance in the identification of current habitat that may be at high risk from those same influences which could be targeted for restoration work.

2. BACKGROUND

2.1 History of the study area

The project study area of Indian Creek is a tributary to the South Fork Eel River in Mendocino County, California. As an area containing a significant amount of anadromous fish habitat, this and neighboring watersheds have a very high priority in ongoing and future watershed restoration work (PWA, 2007, PWA, 2015). The Indian Creek watershed area comprises 27.1 square miles, containing approximately 39 miles of blue line streams (Figure 4). The three anadromous fish populations of interest all have identified spawning grounds in the Indian Creek watershed (CA DFW, 2016). The great majority of the Indian Creek watershed ownership was previously held by multiple logging companies and recently transferred to private hands (PWA, 2015). Majority property ownership of the Indian Creek watershed is currently held primarily by two organizations: Redwood Forest Foundation, Inc., (RFFI) and the Lost Coast Forestlands, LLC (LCF) (Humboldt County GIS, 2017) (Figure 5).

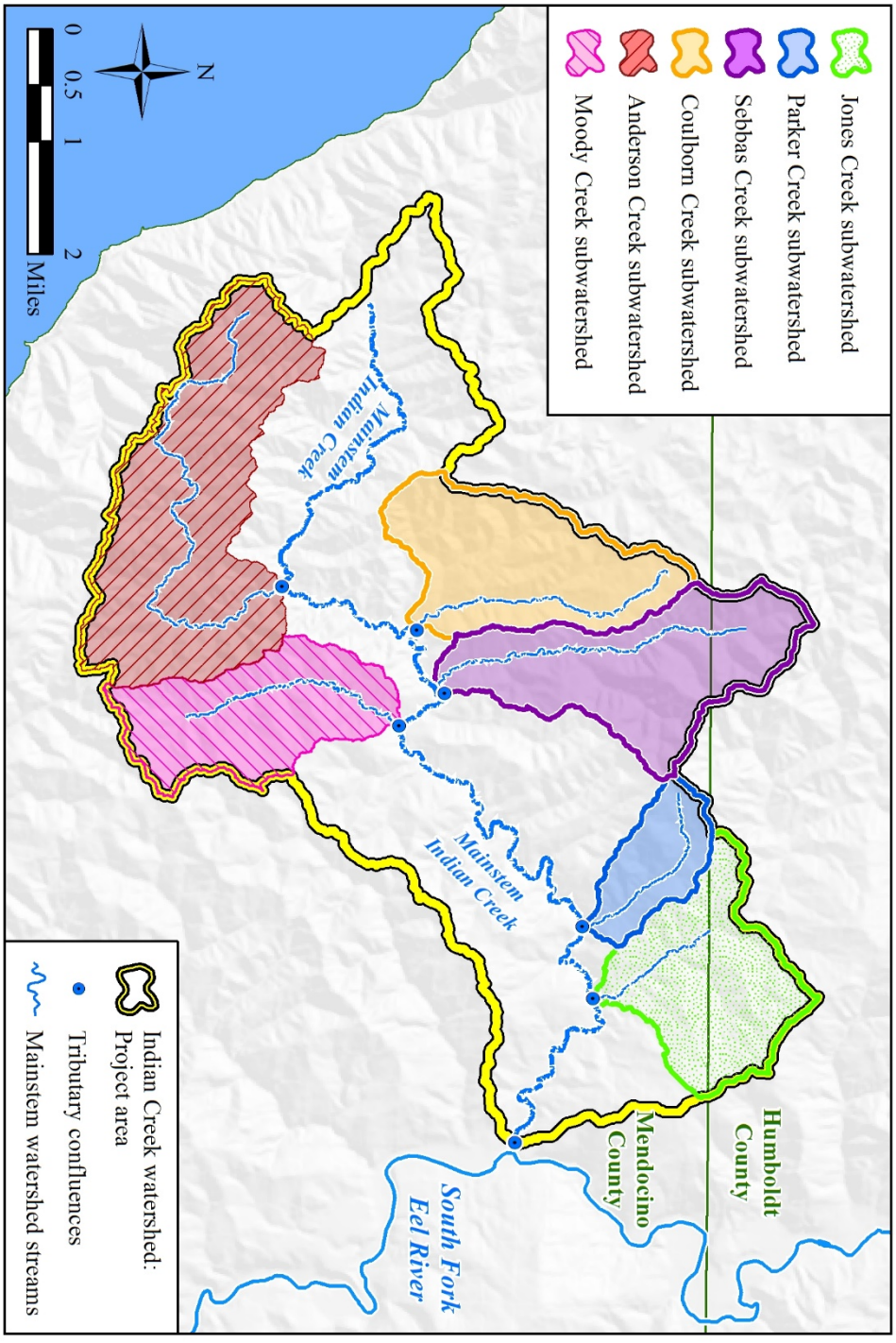

Figure 4. Detailed map of the Indian Creek watershed, denoting primary tributaries to Indian Creek and named subwatersheds, Humboldt and Mendocino Counties, California.

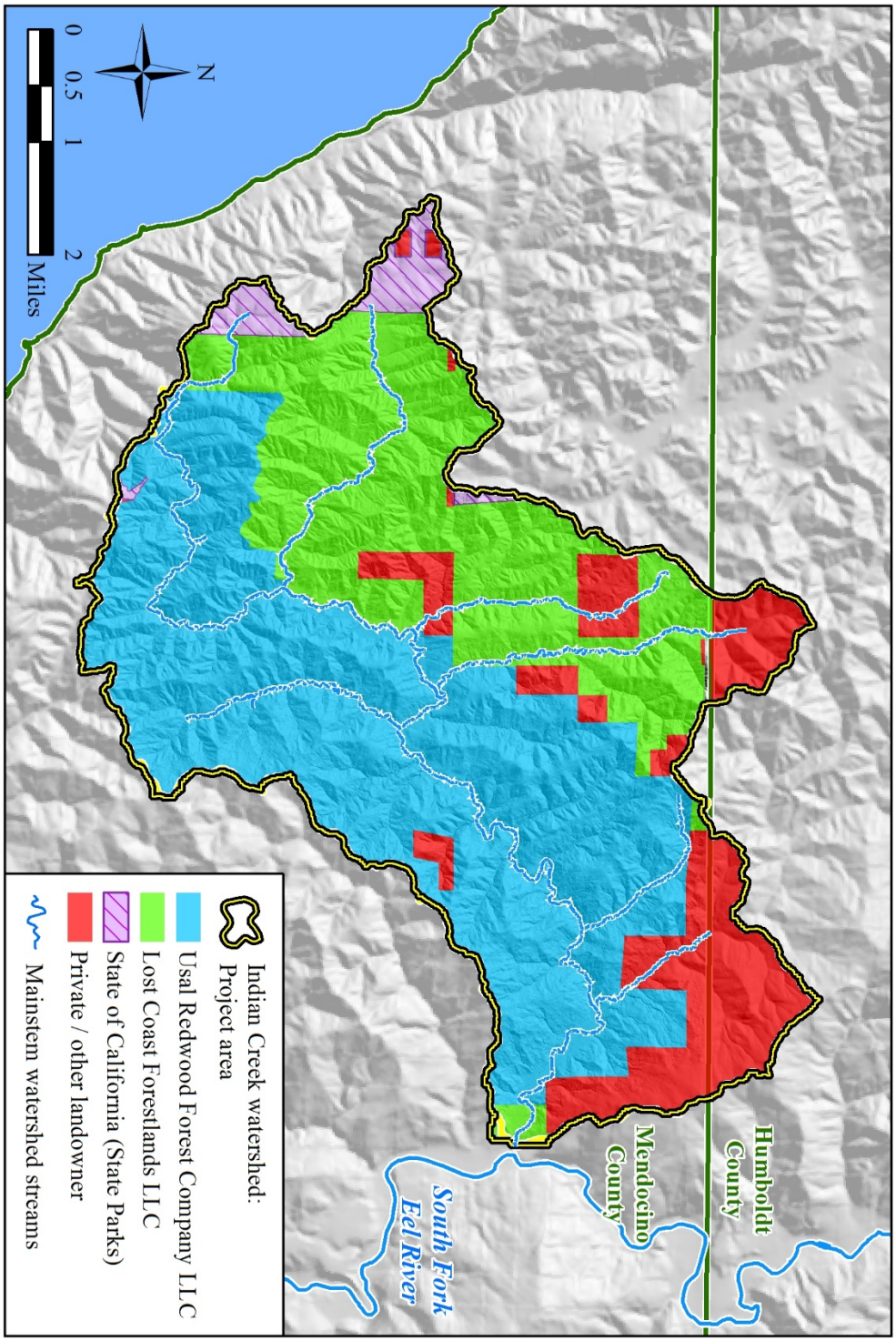

Figure 5. Detailed map of the Indian Creek watershed, denoting primary land ownership, Humboldt and Mendocino Counties, California.

The Indian Creek watershed, along with many neighboring watersheds, has experienced significant negative anthropogenic disturbances that have affected its physical landscape. Within the last century, much of the area had been clear-cut logged, stripping the topography of native old-growth forest. Roads and railroads constructed to allow access for commercial logging have interrupted historic migratory salmonid spawning streams, both by creating artificial barriers to fish passage as well as vastly increasing sediment delivery to streams. Physical remnants of these practices still exist on the landscape (Appendix F), and current property owners regularly cooperate with private consultant firms such as Pacific Watershed Associates (PWA) to restore or mitigate the negative effects of those types of historic disturbances. Restoration of streams via engineered alteration of the negatively affected stream channel, decommissioning and/or upgrading of roads hydrologically connected to streams, and improvement and/or creation of salmonid habitat in streams by installation of large woody debris structures are all viable and regularly used methods to enhance and rehabilitate salmonid habitat. All these methods are currently being used in various locations throughout the Indian Creek watershed, with much work still to be done.

2.2 Geospatial modeling as a research tool

Use of geospatial tools in academic and professional environments allows numerous benefits for researchers. Visualization in a geographic context is key to any study examining spatial distributions of data, allowing multivariate predictive analyses to

be interpreted and presented in a comprehensible manner. GIS software packages like ESRI ArcMap, QGIS, and Grass GIS are used regularly when modeling the natural environment, such as when examining distributions of species, habitat suitability, and geomorphic processes. A related study by Ames et. al. (2009) used GIS-derived watershed characteristics when estimating stream channel morphology in Idaho. A variety of geospatial covariates were examined and used for model comparison when attempting to predict stream widths and depths. The authors concluded that for their study area, while drainage areas of the streams in question and localized precipitation had the greatest predictive power, when attempting to model similar morphological characteristics in smaller areas, higher resolution location-specific data would yield better results.

Meixler and Bain (2012) developed a geospatial fish habitat prediction model that incorporated categorized covariates for the watershed landscape and stream system and predicted potential habitat for 146 species of fish in western New York. This is one among many demonstrations of the potential flexibility and robust nature of using GIS as a modeling tool. Large amounts of data (both quantitative and categorical) can be processed for large numbers of variables to derive potential outcomes for many species. However, modeling high resolution, large volume datasets with many covariates can significantly increase software processing time and care must be taken when interpreting large volumes of results in a practical and logistical sense. Cook and Venkatesh (2009) noted significant differences in accuracy of flood inundation areas in their comparative geospatial study of different resolutions of DEMs. Higher resolution DEMs (1 meter

resolution, as opposed to 10 meter) can provide clearer and more accurate estimations when modeling the physical environment, but that resolution requires significant increases in computing power.

In an attempt to model Coho Salmon occupancy, Anlauf-Dunn et. al. (2014) integrated a number of geospatial components into their modeling strategy, including geospatially derived flow length distances from ocean to habitat. Those flow lengths, in addition to other physical stream variables such as wood volumes, local pool complexities, gravel morphology, and riffle depths, allowed the researchers to underscore the importance of areas accessible to the species, while pinpointing other geospatial locations where instream habitat had been degraded and could be improved. Similarly, Gard (2013) used River2D (a two-dimensional hydraulic and habitat model) to model habitats in stream systems scheduled for restoration efforts. Gard geospatially examined multiple habitat scenarios for fall-run Chinook salmon based on the stream area restoration design, before-, immediately after-, and post-flow event to the restoration project. Again, high resolution local geospatial information proved key to the study, which provided insights to the effects of the restoration work and the differential in effectiveness of those efforts for spawning and rearing habitats. Coarser, less resolved, but more easily available geospatial data for the area would not have been appropriate for the modeling exercise, as the resolution of that data exceeded the scale of geomorphic changes being modeled. Therefore, field surveyed data, such as stream flows and site-specific stream geomorphic characteristics, were necessary to obtain realistic results.

Goodman, et. al. (2015) modeled potential habitat that would be affected by restoration efforts on the northern Trinity river, directly downstream of the Lewiston Dam, Trinity County, California, using stream morphological data recorded with a geospatial context. This field-acquired data, such as stream depth, mean column velocity, and cover, proved invaluable when examining changes in flow velocities and depths at different distances from the dam. The authors modified demonstration flow assessments (used to assess in-stream habitats of different species and evaluate habitat for management purposes) to reduce subjectivity of those studies, allowing a more objective approach. This approach assisted in finding better practices of quantifying analyses performed in a geospatial context. That type of reproducible quantification is of great value when agencies are conducting restoration activities at small to large geospatial extents.

Integration of statistical prediction with geospatial modeling is commonplace. Lecomte, et al. (2013) developed a Bayesian model with predictive geospatial outputs for multiple species based on multiple physical environmental variables. In this context, the geospatial outputs derived from the Bayesian predictive model were rasterized probability of occurrence and distribution surfaces for species of interest. The Bayesian hierarchical model developed was successfully used to create areal geospatial outputs of probability surfaces predicting aquatic biomass of multiple species using covariates of sediment type, depth, and temperature.

Similarly, Burton, et. al. (2016) developed a GIS modeling tool integrating statistical predictions of the impacts of hydraulic fracturing on groundwater. Proximity,

least-cost pathway, and cluster analyses were used to derive probability surfaces forecasting changes in total beryllium amounts in groundwater in relation to spatial proximity to well locations. Similar surfaces can be generated when modeling species habitat and distribution, which requires acquisition of geospatial variables over a surface area, relating those covariates within a defined context, and then deriving a probability density surface using presence/absence data as response.

2.3 Statistics in geospatial modeling

In general, a response curve denotes the relationship between some input (or covariate) needed to produce a certain output (or response). It is important for the researcher to select a model (and its associated response mechanism) based upon the appropriate nature of that model: i.e. a choice or choices derived from specific information regarding the system in question. A wide array of models supporting multivariate analysis exist, yielding different types of response curves. Burnham and Anderson (2010) and Plant (2012) discuss numerous statistical models, all of which can, in some way, be applied in a geospatial context. These can include, but not limited to regression splines, boosted regression trees, and generalized linear, additive, and mixed models, each using unique methodologies to produce predictive response formulae. The authors emphasize the critical importance of intelligent model selection and application, based on the nature of the data and type of phenomenon to be examined. The authors also emphasize the importance of retaining parsimony in developed models, i.e. developing a model framework that achieves the desired level of prediction using the

fewest covariates possible and still retaining the capacity to reasonably explain the individual contributions and interactions of those covariates.

Additive models, such as in a linear regression equation, can use a linear least-squares fit that is computed for one or more covariates to predict a response variable in the form:

$$Y = b_0 + b_1*X_1 + ... + b_m*X_m$$

where Y denotes the response variable, b_0 the intercept, and $b_{1\text{-}m}$ the various coefficients of the values of covariates $X_{1\text{-}m}$. Generalized linear models differ from the general linear model in that the distributions of the response can be non-normal and not necessarily continuous. Generalized additive models combine aspects of additive models with generalized linear models to maximize the quality of prediction of a response variable from various distributions by estimating non-parametric functions of the predictor variables which are connected to the response by a "link" function:

$$g(E(Y)) = b_0 + f_1(x_1) + f_2(x_2) \ ... + f_m(x)$$

where Y denotes the response variable, E() the exponential family distribution, g() the link function, b_0 the intercept, and $f_{1\text{-}m}$ the various smoothing functions (parametric or non-parametric) for the values of covariates $X_{1\text{-}m}$. Based on user definitions, these smoothing functions can be tailored for more generalized or specific fits to the data. Highly specific fitting in this context may yield applicable response predictions for very specific datasets, but care must be taken when applying those predictions elsewhere. Conversely, less specific fitting can allow greater versatility when using model predictions of the phenomenon in other contexts.

In general, habitat suitability modeling relates a set of ecological covariates to the likelihood of occurrence for a species, estimating the relationship between occurrences and the environments at the occurrence locations (Elith, et al., 2011). Of key importance in a suitability analysis is the judicious selection of appropriate environmental variables, focus on an appropriate scale of measurement, and acquisition of presence data (and, if available, absence data, as absence of evidence is not evidence of absence). MaxEnt (Phillips, 2017) uses geospatial environmental variable raster covariates and point location presence data to derive habitat probability surfaces using maximum entropy modeling (Elith et al., 2011).

Valavanis, et al., (2008) compared a number of different methodologies for modeling essential fish habitat, noting that a generalized additive model (GAM) is a commonly used method to model continuous, non-linear natural systems. A parametric model, the GAM uses spline functions when generating response curves. The GAM response curve has a number of "knots", or inflection points, the number of which are controlled by a gamma factor acting to "smooth" the response curve, ideally preventing the model from over-fitting to the dataset. An overabundance of "knots" in the response curve would yield a statistical model that is too data-specific, thus potentially unreliable predictions when used in another context or different dataset.

Guisan, et. al. (2002) and Leathwick, et. al. (2006), also discussed the use of both generalized linear and generalized additive models and their uses in species distribution modeling. Response curves developed denoted a range of non-linear systems, with the models all performing in a fairly robust way. Leathwick noted that GAMs outperformed

multivariate adaptive regression techniques when explaining the responses of the study covariates. Suarez-Seoane, et. al. (2002) used a generalized additive model when geospatially predicting habitat responses of agricultural birds in Spain. In that case, the GAMs were built to predict presence-absence as a response to covariates. The habitats for the three species of interest were able to be distinguished from one another using the GAM model responses. Receiver operating characteristic (ROC) plots showed the developed models to be successful and robust. Methodology using generalized linear models (GLMs) was also attempted successfully, but the resulting response curve would only rarely have been observed in nature due to its idealized form.

2.4 Lidar data

Lidar (acronym for Light Detection And Ranging) is a method of remote sensing which uses pulsed electromagnetic radiation to acquire high precision elevation information (Wehr & Lohr, 1999). Equipment used to capture lidar data consists of a laser emission device, a scanner, and a specialized GPS receiver. Data can be acquired from any number of environments where precise distance information would prove useful, and both topographic elevation and bathymetric depths are regularly collected. Topographic lidar data is most often collected via airborne platform, either an aircraft (most often used for large areas of landscape) or unmanned aerial vehicle (UAV) for smaller, project-specific sites. Precise measurement of distance logically allows precise measurement of elevation and/or precise creation of three-dimensional models. The laser pulses from the acquisition system can split into multiple returns, based upon how many

objects are on and above ground surface (e.g. canopy, anthropogenic artifacts, etc.). First returns are generally associated with the most elevated features on the landscape, whereas final returns usually represent the bare-earth ground surface. These various returns are used to generate a point cloud dataset, classified by the agency performing the acquisition into multiple categories and converted to a LASer (LAS) data exchange file dataset, from which bare-earth DEM datasets can be derived. Working in tandem with precise GPS positioning, large areas of landscape can thus have accurate, precise DEMs constructed which can be used for any number of applications, such as geospatial and hydrologic modeling, engineering, and geomorphic mapping. As not all of the landscape has this caliber of precise data available, it is extremely important to develop methods and tools to effectively use lidar data whenever possible to best utilize the resources when available and to justify their acquisition for areas where they are not currently available.

3. MATERIALS AND METHODS

3.1 Study site

To achieve the research objectives, a Northern California watershed area was located that fulfilled three conditions:

1. The watershed area contains streams that host anadromous habitat of the species of interest.
2. On-site surveys for anadromous spawning habitat took place within the watershed and specific spawning use habitat (redds) for the threatened species was identified.
3. High-resolution lidar-developed digital elevation models (DEMs) of the area exist and can be used for model development and calibration.

In coordination with geologic consulting firm Pacific Watershed Associates, Indian Creek (Figures 1), a tributary to the South Fork Eel River, was found to fulfill the stated criteria. Located 127 kilometers south of Eureka, California, Indian Creek has been the focus of a significant amount of restoration research and implementation funded by both private and public agencies. The Eel River watershed (Figure 2) has historically held large extents of salmonid habitat, though that habitat has been significantly reduced in size and scope due to anthropogenic influences such as commercial timber harvest, private landscape development for housing, and poorly maintained road networks (PWA 2015).

Indian Creek is located primarily in Mendocino County, California, west of the South Fork Eel River, downstream from Leggett, immediately north and west of Piercy (39° 58' 4.076" N, 123° 52' 56.698" W). The project area watershed houses relatively productive anadromous fish-bearing tributaries connected to the South Fork Eel River. Adjacent watersheds include Wildcat Creek, Bear Pen Creek, Standley Creek, and Piercy Creek (Figure 4).

3.2 Data

While developing a watershed restoration plan for Coho Salmon species recovery in the South Fork Eel River, PWA (2015) conducted numerous geomorphic stream surveys in the Indian Creek and neighboring watersheds (Figure 8). The instream assessment protocol of these geomorphic surveys was intended to facilitate future wood-loading restoration projects throughout the watershed and were conducted along mainstem fish-bearing streams in the Indian Creek, Piercy Creek, Standley Creek, Bear Pen Creek, and Wildcat Creek watersheds. Stream geomorphic data, including peak and average bankfull widths and depths (Figures 6, 7, 8, and 9) and estimations of substrate particle size percentages (Table 1) were collected at 500 foot stations along selected reaches using a modified Rosgen classification system (Rosgen, 1994) with additional substrate data as per Montgomery & Buffington (1997). In this context, bankfull width was defined as the channel width at bankfull discharge, where the stage is delineated by the presence of a floodplain at the elevation of incipient flooding and indicated by

deposits of fine sediments such as sand or silt at the active scour mark, break in stream bank slope, and/or perennial vegetation limit (CA DFW 2010). Bankfull discharge is further defined as the dominant channel forming flow, with a recurrence interval of 1.5 years (CA DFW 2010).

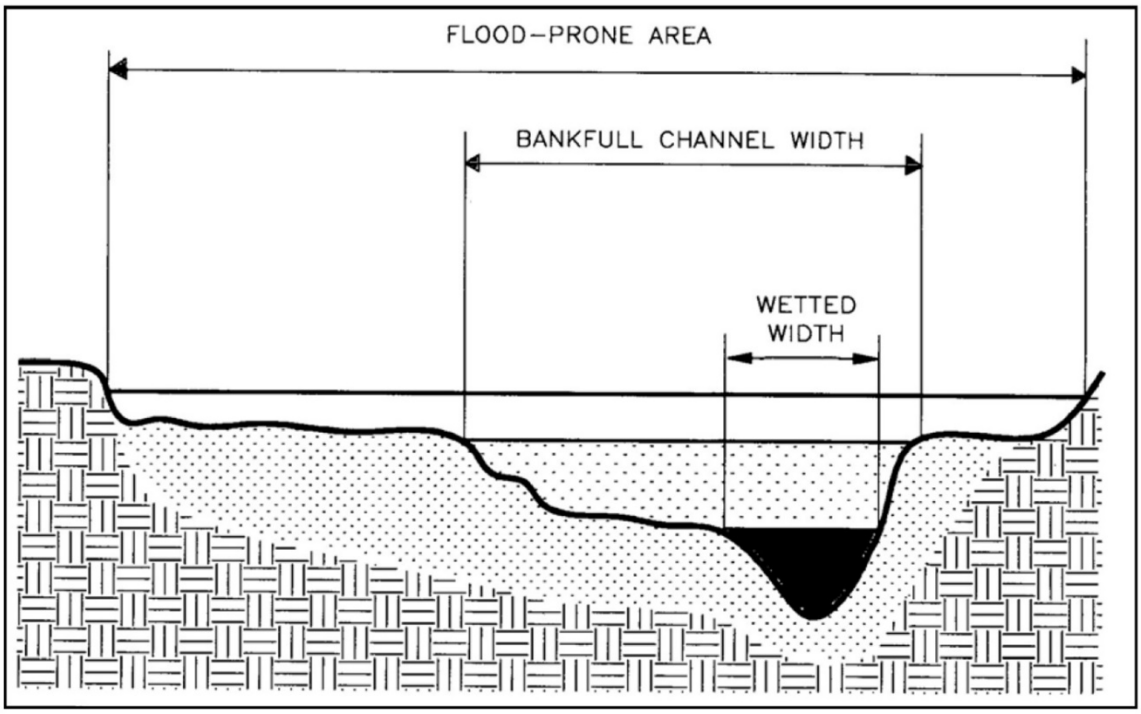

Figure 6. Channel cross-section, as denoted by CDFW Fisheries Restoration Grant Program (FRGP) California Salmonid Stream Habitat Restoration Manual Vol. II (2010), page III-4.

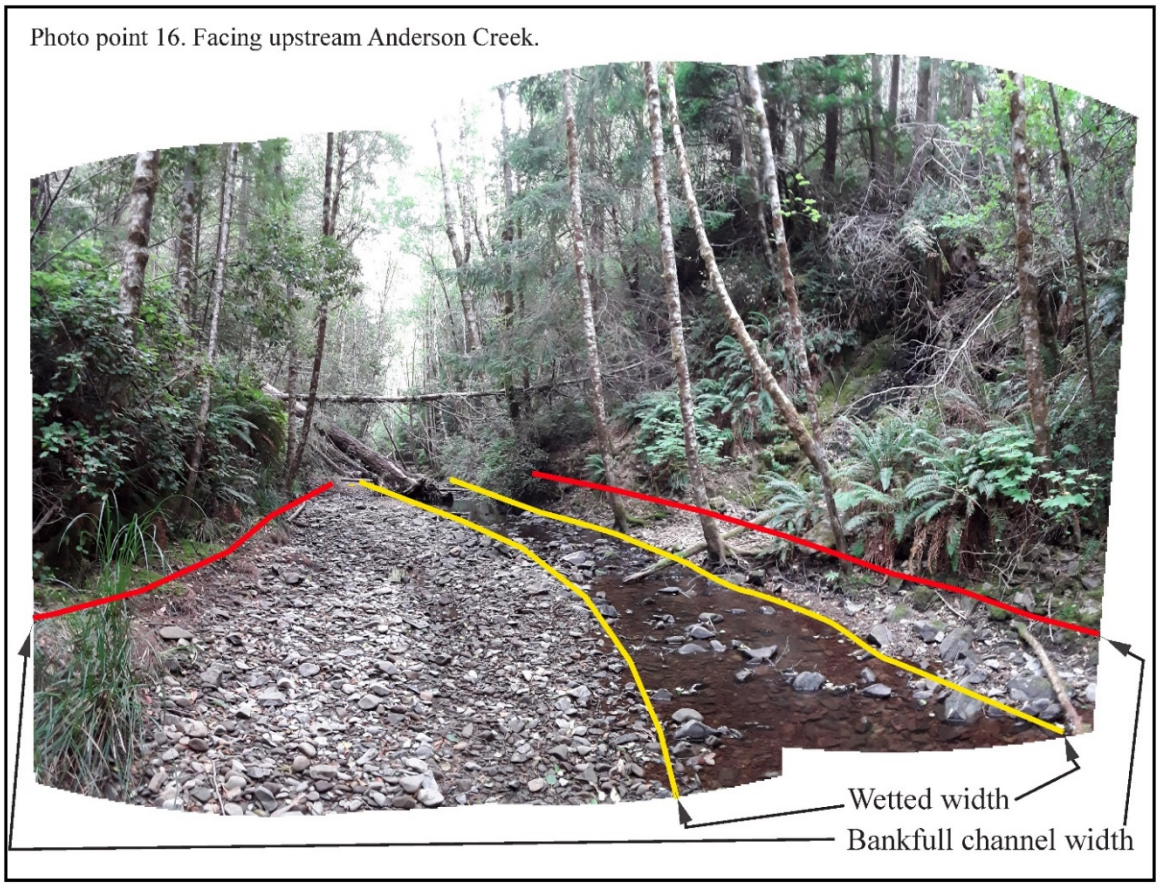

Figure 7. Project location - stream corridor of Anderson Creek, facing upstream, wetted and bankfull channel widths delineated (Photo point 16, Appendix F).

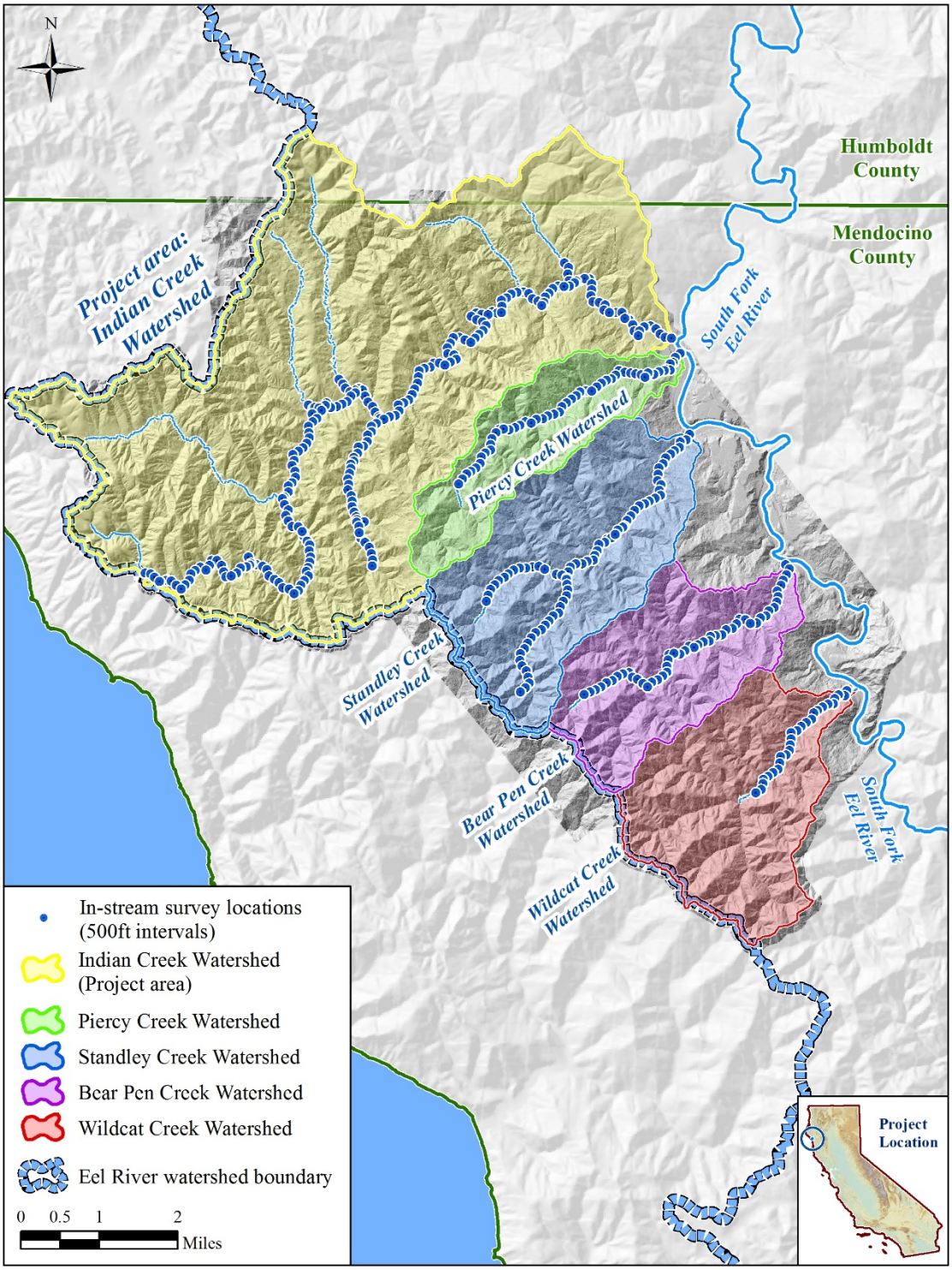

Figure 8. Locations of in-stream surveys in Indian Creek and neighboring watersheds.

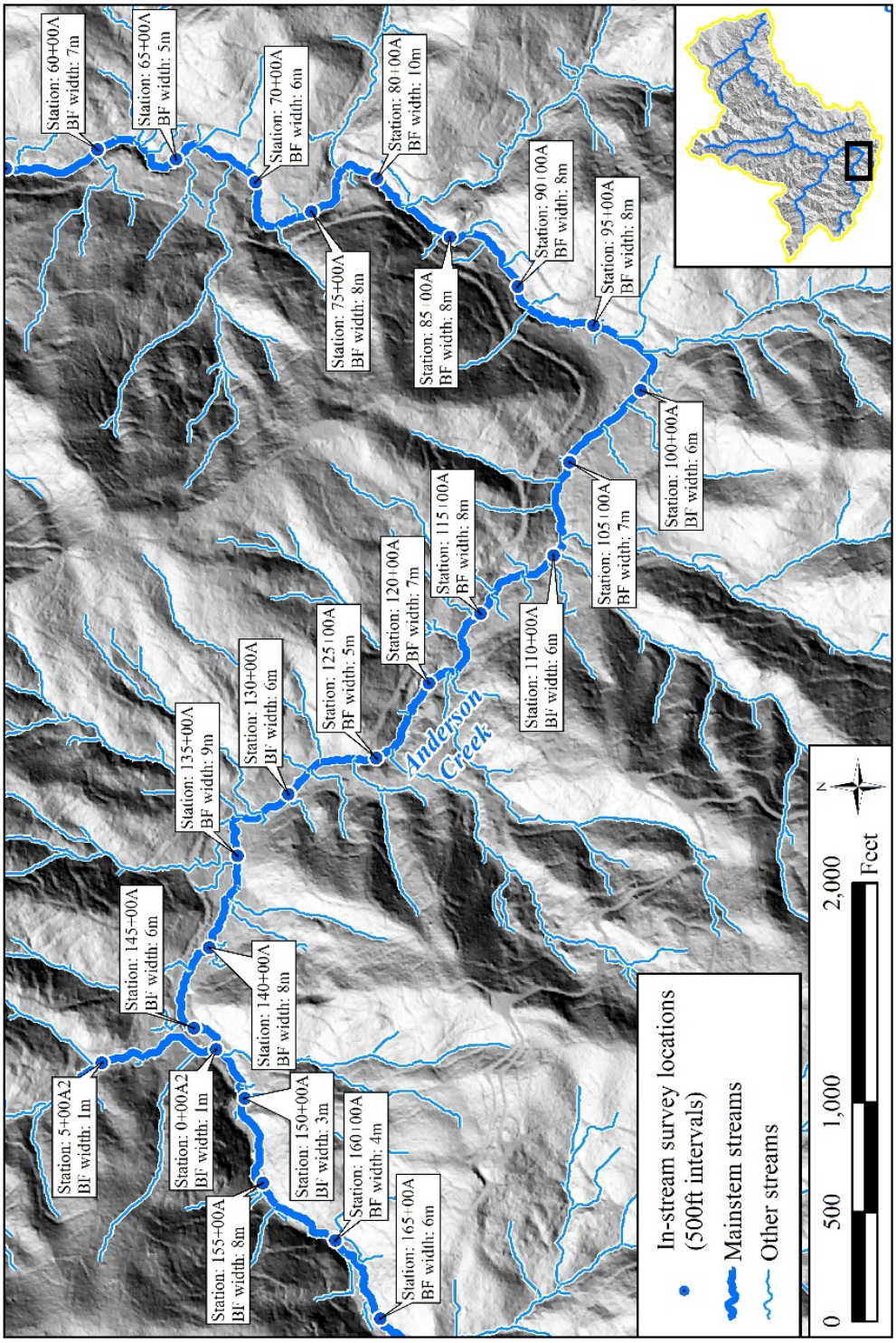

Figure 9. Closeup of selected area within Indian Creek watershed showing in-stream survey locations.

Table 1. Instream protocol for substrate classification – particle size.

Substrate class:	Size range (mm)
Substrate: Bedrock	>2048
Substrate: Boulder	256-2048
Substrate: Cobble	64-256
Substrate: Gravel	2-64
Substrate: Sands/silts	0.062-2
Substrate: Fine grain cohesives	< 0.062

Spawning habitat data for the species of interest was obtained from the California Department of Fish and Wildlife in October 2016 (CDFW). CDFW conducts regular surveys of anadromous fish-bearing streams as part of their population monitoring and to help pinpoint fish habitat and spawning grounds. Numerous habit surveys were conducted throughout the Eel River watershed, many specifically within the Indian Creek watershed (Figures 10, 11, and 12). Species identification for each redd was assigned by nearest species proximity within the stream if no specific fish was found to be associated with a particular redd. From 2010-2015, a total of 673 redd locations (275 identified as California Coastal Chinook, 248 identified as Coho Salmon, and 150 identified as steelhead) were found in the Indian Creek watershed within mainstem streams not blocked by fish barriers. CDFW has allowed the author the use of this data, which was used as a guide to locate stream reaches with known habitat to calibrate model inputs and interpret modeling results. While CalFish (2012) has denoted significant portions of the Indian Creek watershed as anadromous fish habitat, those extents represent simplistic

linear features without the locational specificity that CDFW stream surveys have acquired. That specificity of survey data can allow greater accuracy during model parameterization and better reliability of model outputs.

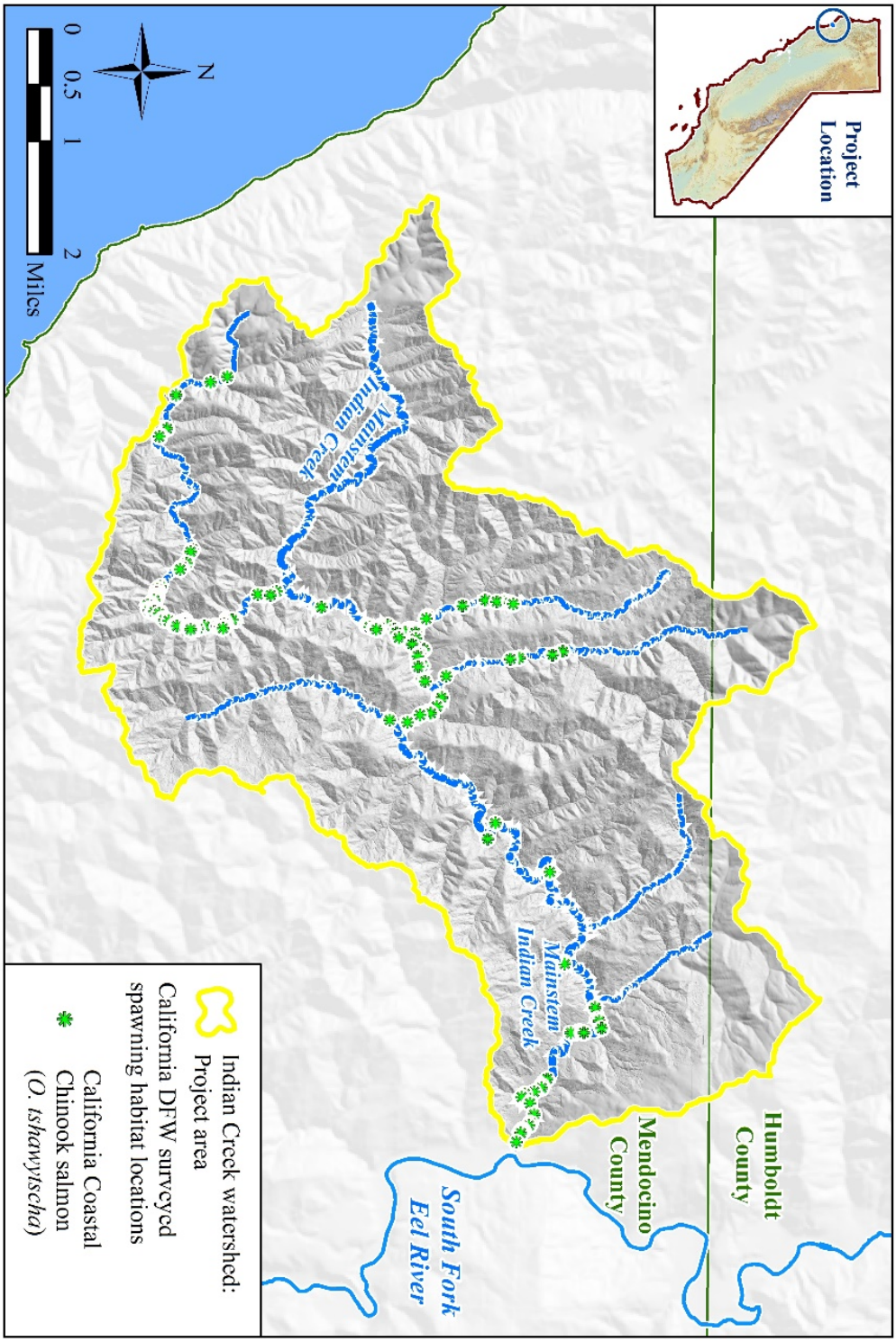

Figure 10. Locations of CDFW field-surveyed California Coastal Chinook redds.

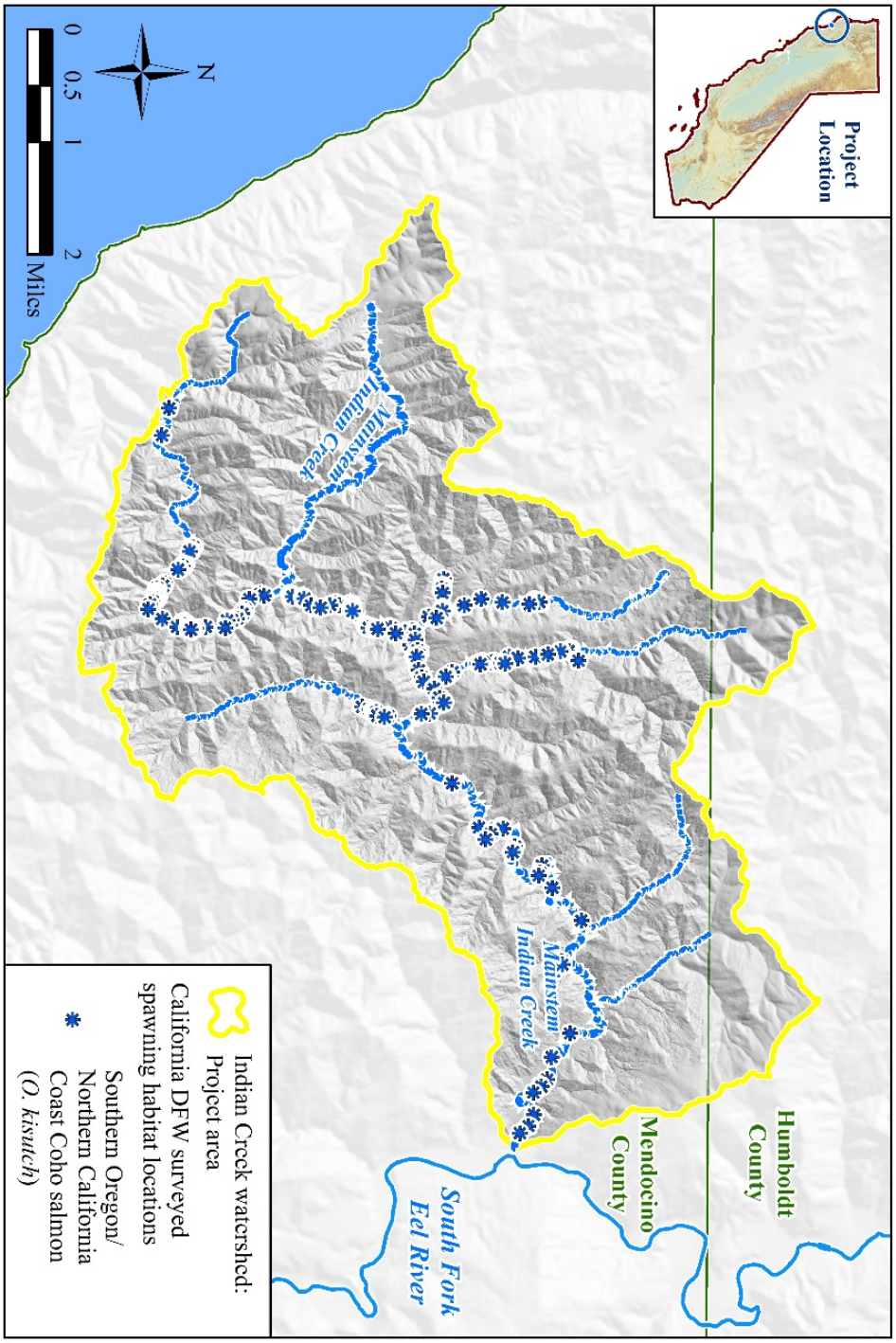

Figure 11. Locations of CDFW field-surveyed Southern Oregon / Northern California Coast Coho Salmon redds.

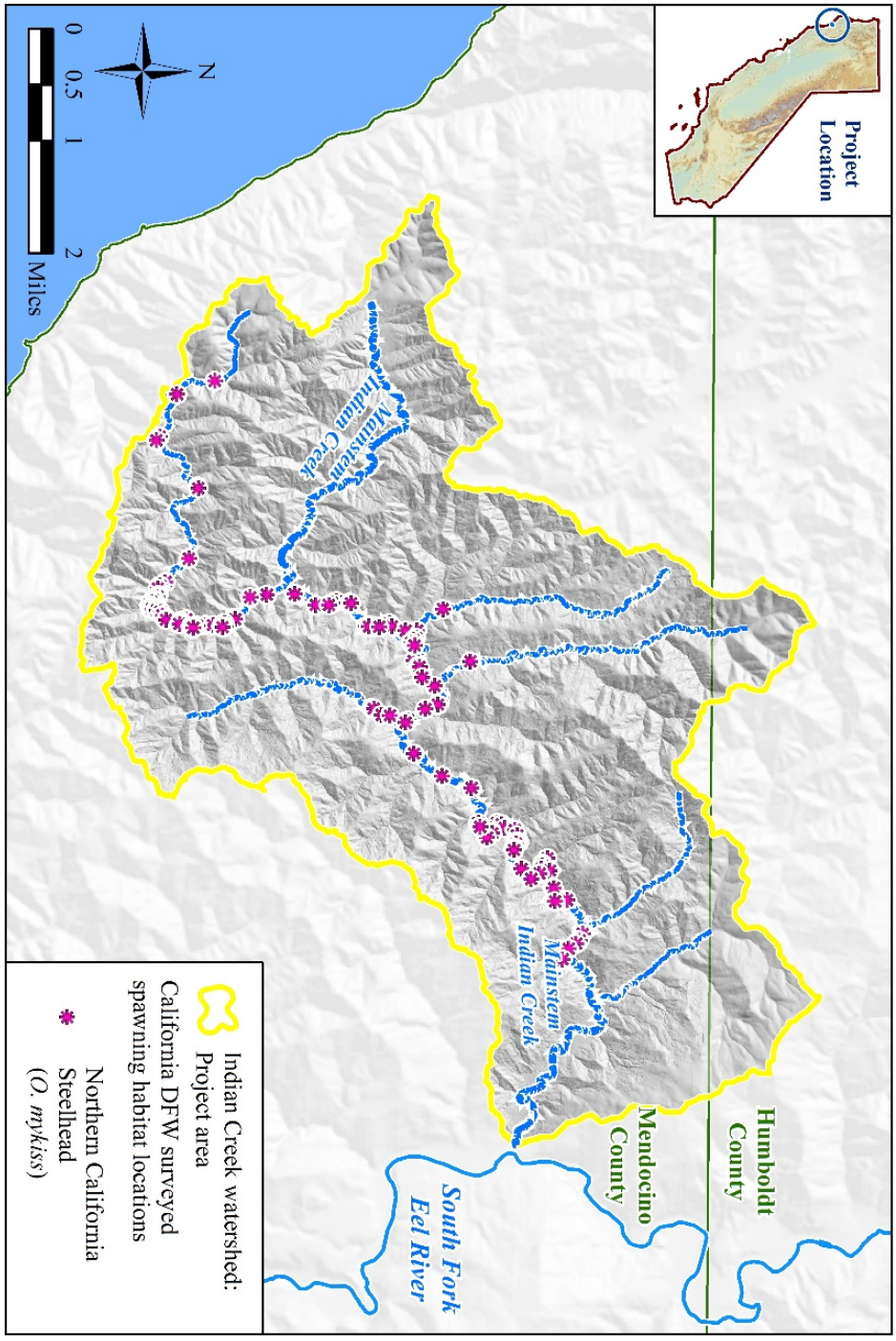

Figure 12. Locations of CDFW field-surveyed Northern California Steelhead redds.

RFFI and LCF, as part of their land management activities and restoration efforts, acquired 1-meter resolution lidar-generated digital elevation models covering significant portions of their properties, including the majority of the Indian Creek watershed (86.82%) and a number of neighboring watersheds to the south: Piercy Creek, Standley Creek, Bear Pen Creek, and Wildcat Creek (Figure 14). The DEM was created from lidar data collected with a Leica ALS70 sensor at an altitude of 1300 meter at a collection density of 8 points / meter^2 (Quantum Spatial, 2013). In the Indian Creek watershed area, lidar data collected had an average absolute accuracy of 0.003 m and an average vertical relative accuracy of 0.05 m (Quantum Spatial, 2013). This data represents 100 % coverage of neighboring watersheds, all of which have had similar anthropogenic disturbance, similar geology, and are all tributaries to the South Fork Eel River (Figure 2). In order to derive a better representation of contributing areas for streams throughout the Indian Creek watershed (Figure 14), 10 m DEM acquired from the USDA geospatial data repository (2018) was resampled using a bicubic process to 1 m and then merged with the lidar DEM data to fill gaps in the 1m DEM data to achieve 100 % watershed coverage. This allowed DEM coverage for the remaining watershed area (86.82 % covered by lidar DEM data, 13.18% covered by resampled 10m DEM data). This process was necessary, as contributing areas to streams throughout the watershed are used as a covariate in the modeling analysis. It was assumed that the geospatial extents of the watershed requiring fill coverage would not differ significantly in contributing area representation from an ideal situation of 100 % lidar DEM coverage.

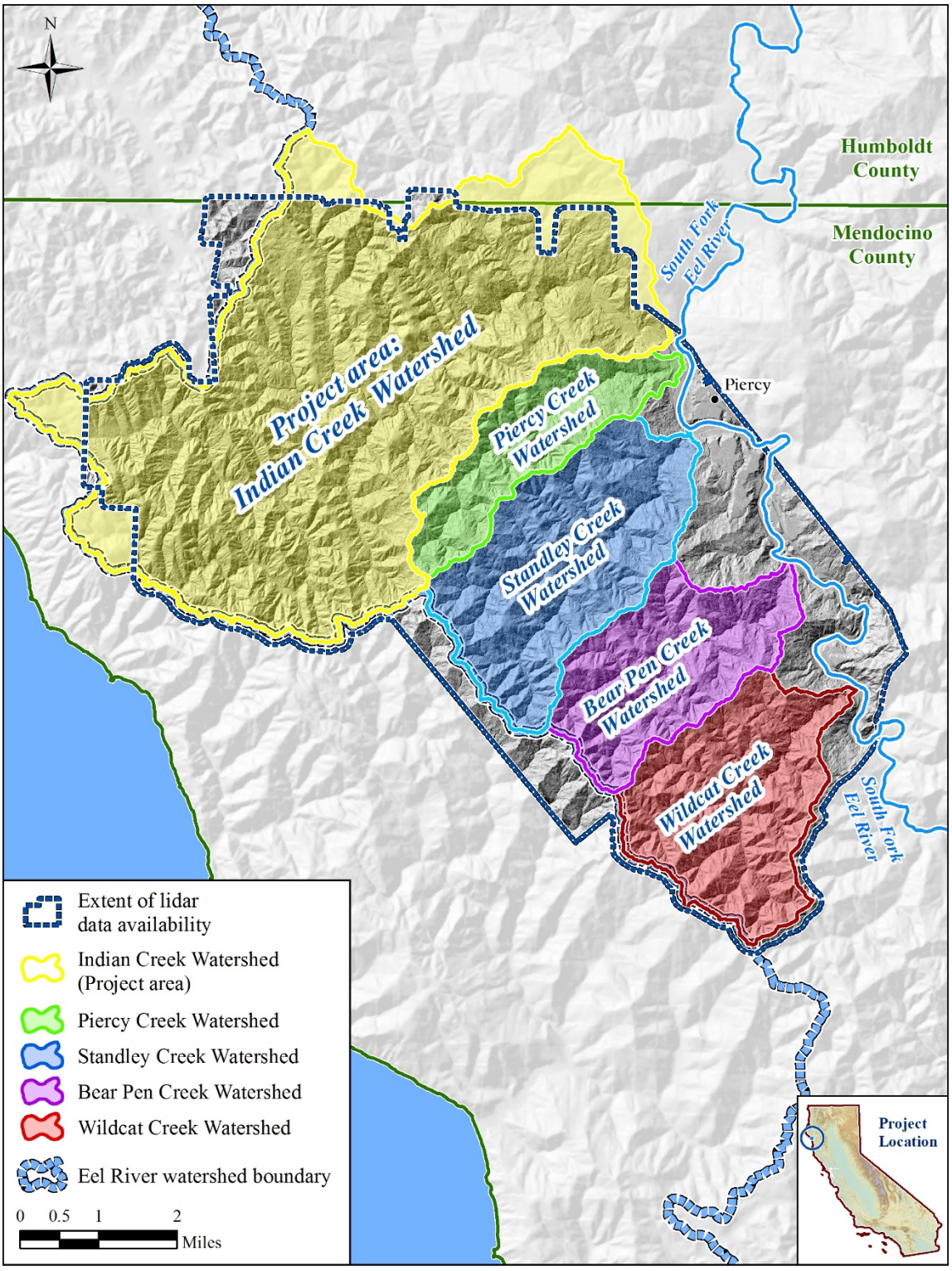

Figure 13. Extent of acquired 1m resolution lidar DEM data.

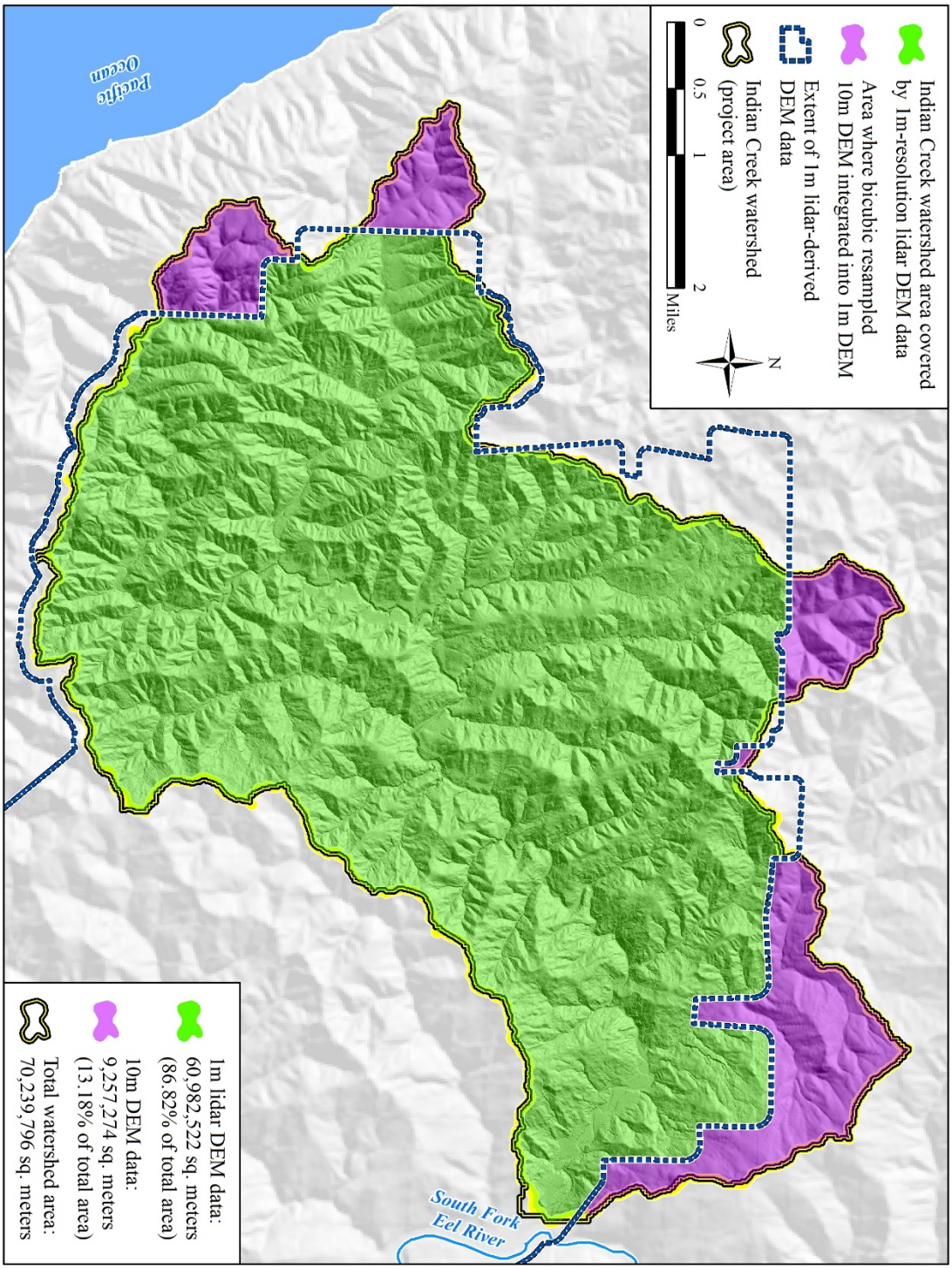

Figure 14. Extent of 1m resolution lidar DEM data within the Indian Creek watershed and areas of 10m resolution DEM data used to obtain full contributing area coverage.

3.3 Methodology

3.3.1 Digital Elevation Model analysis and processing

A 10 meter DEM was used to fill in geospatial gaps of drainages where 1 meter data was unavailable, and sufficiently buffered sections of the 10 meter DEM were extracted to ensure complete drainage coverage (and thus correct flow accumulation metrics) of 1 meter data gaps (Figure 10). The 10m DEM extracted data were then resampled to 1 meter resolution using a bicubic resampling process to ensure compatibility between the datasets, though this does not improve the quality of the 10 meter data. The resampled DEMs were then integrated with the 1 meter resolution DEMs into a single dataset.

The complete DEM surface was then used to hydrologically model the Indian Creek watershed area, generating fill (FILL), flow direction (FDR), and flow accumulation (FAC) rasters. The Raster Calculator tool was used to delineate a synthetic stream raster grid using a 2500-cell contributing area as a threshold (Foster, 2012). A polyline stream network representing the modeled thalweg was then developed. This synthetic thalweg stream network was used for visualization and spot-checking to ensure each step of the modeling process was performing as expected.

The first step taken in the analysis of DEM data was to derive a synthetic hydrologic network that mirrored as closely as possible actual field conditions. During Foster's (2010) geologic survey of the neighboring Standley Creek watershed (Figure 13), it was field-verified that a 10000 meter^2 contributing area was ideal as a threshold

when deriving a synthetic linear stream network from DEM data. Foster and Kelsey (2012) revisited the study area and refined metrics associated with the contributing area to 2500 meter^2. Using a 2500 meter^2 contributing area threshold for stream inception allowed the resulting hydrologic network to match on-ground conditions in the Indian Creek watershed in terms of hydrologic extent and density. As Standley Creek is in direct proximity to Indian Creek, lying within the same geologic unit (Jennings, 1960), climatic regime (USDA 2016), sharing similar vegetative landcover (PWA 2015), and having the same types of historical anthropogenic disturbances (PWA 2015) it was assumed that streams within the Indian Creek watershed have a very similar inception area threshold. Additional accounts from professionals that are familiar with the landscape (PWA engineering geologist Thomas Leroy, and CDFW fisheries biologist Seth Ricker) further support this assumption by the author. Field verification at selected locations in the Indian Creek watershed by the author also confirmed this (Appendix F, photo points). This synthetically derived linear hydrologic network, representing the mathematical path of the thalweg as derived from the DEM data acts as a key base component to the stream morphological and spawning habitat models.

After a reliable synthetic stream network had been created, a statistical model to predict bankfull stream widths in the Indian Creek watershed was developed, parameterized, and validated using field-acquired geomorphic stream survey data from the Indian Creek and the neighboring, environmentally similar watersheds (Figure 8). Based on background research, it was decided to use a generalized additive model (GAM) due to its flexibility in modeling non-linear and threshold response systems. The

bankfull width of a stream can vary significantly over the course of its flow, due to variations of slope, geology, accumulation area, vegetation, bed material, and contributing streams (Dunne and Leopold, 1978, Faustini, et. al. 2009). These types of variations in a multivariate response system in a natural environment makes the GAM model an appropriate choice in this context.

After performing sensitivity testing, the predictive bankfull width model was then applied in a geospatial context by using R-Studio in conjunction with ArcMap to process acquired data and output geospatial products. Using the derived hydrologic network of the thalweg, a toolset to create a geospatial morphological representation of the bankfull stream corridor was created and field verified in selected locations (Figures 15-17, Appendix F). This toolset, Numerically Interpolated Flow Track Inferencing (NIFTI), allowed the development of continuous raster surfaces representing the entirety of the Indian Creek watershed stream network corridors with each of the chosen covariates. The resultant raster covariates derived from this geospatial data analysis and model development (flow accumulation, slope, substrate, distance from the confluence of Indian Creek with the SF Eel River) were then used to predict habitat suitability using the species distribution / habitat suitability modeling software MaxEnt (Phillips, et. al. 2018). At each stage of the process, potential sources of uncertainty and when sensitivity testing should take place were noted and performed.

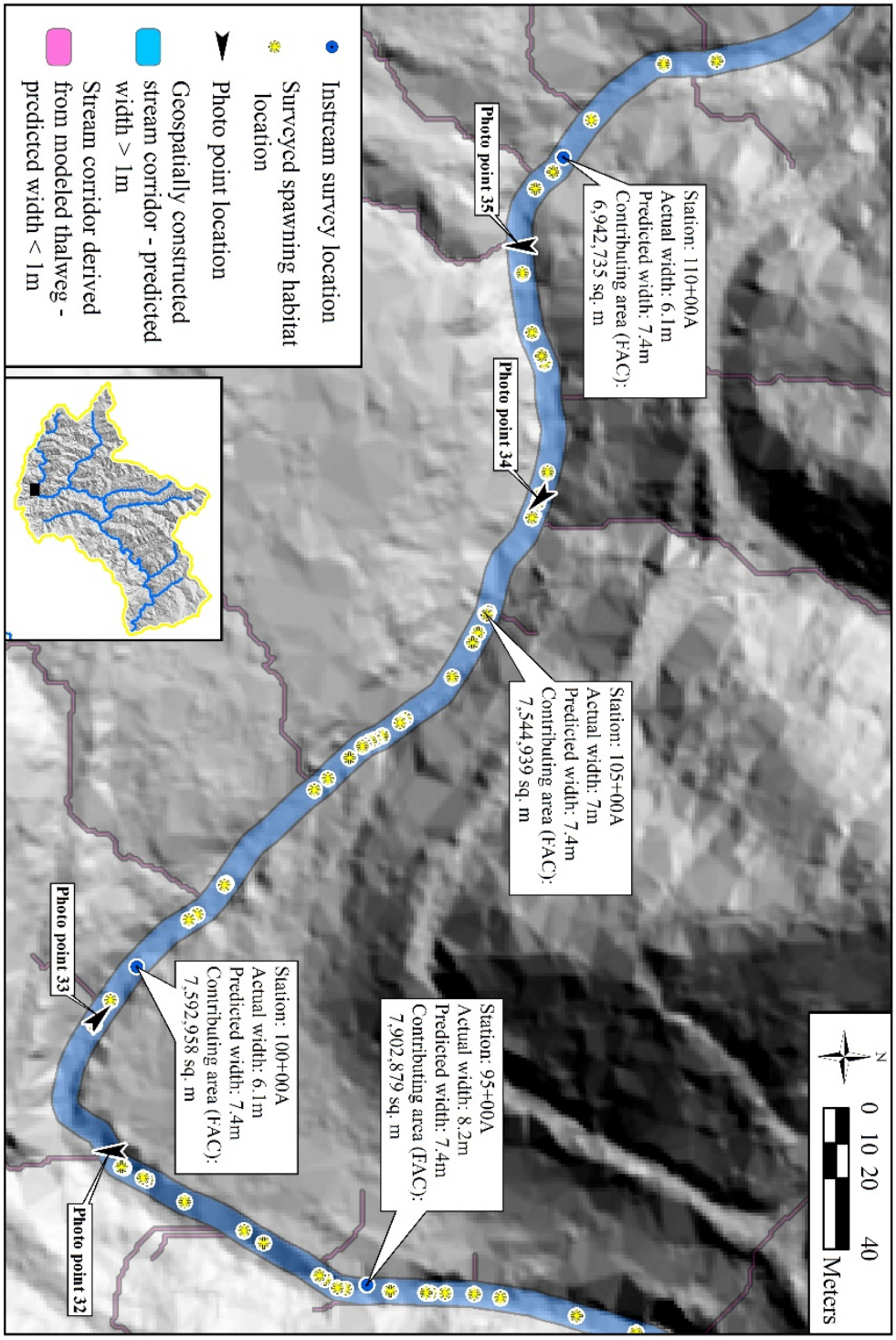

Figure 15. Geospatially reconstructed stream corridor with actual and predicted widths, Anderson Creek, Indian Creek watershed. See also Section 3.3.4.

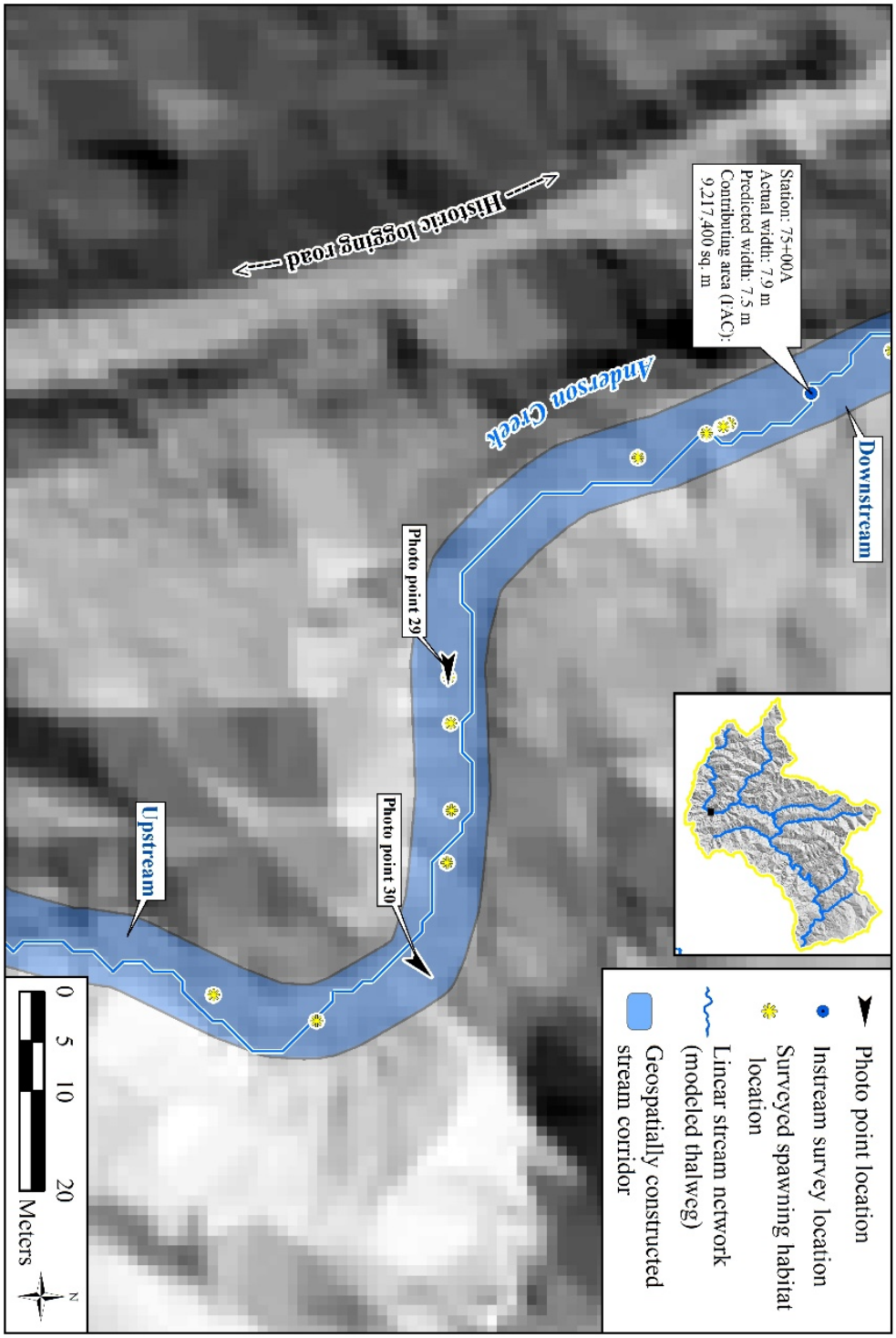

Figure 16. Detailed view of geospatially reconstructed stream corridor with photo point locations, Anderson Creek, Indian Creek watershed.

Figure 17. Geospatially reconstructed stream corridor with actual and predicted width at Photo Point 29, Anderson Creek, Indian Creek watershed. Pictured are Thomas Leroy (PWA) on left and Seth Ricker (CDFW) on right. Note historic railroad track (c. 1900).

3.3.2. In-stream survey data analysis and processing

Geomorphic stream survey data were also processed so that data could be used in development of a model predicting bankfull widths. The initial tasks performed on and with stream survey data of the project area were to geospatially correct in-stream survey points by moving them by the minimal distance to the nearest linear feature of the synthetic stream network. The accuracy of the positions of the survey point data ranged between 2 and 5 meters due to global positioning system (GPS) unit quality and the

location of the survey points in an inner-gorge area. During initial review of the data, it was found that some stream survey points had fallen on roads and hillslopes directly adjacent to the stream. This geospatial relocation was performed to ensure survey data could be reliably associated with the most appropriate stream data values derived from the FAC and Slope rasters.

Though survey points had been taken at 500 foot intervals of selected streams, it would not have been appropriate to denote 500 foot intervals of the synthetic stream network and locate the data at those interval points, as those synthetic stream networks tend to have an overly complex nature resulting from the resolution of the 1 m DEM. That overly complex nature (mirroring the path of the modeled thalweg) renders length calculations and assumptions erroneous in some cases. Of the 430 stream geomorphic survey point features, only 2 needed to be snapped to within a distance greater than 5 meters. One of those was a stationing located at the confluence of Indian Creek with the Eel River, where the meander of the thalweg was the greatest and the channel the widest, thus indicating potential channel migration or slight morphological change in the thalweg at that area between the time when the DEM was acquired, and the stream survey was performed. After examination of the hillshade and consultation with the field crew that had acquired the data in the area of the second point, it was determined that the second point was located in an inner-gorge area where satellite signal reception was poor. Survey stations (428 total) survey stations were relocated less than a 2 m distance. Thus, it was assumed that the synthetic stream network representing the thalweg of the stream corresponds closely to the survey coordinate information. This in turn indicates that the

physical variable attributes to be associated with the synthetic network do not vary greatly from those associated with the actual stream system.

The stream survey data was then geospatially joined and specific FAC and Slope raster cell values with each stream survey point coincident at that cell were integrated into the data table. A unique identification to each stream survey point was then added, utilizing the attribute table for that feature dataset.

After initial analysis and model development, it was necessary to incorporate geospatial information from points of stream inception. Thus, a geometric network of point data was derived from the inception points of the modeled linear stream. FAC and slope raster cell values at those spatial locations were then geospatially associated with those points. This data table was integrated into the stream survey data, together with unique identifications for each geospatial position. The entirety of this data was then exported as a database and converted to a table of comma separated values (CSV file).

3.3.3. Spawning Habitat Survey data analysis and processing

CDFW spawning habitat data served as presence data input. Rasters representing the stream bankfull morphology with assigned contributing areas, slope information extracted from the DEM, distance of fish travel from the confluence of Indian Creek with the South Fork Eel River, and substrate information derived from the geomorphic stream surveys were used as raster covariates (Figures 18-26).

A total of 672 CDFW field-verified spawning ground locations surveyed in the South Fork Eel River watershed fell within the Indian Creek watershed. A further 23 were within the neighboring Piercy Creek watershed, 10 within Standley Creek

watershed, and 7 within the Wildcat Creek watershed. Initial tasks performed on and with spawning habitat survey data of the project area were similar to the preprocessing of stream geomorphic survey data. Spawning point data were geospatially relocated by the minimal distance to the nearest linear feature of the synthetic stream network to ensure that spawning habitat data fell within the modeled stream system. The accuracy of the survey point data was roughly 10 m.

3.3.4. Modeling bankfull stream corridor in the project area

The stream survey data table from Indian Creek, Piercy Creek, Standley Creek, Wildcat Creek, and Bear Pen Creek, with geospatially joined raster values from the FAC and Slope raster cell values, were imported into R statistical processing software (R Core Team, 2013). A series of generalized additive models (GAMs) were developed using covariates of FAC and Slope to predict stream width. Other variables extracted from the DEM (such as flow lengths) were eliminated as candidates for this stage of model development as they directly covaried with FAC values, and thus might have incorporated a confounding influence on the model. The possibility also existed that modeled stream structures might be overly complex in nature and could exhibit lengths that do not correspond with naturally occurring stream features.

During stream width model development, varying degrees of gamma ("smoothing") thresholds were examined to allow for model prediction flexibility while still predicting with a reasonable degree of field-verified accuracy. A predictive model using a 1.4 gamma factor was found to be optimum. Response curves from models derived using smaller gamma values tended to exhibit over-fitting, so it was decided that

they would not be suitable for extrapolation as they were too model-specific or showed inexplicable curvilinear anomalies. Models derived using gamma values greater than 1.4 seemed to not capture intricacies of the phenomenon that would have provided insight to both the model and/or data – overly "smooth" response curves lost the uniqueness of the dataset specific to the Indian Creek watershed. The model was cross validated 10000 times using a random 70% / 30% training / test data ratio and was found to be able to explain 93.3 % of the variance. The p-value for FAC as a predictor component to the model was $2x10^{-16}$. Slope, though the p-value was 0.123, was left in the model as it was noted during calibration of multiple models using subsets of stream station data that p-values continued to decrease rapidly as the number of stream data stations increased. Observations made during field visits to stream locations with high slope indicated that inclusion of slope as a predictive variable in this context would hold value. Future work could potentially include model development and data acquisition focusing on sections of the stream system with higher slope values, thus providing additional data that may prove valuable when calibrating slope as a covariate (Appendix A).

Bootstrapping tests with 70/30, 50/50, and 25/75 subsample percentages repeated 1000 times showed that the model performed consistently for internal validation. Using smaller percentages of the data (50 %, then 25 %) to predict larger proportions displayed a small drop in the percentage of deviance explained by the model. This indicates that the large size of the dataset allows for some flexibility when using a small percentage of the data to perform inference overall while only having a relatively small increase in uncertainty when doing so.

Predictions from the stream width model were geospatially associated with the synthetic thalweg stream network. Using the predicted widths and the original DEM an automated process was developed and used to create a geospatial representation of bankfull stream morphological corridor. Using the NIFTI toolset, a geospatially reconstructed stream corridor was developed and field-verified. This allowed continuous raster datasets representing the stream corridor to be developed and assigned values corresponding to the contributing areas (FAC), slope, distance from the confluence of Indian Creek with the South Fork Eel River, and percentages of delineated substrate (Table 1, Figures 18-26, Appendix G). Substrate values for the geospatial extents of the stream system were assigned in two ways: 1.) between survey stations with known substrate percentages, known values were geospatially assigned to raster extents 50% of the distance between stations, and 2.) for stream reaches outside of known locations, a geospatial similarity analysis based on flow accumulation and slope was used to predict and assign substrate percentages. As flow accumulation and slope were found to be significant ($p << .01$) though weak (12-22% of variance explained) predictors of substrate percentage, it was decided to move forward with that assignment, rather than proceed with no data for those extents.

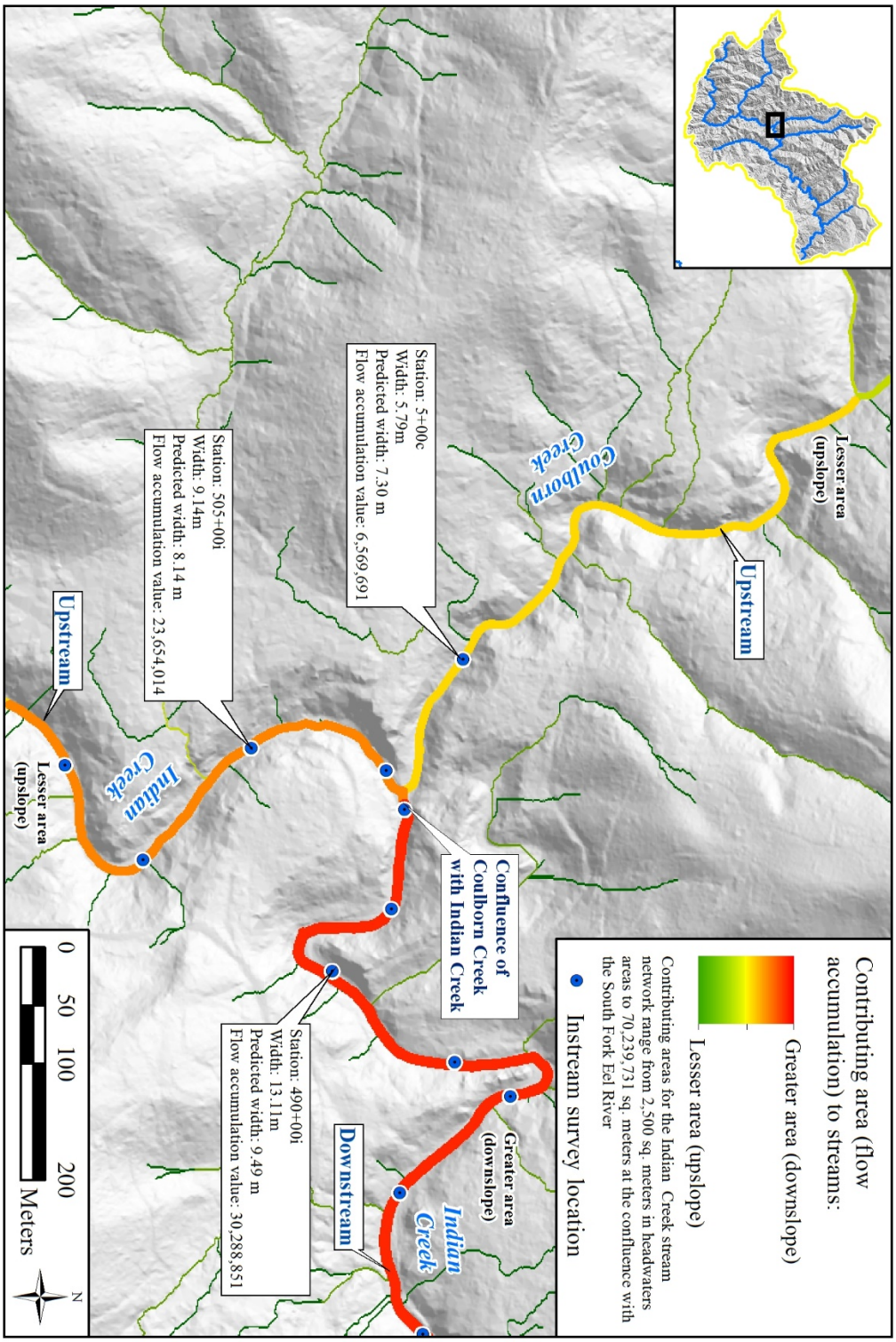

Figure 18. Selected area of raster covariate environmental variable used for MaxEnt probability surface creation – contributing areas (FAC).

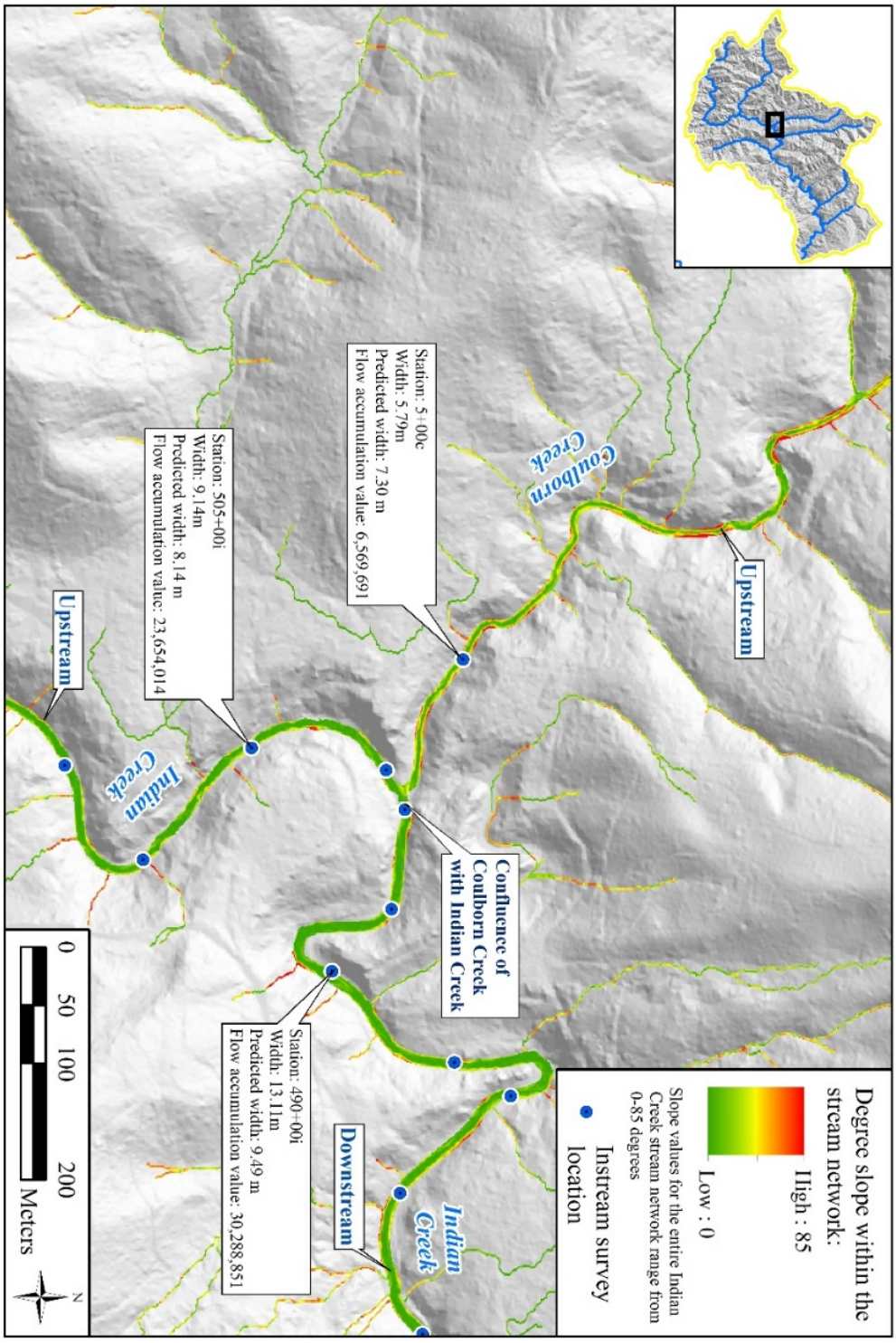

Figure 19. Selected area of raster covariate environmental variable used for MaxEnt probability surface creation – degree slope.

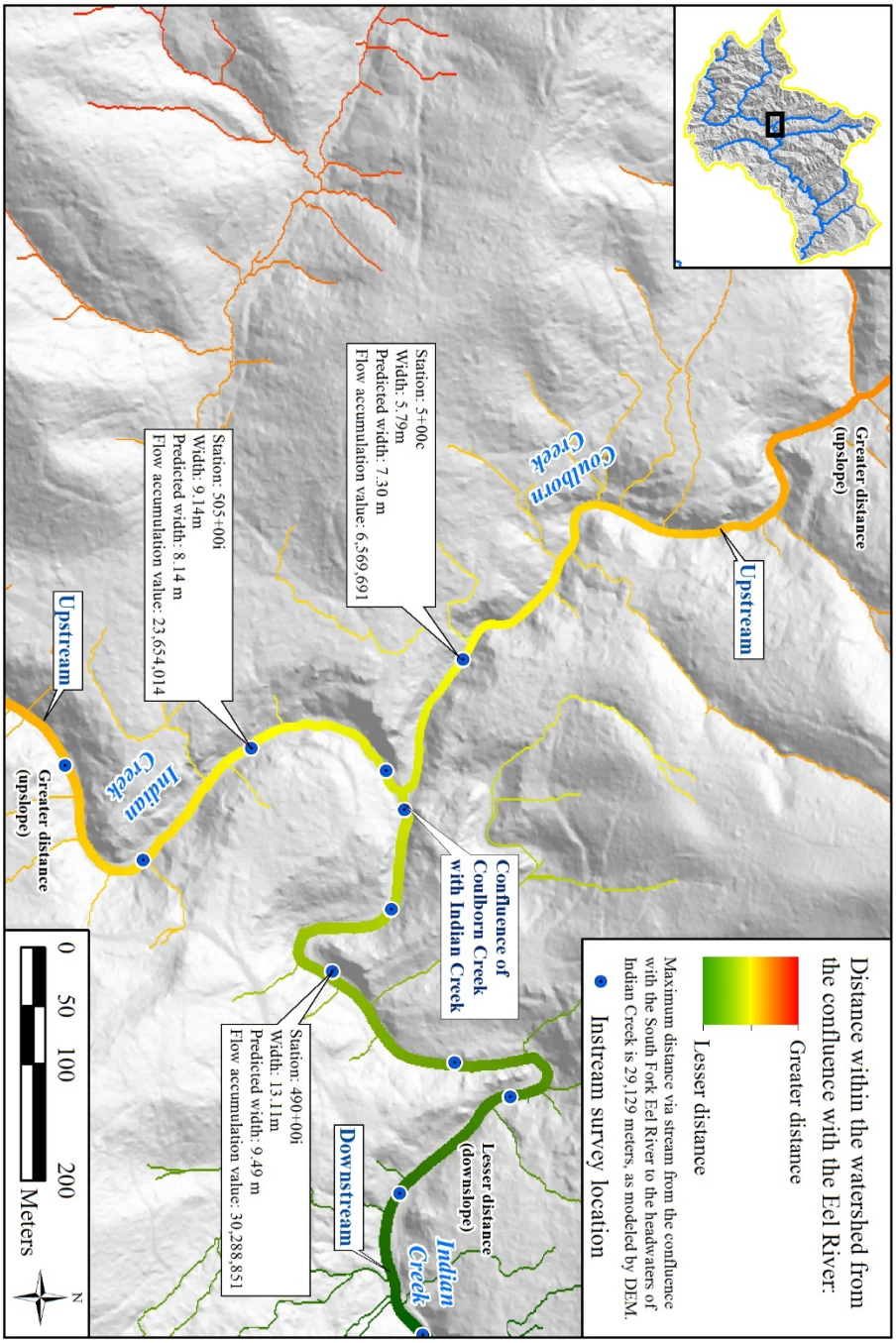

Figure 20. Selected area of raster covariate environmental variable used for MaxEnt probability surface creation – distance from the confluence of Indian Creek with the Eel River.

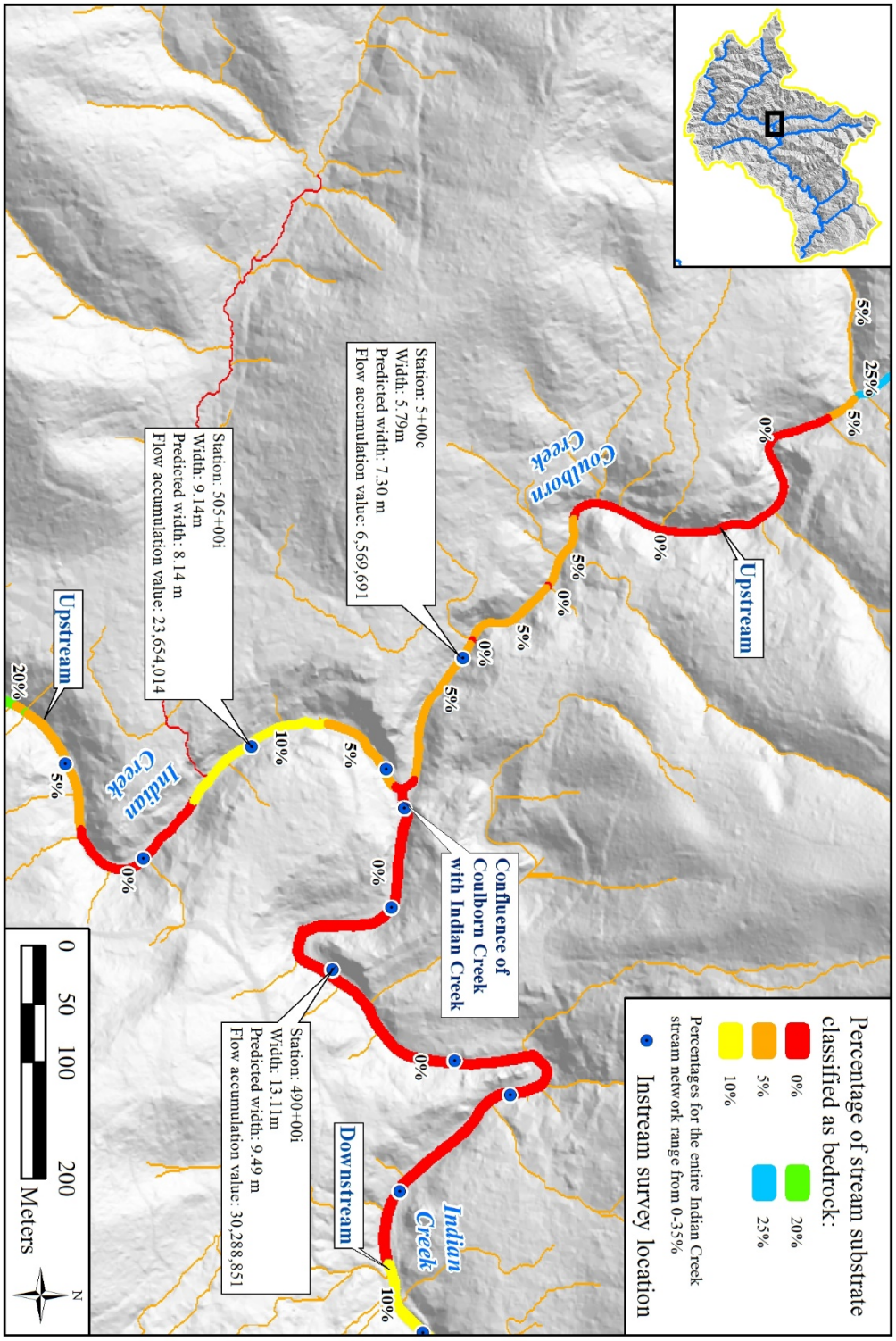

Figure 21. Selected area of raster covariate environmental variable used for MaxEnt probability surface creation – bedrock substrate classification.

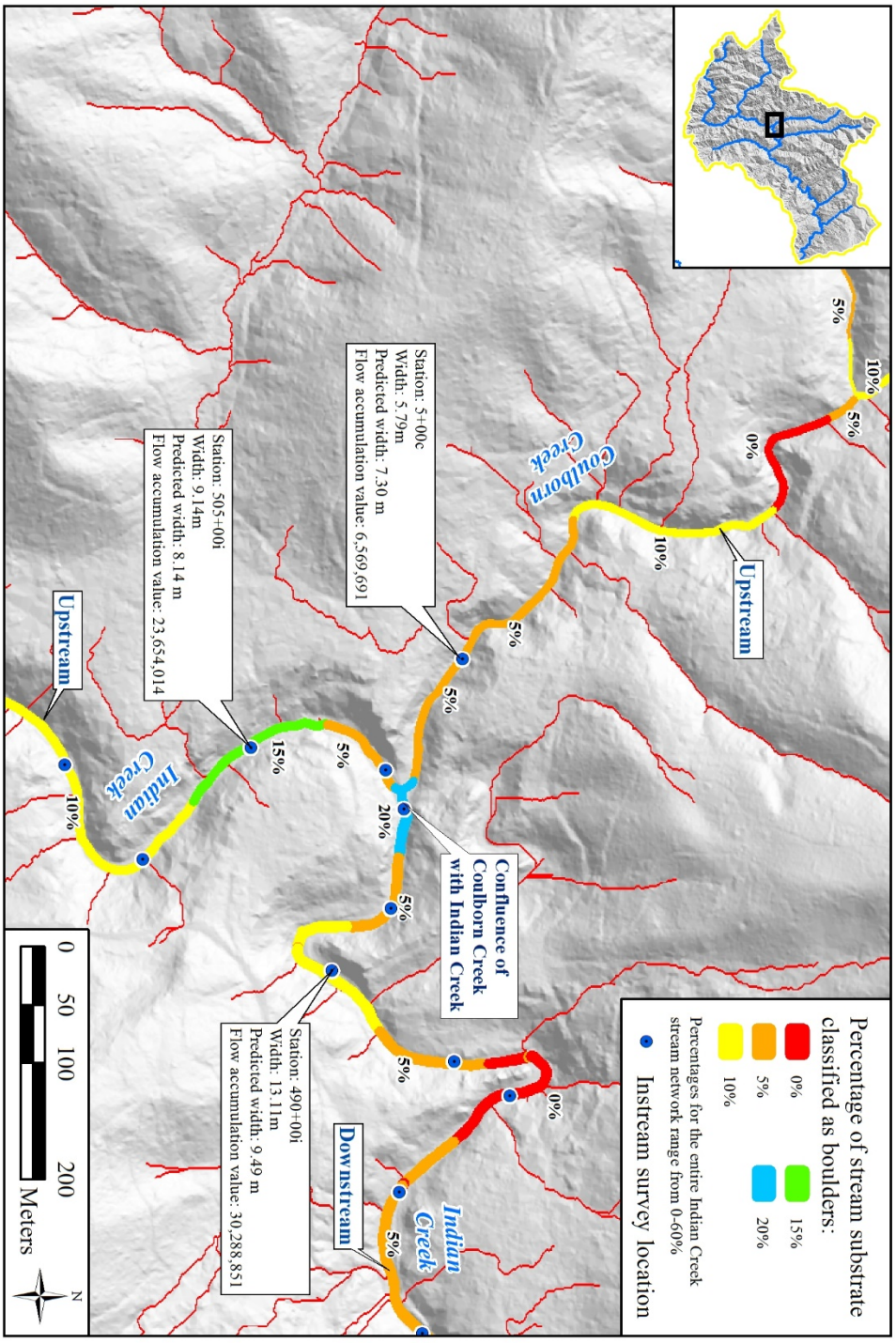

Figure 22. Selected area of raster covariate environmental variable used for MaxEnt probability surface creation – boulder substrate classification.

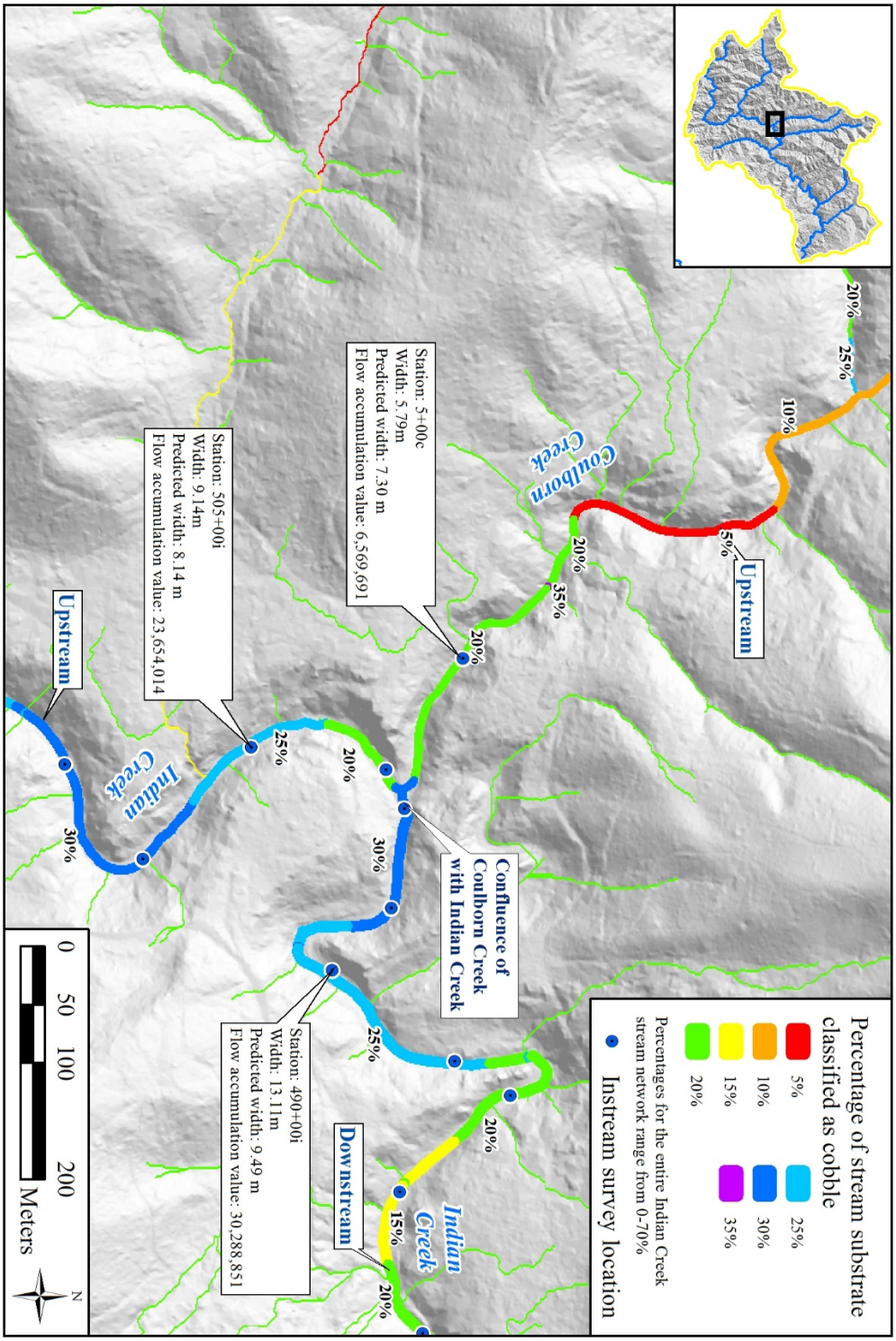

Figure 23. Selected area of raster covariate environmental variable used for MaxEnt probability surface creation – cobble substrate classification.

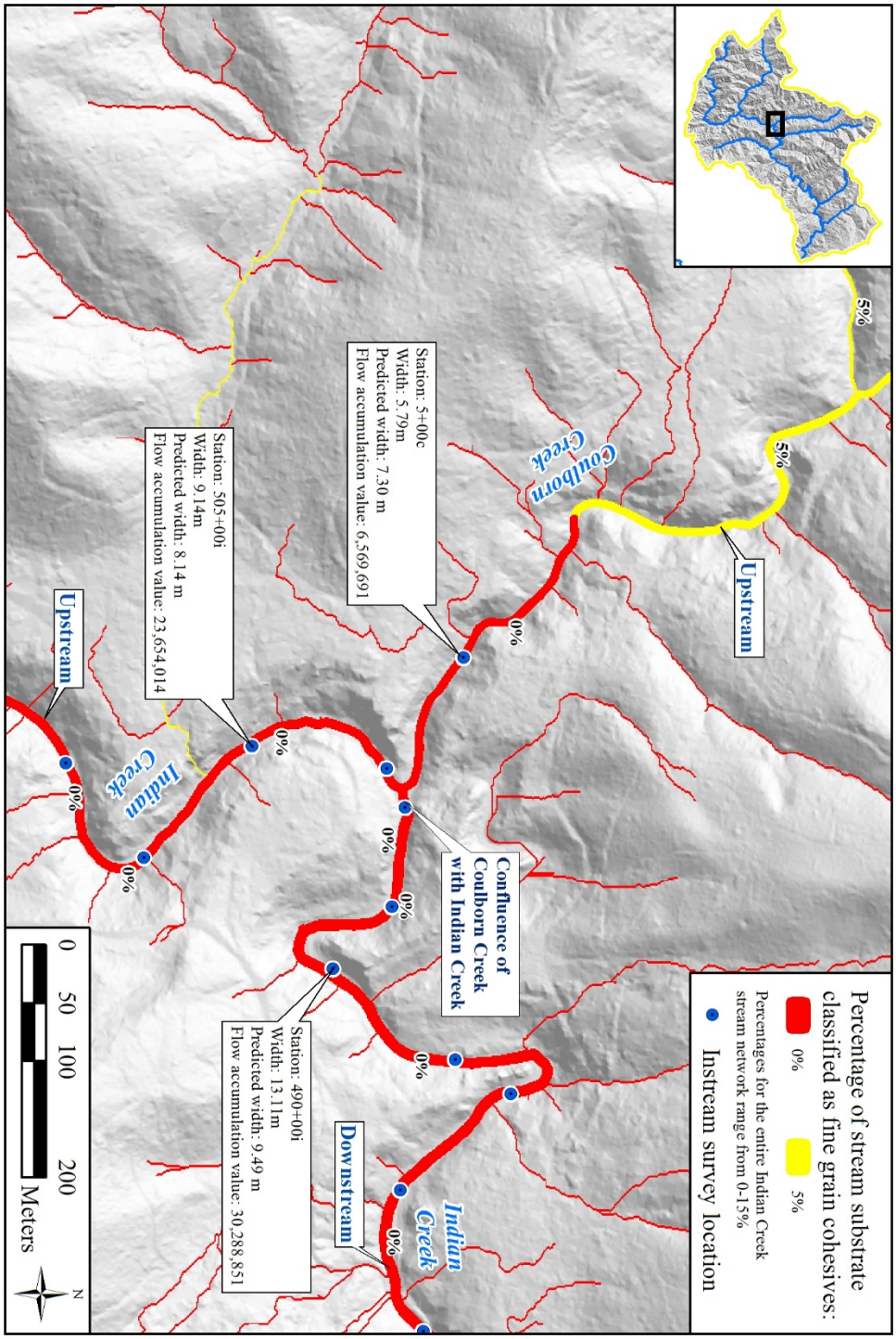

Figure 24. Selected area of raster covariate environmental variable used for MaxEnt probability surface creation – fine grain cohesive substrate classification.

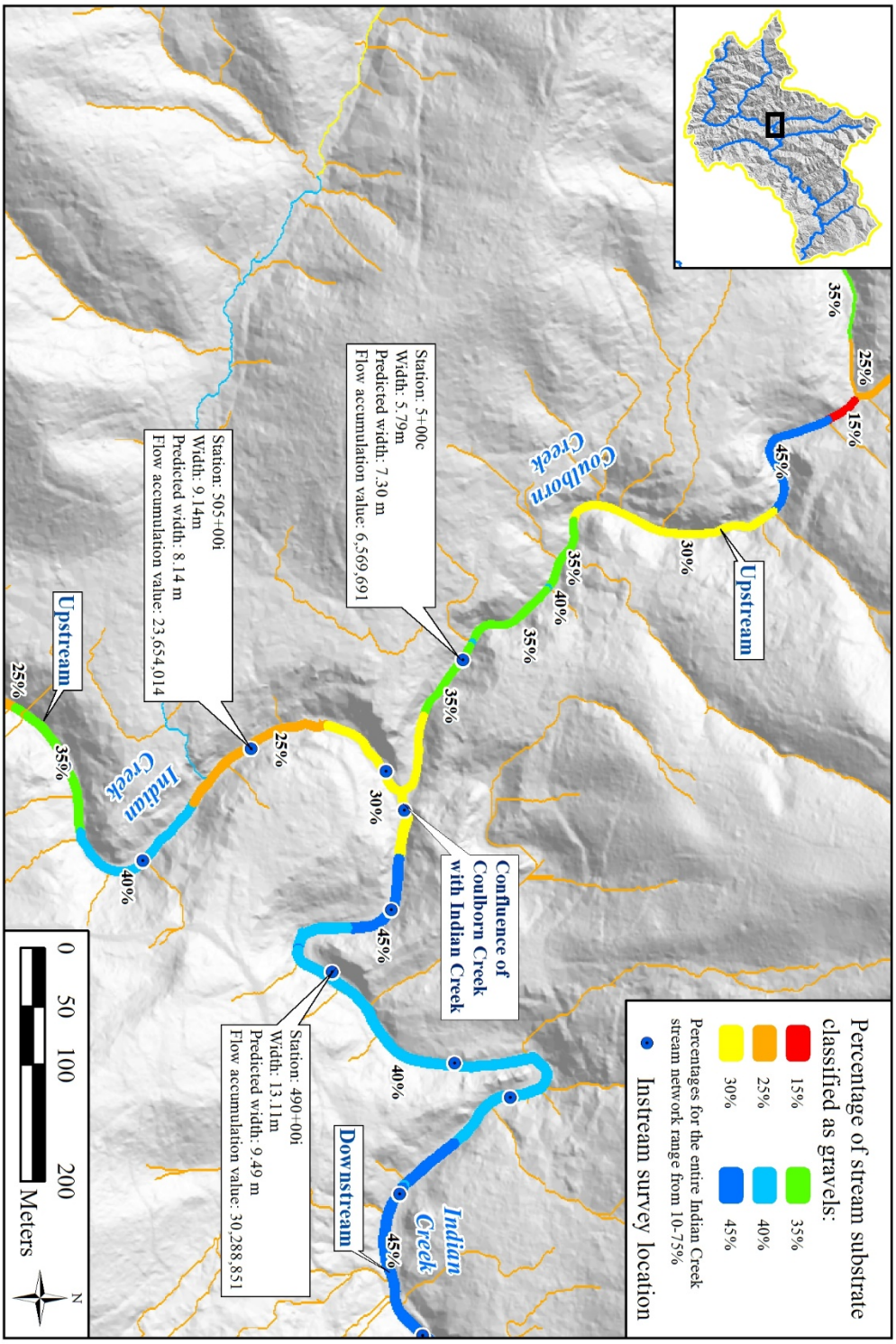

Figure 25. Selected area of raster covariate environmental variable used for MaxEnt probability surface creation – gravel substrate classification.

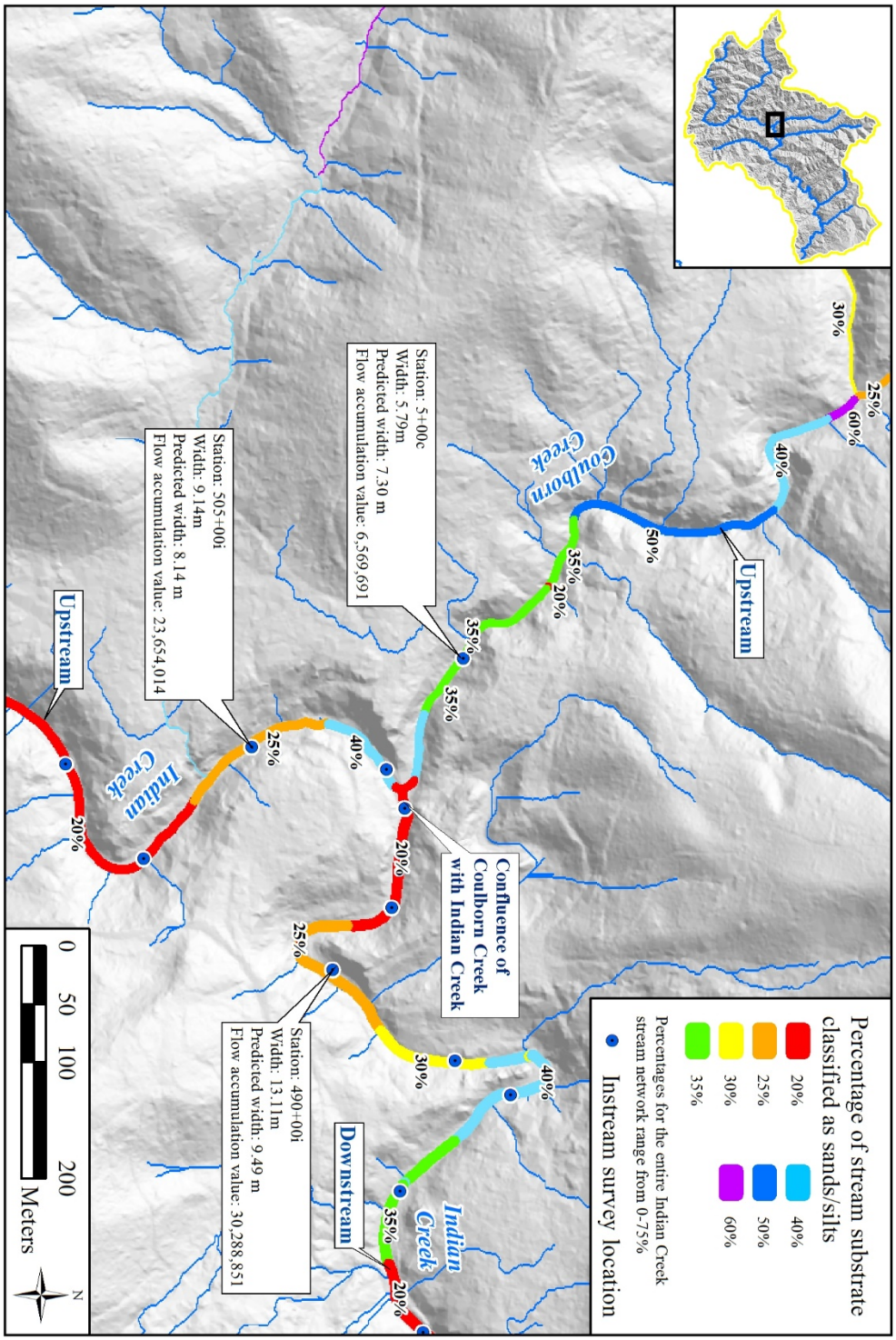

Figure 26. Selected area of raster covariate environmental variable used for MaxEnt probability surface creation – sands / silts substrate classification.

3.3.5. Habitat suitability modeling

To model the probability for spawning habitat throughout the Indian Creek watershed stream system, the geospatially constructed raster covariates and spawning habitat presence data were utilized in MaxEnt (Phillips, et. al. 2017, 2018) to derive habitat probability surfaces. MaxEnt (acronym for Maximum Entropy) is a geospatial statistical package used to model species distributions from presence-only location data and continuous raster covariates. MaxEnt was used to develop probability surfaces for spawning habitat for the three species of interest in the Indian Creek watershed using raster covariates of FAC, degree slope, distance within the watershed from the confluence of Indian Creek with the South Fork Eel River, and percentages of substrate as derived from the habitat typing stream surveys in the Indian Creek and neighboring watersheds (typing system as developed by Flosi, (2014)). A critical component of this analysis was the development of the geospatial reconstructions of the stream systems using NIFTI, as MaxEnt requires accurate continuous raster surfaces of predictor variables to have accurate, interpretable results. Occurrence data from all three species of interest were used individually. A 70 % / 30 % cross-validation with random sub-sampling for 100 repetitions was performed for model validation, which allowed assessment of how well the model performs for an independent data set. In this instance, a random selection of 70 % of the data was used to validate the remaining 30 %. Jackknifing for variable importance was also performed during this cross-validation, as this resampling technique tests for variance and bias estimation by systematically leaving out each observation from the dataset, calculating the estimate, and then finding the average of the calculation.

These operations in MaxEnt were used to derive raster probability surfaces for each of the three species of interest.

RESULTS

Using the continuous raster covariates developed with NIFTI, stream geomorphic data, and habitat presence data, spawning habitat probability surfaces were obtained using MaxEnt (n.b. due to the spatial resolution and number of covariates, as well as the task of deriving three probability surfaces using 100 replications for cross-validation and jackknifing for variable importance, total computer processing time for the modeling exercise was 4 days 3 hours, with 3.5 terabytes of resulting data). Figures 27, 28, and 29 show probability surfaces generated during the modeling process at watershed scale.

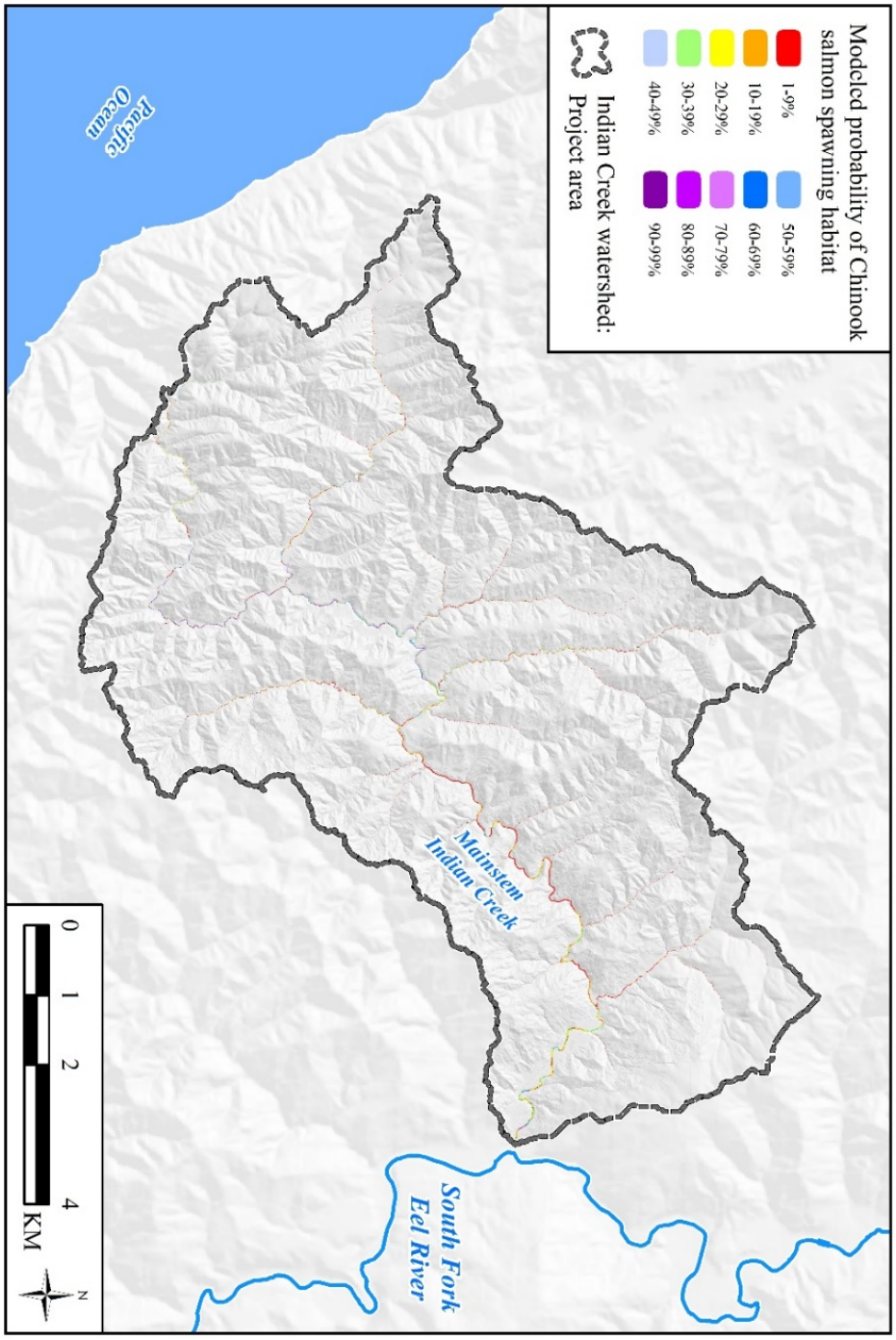

Figure 27. MaxEnt results – Chinook spawning habitat, overview map for Indian Creek watershed. Mean AUC for 100 replicated runs = 0.954; standard deviation = 0.036. Note – not all data may be represented visually at this scale.

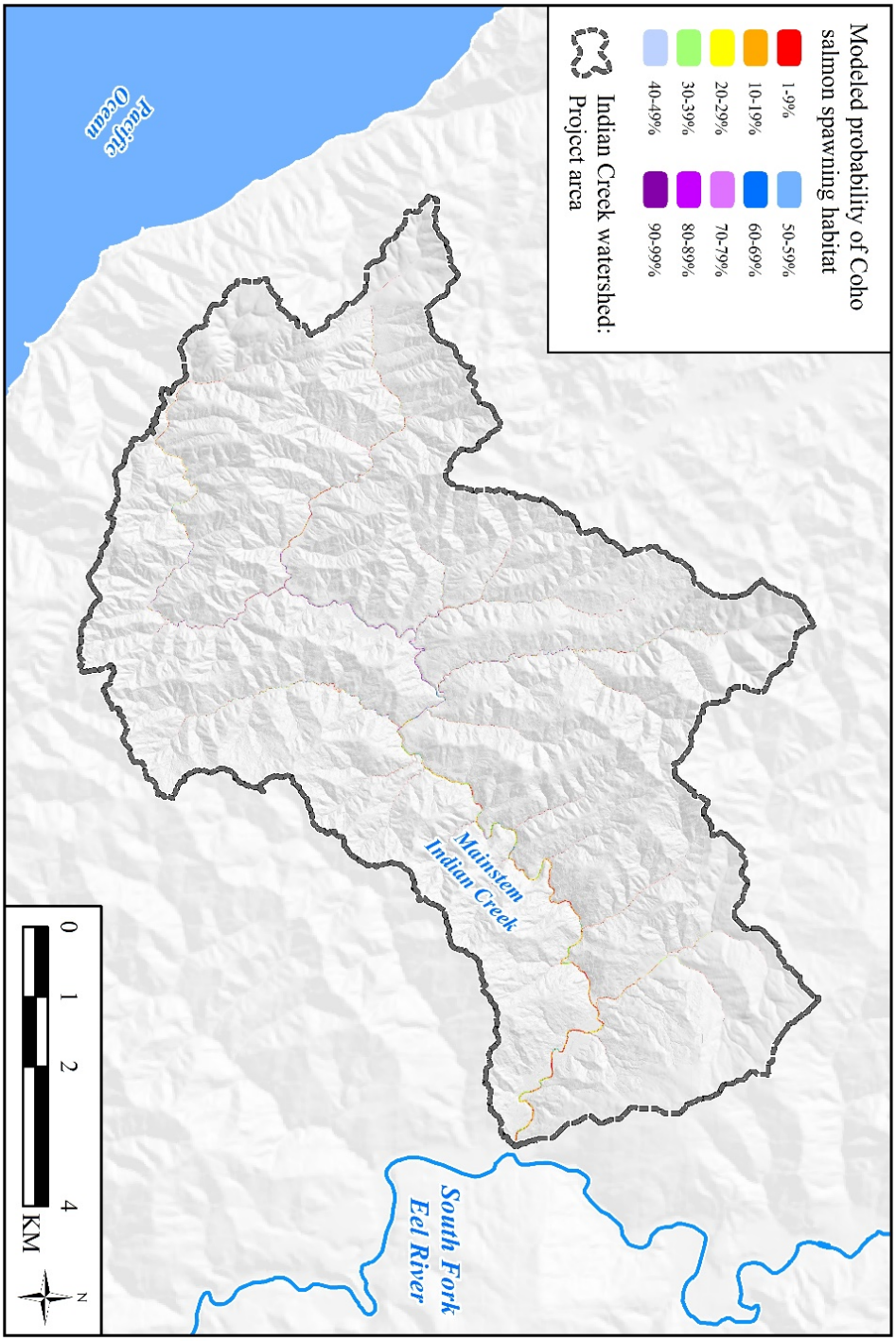

Figure 28. MaxEnt results - Coho spawning habitat, overview map for Indian Creek watershed. Mean AUC for 100 replicated runs = 0.951; standard deviation = 0.034. Note – not all data may be represented visually at this scale.

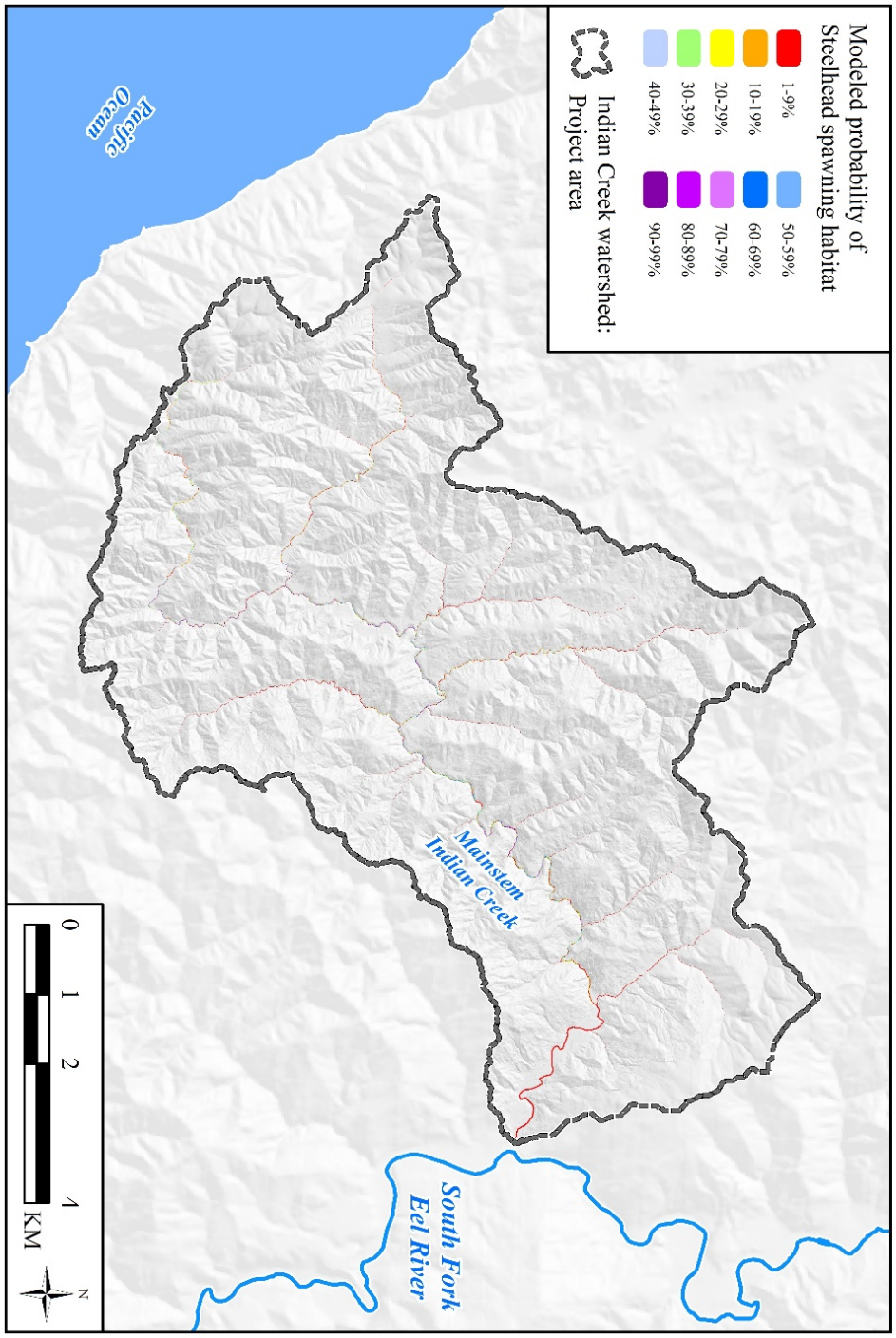

Figure 29 MaxEnt results - Steelhead spawning habitat, overview map for Indian Creek watershed. Mean AUC for 100 replicated runs = 0.958; standard deviation = 0.036. Note – not all data may be represented visually at this scale.

Probability surface results were incorporated into maps and field-verified for geospatial and interpretive accuracy with Thomas Leroy and CDFW Fisheries biologist Seth Ricker - selected project areas with specific probability surfaces are shown in Figures 30, 36, and 42. Figures 31, 37, and 43 show the same geospatial extents with the uncertainty (standard deviation) surface for their respective species, and figures 32-35, 38-41, and 44-47 show charted areas of probability percentages for modeled streams. Tables 2-10 are probability areas in tabular format, broken into specific geospatial extents. Response curves for specific geospatial covariates are included in Appendix C, together with jackknifing results. Small scale probability surface maps for each of the three study species are given in overview in Appendix B, as well as at selected photo points included in Appendix F.

Areas of spawning habitat probability for each species have been itemized as follows:

1. Areas of specific probabilities for entirety of modeled stream system
2. Areas of specific probabilities for modeled streams with bankfull widths predicted to be >= 1m
3. Areas of specific probabilities for modeled streams with bankfull widths predicted to be < 1m

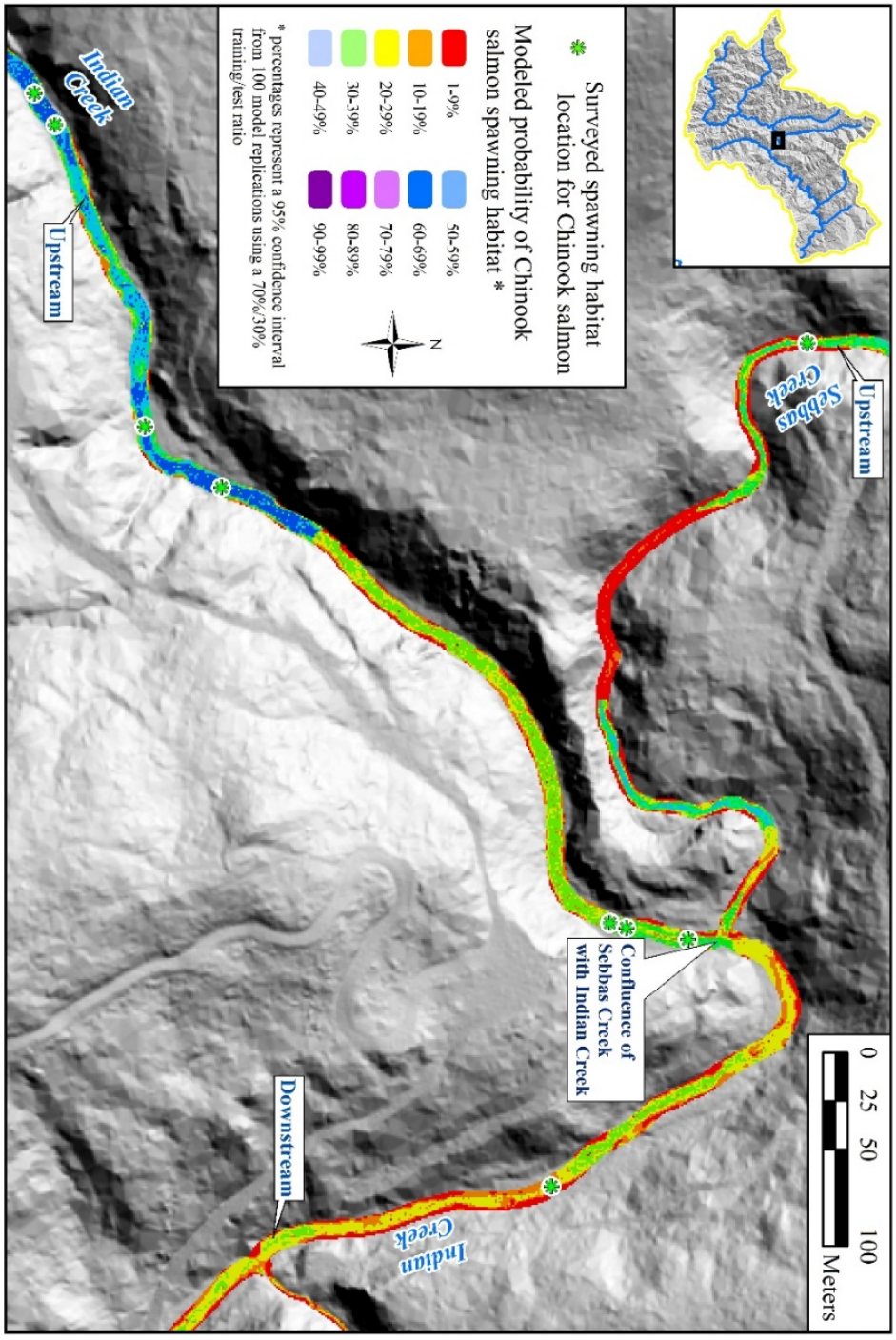

Figure 30. Selected area of probability surface for Chinook salmon spawning habitat. The average test AUC for 100 replicate runs is 0.954, and the standard deviation is 0.036.

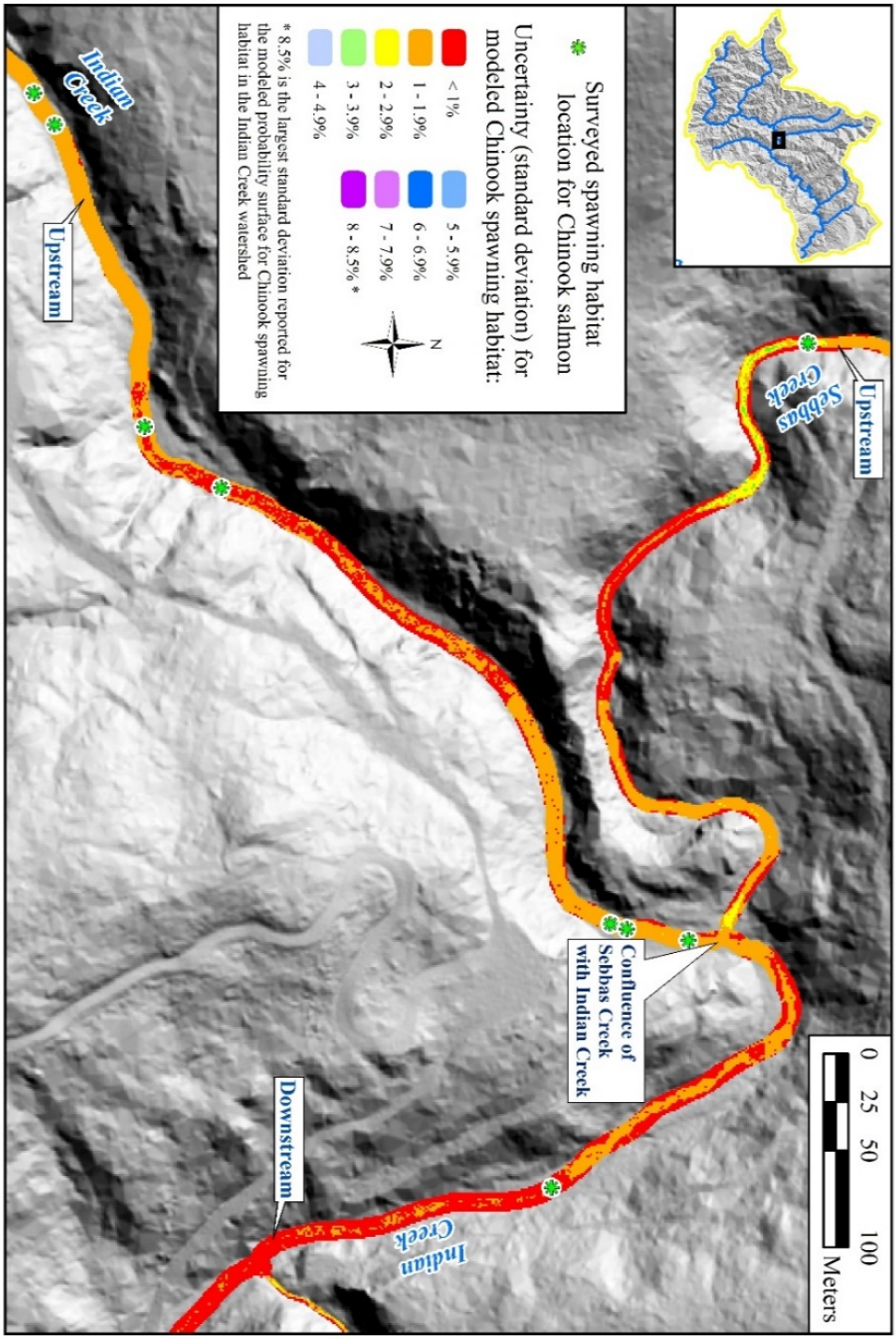

Figure 31. Selected area of uncertainty surface (standard deviation) for Chinook salmon habitat model.

Table 2. Summary of geospatially derived spawning habitat probabilities, by total area, for Chinook salmon for all streams in the geospatially modeled Indian Creek stream system.

Probability of spawning habitat: Chinook	Percentage of total modeled stream system	Area of modeled stream system (m^2)
< 1%	77.66%	1,227,337
1 - 4.9%	4.21%	66,492
5 - 9.9%	3.91%	61,798
10 - 14.9%	2.55%	40,274
15 - 19.9%	1.89%	29,876
20 - 24.9%	1.64%	25,912
25 - 29.9%	1.36%	21,514
30 - 34.9%	1.24%	19,585
35 - 39.9%	0.90%	14,160
40 - 44.9%	0.70%	11,010
45 - 49.9%	0.55%	8,650
50 - 54.9%	0.51%	7,999
55 - 59.9%	0.44%	7,010
60 - 64.9%	0.39%	6,154
65 - 69.9%	0.40%	6,299
70 - 74.9%	0.38%	5,976
75 - 79.9%	0.38%	6,021
80 - 84.9%	0.26%	4,164
85 - 89.9%	0.26%	4,107
90 - 94.9%	0.22%	3,524
95 - 99.87%	0.17%	2,608
Total area (sq. meters):	100%	1,580,470

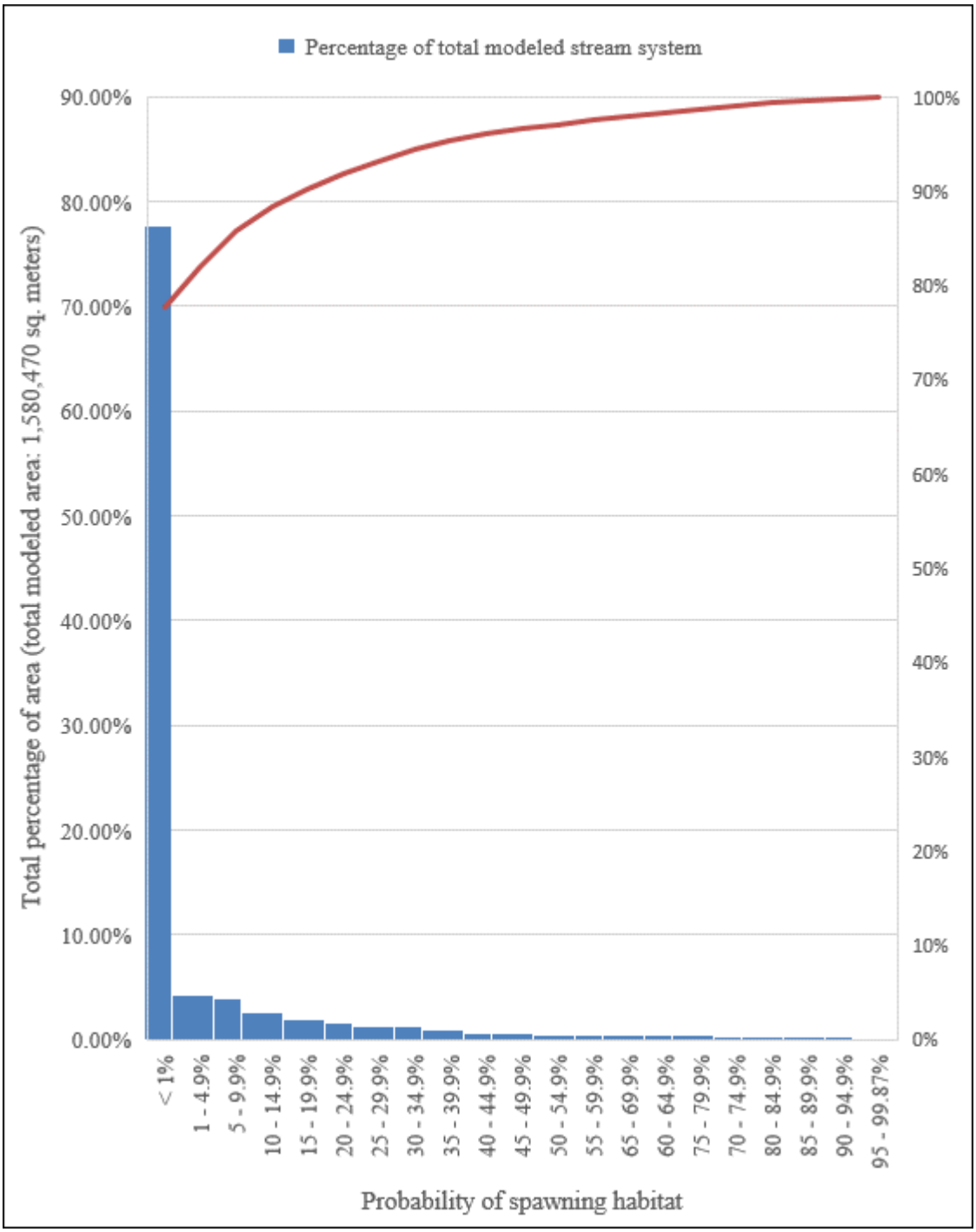

Figure 32 Pareto chart denoting summary of geospatially derived spawning habitat probabilities, by total area, for Chinook salmon for all streams in the geospatially modeled Indian Creek stream system.

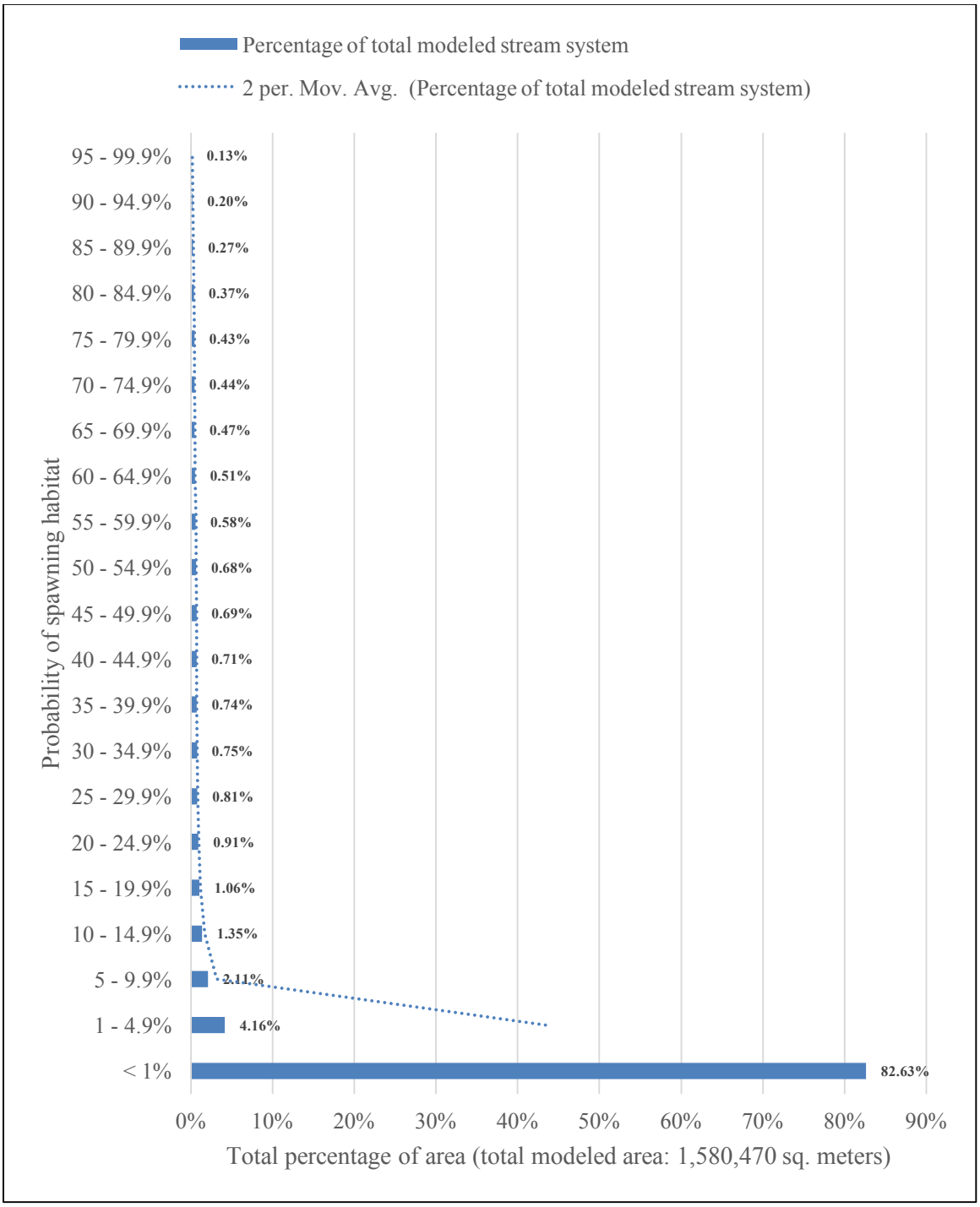

Figure 33. Bar chart denoting summary of geospatially derived spawning habitat probabilities, by total area, for Chinook salmon for all streams in the geospatially modeled Indian Creek stream system.

Table 3. Summary of geospatially derived spawning habitat probabilities, by total area, for Chinook salmon for all streams with predicted bankfull widths >= 1m in width in the geospatially modeled Indian Creek stream system.

Probability of spawning habitat: Chinook	Percentage of total modeled stream system	Area of modeled stream system (m^2)
< 1%	10.00%	38,959
1 - 4.9%	16.53%	64,388
5 - 9.9%	15.80%	61,559
10 - 14.9%	10.33%	40,233
15 - 19.9%	7.66%	29,854
20 - 24.9%	6.65%	25,911
25 - 29.9%	5.52%	21,497
30 - 34.9%	5.02%	19,569
35 - 39.9%	3.63%	14,148
40 - 44.9%	2.82%	10,994
45 - 49.9%	2.22%	8,639
50 - 54.9%	2.05%	7,999
55 - 59.9%	1.80%	7,010
60 - 64.9%	1.58%	6,154
65 - 69.9%	1.62%	6,299
70 - 74.9%	1.53%	5,976
75 - 79.9%	1.55%	6,021
80 - 84.9%	1.07%	4,164
85 - 89.9%	1.05%	4,107
90 - 94.9%	0.90%	3,524
95 - 99.87%	0.67%	2,608
Total area (sq. meters):	100%	389,613

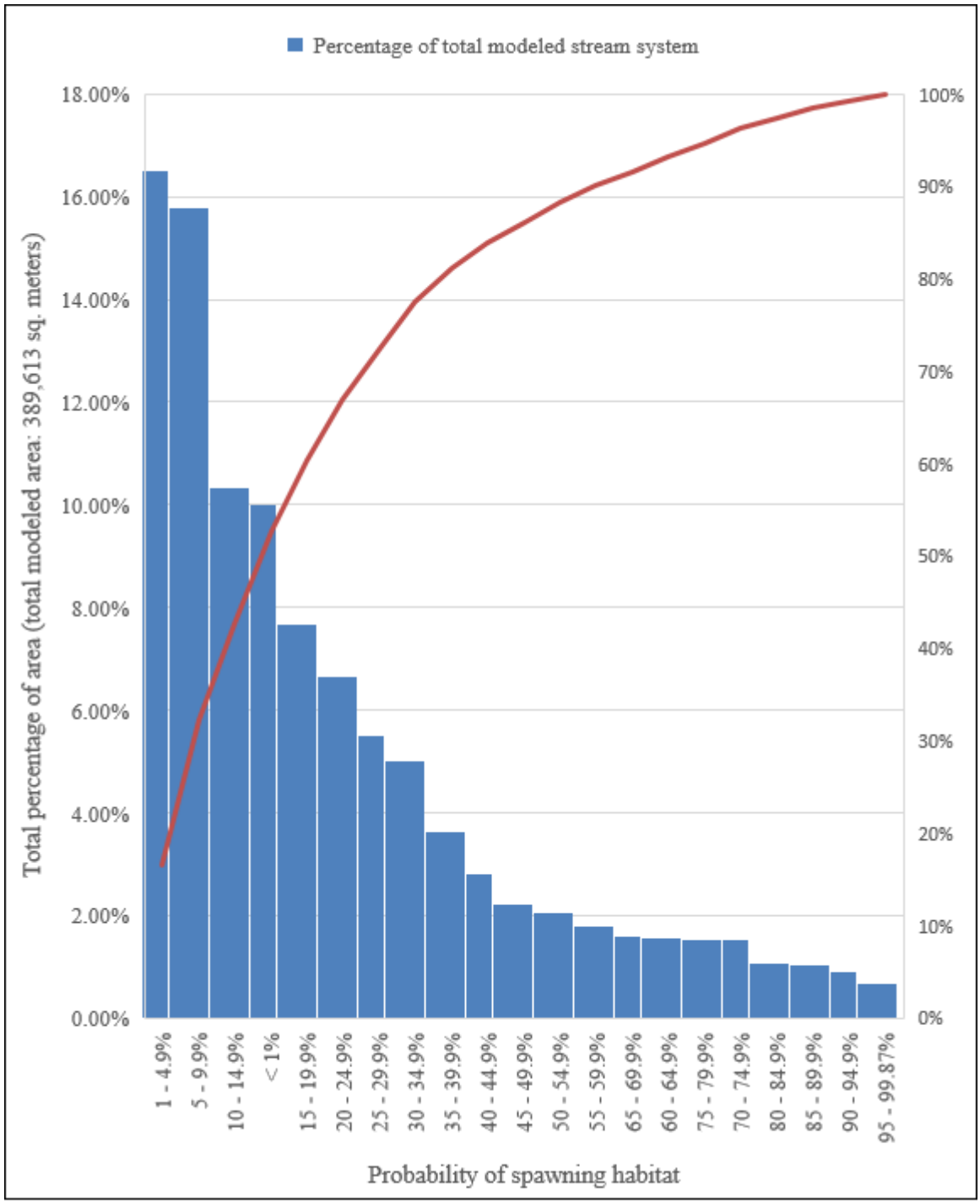

Figure 34. Pareto chart denoting summary of geospatially derived spawning habitat probabilities, by total area, for Chinook salmon for all streams >= 1m bankfull width in the geospatially modeled Indian Creek stream system.

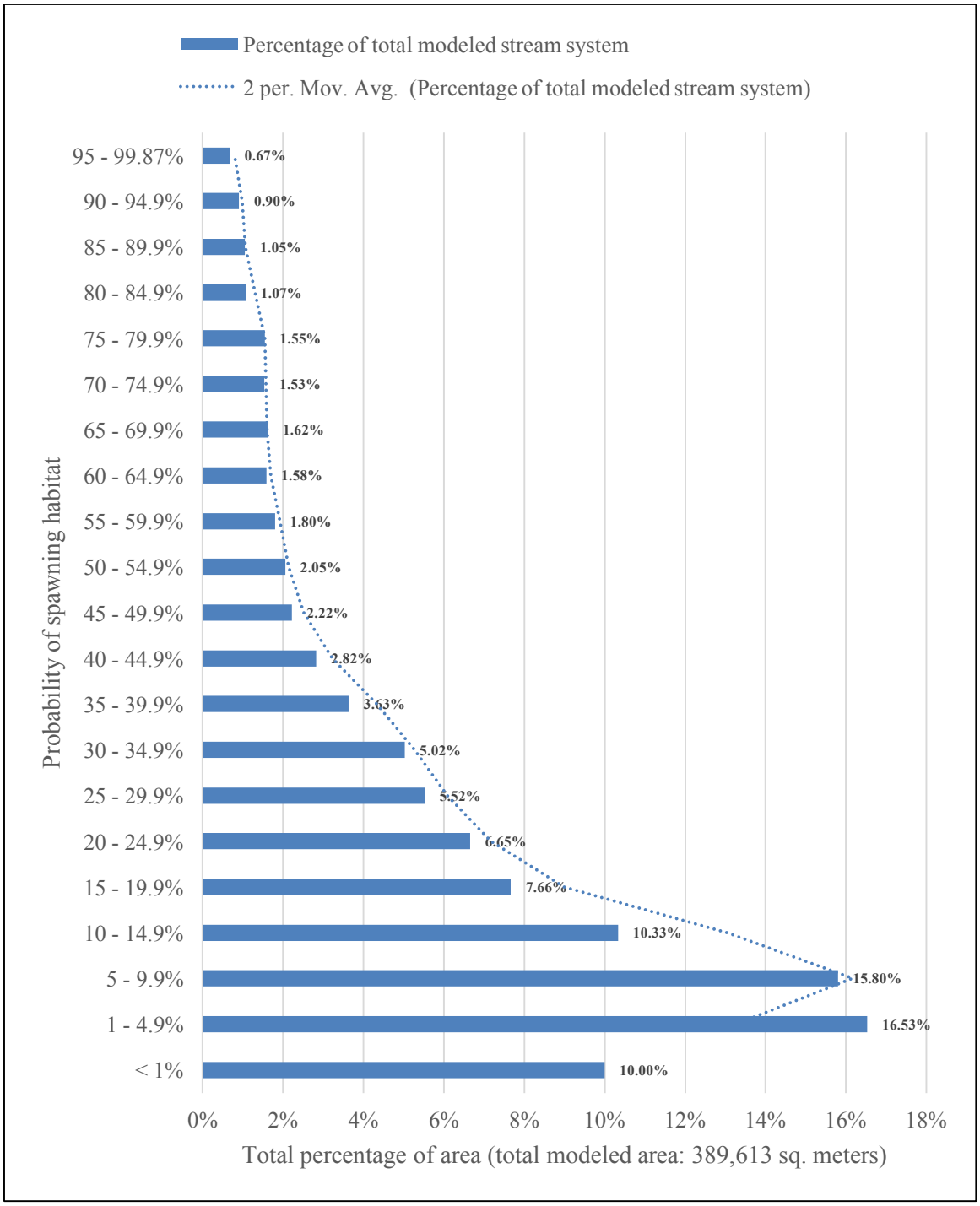

Figure 35. Bar chart denoting summary of geospatially derived spawning habitat probabilities, by total area, for Chinook salmon for all streams >= 1m bankfull width in the geospatially modeled Indian Creek stream system.

Table 4. Summary of geospatially derived spawning habitat probabilities, by total area, for Chinook salmon for all streams with predicted bankfull widths < 1m in width in the geospatially modeled Indian Creek stream system.

Probability of spawning habitat: Chinook	Percentage of total modeled stream system	Area of modeled stream system (m^2)
< 1%	99.7918%	1,188,378
1 - 4.9%	0.1767%	2,104
5 - 9.9%	0.0201%	239
10 - 14.9%	0.0034%	41
15 - 19.9%	0.0018%	22
20 - 24.9%	0.0001%	1
25 - 29.9%	0.0014%	17
30 - 34.9%	0.0013%	16
35 - 39.9%	0.0010%	12
40 - 44.9%	0.0013%	16
45 - 49.9%	0.0009%	11
Total area (sq. meters):	100%	1,190,857

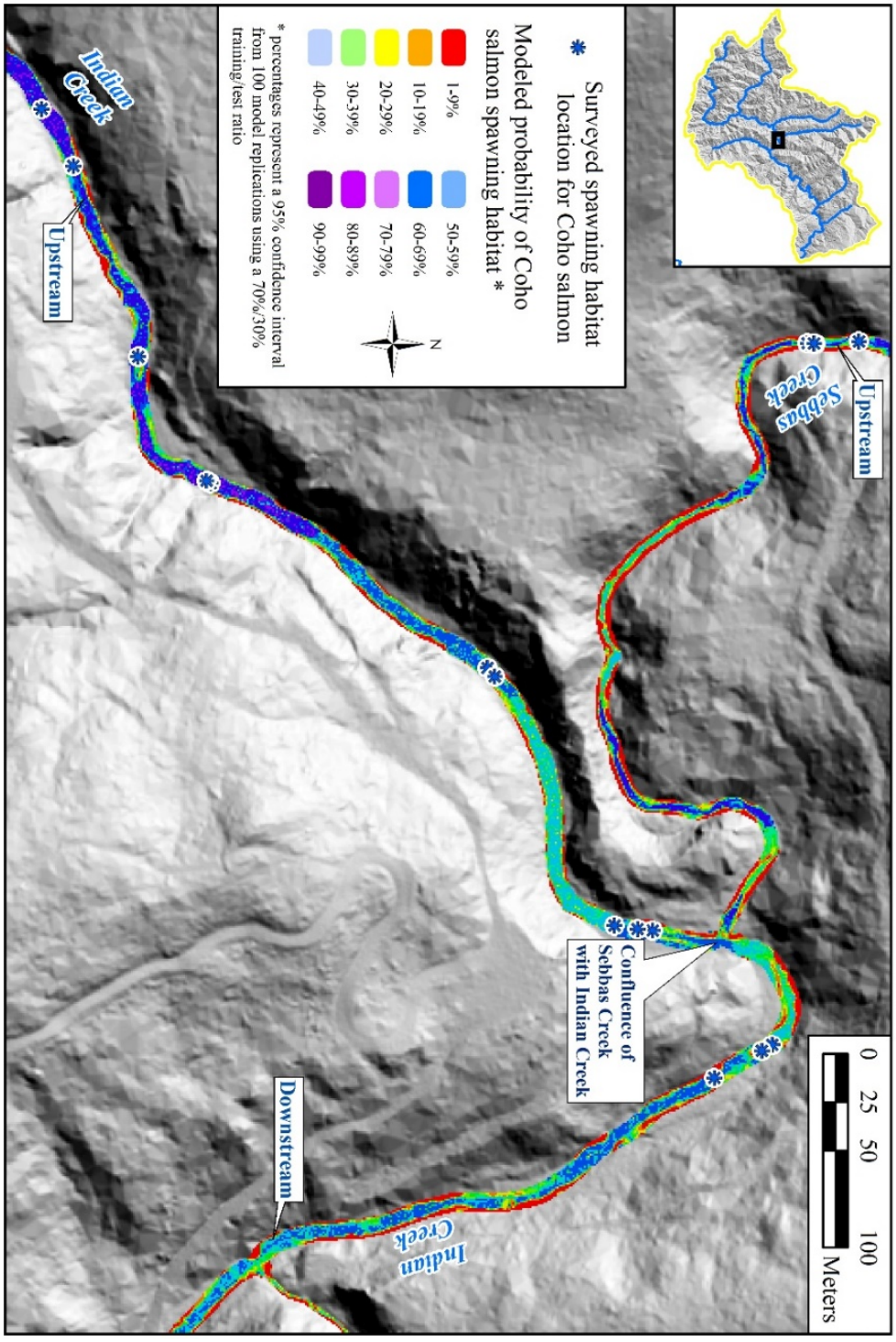

Figure 36. Selected area of probability surface for Coho Salmon spawning habitat developed using MaxEnt. The average test AUC for 100 replicate runs is 0.951, and the standard deviation is 0.034.

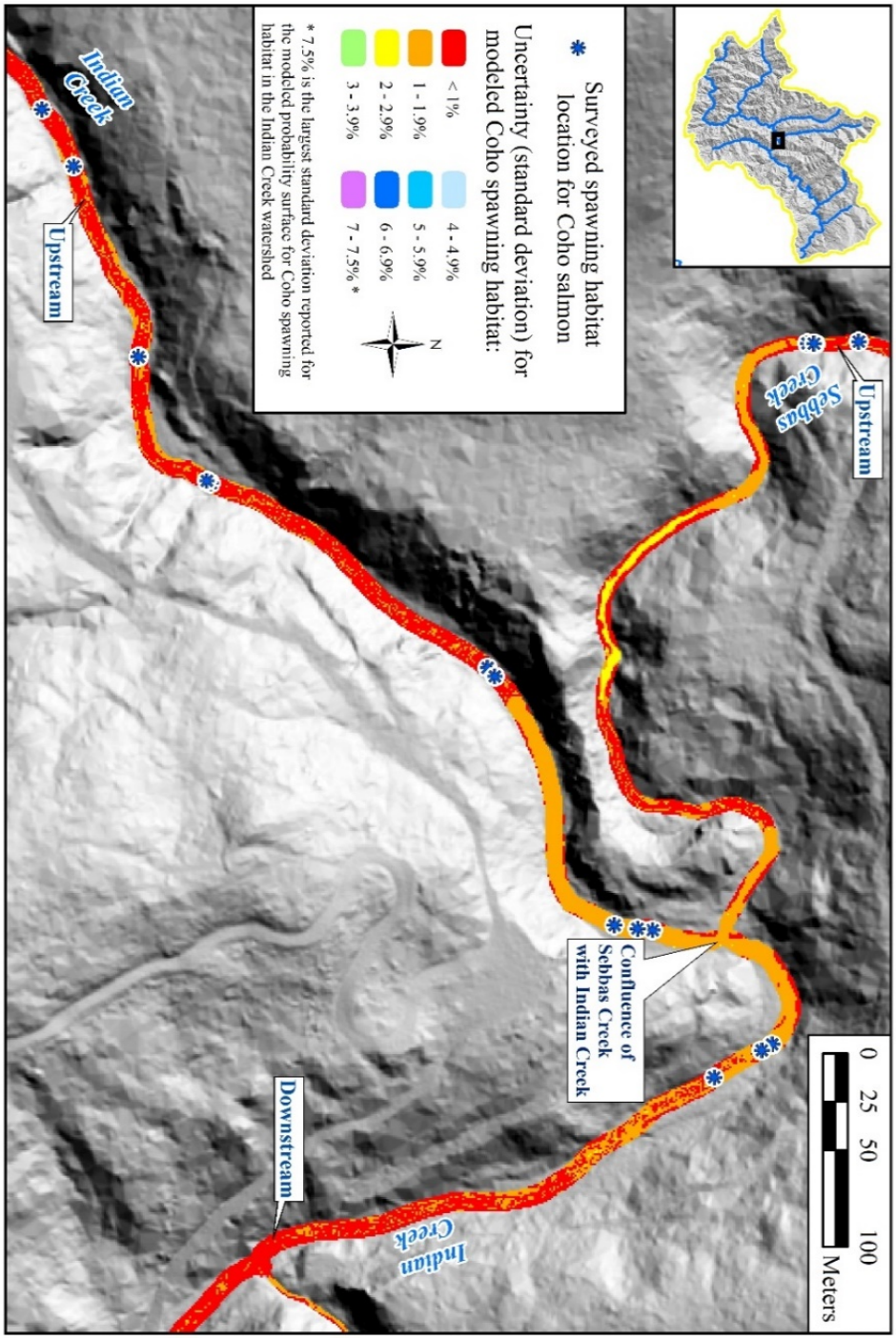

Figure 37. Selected area of uncertainty surface (standard deviation) for Coho Salmon habitat model.

Table 5. Summary of geospatially derived spawning habitat probabilities, by total area, for Coho Salmon for all streams in the geospatially modeled Indian Creek system.

Probability of spawning habitat: Coho	Percentage of total modeled stream system	Area of modeled stream system (m^2)
< 1%	78.01%	1,232,941
1 - 4.9%	3.50%	55,307
5 - 9.9%	2.64%	41,682
10 - 14.9%	2.32%	36,657
15 - 19.9%	2.19%	34,668
20 - 24.9%	1.71%	27,005
25 - 29.9%	1.58%	24,996
30 - 34.9%	1.18%	18,612
35 - 39.9%	0.99%	15,594
40 - 44.9%	0.62%	9,877
45 - 49.9%	0.51%	8,075
50 - 54.9%	0.51%	8,104
55 - 59.9%	0.43%	6,836
60 - 64.9%	0.39%	6,140
65 - 69.9%	0.49%	7,786
70 - 74.9%	0.54%	8,577
75 - 79.9%	0.57%	9,037
80 - 84.9%	0.59%	9,350
85 - 89.9%	0.64%	10,128
90 - 94.9%	0.50%	7,975
95 - 99.9%	0.07%	1,123
Total area (sq. meters):	100.00%	1,580,470

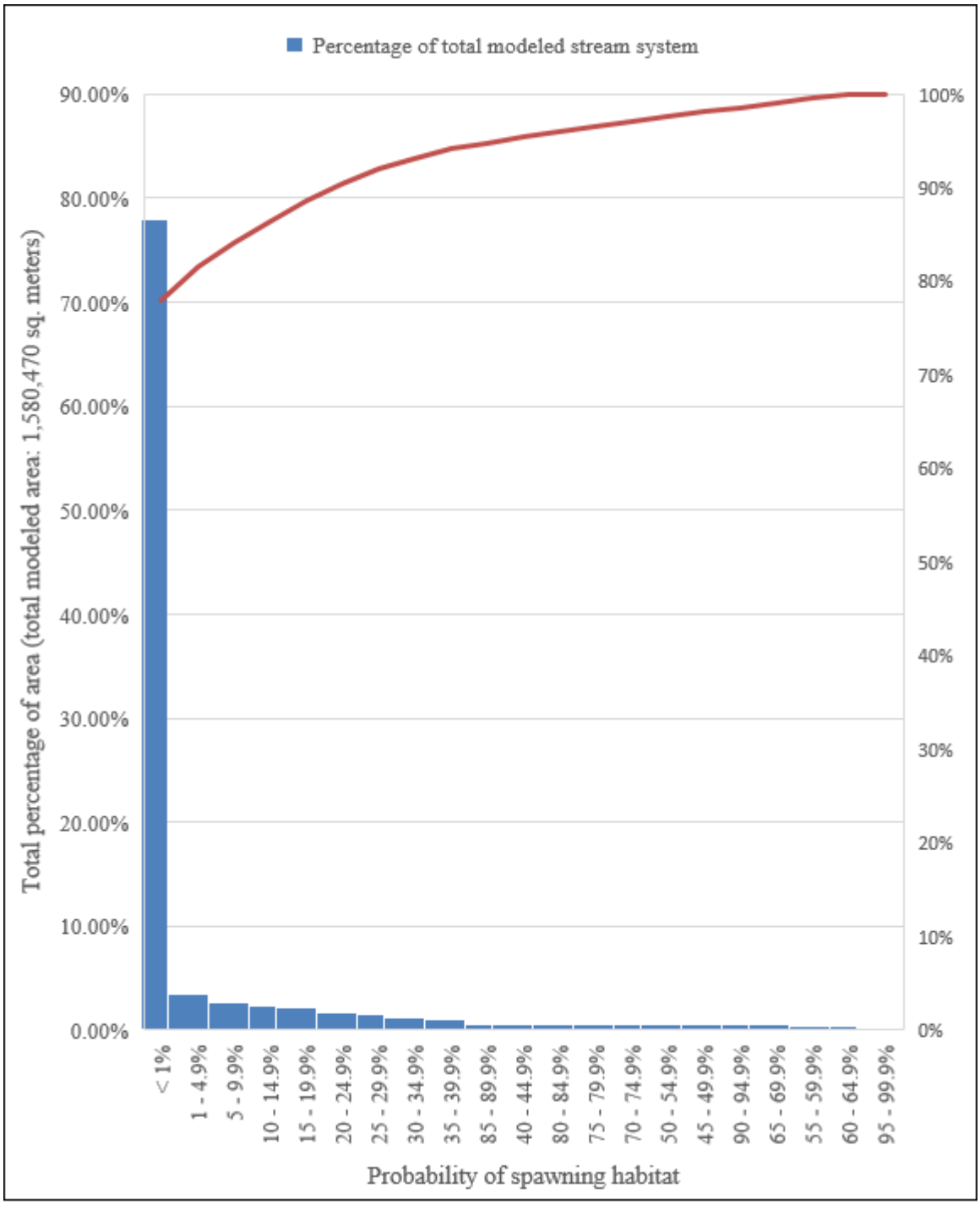

Figure 38. Pareto chart denoting summary of geospatially derived spawning habitat probabilities, by total area, for Coho Salmon for all streams in the geospatially modeled Indian Creek stream system.

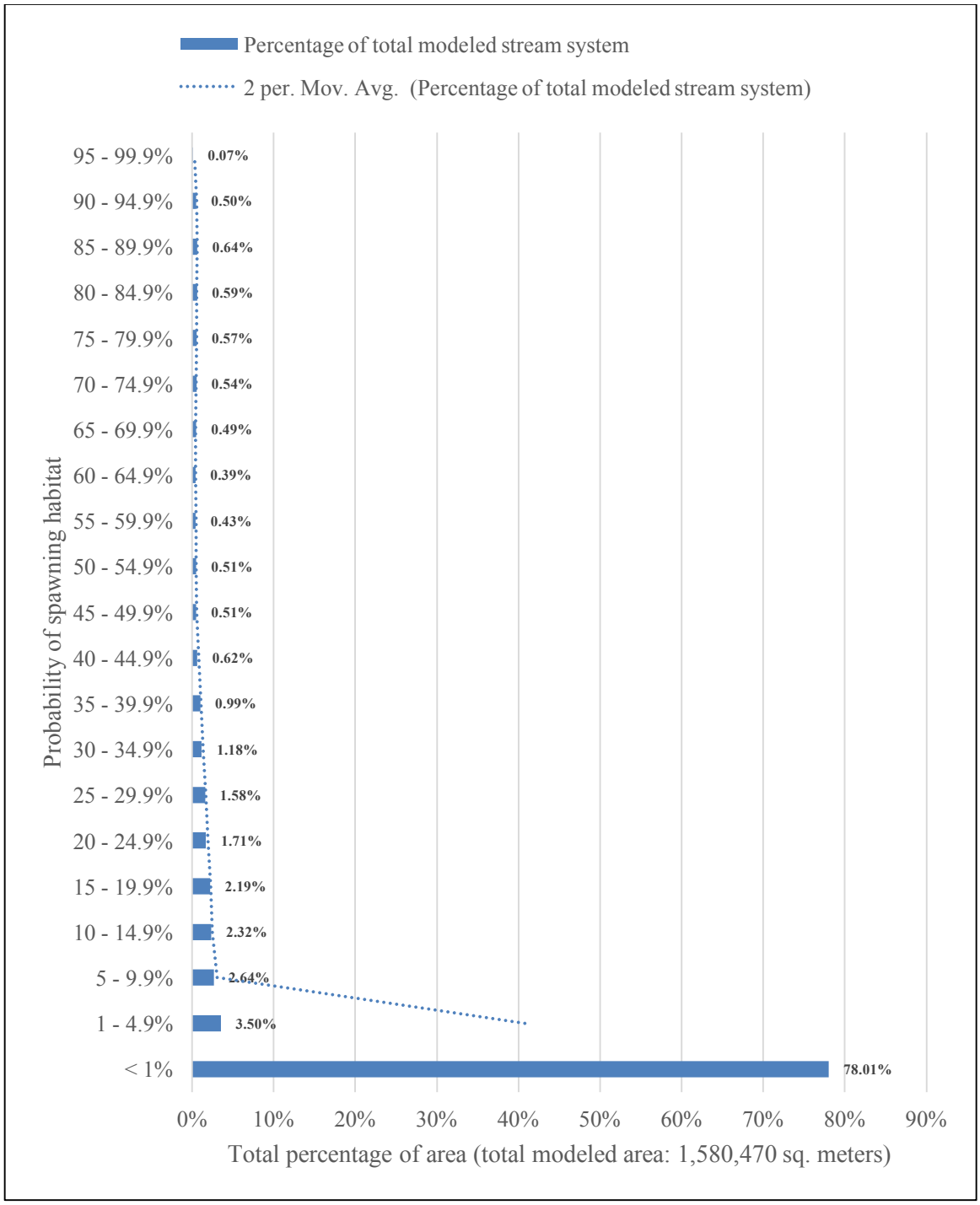

Figure 39. Bar chart denoting summary of geospatially derived spawning habitat probabilities, by total area, for Coho Salmon for all streams in the geospatially modeled Indian Creek stream system.

Table 6. Summary of geospatially derived spawning habitat probabilities, by total area, for Coho Salmon for all streams with predicted bankfull widths >= 1m in width in the geospatially modeled Indian Creek stream system.

Probability of spawning habitat: Coho	Percentage of total modeled stream system	Area of modeled stream system (m^2)
< 1%	11.50%	44,801
1 - 4.9%	13.61%	53,014
5 - 9.9%	10.67%	41,564
10 - 14.9%	9.37%	36,522
15 - 19.9%	8.89%	34,621
20 - 24.9%	6.93%	26,981
25 - 29.9%	6.40%	24,942
30 - 34.9%	4.77%	18,567
35 - 39.9%	4.00%	15,593
40 - 44.9%	2.54%	9,877
45 - 49.9%	2.07%	8,075
50 - 54.9%	2.08%	8,104
55 - 59.9%	1.75%	6,836
60 - 64.9%	1.58%	6,140
65 - 69.9%	2.00%	7,786
70 - 74.9%	2.20%	8,577
75 - 79.9%	2.32%	9,037
80 - 84.9%	2.40%	9,350
85 - 89.9%	2.60%	10,128
90 - 94.9%	2.05%	7,975
95 - 99.9%	0.29%	1,123
Total area (sq. meters):	100.00%	389,613

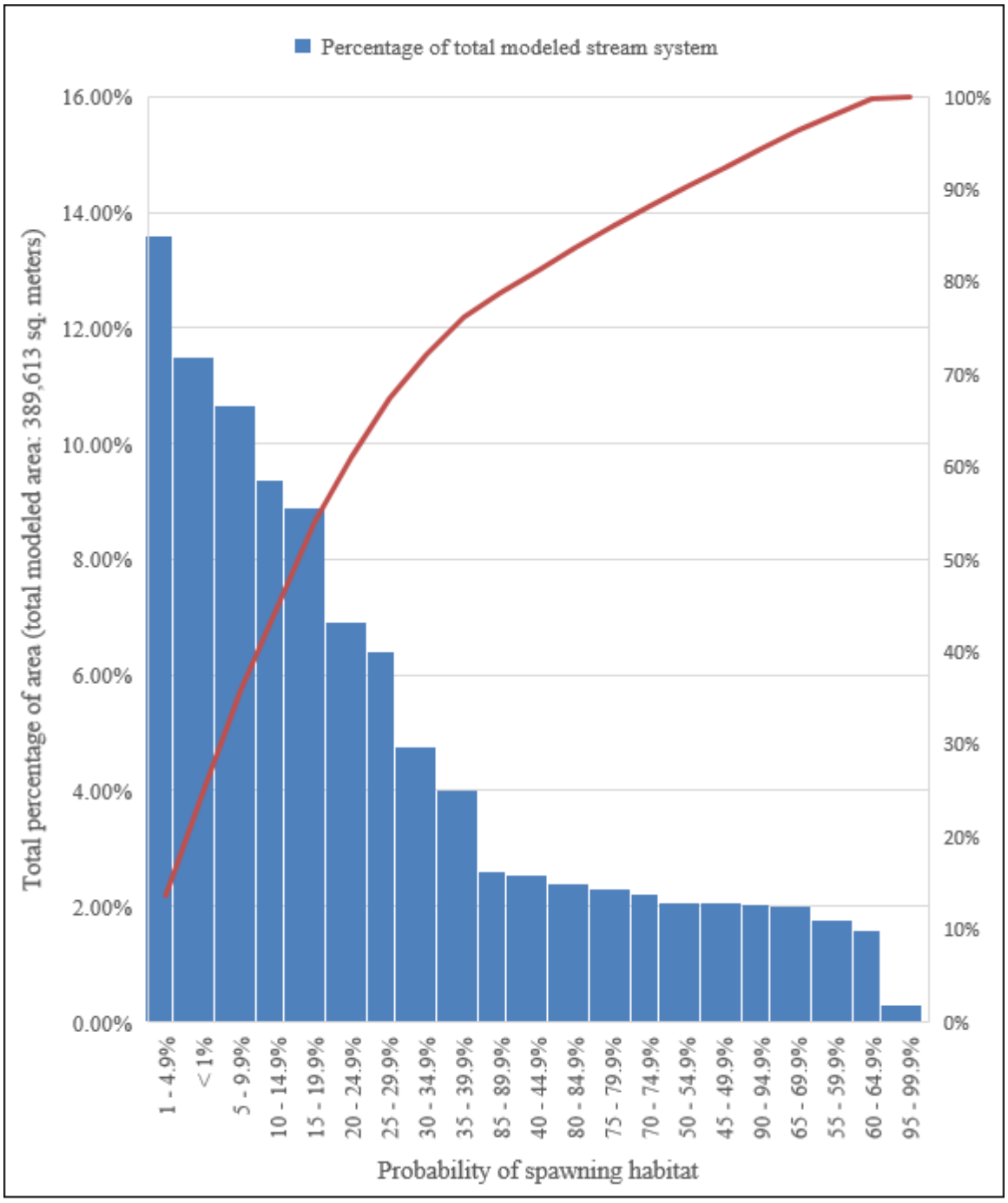

Figure 40. Pareto chart denoting summary of geospatially derived spawning habitat probabilities, by total area, for Coho Salmon for all streams >= 1m bankfull width in the geospatially modeled Indian Creek stream system.

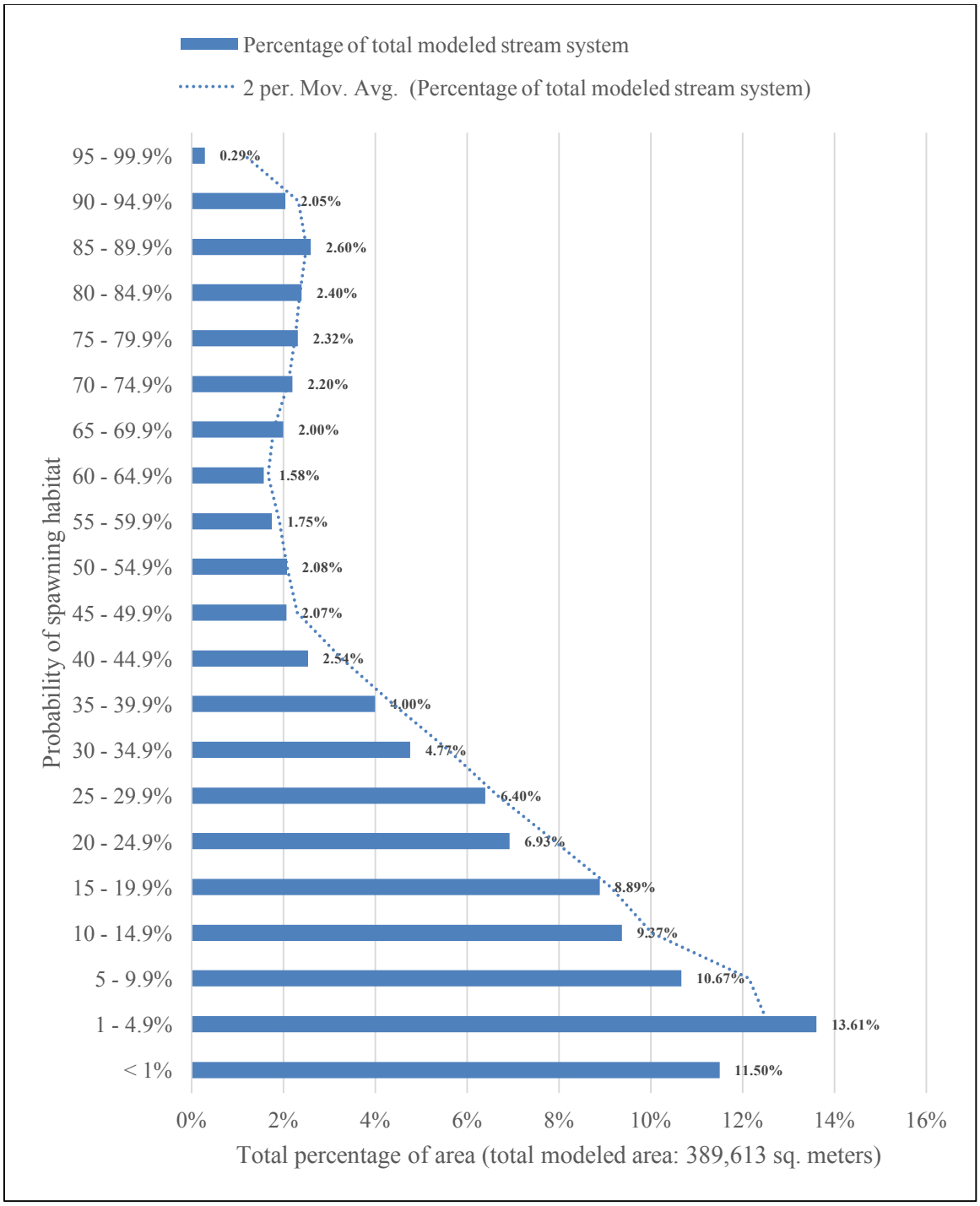

Figure 41. Bar chart denoting summary of geospatially derived spawning habitat probabilities, by total area, for Coho Salmon for all streams >= 1m bankfull width in the geospatially modeled Indian Creek stream system.

Table 7. Summary of geospatially derived spawning habitat probabilities, by total area, for Coho Salmon for all streams with predicted bankfull widths < 1m in width in the geospatially modeled Indian Creek stream system.

Probability of spawning habitat: Coho	Percentage of total modeled stream system	Area of modeled stream system (m^2)
< 1%	99.7718%	1,188,140
1 - 4.9%	0.1926%	2,293
5 - 9.9%	0.0099%	118
10 - 14.9%	0.0113%	135
15 - 19.9%	0.0039%	47
20 - 24.9%	0.0020%	24
25 - 29.9%	0.0045%	54
30 - 34.9%	0.0038%	45
35 - 39.9%	0.0001%	1
Total area (sq. meters):	100.00%	1,190,857

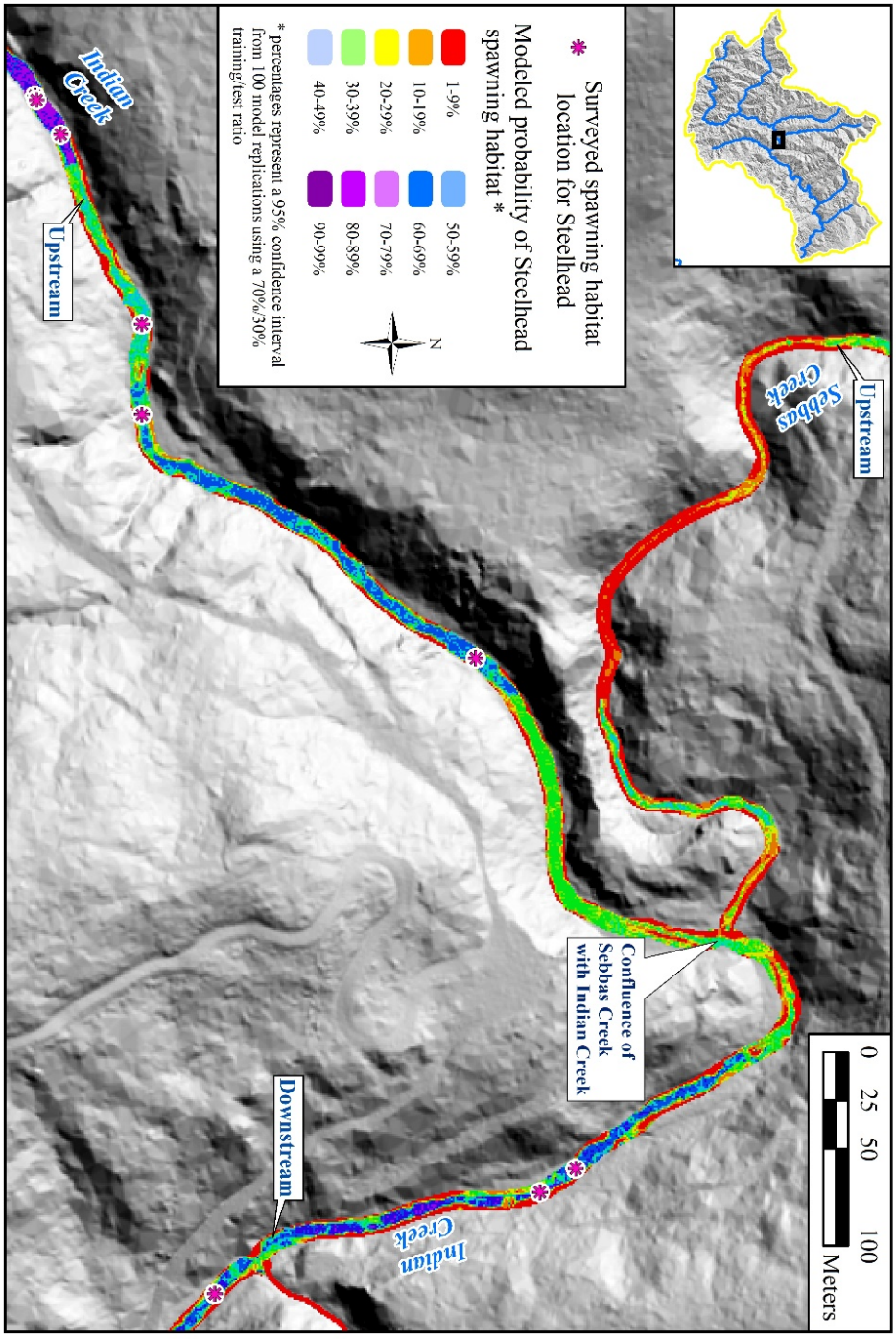

Figure 42. Selected area of probability surface for Steelhead spawning habitat developed using MaxEnt. The average test AUC for 100 replicate runs is 0.958, and the standard deviation is 0.036.

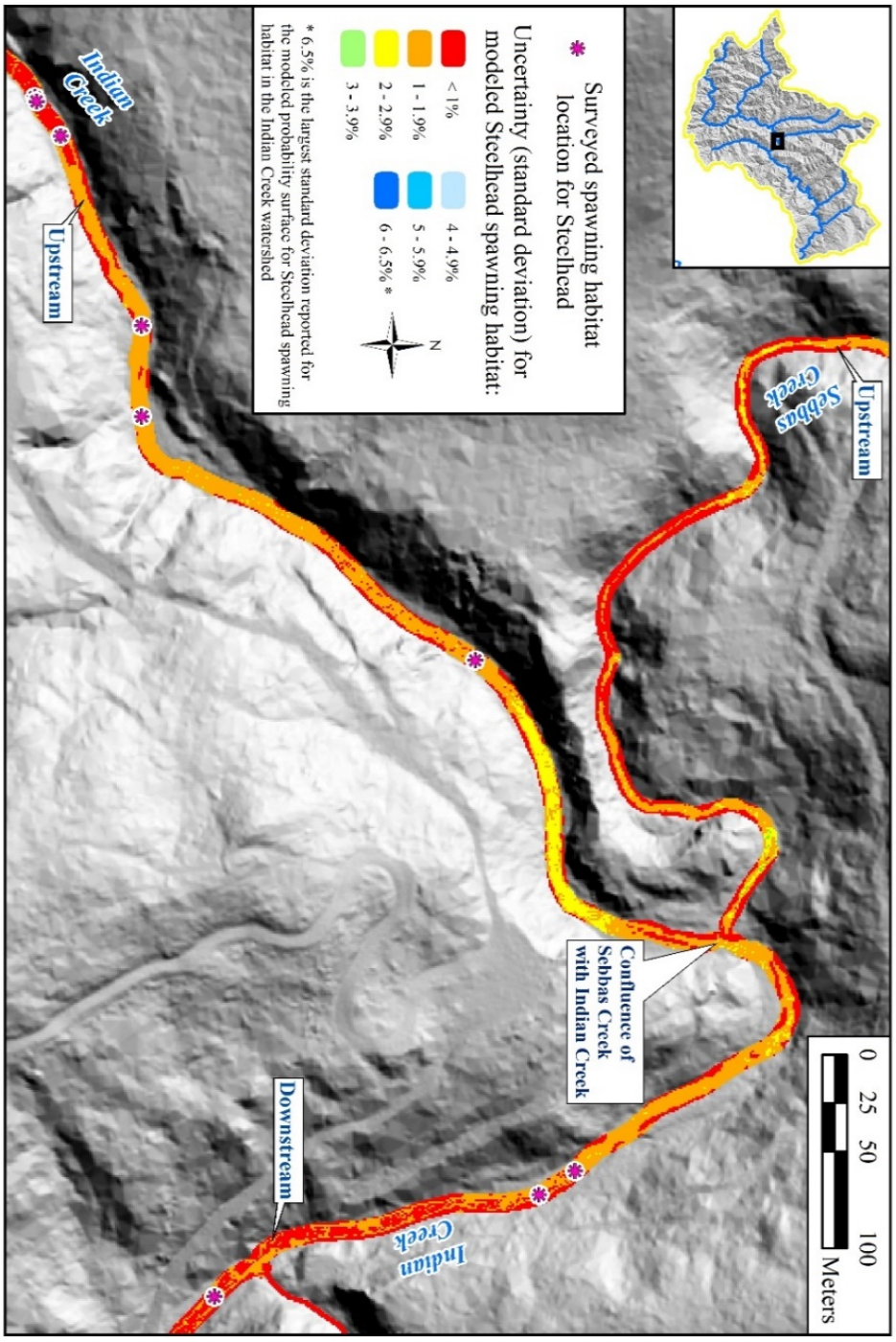

Figure 43. Selected area of uncertainty surface (standard deviation) for Steelhead habitat model.

Table 8. Summary of geospatially derived spawning habitat probabilities, by total area, for Steelhead for all streams in the geospatially modeled Indian Creek stream system.

Probability of spawning habitat: Steelhead	Percentage of total modeled stream system	Area of modeled stream system (m^2)
< 1%	82.63%	1,305,940
1 - 4.9%	4.16%	65,784
5 - 9.9%	2.11%	33,325
10 - 14.9%	1.35%	21,403
15 - 19.9%	1.06%	16,719
20 - 24.9%	0.91%	14,329
25 - 29.9%	0.81%	12,817
30 - 34.9%	0.75%	11,887
35 - 39.9%	0.74%	11,643
40 - 44.9%	0.71%	11,181
45 - 49.9%	0.69%	10,921
50 - 54.9%	0.68%	10,671
55 - 59.9%	0.58%	9,216
60 - 64.9%	0.51%	8,138
65 - 69.9%	0.47%	7,431
70 - 74.9%	0.44%	6,946
75 - 79.9%	0.43%	6,754
80 - 84.9%	0.37%	5,884
85 - 89.9%	0.27%	4,331
90 - 94.9%	0.20%	3,094
95 - 99.9%	0.13%	2,056
Total area (sq. meters):	100.00%	1,580,470

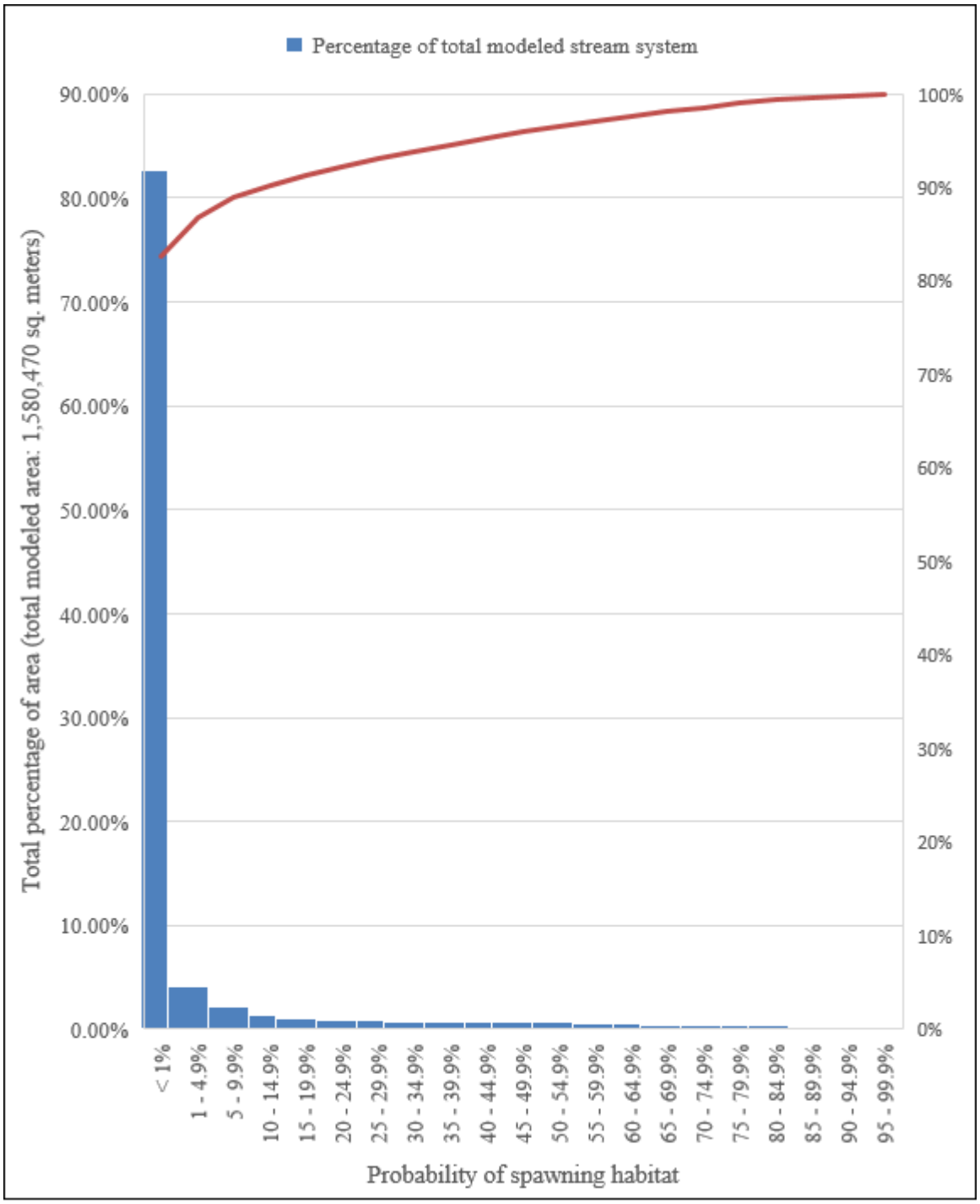

Figure 44. Pareto chart denoting summary of geospatially derived spawning habitat probabilities, by total area, for Steelhead for all streams in the geospatially modeled Indian Creek stream system.

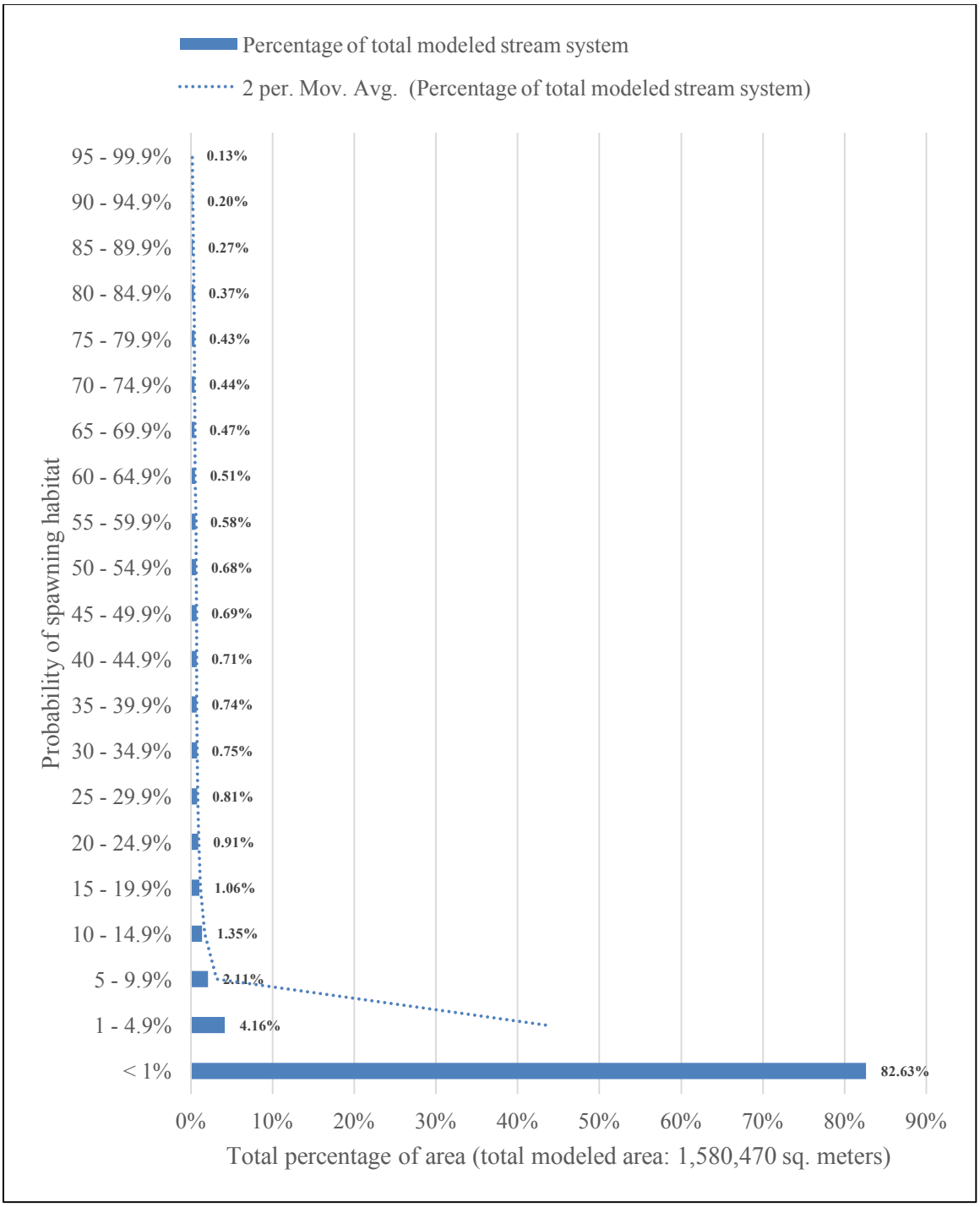

Figure 45. Bar chart denoting summary of geospatially derived spawning habitat probabilities, by total area, for Steelhead for all streams in the geospatially modeled Indian Creek stream system.

Table 9. Summary of geospatially derived spawning habitat probabilities, by total area, for Steelhead for all streams with predicted bankfull widths >= 1m in width in the geospatially modeled Indian Creek stream system.

Probability of spawning habitat: Steelhead	Percentage of total modeled stream system	Area of modeled stream system (m^2)
< 1%	29.91%	116,521
1 - 4.9%	16.53%	64,389
5 - 9.9%	8.54%	33,282
10 - 14.9%	5.49%	21,403
15 - 19.9%	4.29%	16,719
20 - 24.9%	3.68%	14,329
25 - 29.9%	3.29%	12,817
30 - 34.9%	3.05%	11,887
35 - 39.9%	2.99%	11,643
40 - 44.9%	2.87%	11,181
45 - 49.9%	2.80%	10,921
50 - 54.9%	2.74%	10,671
55 - 59.9%	2.37%	9,216
60 - 64.9%	2.09%	8,138
65 - 69.9%	1.91%	7,431
70 - 74.9%	1.78%	6,946
75 - 79.9%	1.73%	6,754
80 - 84.9%	1.51%	5,884
85 - 89.9%	1.11%	4,331
90 - 94.9%	0.79%	3,094
95 - 99.9%	0.53%	2,056
Total area (sq. meters):	100.00%	389,613

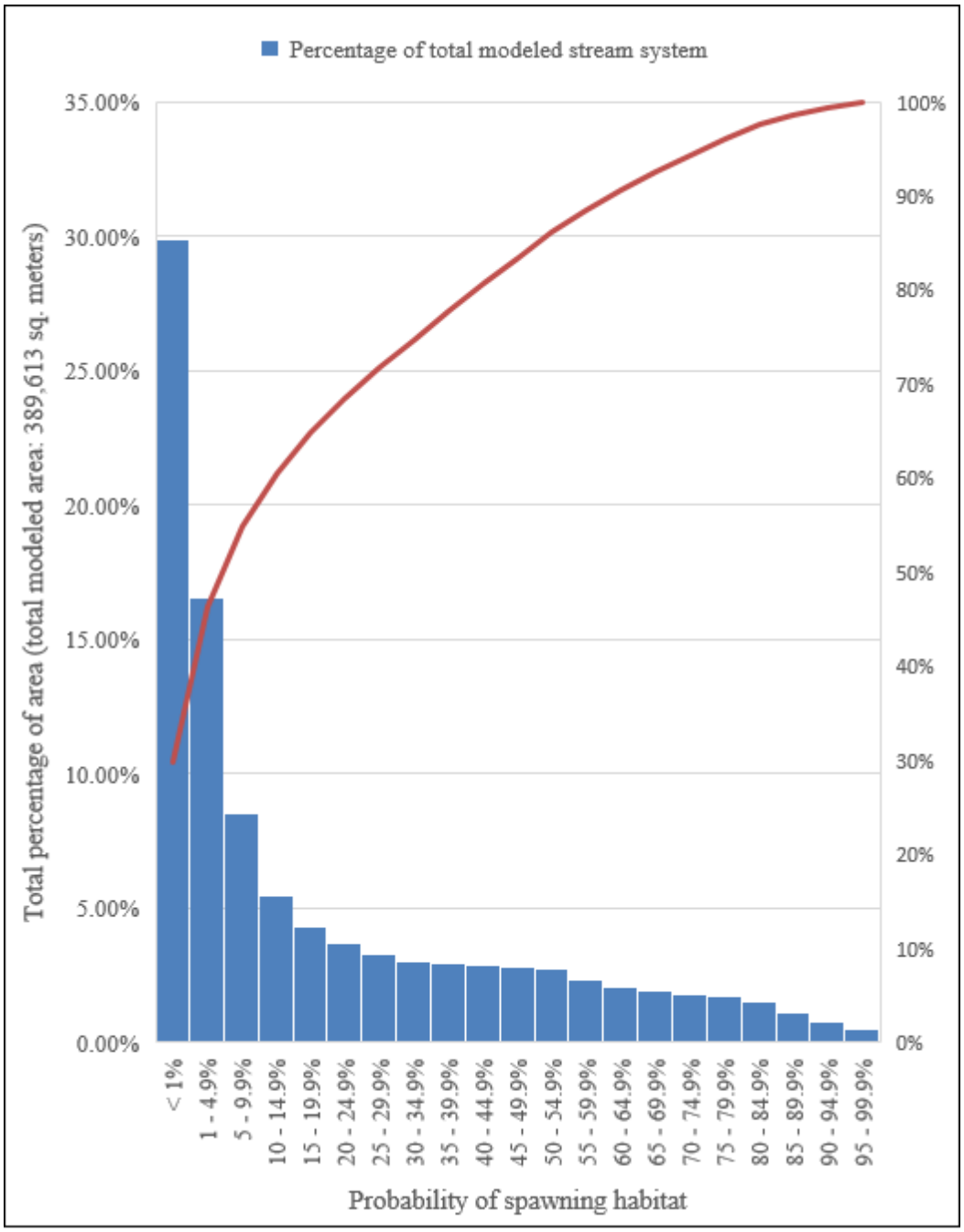

Figure 46. Pareto chart denoting summary of geospatially derived spawning habitat probabilities, by total area, for Steelhead for all streams >= 1m bankfull width in the geospatially modeled Indian Creek stream system.

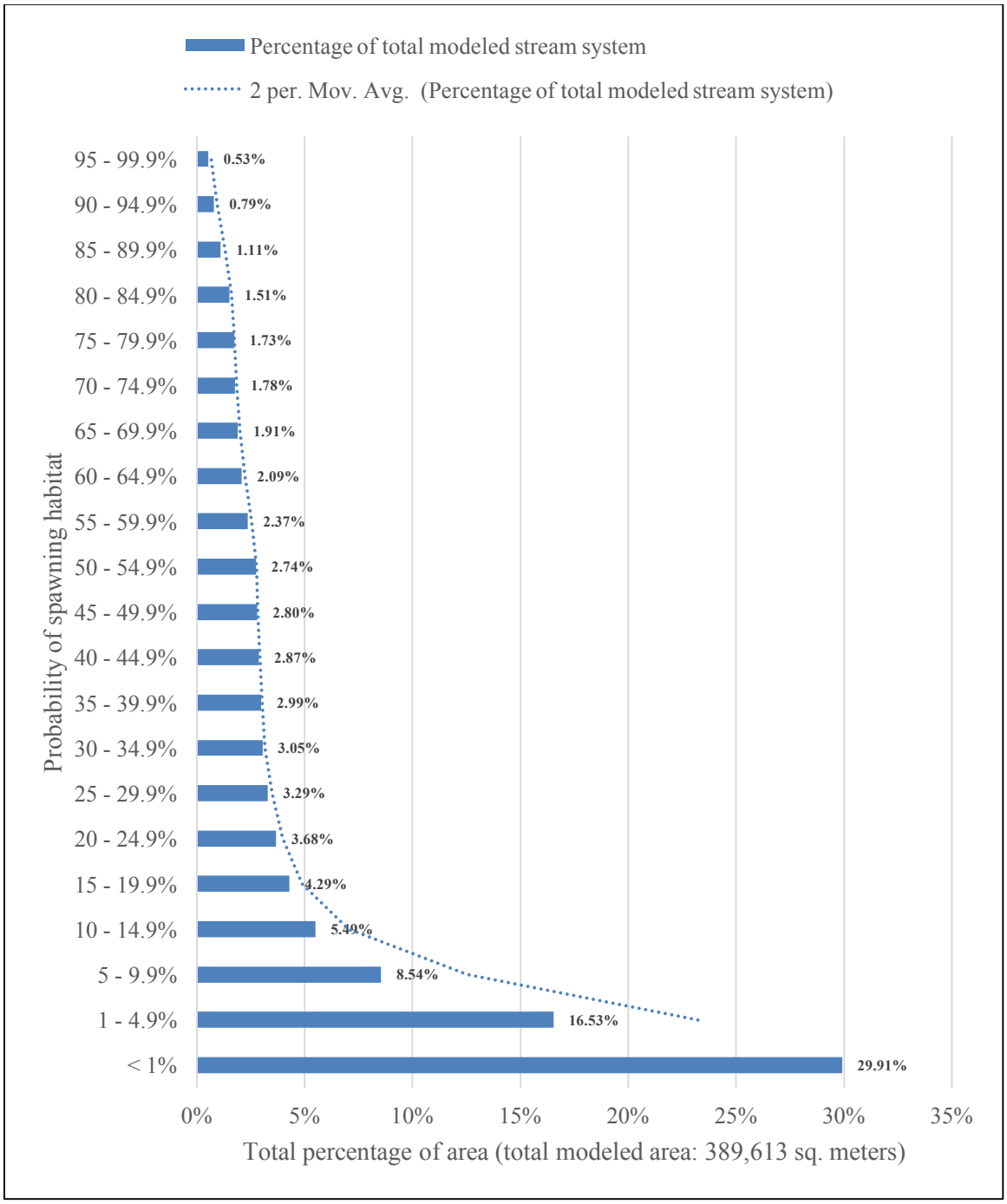

Figure 47. Bar chart denoting summary of geospatially derived spawning habitat probabilities, by total area, for Coho Salmon for all streams in the geospatially modeled Indian Creek stream system.

Table 10. Summary of geospatially derived spawning habitat probabilities, by total area, for Steelhead for all streams with predicted bankfull widths < 1m in width in the geospatially modeled Indian Creek stream system.

Probability of spawning habitat: Steelhead	Percentage of total modeled stream system	Area of modeled stream system (m^2)
< 1%	99.8792%	1,189,419
1 - 4.9%	0.1171%	1,395
5 - 9.9%	0.0036%	43
Total area (sq. meters):	100.00%	1,190,857

4. DISCUSSION

4.1. Development of the Numerically Interpolated Flow Track Inferencing (NIFTI) toolset

In order to develop a prediction for anadromous salmonid species spawning habitat in the Indian Creek watershed that comprised not only linear stream lengths, but also stream area, it was necessary to first develop a rasterized surface that defined as best possible the areal extent of that stream system. To this purpose, the 1m DEM data and geomorphic data unique to the Indian Creek watershed were utilized to develop a toolset that, given inputs of bankfull widths, high resolution DEM data, and a contributing area threshold for stream inception, can output a continuous surface representing a predicted bankfull stream corridor network for the extent of that DEM data. The corridor does not represent a simplistic width prediction, but rather a geospatial reconstruction of the morphology of the stream, taking into account local micro-scale variations in slope, channel constraint, and sinuosity. Successfully tested and field-verified for accuracy in the Indian Creek watershed, this toolset can, in theory, be applied to other watershed where those same inputs exist. Current calibration when using the NIFTI toolset has successfully yielded accurate surfaces for neighboring watersheds which share the same geologic, biogeographic, and historical land usage as Indian Creek. Additional development of the toolset includes automation of the toolset utilizing componentry of ESRI ArcMap Model Builder, R-ArcGIS Bridge, Spatial Analyst, and Python. Given

inputs of bankfull depths or flood-prone widths at specific locations, NIFTI can also output predictive watershed-wide surfaces for those variables as well. Cross sectional data used for hydrologic and hydraulic modeling can easily be extracted using current outputs, and further development will automate this process. There are numerous potential applications where the NIFTI toolset can be used by state and private agencies for natural resources management, health and human safety, environmental restoration, etc.

4.2 Uncertainty and limitations for the NIFTI toolset

The reliability of a geospatial surface derived using NIFTI is greatly increased with the use of high-resolution DEM data and the frequency and reliability of stream morphological inputs within the watershed being modeled. The statistical models used for the NIFTI analysis of data inputs rely upon the strengths of the inputs. In the case of the Indian Creek watershed NIFTI analysis, inputs came from the 427 in-stream surveys throughout the Indian Creek and neighboring watersheds (Figure 45).

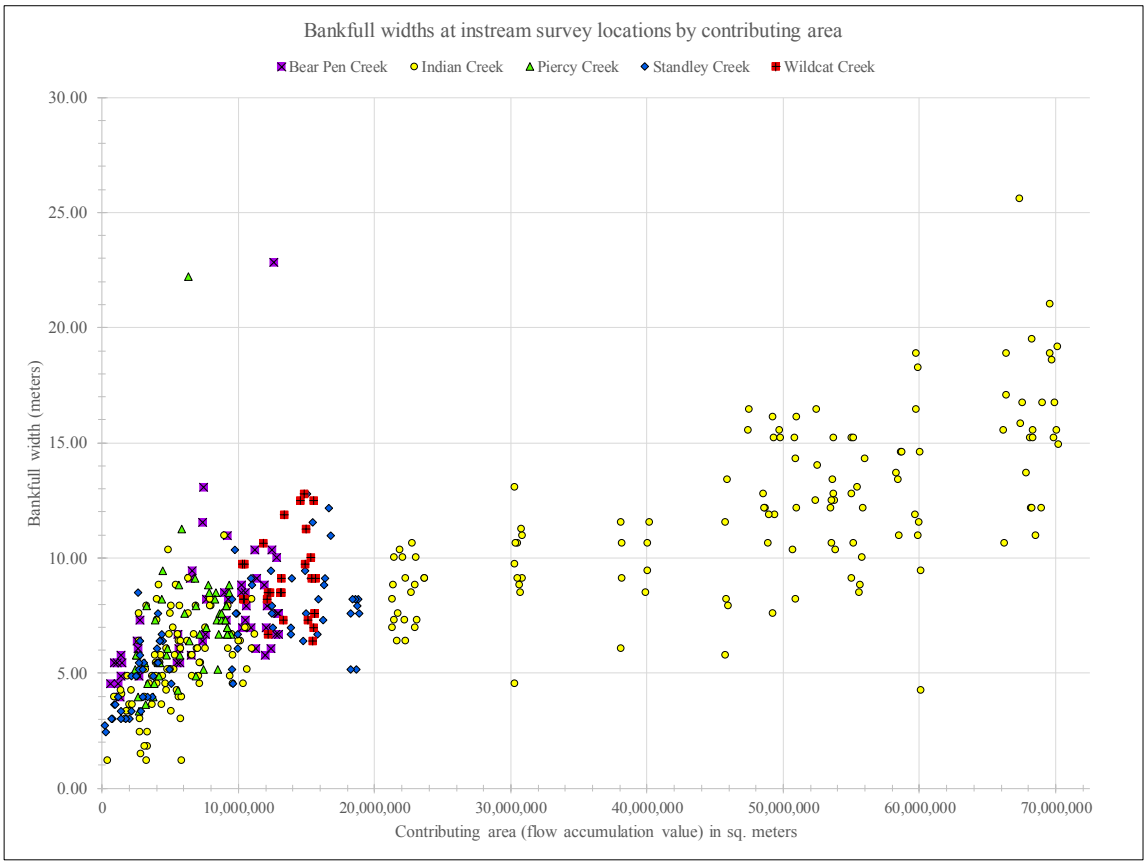

Figure 48. Bivariate scatterplot showing relative locations of in-stream surveys (by proxy of contributing areas) and the bankfull widths at those locations in the Indian Creek and neighboring watersheds.

As can be seen in Figure 48, the majority of the in-stream survey data is spatially located in the surveyed watersheds at areas of relatively low contributing areas, whereas the Indian Creek watershed has surveys in areas in streams that have much larger contributing areas. This is corroborated by Figure 8. Thus, the NIFTI-derived surfaces using this dataset have a relatively higher degree of certainty in areas that have relatively low flow accumulation values. This has a coincidental, yet ancillary, benefit for this specific analysis, as those same areas tend to have higher incidences for presences of

spawning habitat. Thus, in areas where there is potentially a high degree of spatial interest, there is also a higher degree of reliability for rasters derived using the NIFTI-constructed stream surface.

An additional source of uncertainty emanates from lumping geomorphic data from neighboring watersheds. It was assumed that since neighboring watersheds underwent the same land management practices (and thus have similar biogeography) and similar geology (the entire area is defined as Coastal Franciscan) and similar climate, the morphological responses of streams in these watersheds would be similar to that of Indian Creek. During NIFTI stream morphology model development, it was found that there were no significant statistical differences between predictive models for Indian Creek and its neighbors. However, if there are unforeseen confounding factors then corrective steps would need to be taken.

Stream corridors geospatially constructed using NIFTI are unreliable when the predicted widths of those streams are less than the resolution of the DEM data. Furthermore, it was found that in areas with high degrees of localized micro-scale anthropogenic disturbance, such as in direct proximity to stream crossings or stream diversions via inboard ditches, predicted corridors became subject to a higher degree of anthropogenic “noise” and displayed artificial sinuosity. However, it was found during field reconnaissance that the majority of anthropogenic effects on the NIFTI datasets derived for the Indian Creek watershed occurred in locations where the predicted stream corridors had bankfull widths predicted to be less than 1m. This subset of the predicted spawning habitat data was extracted for other reasons (see 4.4).

4.3 Habitat suitability modeling

Based on field verification and interpretation, the modeled spawning habitat surfaces derived from MaxEnt accurately represent the situation on the ground. As can be seen in Photo Points 1-40 (Appendix F), higher modeled probabilities of spawning habitat generally occur in areas of the stream system where habitat occurs naturally. Areas of water availability (by proxy of contributing area / FAC), low gradient, unconstrained channels, and higher incidence of gravels, all denote higher probability of spawning habitat. As can be seen in the included photo points, extreme right and left banks, particularly in constrained stream channels, still lie both within the surveyed and predicted stream corridors yet show a marked decrease in habitat probability (Photo Points 6, 10, 11, 20, 26, 36, 37, and 39). This indicates that the habitat model is showing sensitivity to the higher slopes on those channel banks and denotes a lower probability in those outlying areas. Photo Points 6, 20, 26, and 39 show areas of the stream channel with highly constrained channel morphology which, though modeled accurately for bankfull width, still yield a surface with very low habitat probabilities due to high slopes on both the left and right banks. Conversely, in those same channels, the stream centers can display previously noted favorable characteristics and increased habitat suitability.

Photo Points 5a and 5b show a detailed view of a bedrock cascade directly east of the confluence of Anderson Creek with the mainstem of Indian Creek. As shown in the spawning habitat probability maps, there is a marked decrease in the area of the cascade, with higher probabilities outside the cascade zone. This could indicate another

immediately, easily interpretable visualization and confirmation of the accuracy of the modeling process. Similarly, Photo Point 8 shows another cascade, with a correspondingly sharp decrease in spawning habitat probability at that location due to slope. Photo Points 36, 37, 38, and 40 show streams that are still heavily influenced by historic anthropogenic disturbance, as the stream bed at these locations underwent radical morphological change due to poor watershed management practices - including clear-cutting timber extraction - and represent areas that are still in a recovery process. The historical railroad tracks that can be seen in Photo Points 27 and 29 give insight as to the landscape morphology of a century ago. In many cases, the stream bed and surrounding channel sides were forcibly altered as a standard land-use practice.

Areal statistics from the spawning habitat probability surfaces have been presented three ways: globally, for streams predicted to be greater than or equal to 1m bankfull width, and for streams predicted to be less than 1m bankfull width. This was done for two reasons: 1.) It was found during the NIFTI modeling calibration that streams with width predictions less than the resolution of the DEM inputs would yield potentially erroneous results for predicted stream corridor morphology, and 2.) After the modeling process in MaxEnt was performed, it was found that streams predicted to be less than 1m bankfull width displayed less than 1% probability for habitat, which was confirmed during field verification by the author, Thomas Leroy, and CDFW fish biologist Seth Ricker.

During analysis, before incorporation of raster covariates into MaxEnt, a decision was made to minimize the impact of erroneous stream morphology constructed in areas

of highest uncertainty (i.e. areas where streams were predicted to be less than 1m bankfull width) by utilizing the thalweg network as stream centerlines rather than NIFTI-derived surfaces. As seen in Figure 11a and 12a-f, the final raster covariates serving as inputs to MaxEnt had continuous surfaces where the stream networks were derived from 1.) NIFTI-derived stream morphology for streams greater than or equal to the resolution of the DEM and 2.) Streams as predicted by simple linear threshold response to contributing area for streams less than 1m predicted bankfull width, until there occurred an intersection between surfaces, at which point NIFTI-derived surfaces took precedence. The intention was to produce raster covariates which could be utilized to derive a probability surface from MaxEnt while minimizing potential for uncertainty, anthropogenic or otherwise.

Thus, to better and more effectively communicate modeling results on streams where there was both a reasonably high degree of real-world confidence for habitat to actually exist as well as highly reliable results for probability of spawning habitat in those areas, metrics were derived and partitioned out as shown in Figures 27-44, and Tables 2-10. This can also be seen as presented in Photo Points 22, 30, 32, and 35. These areas served as excellent calibration points for additional model interpretation.

Jackknifing during spawning habitat model development (Appendices C, D, E) revealed that, in each case, contributing area (FAC), degree slope, and distance from the confluence of Indian Creek with the South Fork Eel River were the top three contributing variables. Contributing area (FAC) can be seen as a proxy for the presence of water at any specific location within the stream system, and thus would be an excellent indicator

of whether or not a fish could spawn at that location. Regarding slope, a stream reach with a high slope value overall tends to have higher velocities and/or be constrained due to morphology at that location, and thus have negative effects on the presence of pool/riffle areas.

In review and interpretation of the bivariate response curves for distances within the watershed from the confluence of Indian Creek with the South Fork Eel River, it was noted that both Chinook and Steelhead seemed to generally favor the upper watershed areas (as interpreted from the general increase in probability based on increasing distance from the confluence) while Coho seemed to prefer upper/mid-range distances. Keeping in mind that caution must be used when interpreting a bivariate response in a multivariate system, it seems that this may be due to a potential higher athleticism in Chinook and Steelhead species (thus, a willingness to expend more energy toward reaching upper watershed areas) whereas Coho may prefer upper/mid-ranges of watershed streams.

When reviewing and interpreting substrate bivariate response curves it was noted that in most cases variable importance decreased greatly, as reported by the jackknifing processes in relation to contributing areas, slope, and distances from the confluence. Again, a high degree of caution must be used when interpreting these responses for substrate values, as they are spatially and geologically autocorrelated. This decrease in importance for each of the substrate covariates could potentially be due to the method associated with their geospatial assignment (as discussed in Section 4.4) or due to interactions based on their geologic, geomorphic, and geospatial relationships.

As a whole, the resulting probability surfaces will serve as an excellent toolset and reference when planning future restoration efforts in the Indian Creek watershed. For example, the Moody Creek subwatershed has a fish barrier (embedded log jam) not far upstream from the confluence of Moody Creek with the mainstem Indian Creek (Figure 16). The total modeled area for streams greater than or equal to 1 meter predicted width (streams with highest modeled potential for spawning habitat) is 21691 meter^2. However, the great majority of this modeled area is inaccessible to fish due to the fish barrier, with 15969 meter^2 essentially walled off from access, leaving only 5992 meter^2 open as spawning habitat. Based on these findings and additional field inspection, this may be an ideal work location when considering future restoration projects. This modeling analysis allows additional insight when consideration of many other potential projects throughout the Indian Creek watershed.

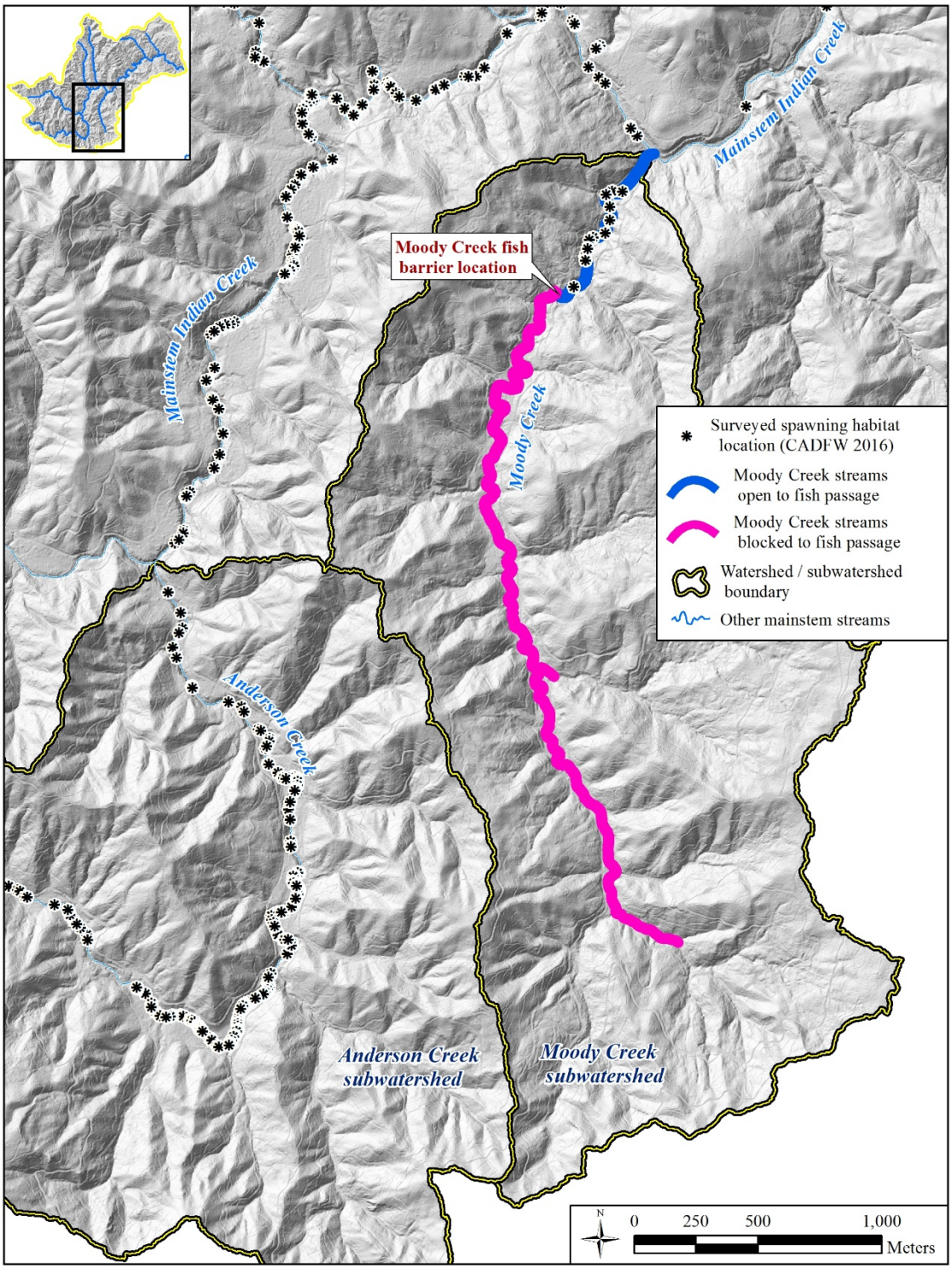

Figure 49. Location of fish barrier in the Moody Creek subwatershed, Indian Creek watershed.

4.4 Uncertainty and limitations of analysis

Sources for uncertainty and inherent limitations for this modeling process and results are numerous. All modeling results are derived from and share spatial relationships with products derived from the DEM. Errors and uncertainties associated with the DEM (physical acquisition of the data, recency of the data, anthropogenic or natural alterations rendering the data inaccurate, etc.) are thus shared with all modeling results. During field visits for model calibration and field-verification, it was noted in some areas that recent anthropogenic influences on the stream morphology had significant changes that were not reflected on the DEM, as that data had been acquired before the changes had occurred. As shown in Photo Points 16, 17, and 31, relatively recent restoration work conducted by PWA can significantly alter the morphology of the stream bank. Large woody debris structures emplaced as part of fish habitat improvement projects to create pool/riffle spawning habitat also have significant effects on morphology that post-date data acquisition.

Conversely, there is the potential for negative effects to occur to habitat probability that would not be confirmed by the data available. Both anthropogenic and natural occurrences can have drastic effects on stream morphology. Fill failures associated with historic roads and stream crossings can have immediate effects, inundating the stream system (and salmonid spawning gravels) with large amounts of fine-grained sediment. Naturally occurring log jams or landslides can occur due to storm

events or threshold changes in the landscape. All these processes can have effects on the stream system that the modelling process used in this study would not have been able to characterize without extensive field-checking.

Additional sources of uncertainty with this specific analysis occur with the use of raster covariates assigned substrate values (Figures 12d-i). Three methods were developed and utilized to assign specific substrate values to the stream network:

1.) For stream reaches between in-stream survey locations, it was decided to extrapolate substrate values evenly between stations. Thus, the substrate percentages for each station were assigned to the stream network up to 50% of the geospatial distance to the next closest survey location. Further, substrate contribution percentages reported from MaxEnt do not reflect contributions for a model derived from only stream areas greater than or equal to 1 meter modeled width.

2.) For stream reaches that did not have survey locations, yet whose contributing areas numerically matched other surveyed stream reaches, values of substrate were assigned via a similarity analysis utilizing contributing area as the deciding variable. While attempting to utilize a predictive model for substrate as derived from DEM information (contributing area and slope) it was found that while contributing area was a significant predictor for each substrate value ($p << .01$), only between 12-22 % of the variance was explained by contributing area. Thus, while better than simply random assignment, there is a high degree of uncertainty associated with using contributing area as a predictor for substrate. As such, it

was decided to perform the similarity analysis and substrate value assignment using contributing area in the absence of anything more useful.

3.) For stream reaches outside the values of contributing area information as derived from in-stream surveys (i.e. with very small contributing areas such as the very small streams seen in Figures 12d-i) it was decided to assign substrate values as per the in-stream survey at the watershed location with the minimum contributing area value. This had the effect of assigning substrate values to a great majority of the stream system to be equal to that of the in-stream survey farthest upward to the headwaters areas in the watersheds where survey data exist. Parallel to this, the great majority of stream areas that were assigned these specific values were also streams denoted as being less than 1m predicted bankfull width, and thus had areal metric derived separately, as per Figures 13a-f, 14a-f, 15a-f, and Tables 2-10.

4.) While being treated as independent variables, substrate environmental variable percentages directly relate to one another. The method by which the percentage data was collected was to inventory the stream location and assign percentages of the stream substrate at that location, summing them to 100 % (i.e. a specific survey location might be 10 % gravels, 10 % boulders, 80 % sands/silts, 0 % fine grain cohesives, 0 % cobble, and 0 % bedrock). These percentages were assigned as a group during the similarity analysis – i.e. each geospatial location was assigned a series of percentages based on its similarity to known spatial locations. This may lead to unforeseen interactions within the probability model,

particularly if there are effects from anthropogenic disturbances in the substrate that have not yet been accounted for. Areas where this may occur are shown in Appendix F, Photo Points 36-41.

Other sources of uncertainty for the analysis can potentially be found in both the biogeographic, physical, and humanistic historical geography of the area. There are innumerable effects of the historical land management practices on the current physical landscape. There may be factors overlooked or unaccounted for, or simply processes that have yet to express themselves. Threshold response systems can, by definition, experience significant changes once certain variables reach critical values. As an example, the effects of climate change may have yet to influence this particular environment (and by extension, model) – or they may already influence it in ways not yet known.

Extensive field verification indicates that the modeled spawning habitat probability surfaces would be useable with a high degree of confidence for intelligent decision-making processes for research and habitat restoration. Reproducing the analysis in neighboring, geographically similar watersheds where morphological and high-resolution data already exist is a somewhat lengthy, but straightforward process, and will be conducted as part of future research. The same methodology can be applied to other watersheds with a high degree of confidence in success. As noted above, key to that endeavor would be the acquisition of high-resolution DEM data and similar in-stream morphological surveys, ideally of the same or greater number (to strengthen the predictive power of the NIFTI toolset).

As with any modeling exercise, all individual tools and components produced, and all results derived with this analysis should be used judiciously, intelligently, and, ideally, with a significant amount of care and professional expertise. It is always highly recommended that careful field-verification of modeling results be performed for any analysis of this kind.

5. RECOMENDATIONS FOR FUTURE WORK

5.1 Additional data

1.) Precipitation geospatial data has been acquired for the Indian Creek and surrounding watersheds. It is presumed that, during years of high precipitation, streams would need smaller contributing areas before achieving a critical threshold and becoming a recognizable stream that would qualify as habitat and the converse would logically follow. However, as stream geomorphic data was acquired in a single timeframe and not subject to monitoring over a period of time (thus allowing for measurements to be taken during high/low flow years) it would be erroneous to use a precipitation dataset as a model component until additional data was acquired. Establishing stream monitoring stations to derive a series of subwatershed- and watershed-wide hydraulic responses would be of great value in future modeling endeavors seeking to capture biologic responses to wet and dry years, particularly in the face of climatic change.

2.) Geospatial data denoting vegetation was also acquired for the project area. This data may prove a necessary component in conjunction with precipitation data for an evapotranspiration (ET) component in future model development. Vegetation landcover throughout the Indian Creek and surrounding watersheds has been significantly altered over the last several decades before the properties were acquired by their current owners. Systematic clear-cut logging practices essentially stripped the landscape clean over much of the watershed area, and only relatively recently has the area been allowed to recover.

Further, significant numbers of roads were created to facilitate timber extraction. This drastic artificial alteration of the landscape would have a number of effects – sediment contributions to the stream system could still have negative impacts on potential salmonid habitat, runoff and drainage patterns could still be affected by erosional patterns caused by still-recovering vegetation, and ET contributions from a still-shifting vegetation ecosystem could potentially be different.

3.) Additional high-resolution DEM data for before/after restoration work being performed. There are numerous areas within the Indian Creek and neighboring watersheds that hold great potential for future restoration work. A time-series of high-resolution DEM data acquired pre- and post-restoration, with, ideally, additional yearly-captures, could yield not only a better understanding of watershed-wide responses to restoration work, but also better guide future restoration efforts so as to better utilize restoration funding.

4.) Repeating modeling process utilizing additional covariates. Numerous biological and lifecycle variables for the species of interest were not within the scope of this research, such as food sources, canopy protection, interaction with other species, other salmonid life stages, etc., all of which have potential value in the modeling process and represent opportunities for additional work.

5.) Repeating modeling process utilizing stream area system greater than or equal to 1 meter modeled bankfull width. It may be that percentage contributions for substrate and other covariates are reported heavily weighted towards areas of the stream system where streams are less than 1 meter modeled bankfull width. Rerunning the

model utilizing only areas that are field-verified as able to support spawning habitat use could give greater insight into covariate contributions.

5.2 Model comparison

Collaboration with professional and academic colleagues on using the different models such as the Intrinsic Potential (IP) and Potential Habitat Simulation (PHABSIM) models to generate outputs for comparison and refinement would be of great benefit. Additionally, comparing modeling results from the same and different models in both geographically similar and dissimilar watersheds may have great research potential.

5.3 Expanded NIFTI model development

Additional capabilities for the NIFTI toolset are in development, such as automatically denoting and excluding stream systems blocked by fish barriers, customization of contribution area thresholds, and custom importing of stream geomorphic data. Ultimately, a toolset allowing direct integration of MaxEnt and hydraulic modeling tools such as HEC-RAS will be a long-term goal.

SUMMARY

Research goals of this thesis work – deriving spawning habitat models for Coho Salmon (*O. kisutch*), Chinook salmon (*O. tshawytscha*), and Steelhead (*O. mykiss*) using geospatially constructed stream morphology derived from high-resolution lidar-derived DEMs and field survey data - were successful. A new geospatial toolset, Numerically Interpolated Flow Track Inferencing (NIFTI), was created and utilized with great success to geospatially create stream corridor morphology for raster covariates which were then used in MaxEnt for the modeling process. NIFTI has a great number of potential applications, and the author is in discussion with ESRI development staff to incorporate NIFTI into the ESRI ArcHydro toolset. All MaxEnt-derived modeling products in addition to the NIFTI-derived stream corridor morphology were successfully tested and field-verified by the author, committee member Thomas Leroy, and CDFW Fisheries biologist Seth Ricker. Interpretations of geospatial covariates, effects, and modeling results were explicable and reproducible in other areas. The research methods and their application to the Indian Creek watershed have allowed a greater understanding of the physical systems associated with Indian Creek and neighboring watersheds. These methods and developed toolset will be put to good use in future grant-funded restoration work.

Happiness abounds.

CITATIONS

Ames, D., Rafn, E., Van Kirk, R., Crosby, B. (2009) Estimation of stream channel geometry in Idaho using GIS-derived watershed characteristics. Environmental Modeling & Software, v.24, 444-448.

Anlauf-Dunn K, Ward E, Strickland M, Jones K, Bradford M. (2014) Habitat connectivity, complexity, and quality: predicting adult Coho Salmon occupancy and abundance. Canadian Journal Of Fisheries & Aquatic Sciences [serial online]. December 2014;71(12):1864-1876. Available from: Academic Search Premier, Ipswich, MA.

Beechie, T., Imaki, H., Greene, J., Wade, A., Wu, H., Pess, G., Roni, P., Kimball, J., Stanford, J., Kiffney, P. and Mantua, N. (2013), Restoring salmon habitat for a changing climate. River Res. Applic., 29: 939–960. doi:10.1002/rra.2590

Bi, H, Hongsheng, B., Peterson, W., Lamb, J., & Casillas, E. (2011). Copepods and salmon: Characterizing the spatial distribution of juvenile salmon along the Washington and Oregon coast, USA. Fisheries Oceanography, 20(2), 125.

Bi, H., Ruppel, R., & Peterson, W. (2007). Modeling the pelagic habitat of salmon off the Pacific northwest (USA) coast using logistic regression. Marine Ecology Progress Series, 336, 249-265.

Breslow, S. (2014). Tribal science and farmers' resistance: A political ecology of salmon habitat restoration in the American northwest. Anthropological Quarterly, 87(3), 727-758.

Burnham, K., Anderson, D. (2010). Model selection and multimodal inference: A practical information-theoretic approach. Second edition.

Burton, T., Rifai, H., Hildenbrand, Z., Carlton, D., Fontenot, B., Shug, K. (2016). Elucidating hydraulic fracturing impacts on groundwater quality using a regional geospatial statistical modeling approach. Science of the Total Environment, 545-546, p. 114-126.

California Department of Fish and Wildlife (2016). Allan Renger, Seth Ricker – Anadromous species habitat survey data, September 2016.

CalFish NOAA National Marine Fisheries Service; Gavette, C. (2012). Extent and Ranges of Coastal Chinook Salmon. Retrieved November 22, 2017, from http://www.calfish.org/Home.aspx

CalFish NOAA National Marine Fisheries Service; Gavette, C. (2012). Extent and Ranges of Coho Salmon. Retrieved November 22, 2017, from http://www.calfish.org/Home.aspx

CalFish NOAA National Marine Fisheries Service; Gavette, C. (2012). Extent and Ranges of Winter Steelhead. Retrieved November 22, 2017, from http://www.calfish.org/Home.aspx

Cook, A., Venkatesh, M. (2009). Effect of topographic data, geometric configuration and modeling approach on flood inundation mapping. Journay of Hydrology, v. 377, 131-142.

Dunne, T., & Leopold, L. (1978). *Water in environmental planning*. San Francisco: W.H. Freeman.

Elith, J., Phillips, S., Hastie, T., Dudik, M., Chee, Y., & Yates, C. (2011). A statistical explanation of MaxEnt for ecologists. *Diversity and Distributions, 17*(1), 43-57.

Faustini, Kaufmann, & Herlihy. (2009). Downstream variation in bankfull width of wadeable streams across the conterminous United States. *Geomorphology, 108*(3), 292-311.

Flosi, G. F., Downie, S., Hopelain, J., Bird, M., Coey, R., Collins, B., (2014). California Salmonid Stream Habitat Restoration Manual, Fourth Edition. California Department of Fish and Game, Wildlife and Fisheries Division.

Foster, M. (2010). Knickpoints in Tributaries of the South Fork Eel River, Northern California. n.p.:

Foster, M., Kelsey, H. (2012). Knickpoint and knickzone formation and propagation, South Fork Eel River, northern California. Geosphere, v.8, no. 2, 403-416.

Gard, M. (2013). Modelling changes in salmon habitat associated with river channel restoration and flow-induced channel alterations. River Research and Applications, 30(1), 40-44.

Goodman D, Som N, Alvarez J, Martin A. (2015). A mapping technique to evaluate age-0 salmon habitat response from restoration. Restoration Ecology [serial online]. March 2015;23(2):179-185. Available from: Academic Search Premier, Ipswich, MA.

Guisan, A., Edwards, T., Hastie, T. (2002). Generalized linear and generalized additive models in studies of species distributions: setting the scene. Ecological Modeling, 157, p. 89-100.

Humboldt County GIS (2017). Web Mapping Applications. (n.d.). Retrieved September 1, 2017, from http://www.humboldtgov.org/1357/Web-GIS

Jennings, C.W., and Strand, R.G., 1960, Geologic map of California, Ukiah sheet: California Division of Mines and Geology, scale 1:250,000.

Leathwick, J., Elith, J., Hastie, T. (2006). Comparative performance of generalized additive models and multivariate adaptive regression splines for statistical modelling of species distributions. Ecological Modelling, 199, p. 188-196.

Lecomte, J., Benoit, H., Etienne, M., Bel, L., Parent, E. (2013). Modeling the habitat associations and spatial distribution of benthic macroinvertebrates: A hierarchical Bayesian model for zero-inflated biomass data. Ecological Modeling 265, p. 74-84.

McGlauflin, M, Schindler, D., Seeb, L., Smith, C., Habicht, C., et al. (2011). Spawning habitat and geography influence population structure and juvenile migration timing of sockeye salmon in the wood river lakes, Alaska. Transactions of the American Fisheries Society, 140(3), 763-782.

Meixler, M. S., Bain, M. B. (2012) A GIS Framework for Fish Habitat Prediction at the River Basin Scale, International Journal of Ecology, vol. 2012, Article ID 146073, 10 pages, 2012. doi:10.1155/2012/146073

Montgomery, D. R., Buffington, J. M. (1997). Channel-reach morphology in mountain drainage basins. GSA Bulletin, vol. 109, no 5, p 596-611.

Mull, K. E., Wilzbach, M. A. (2007) Selection of Spawning Sites by Coho Salmon in a Northern California Stream, North American Journal of Fisheries Management, 27:4, 1343-1354, DOI: 10.1577/M06-054.1

NOAA, National Oceanic and Atmospheric Administration (2017), NOAA Fisheries West Coast. "Essential Fish Habitat." NOAA Fisheries West Coast Region, 25 Sept. 2012, www.westcoast.fisheries.noaa.gov/habitat/fish_habitat/efh_consultations_go.html.

Null, S., Medellín-Azuara, J., Escriva-Bou, A., Lent, M., & Lund, J. (2014). Optimizing the dammed: Water supply losses and fish habitat gains from dam removal in California. Journal of Environmental Management, 136, 121-131.

Pacific Watershed Associates, 2007, Standley/Hollow Tree Creek Watershed Assessment and Erosion Prevention Planning Project: Arcata, California, Pacific Watershed Associates Report 07067801, 88 p.

Pacific Watershed Associates, (2015). Usal Forest Watershed Action Plan for Coho Recovery in the South Fork Eel River, Mendocino County, California. PWA Report No. 1501006501.

Phillips, S.J., Anderson, R. P., Dudík, M., Schapire, R.E. (2018) Maxent software for modeling species niches and distributions (Version 3.4.1). Available from url: http://biodiversityinformatics.amnh.org/open_source/maxent/. Accessed on 2018-10-5

Phillips, S.J., Anderson, R. P., Dudík, M., Schapire, R.E., Blair, M. (2017). Opening the black box: an open-source release of Maxent. In Ecography.

Phillips, S.J., Anderson, R. P., Schapire, (2006). Maximum entropy modeling of species geographic distributions. Ecological Modelling, 190:231-259, 2006.

Phillips, S.J., Dudík, M., Schapire, (2004). A maximum entropy approach to species distribution modeling. In Proceedings of the Twenty-First International Conference on Machine Learning, pages 655-662.

Plant, R.E., (2012). Spatial data analysis in ecology and agriculture using R.

R Core Team (2013). R: A language and environment for statistical computing. R Foundation for Statistical Computing, Vienna, Austria. URL http://www.R-project.org/.

Quantum Spatial (2014) South Fork Eel River Watersheds, LiDAR Technical Data Report. Certification: Tucker, Thomas J. Licensed Land Surveyor, State of California, 2013.

Rosgen, D.L. 1994. A classification of natural rivers. Catena, Vol 22: 169-199, Elsevier Science, B.V. Amsterdam.

Simenstad, C., & Cordell, J. (2000). Ecological assessment criteria for restoring anadromous salmonid habitat in pacific northwest estuaries. Ecological Engineering, 15(3), 283-302.

Smith, D, & Brannon, E. (2008). Growth and habitat occupancy of hatchery Coho Salmon in an engineered stream. Transactions of the American Fisheries Society, 137(4), 1108-1119.

Suarez-Seoane, S., Osborne, P., Alonso, J. (2002). Large-scale habitat selection by agricultural steppe birds in Spain: identifying species-habitat responses using generalized additive models. Journal of Applied Ecology, 39, p. 755-771.

United States Department of Agriculture (2018). Geospatial Data Gateway. Retrieved September 1, 2018, from https://datagateway.nrcs.usda.gov

Valavanis, V., Pierce, G., Zuur, A., Palialexis, A., Saveliev, A., Katara, I., Wang, J. (2008). Modeling of essential fish habitat based on remote sensing, spatial analysis and GIS. Hydrobiologia, 612, p. 5-20.

Wehr, & Lohr. (1999). Airborne laser scanning—an introduction and overview. ISPRS Journal of Photogrammetry and Remote Sensing, 54(2), 68-82.

APPENDIX A: BANKFULL WIDTH RESPONSE CURVES

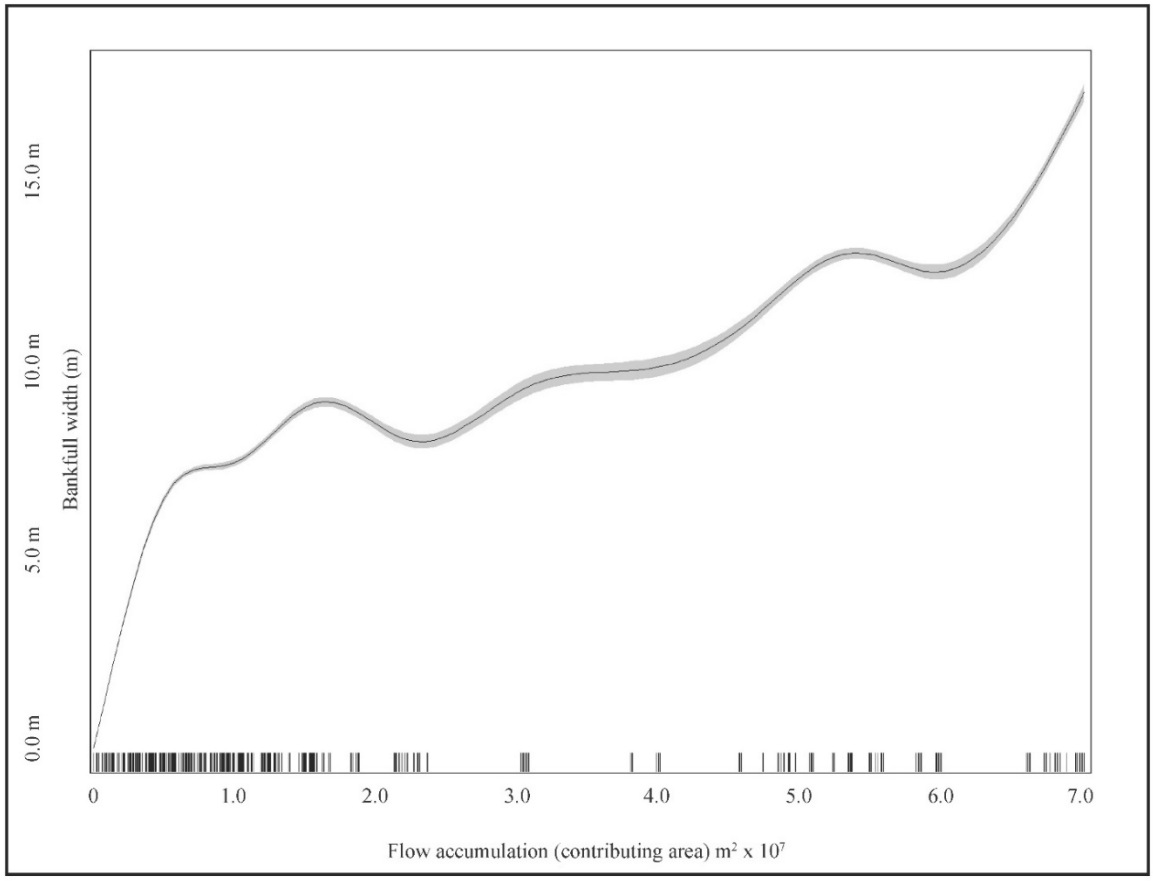

Figure 50. Bivariate response curve representing Bankfull width (m) as a function of contributing area of the stream at a specific geospatial location (FAC). Predictive model developed in R-Studio and utilized geospatially with NIFTI.

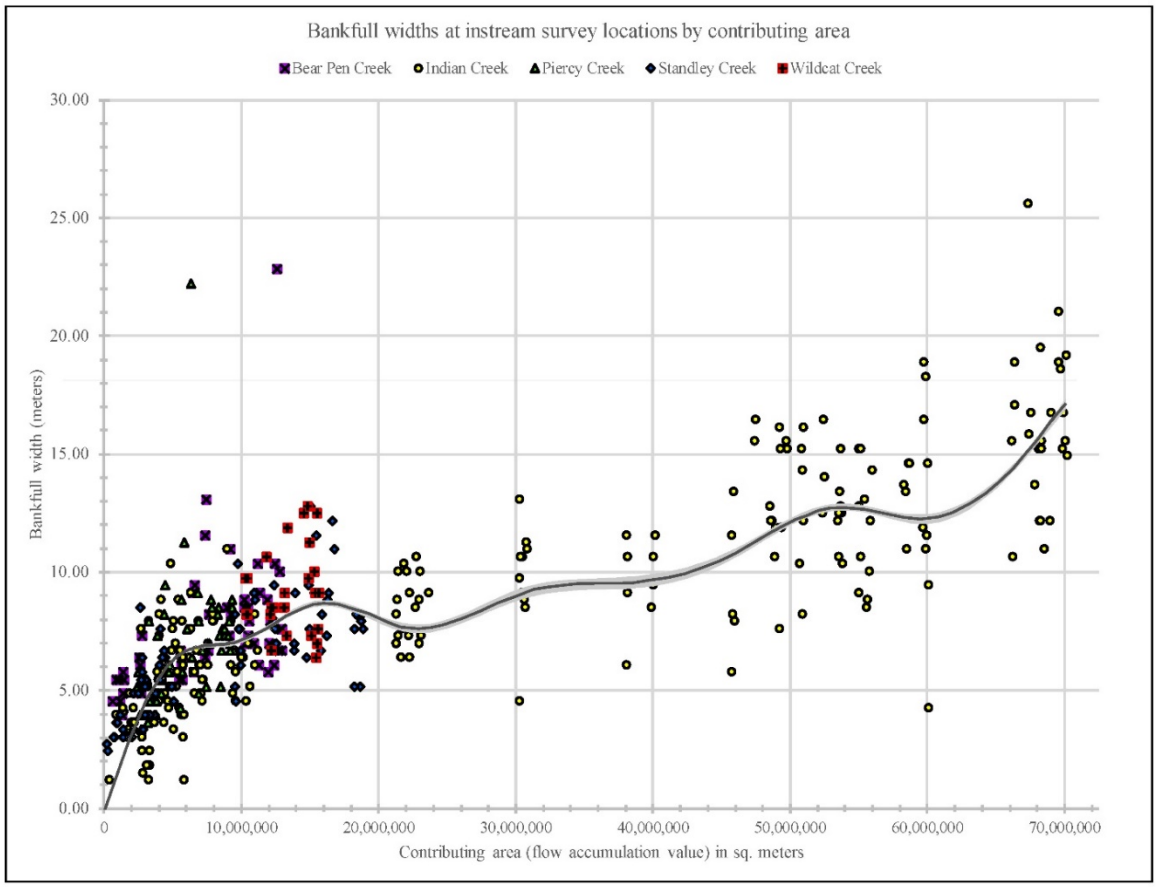

Figure 51. Bivariate response curve representing Bankfull width (m) as a function of contributing area of the stream at a specific geospatial location (FAC) transposed with Figure 15, a scatterplot showing relative locations of in-stream surveys (by proxy of contributing area) and the bankfull widths of those locations.

APPENDIX B: PROBABILITY SURFACES GENERATED WITH MAXENT

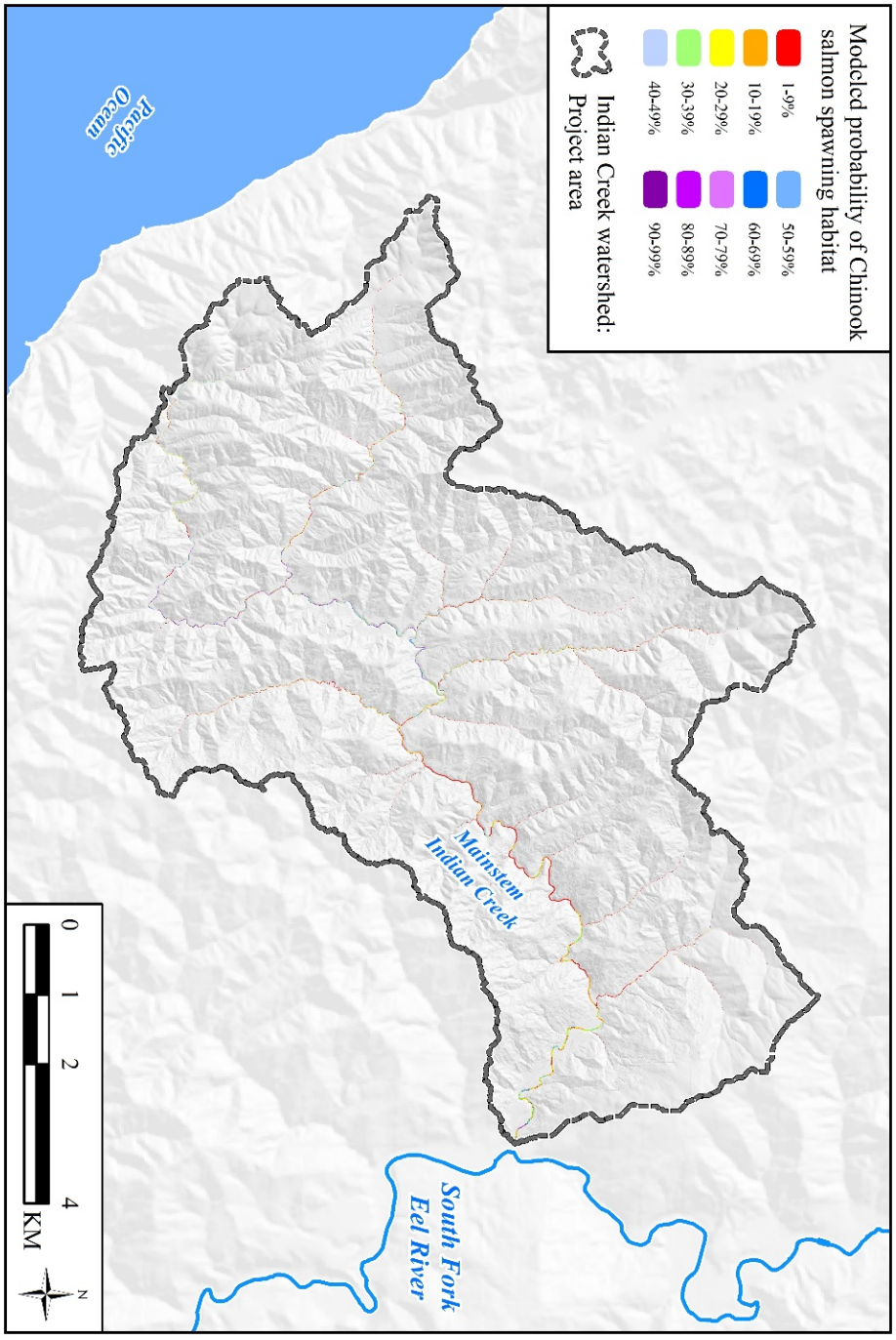

Figure 52. MaxEnt results - Chinook spawning habitat, overview map for Indian Creek watershed. Note – not all data may be represented visually at this scale.

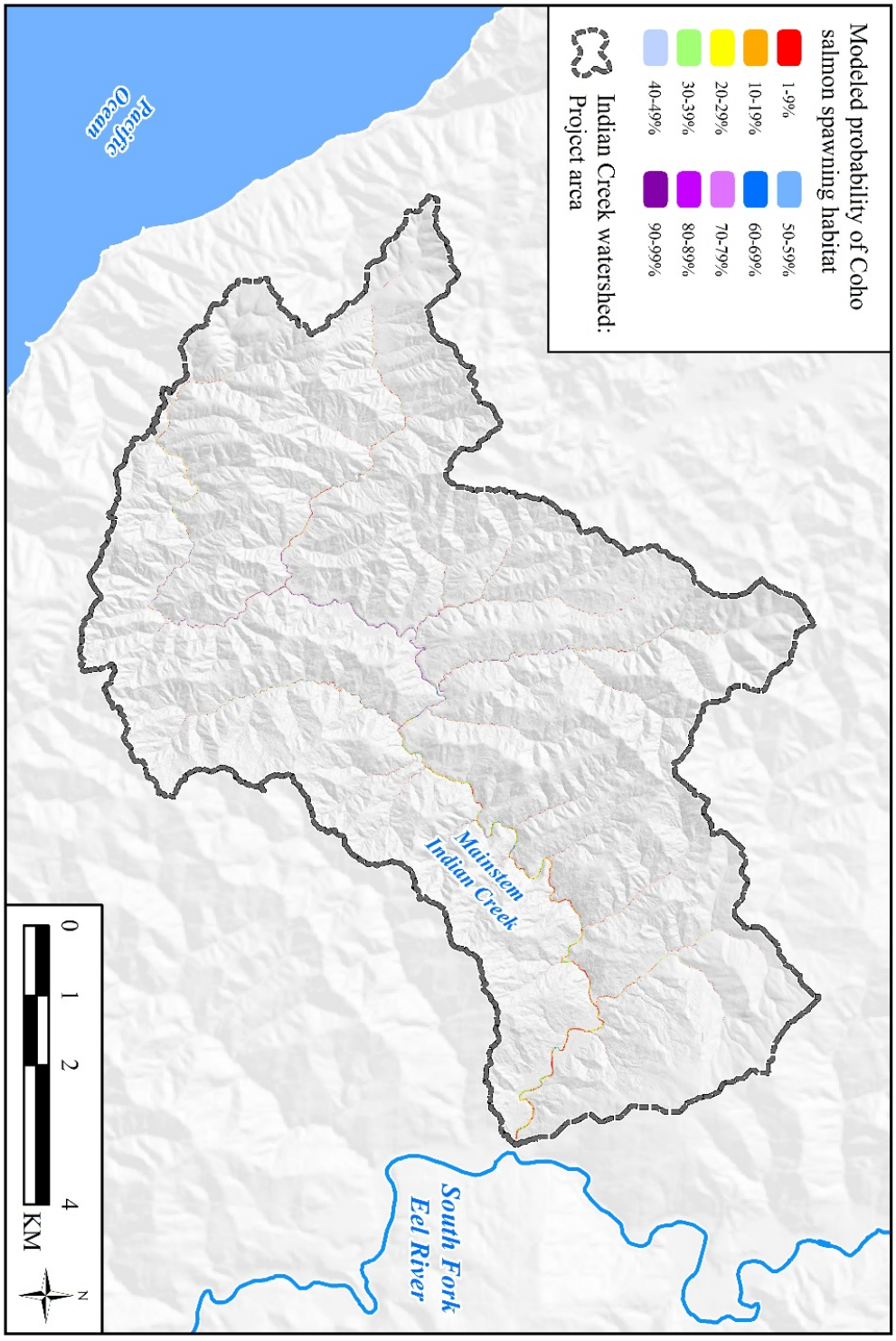

Figure 53. MaxEnt results - Coho spawning habitat, overview map for Indian Creek watershed. Note – not all data may be represented visually at this scale.

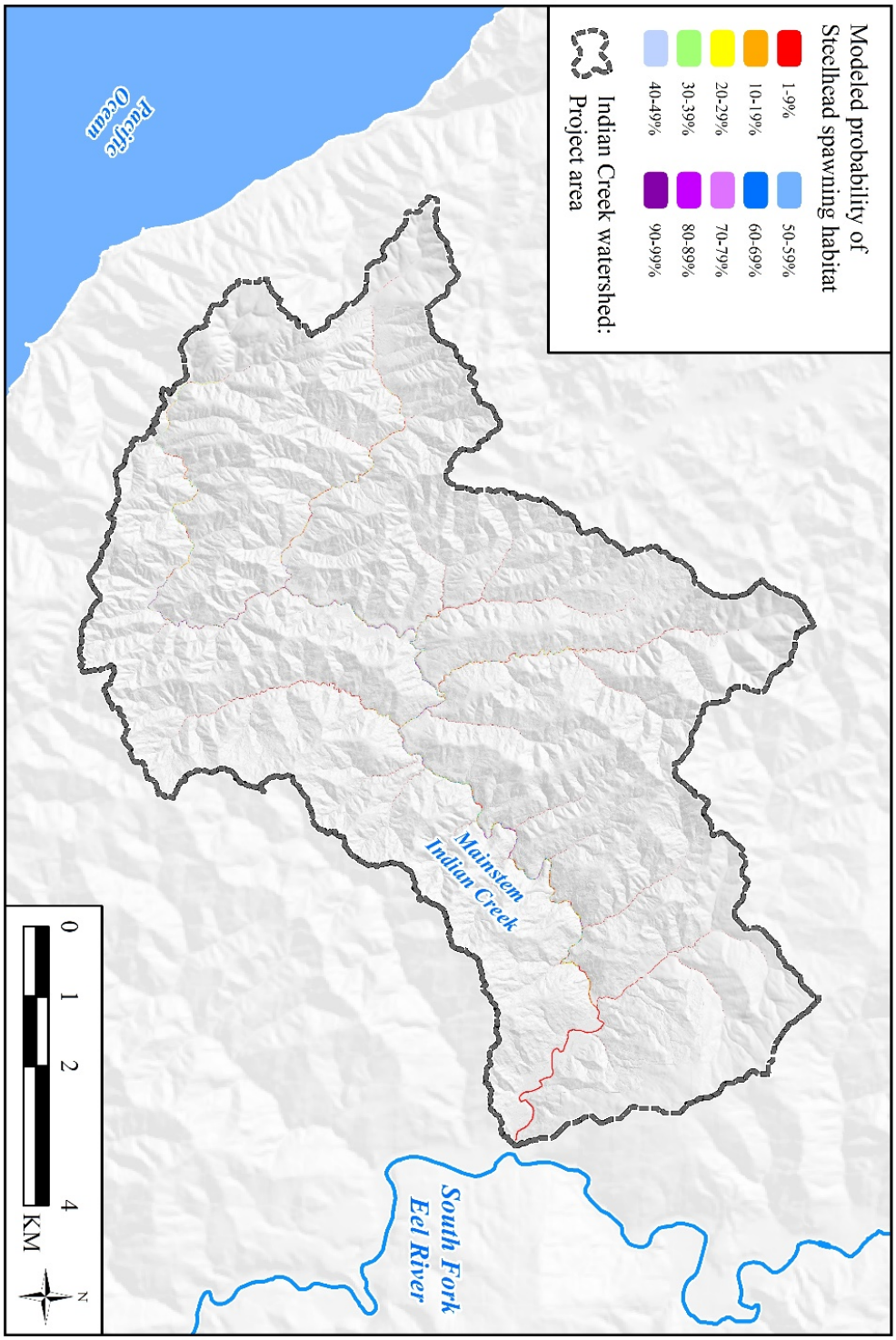

Figure 54 MaxEnt results - Steelhead spawning habitat, overview map for Indian Creek watershed. Note – not all data may be represented visually at this scale.

APPENDIX C: MAXENT MODELING RESULTS - RESPONSE CURVES FOR CHINOOK.

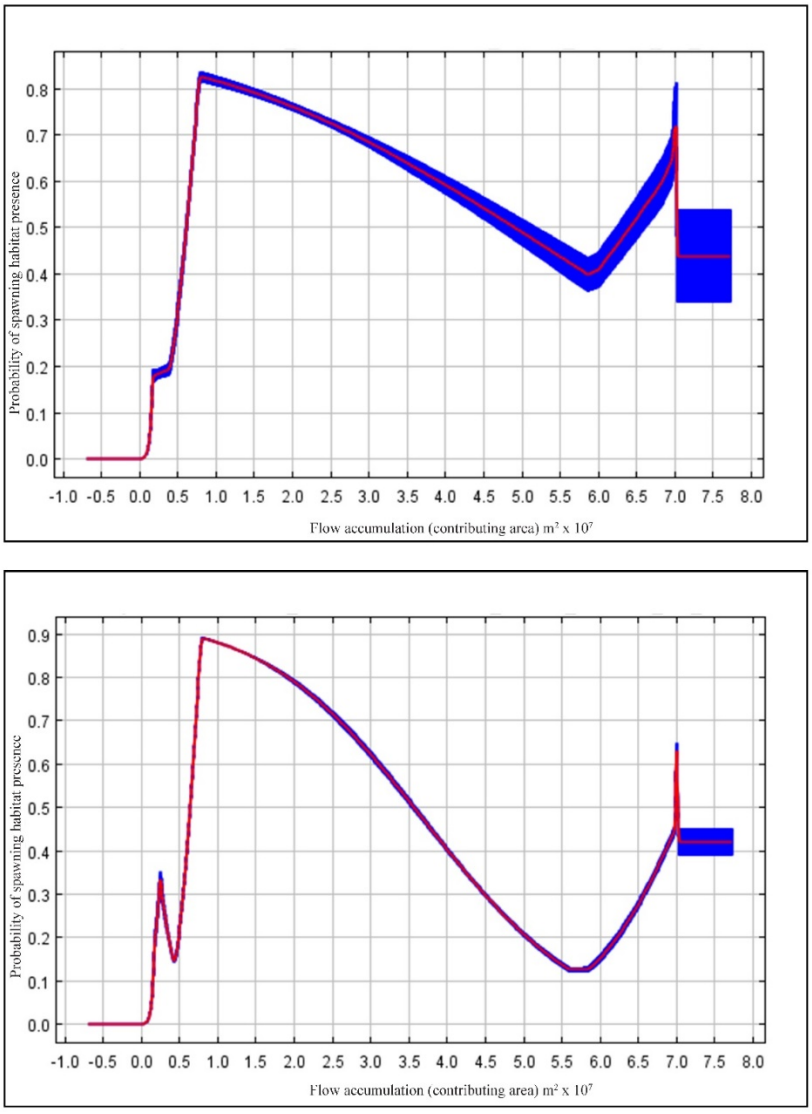

Figure 55. MaxEnt results - Chinook spawning habitat, response curves for flow accumulation (contributing area). Upper curve shows probability response while keeping all other environmental variables constant; lower curve represents response when MaxEnt probability model is derived using only the single variable. Red denotes average response over 100 replicated runs; blue denotes +/- 1 standard deviation.

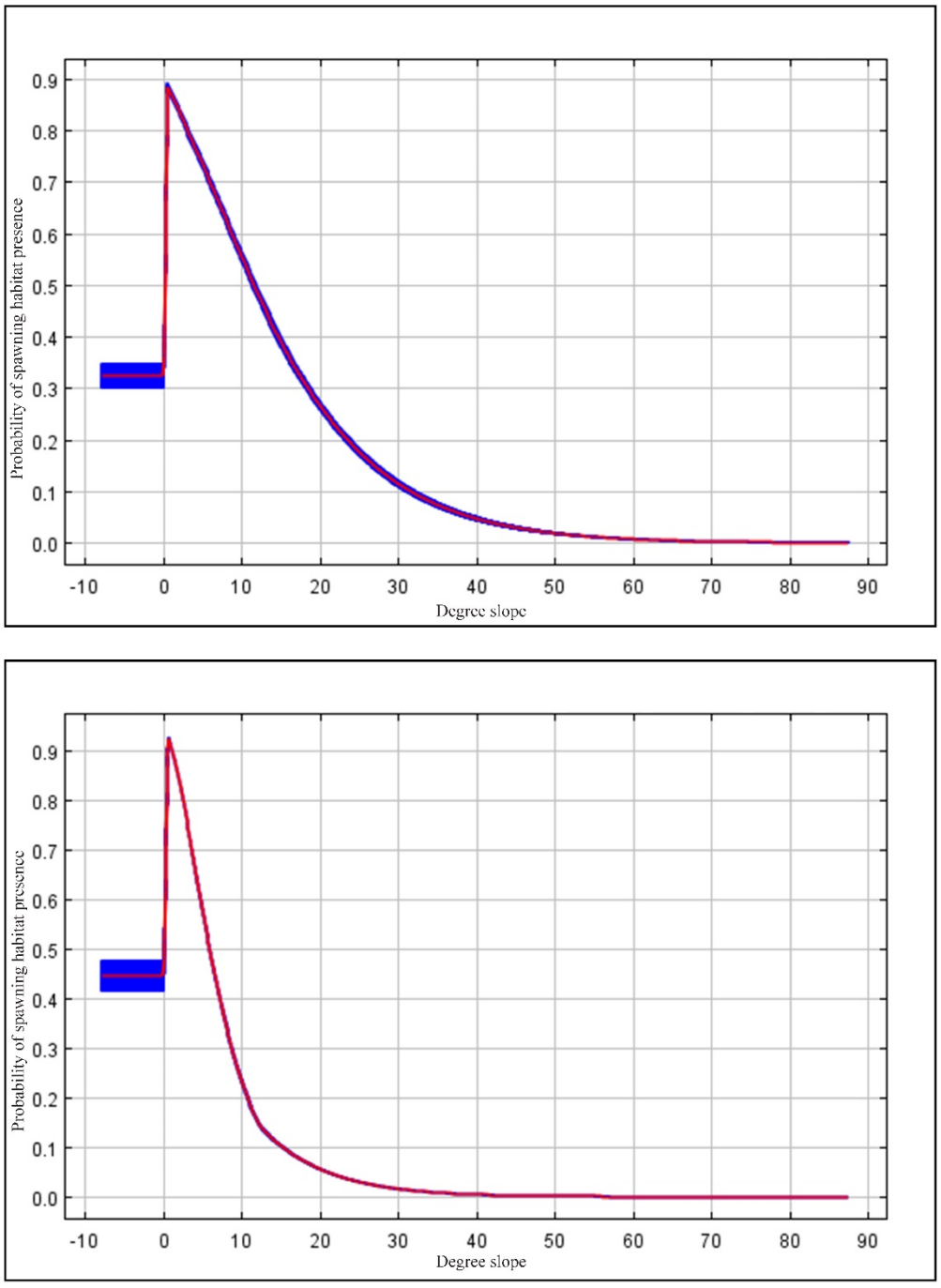

Figure 56. MaxEnt results - Chinook spawning habitat, response curves for degree slope. Upper curve shows probability response while keeping all other environmental variables constant; lower curve represents response when MaxEnt probability model is derived using only the single variable. Red denotes average response over 100 replicated runs; blue denotes +/- 1 standard deviation.

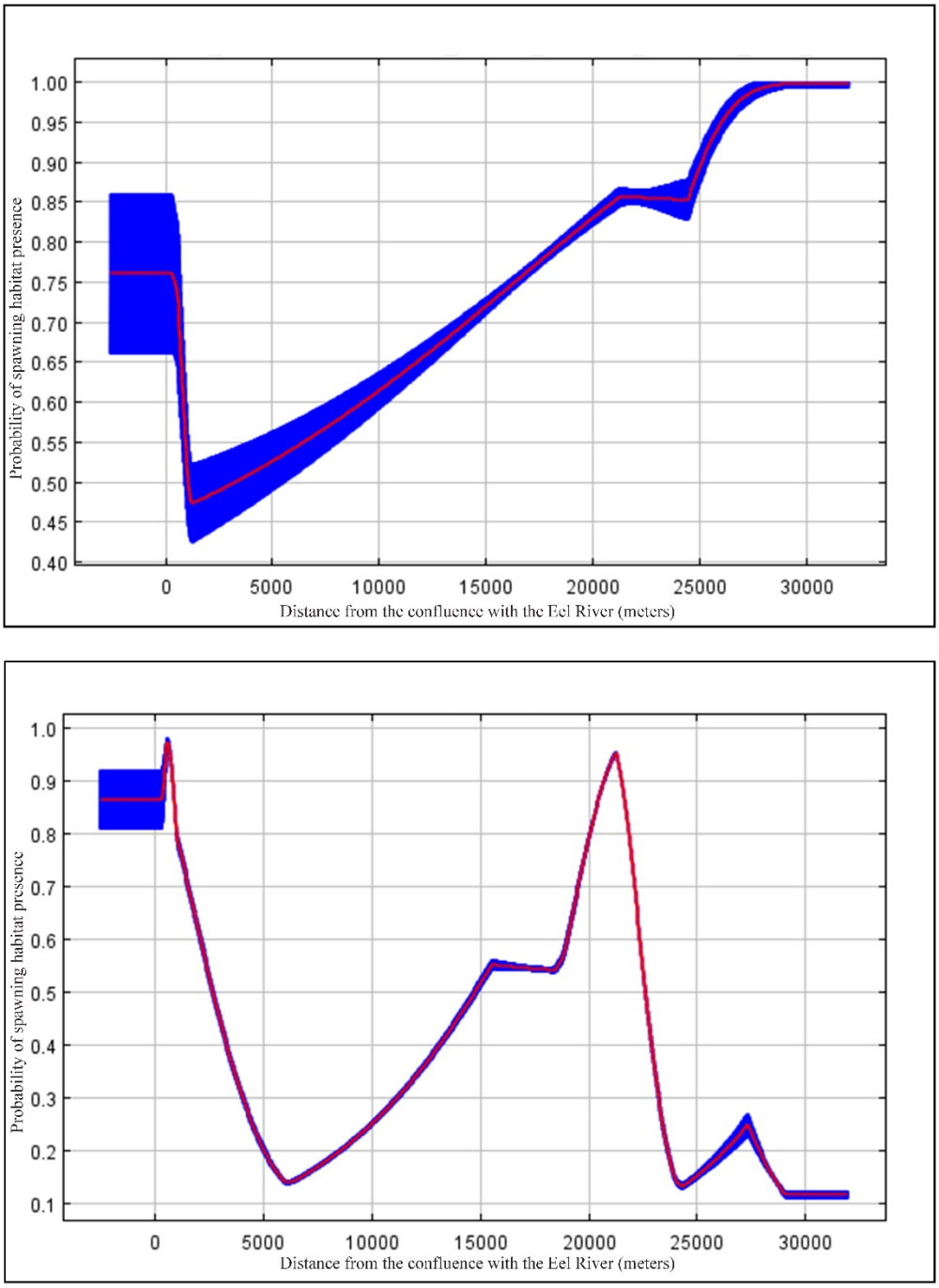

Figure 57. MaxEnt results - Chinook spawning habitat, response curves for distance from the confluence of Indian Creek with the Eel River. Upper curve shows probability response while keeping all other environmental variables constant; lower curve represents response when MaxEnt probability model is derived using only the single variable.

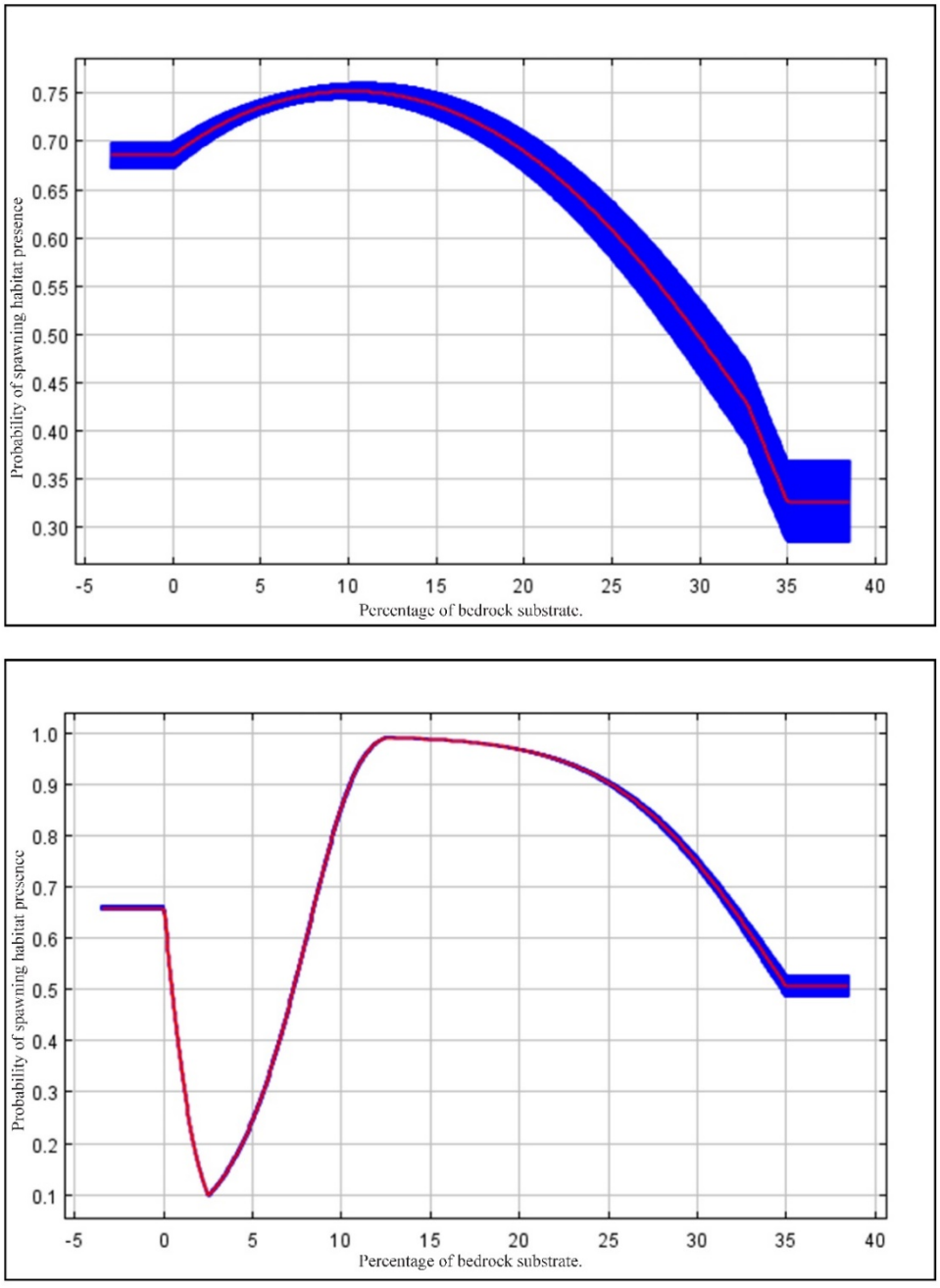

Figure 58. MaxEnt results - Chinook spawning habitat, response curves for percentage of bedrock substrate. Upper curve shows probability response while keeping all other environmental variables constant; lower curve represents response when MaxEnt probability model is derived using only the single variable. Red denotes average response over 100 replicated runs; blue denotes +/- 1 standard deviation.

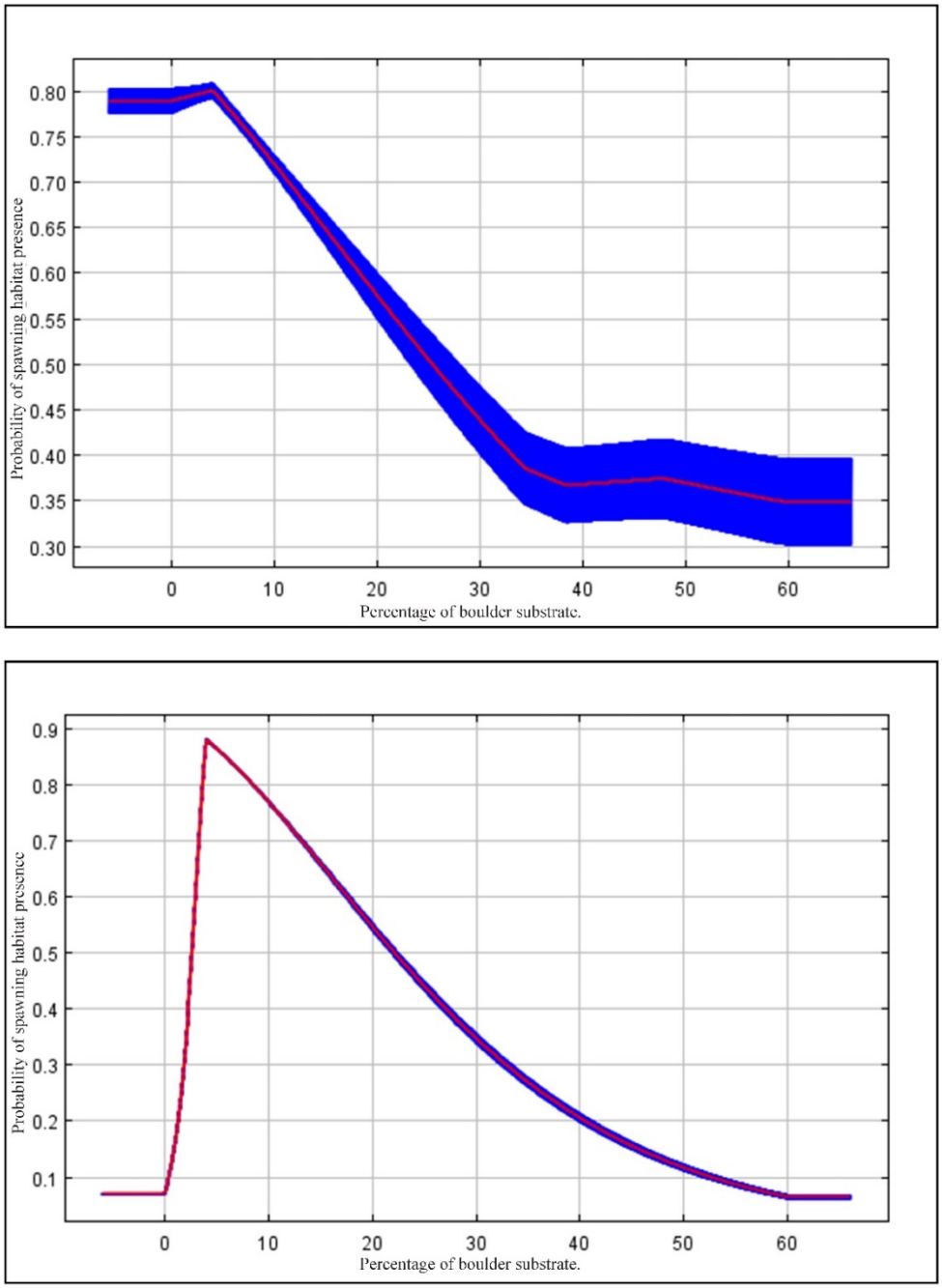

Figure 59. MaxEnt results - Chinook spawning habitat, response curves for percentage of boulder substrate. Upper curve shows probability response while keeping all other environmental variables constant; lower curve represents response when MaxEnt probability model is derived using only the single variable. Red denotes average response over 100 replicated runs; blue denotes +/- 1 standard deviation.

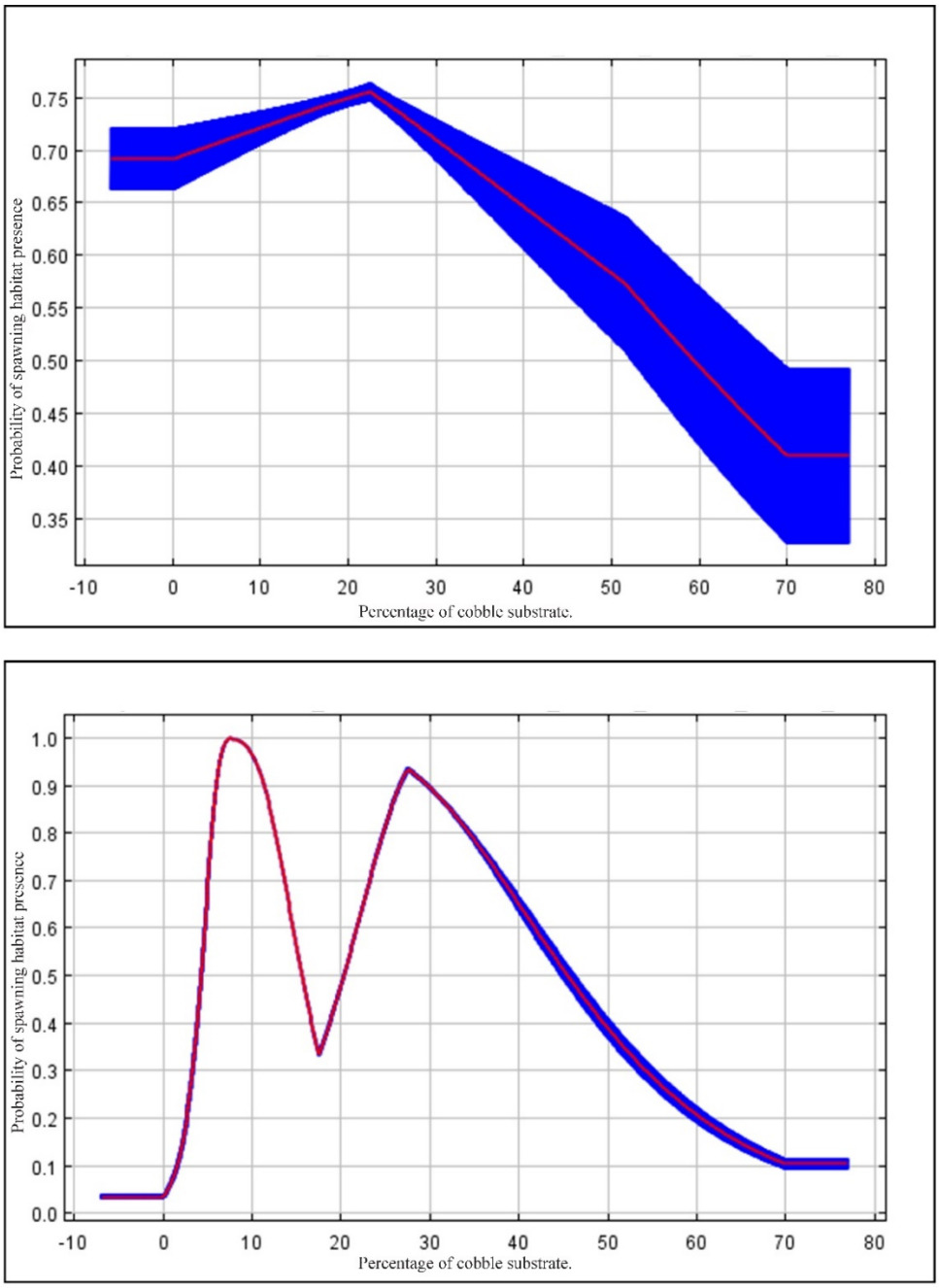

Figure 60. MaxEnt results - Chinook spawning habitat, response curves for percentage of cobble substrate. Upper curve shows probability response while keeping all other environmental variables constant; lower curve represents response when MaxEnt probability model is derived using only the single variable. Red denotes average response over 100 replicated runs; blue denotes +/- 1 standard deviation.

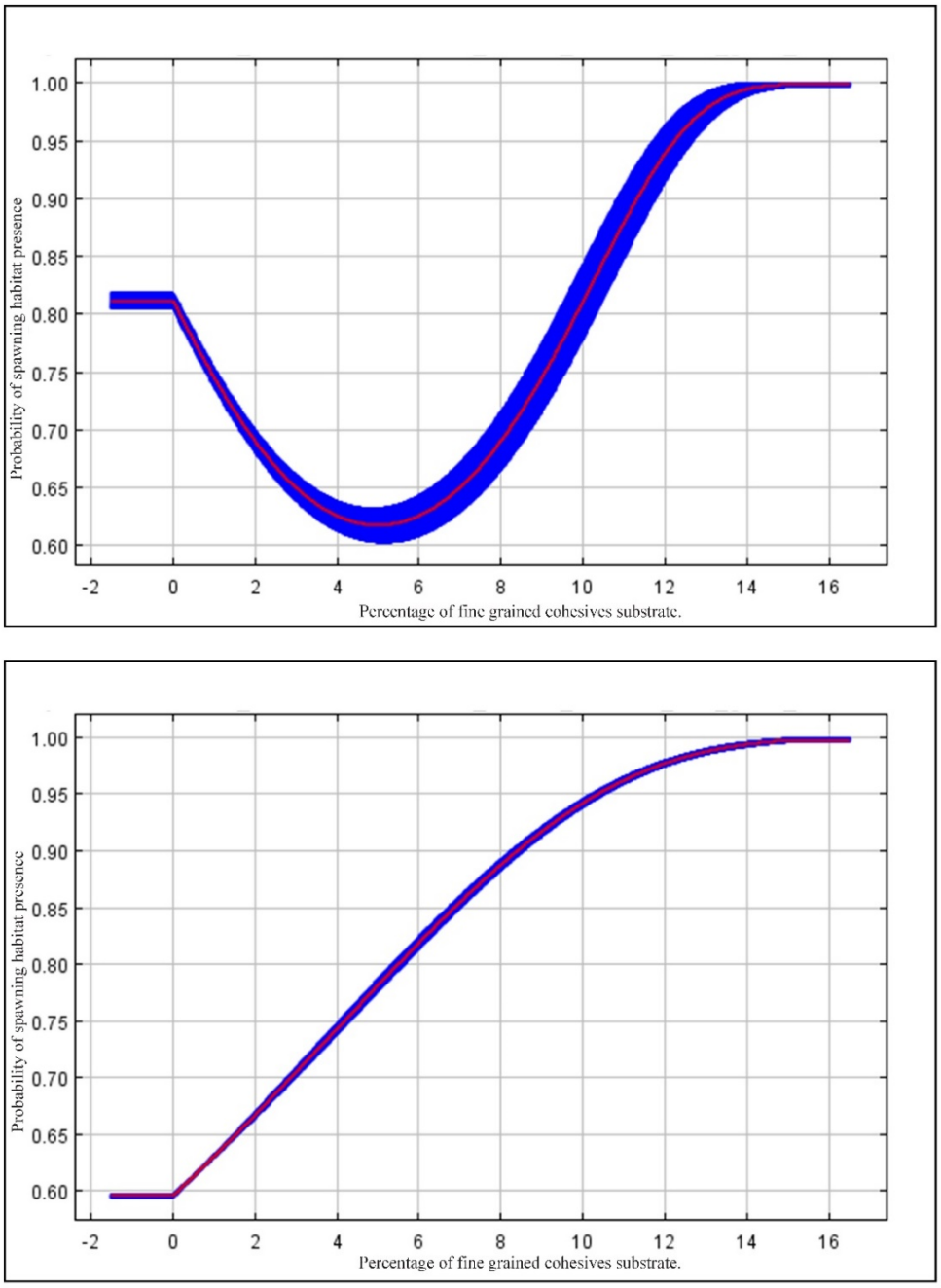

Figure 61. MaxEnt results - Chinook spawning habitat, response curves for percentage of fine grained cohesives substrate. Upper curve shows probability response while keeping all other environmental variables constant; lower curve represents response when MaxEnt probability model is derived using only the single variable. Red denotes average response over 100 replicated runs; blue denotes +/- 1 standard deviation.

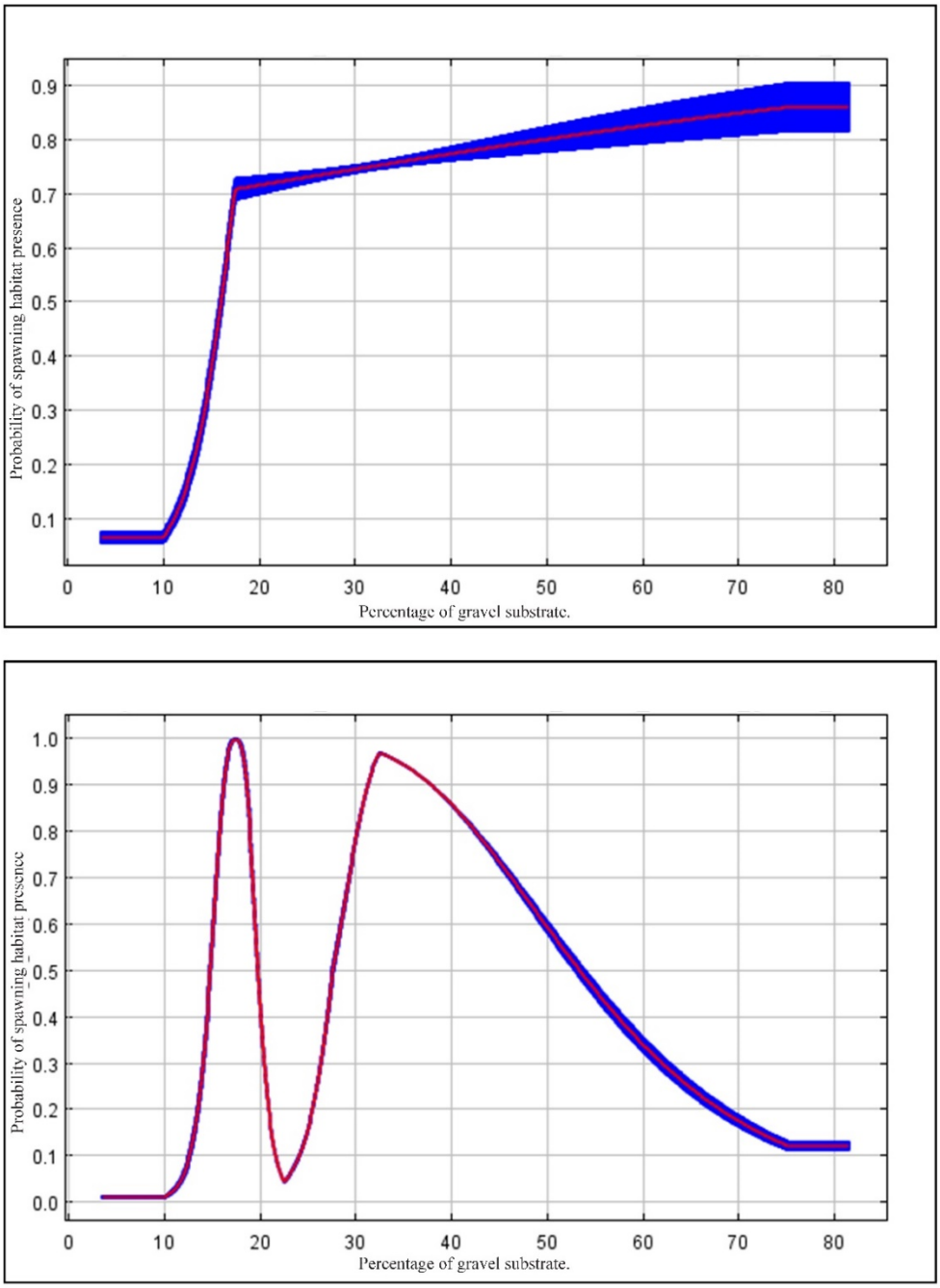

Figure 62. MaxEnt results- Chinook spawning habitat, response curves for percentage of gravel substrate. Upper curve shows probability response while keeping all other environmental variables constant; lower curve represents response when MaxEnt probability model is derived using only the single variable. Red denotes average response over 100 replicated runs; blue denotes +/- 1 standard deviation.

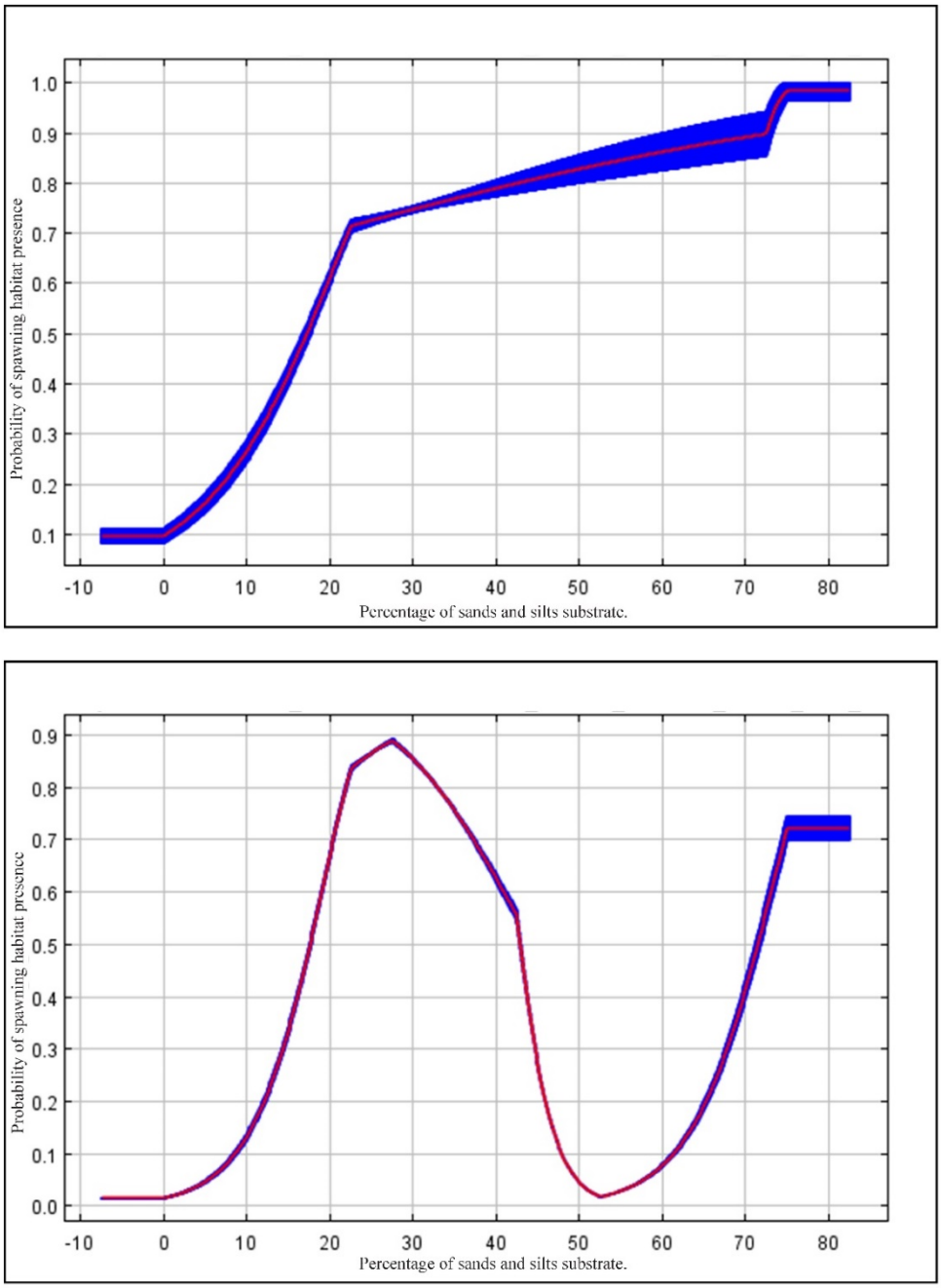

Figure 63. MaxEnt results - Chinook spawning habitat, response curves for percentage of sands and silts substrate. Upper curve shows probability response while keeping all other environmental variables constant; lower curve represents response when MaxEnt probability model is derived using only the single variable. Red denotes average response over 100 replicated runs; blue denotes +/- 1 standard deviation.

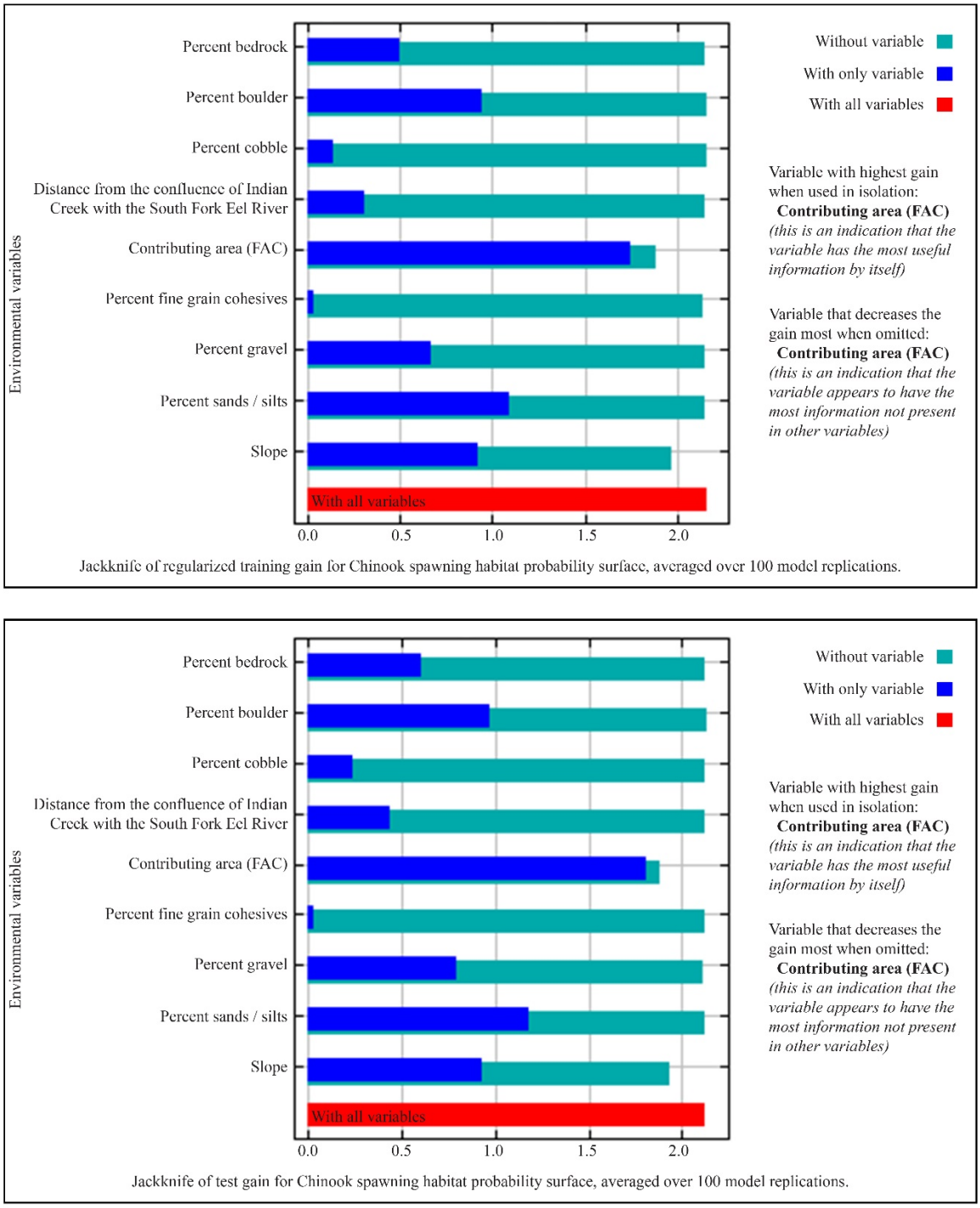

Figure 64. MaxEnt results - Chinook spawning habitat, jackknife tests for environmental variable importance - regularized training gain (upper) and test gain (lower).

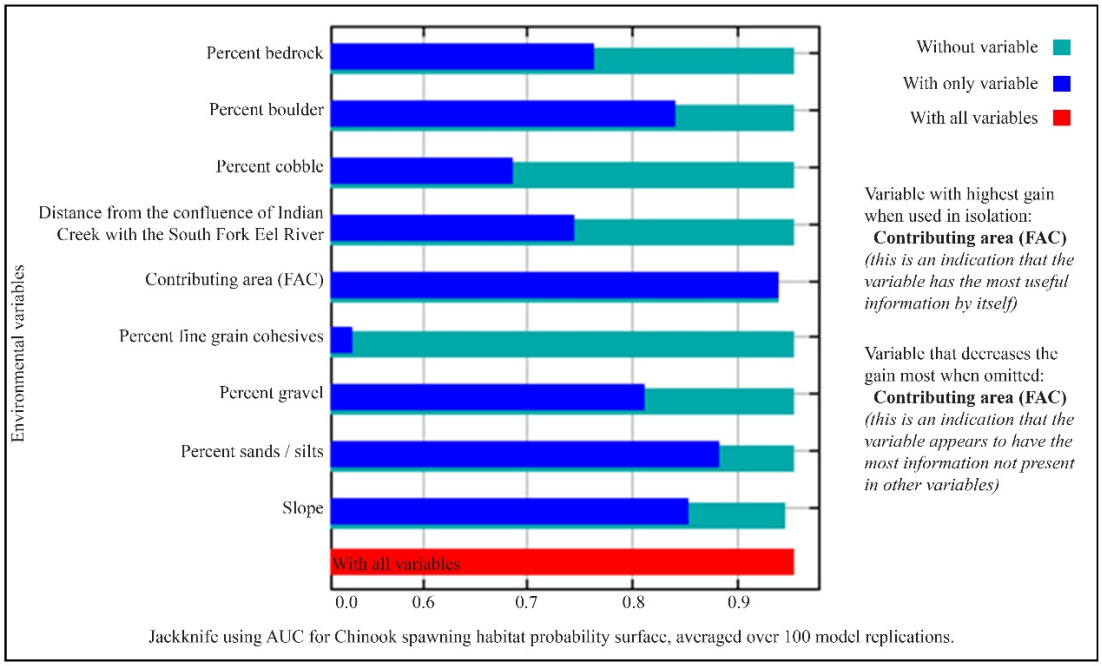

Environmental variable:	Percent contribution	Permutation importance
Contributing area (FAC)	74.70	81.6
Slope	9.40	9.6
Distance from the confluence of Indian Creek with the South Fork Eel River	4.50	2.6
Substrate: Percentage bedrock	1.20	0.7
Substrate: Percentage boulder	1.30	0.6
Substrate: Percentage cobble	0.20	0.8
Substrate: Percentage fine grain cohesives	1.50	1.8
Substrate: Percentage gravel	1.80	0.4
Substrate: Percentage sands/silts	5.30	1.9

Figure 65. MaxEnt results - Chinook spawning habitat, jackknife test using AUC for environmental variable contributions.

APPENDIX D: MAXENT MODELING RESULTS - RESPONSE CURVES FOR COHO SALMON.

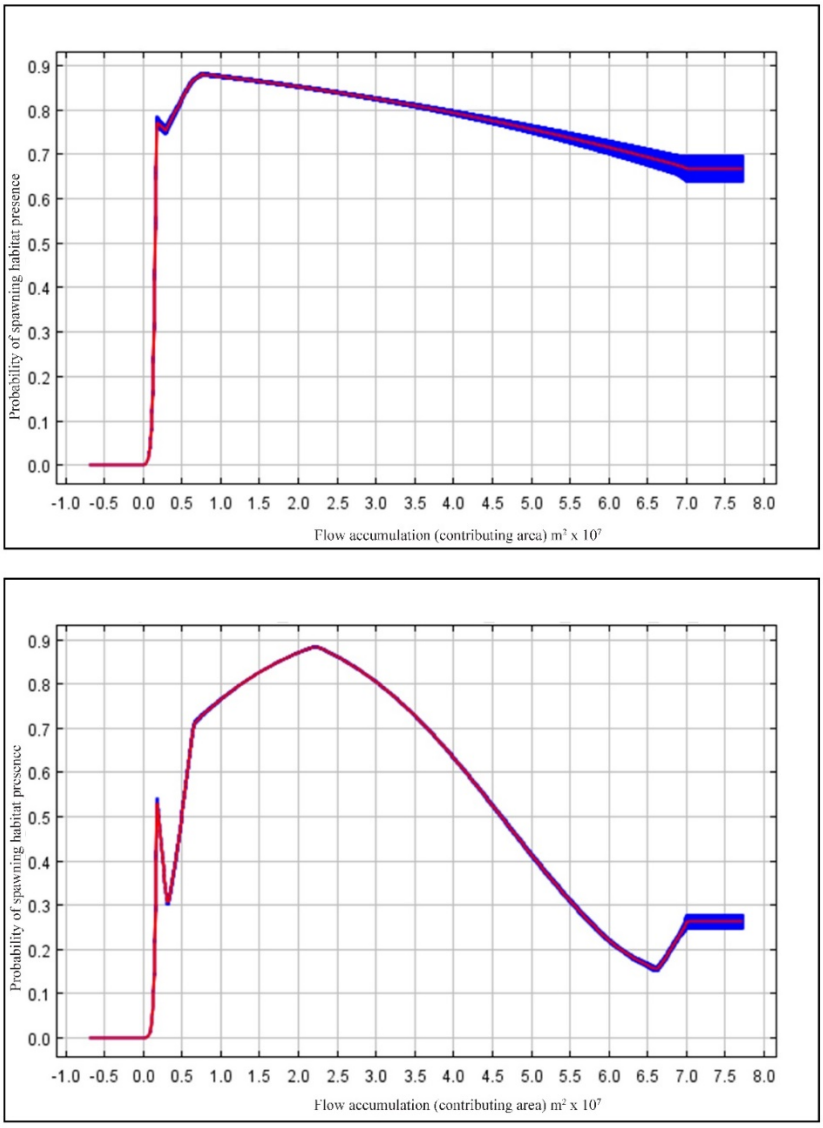

Figure 66. MaxEnt results - Coho spawning habitat, response curves for flow accumulation (contributing area). Upper curve shows probability response while keeping all other environmental variables constant; lower curve represents response when MaxEnt probability model is derived using only the single variable. Red denotes average response over 100 replicated runs; blue denotes +/- 1 standard deviation.

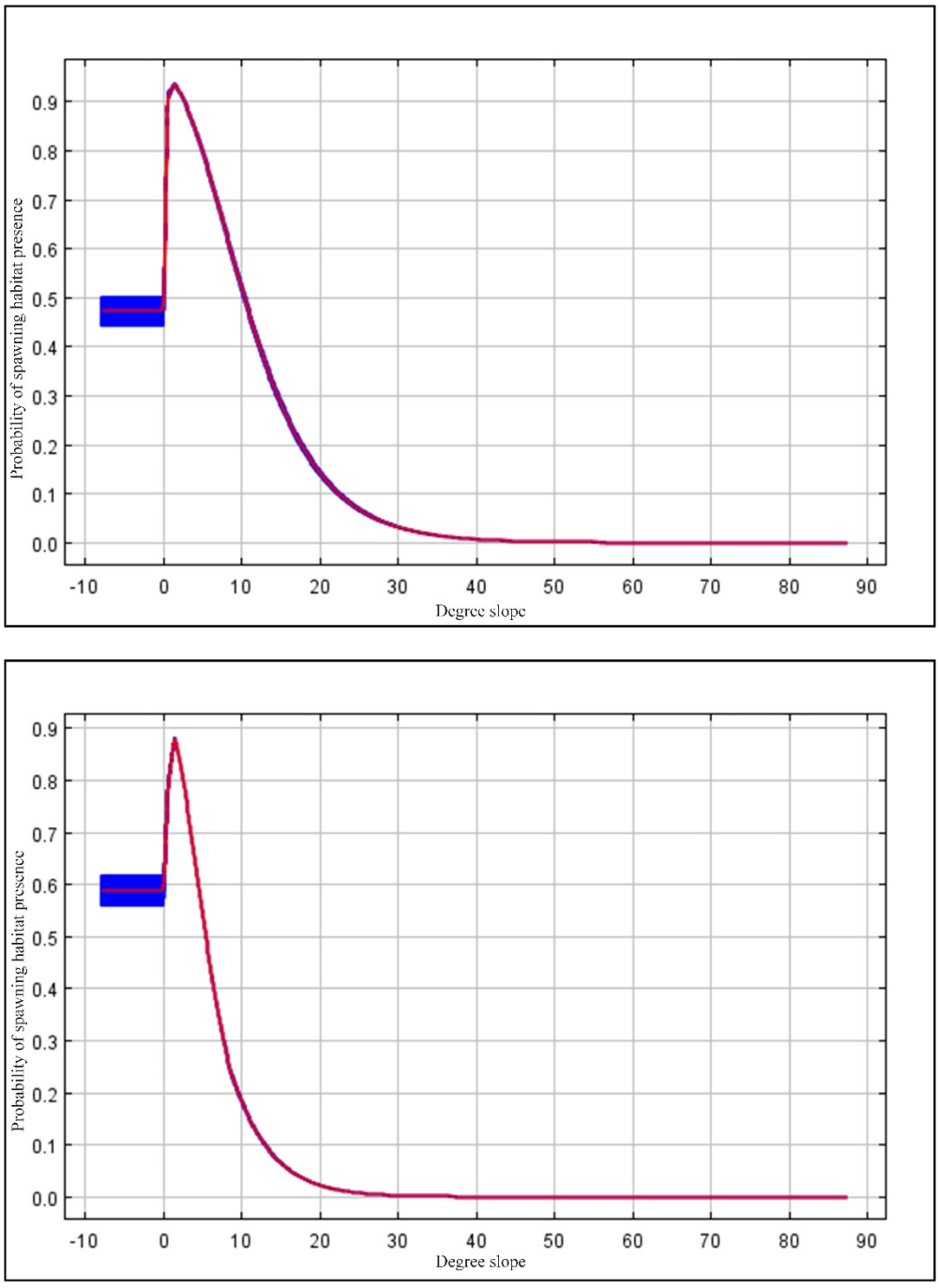

Figure 67 MaxEnt results - Coho spawning habitat, response curves for degree slope. Upper curve shows probability response while keeping all other environmental variables constant; lower curve represents response when MaxEnt probability model is derived using only the single variable. Red denotes average response over 100 replicated runs; blue denotes +/- 1 standard deviation.

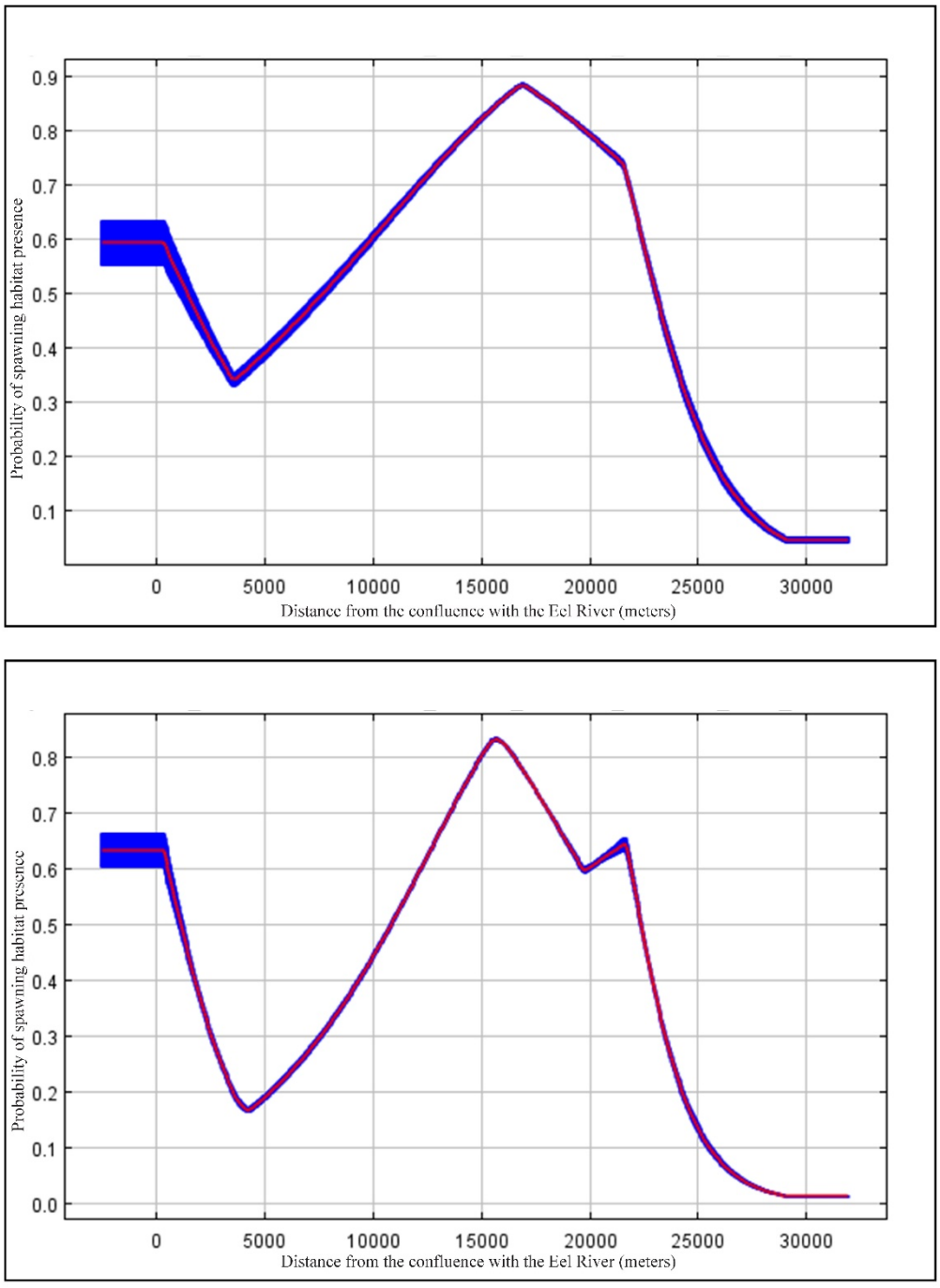

Figure 68 MaxEnt results - Coho spawning habitat, response curves for distance from the confluence of Indian Creek with the Eel River. Upper curve shows probability response while keeping all other environmental variables constant; lower curve represents response when MaxEnt probability model is derived using only the single variable.

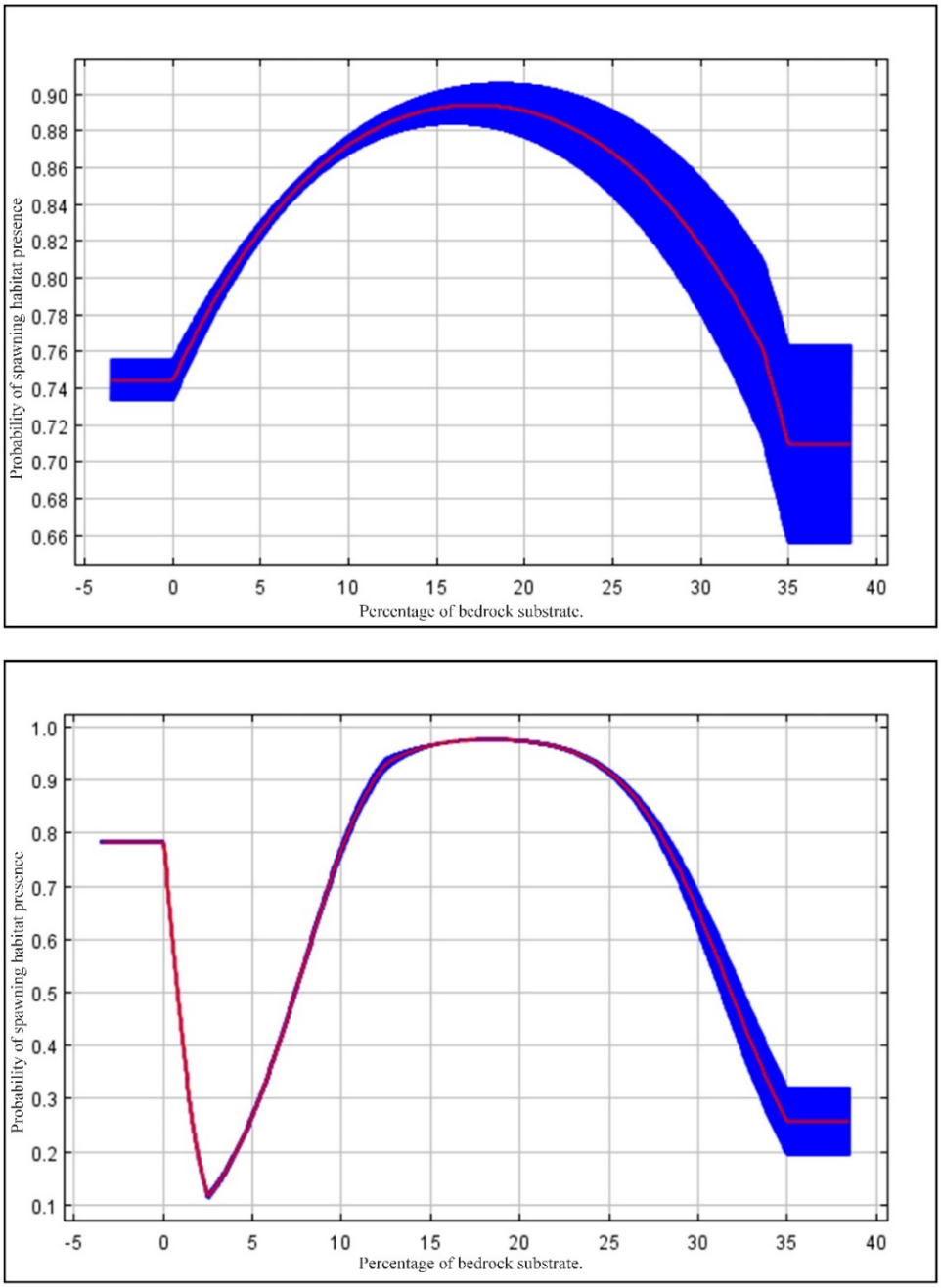

Figure 69 MaxEnt results - Coho spawning habitat, response curves for percentage of bedrock substrate. Upper curve shows probability response while keeping all other environmental variables constant; lower curve represents response when MaxEnt probability model is derived using only the single variable. Red denotes average response over 100 replicated runs; blue denotes +/- 1 standard deviation.

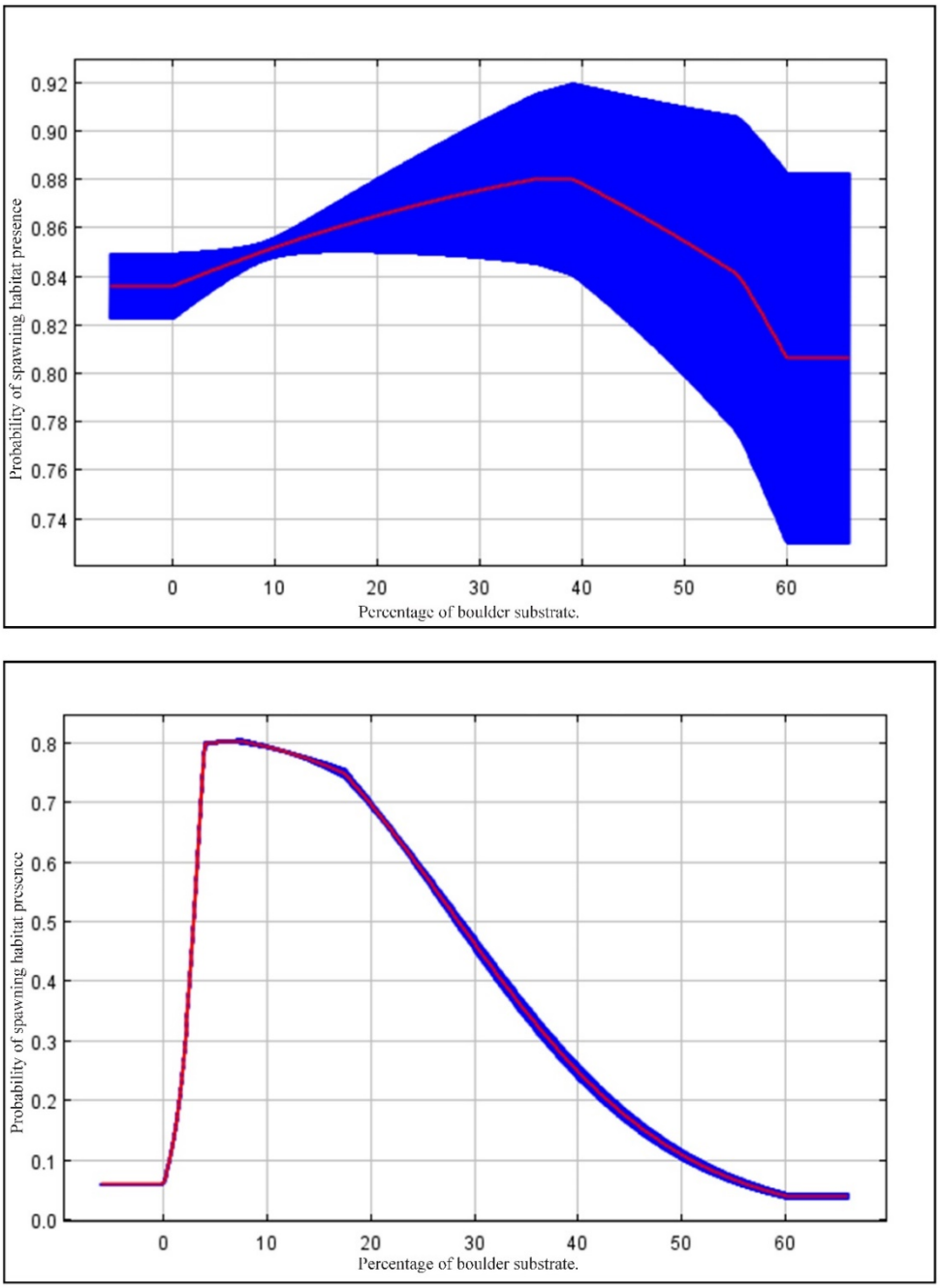

Figure 70. MaxEnt results – Coho spawning habitat, response curves for percentage of boulder substrate. Upper curve shows probability response while keeping all other environmental variables constant; lower curve represents response when MaxEnt probability model is derived using only the single variable. Red denotes average response over 100 replicated runs; blue denotes +/- 1 standard deviation.

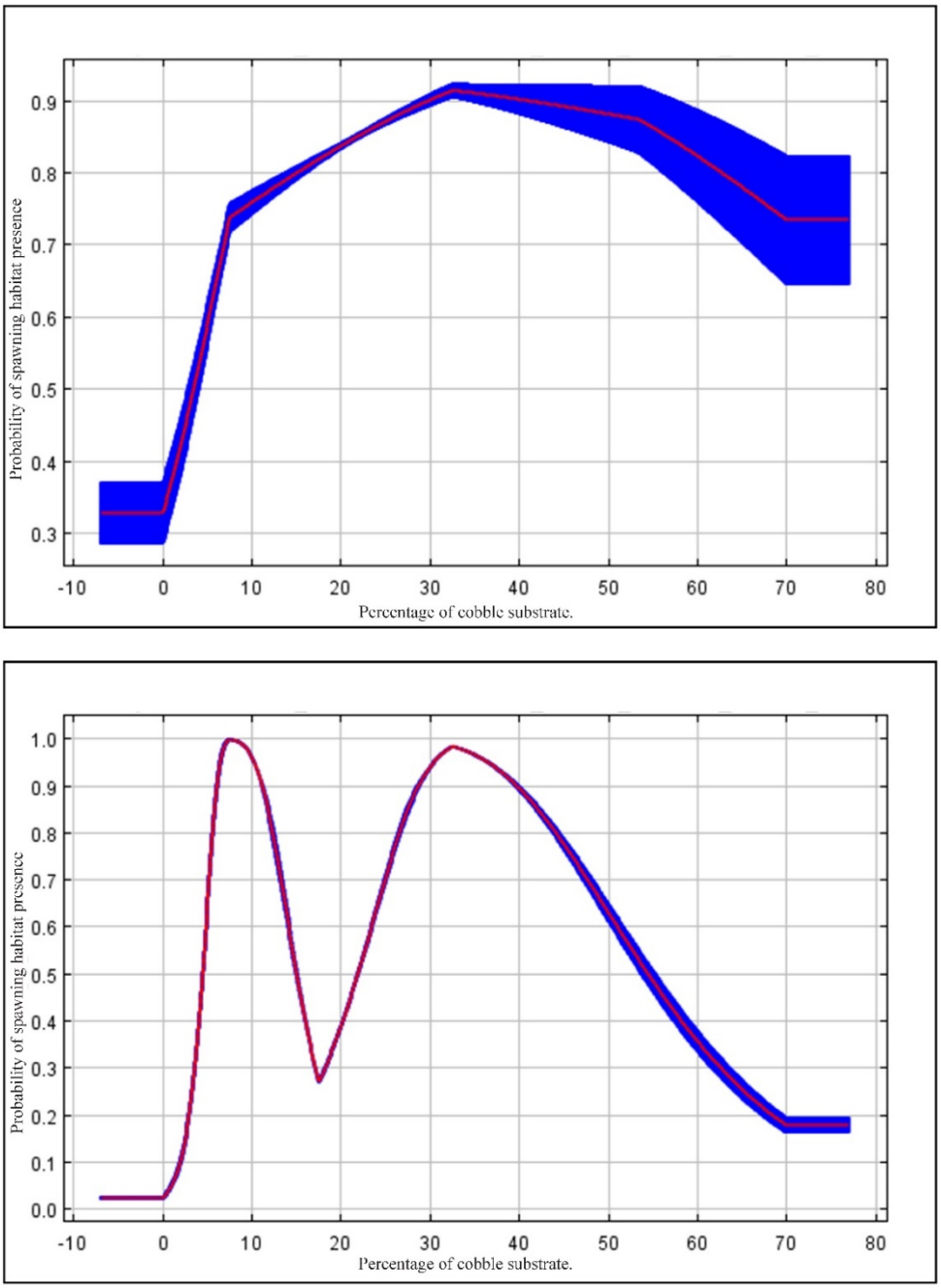

Figure 71. MaxEnt results – Coho spawning habitat, response curves for percentage of cobble substrate. Upper curve shows probability response while keeping all other environmental variables constant; lower curve represents response when MaxEnt probability model is derived using only the single variable. Red denotes average response over 100 replicated runs; blue denotes +/- 1 standard deviation.

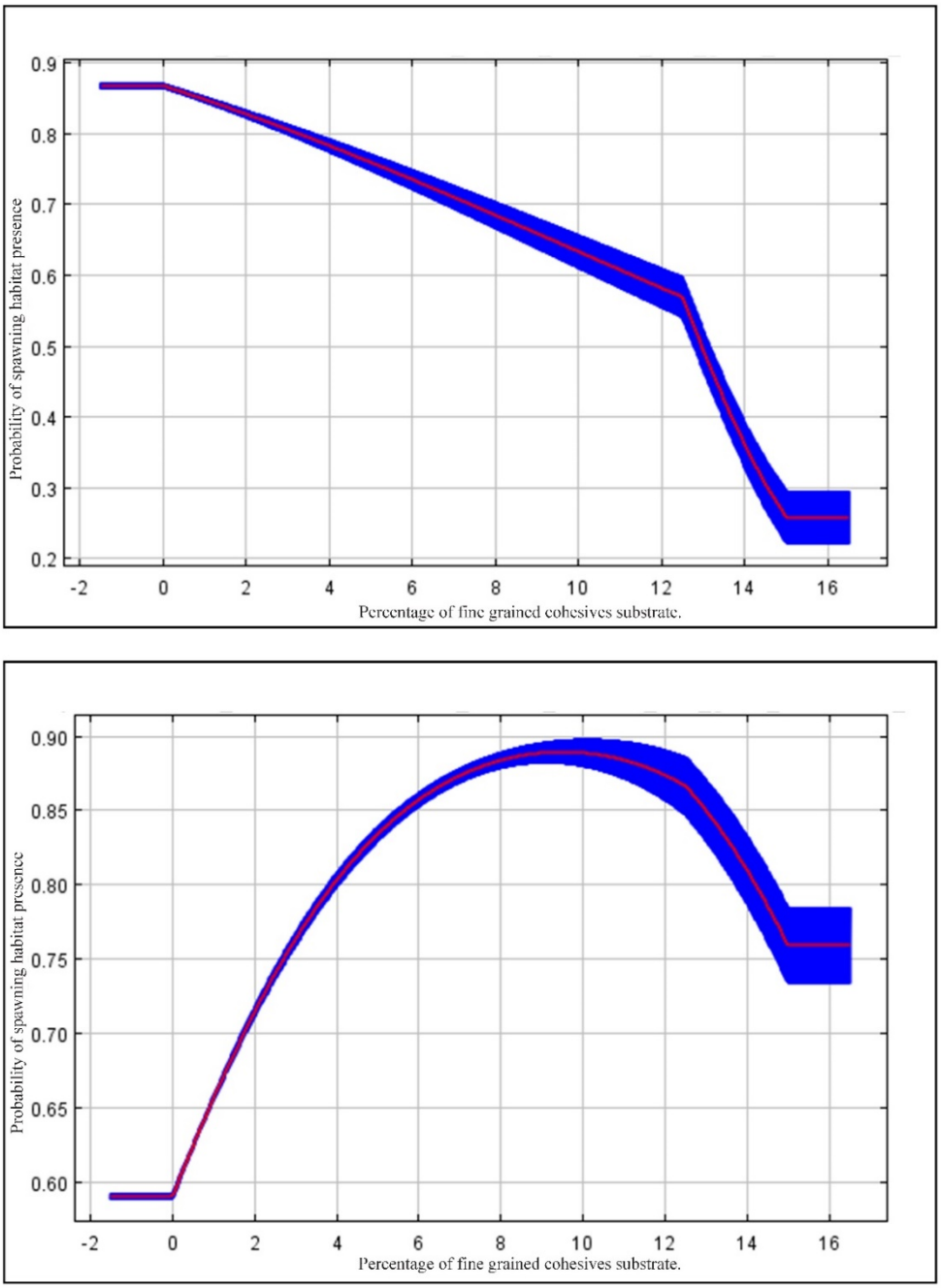

Figure 72. MaxEnt results - Coho spawning habitat, response curves for percentage of fine grained cohesives substrate. Upper curve shows probability response while keeping all other environmental variables constant; lower curve represents response when MaxEnt probability model is derived using only the single variable. Red denotes average response over 100 replicated runs; blue denotes +/- 1 standard deviation.

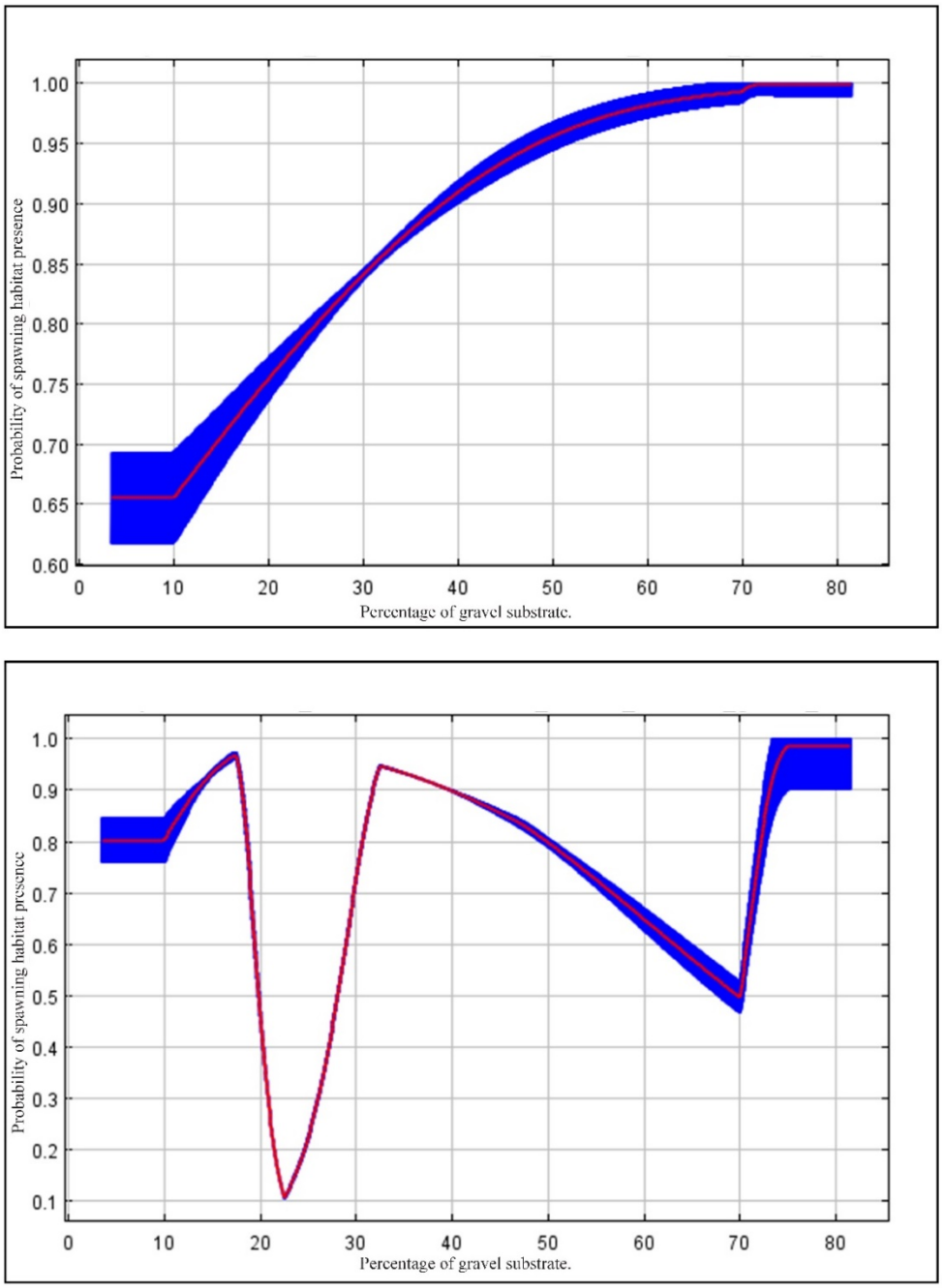

Figure 73. MaxEnt results- Coho spawning habitat, response curves for percentage of gravel substrate. Upper curve shows probability response while keeping all other environmental variables constant; lower curve represents response when MaxEnt probability model is derived using only the single variable. Red denotes average response over 100 replicated runs; blue denotes +/- 1 standard deviation.

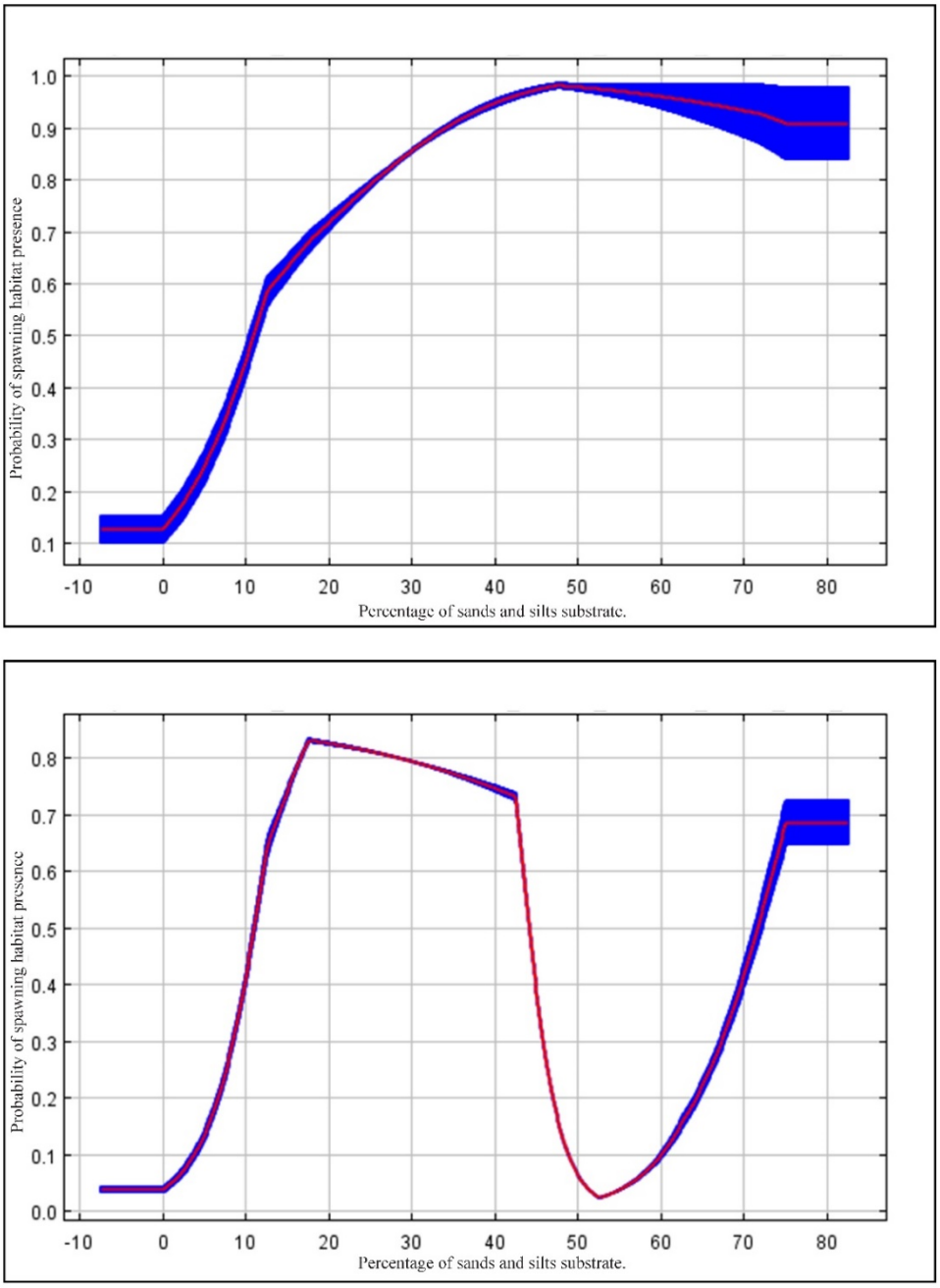

Figure 74. MaxEnt results - Coho spawning habitat, response curves for percentage of sands and silts substrate. Upper curve shows probability response while keeping all other environmental variables constant; lower curve represents response when MaxEnt probability model is derived using only the single variable. Red denotes average response over 100 replicated runs; blue denotes +/- 1 standard deviation.

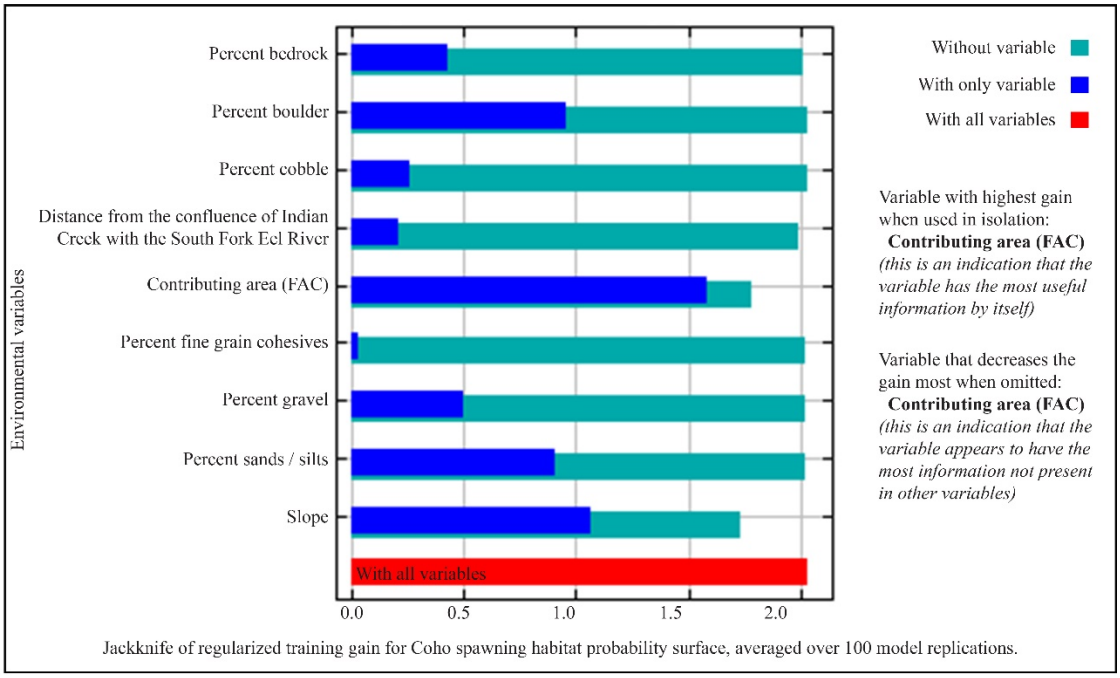

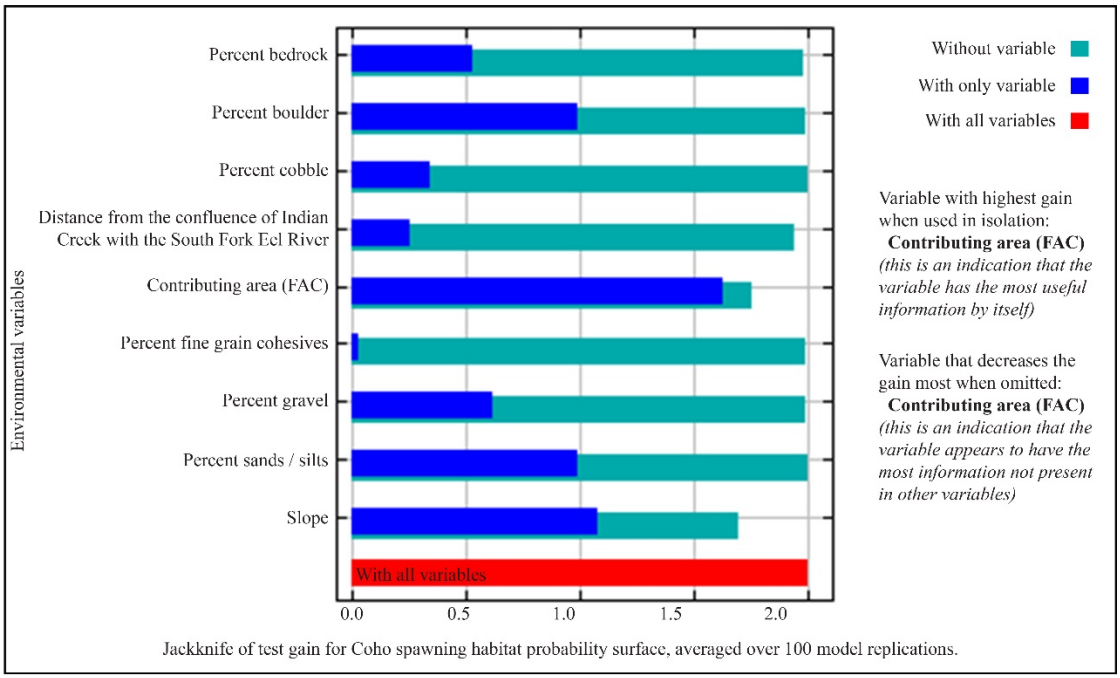

Figure 75. MaxEnt results - Coho spawning habitat, jackknife tests for environmental variable importance - regularized training gain (upper) and test gain (lower).

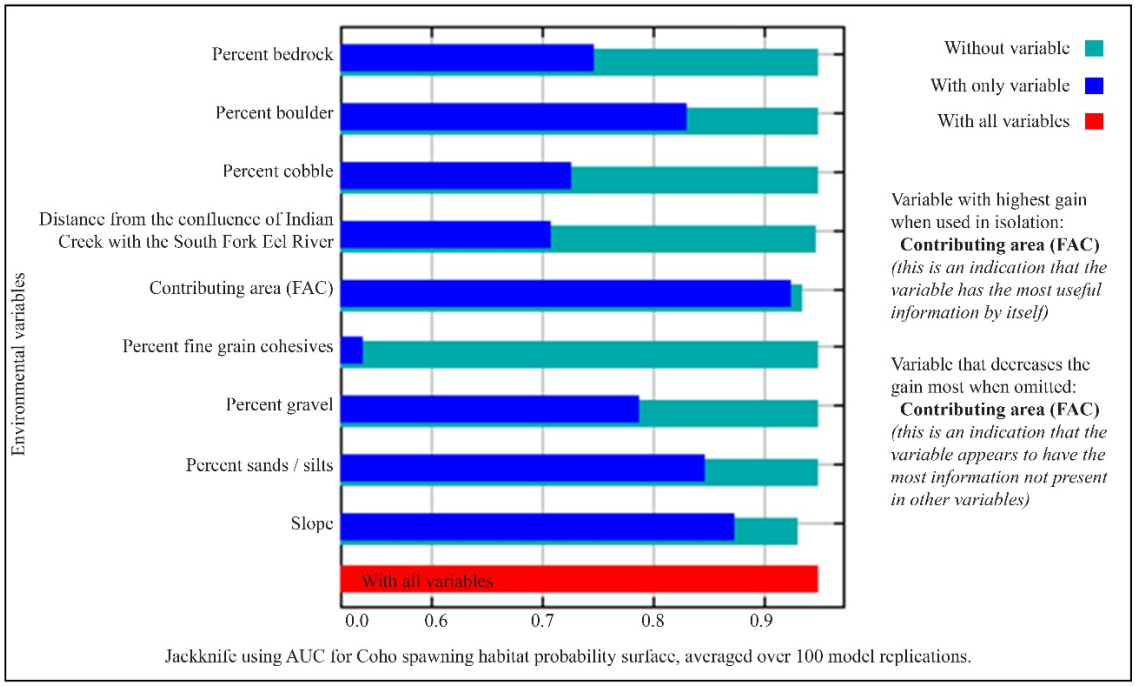

Environmental variable:	Percent contribution	Permutation importance
Contributing area (FAC)	70	72.3
Slope	15.4	15.5
Distance from the confluence of Indian Creek with the South Fork Eel River	9.7	5.1
Substrate: Percentage bedrock	0.9	0.9
Substrate: Percentage boulder	0.6	0.7
Substrate: Percentage cobble	0.8	0.9
Substrate: Percentage fine grain cohesives	0.6	0.5
Substrate: Percentage gravel	0.2	0.5
Substrate: Percentage sands/silts	1.7	3.5

Figure 76. MaxEnt results - Coho spawning habitat, jackknife test using AUC for environmental variable contributions.

APPENDIX E: MAXENT MODELING RESULTS - RESPONSE CURVES FOR STEELHEAD

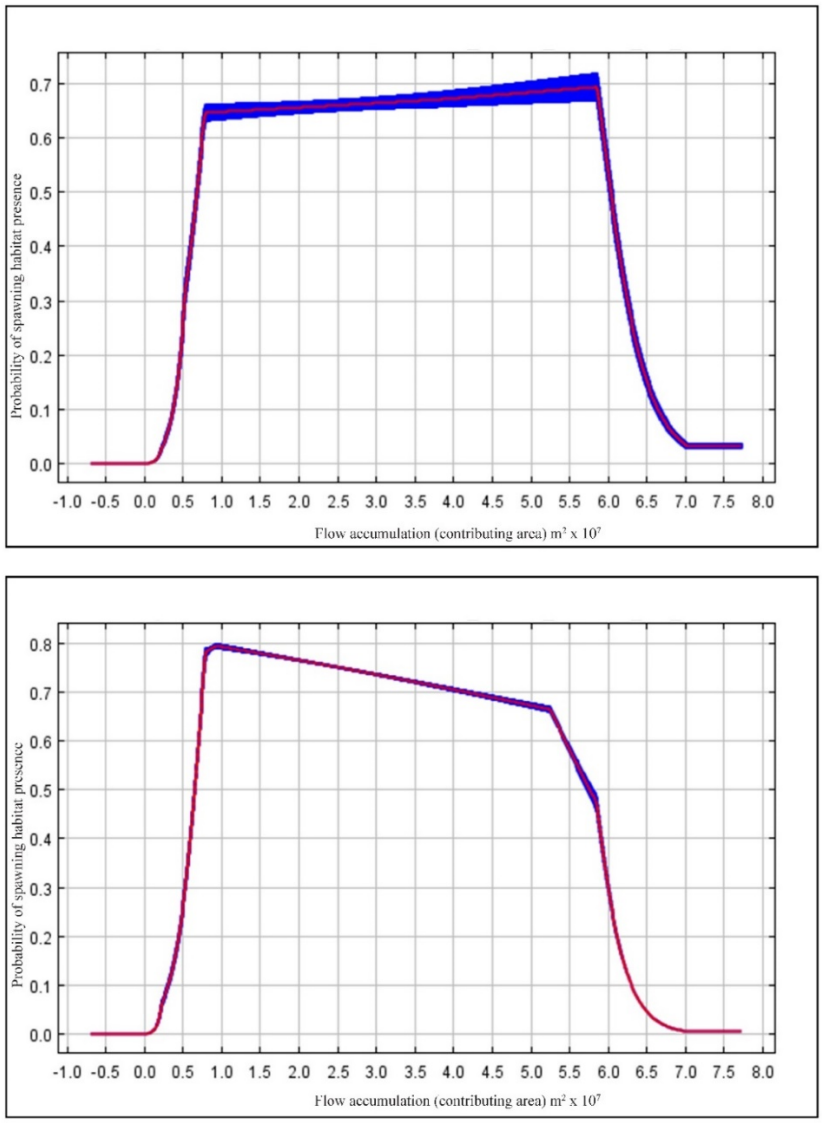

Figure 77. MaxEnt results - Steelhead spawning habitat, response curves for flow accumulation (contributing area). Upper curve shows probability response while keeping all other environmental variables constant; lower curve represents response when MaxEnt probability model is derived using only the single variable. Red denotes average response over 100 replicated runs; blue denotes +/- 1 standard deviation.

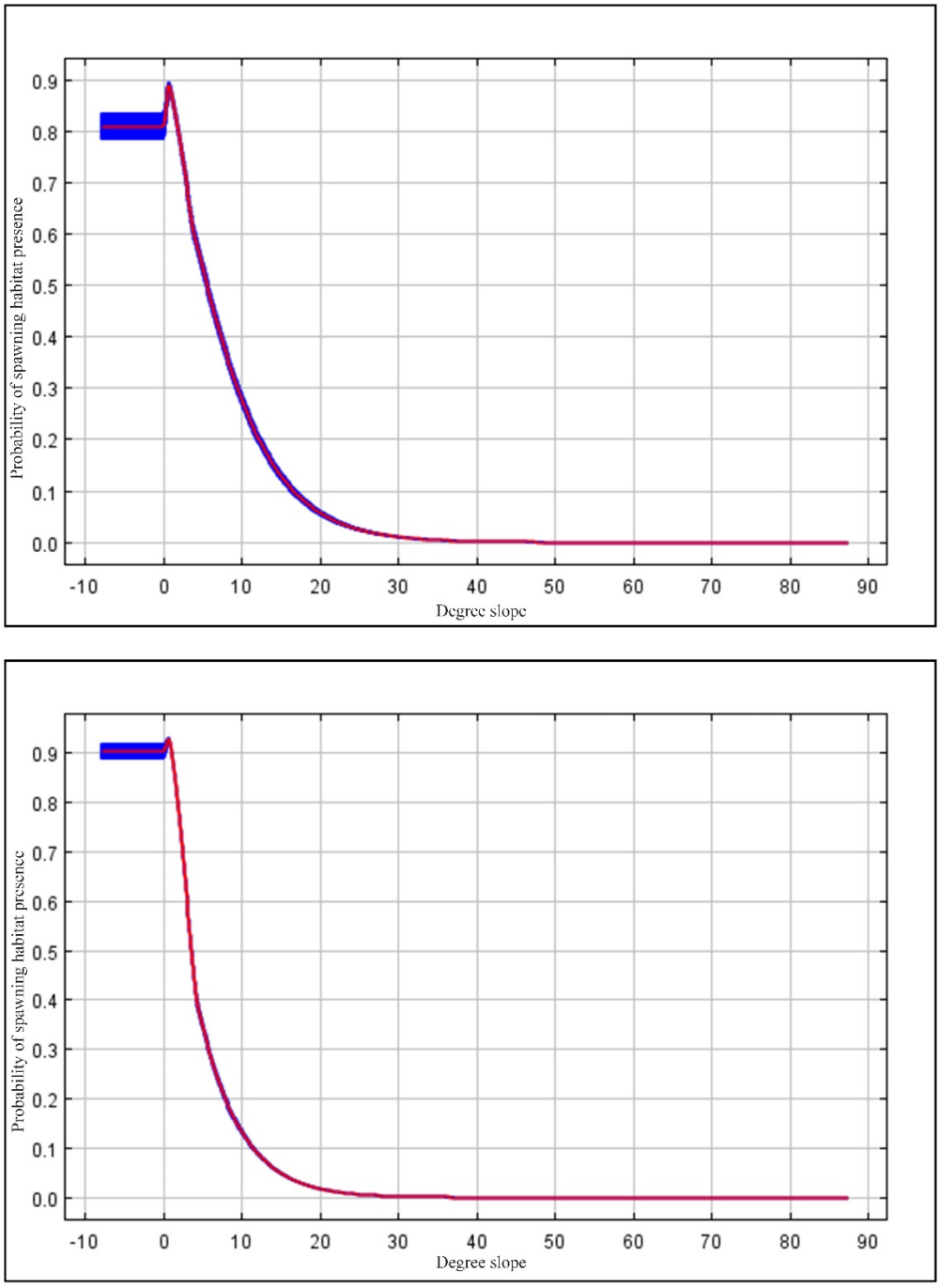

Figure 78. MaxEnt results - Steelhead spawning habitat, response curves for degree slope. Upper curve shows probability response while keeping all other environmental variables constant; lower curve represents response when MaxEnt probability model is derived using only the single variable. Red denotes average response over 100 replicated runs; blue denotes +/- 1 standard deviation.

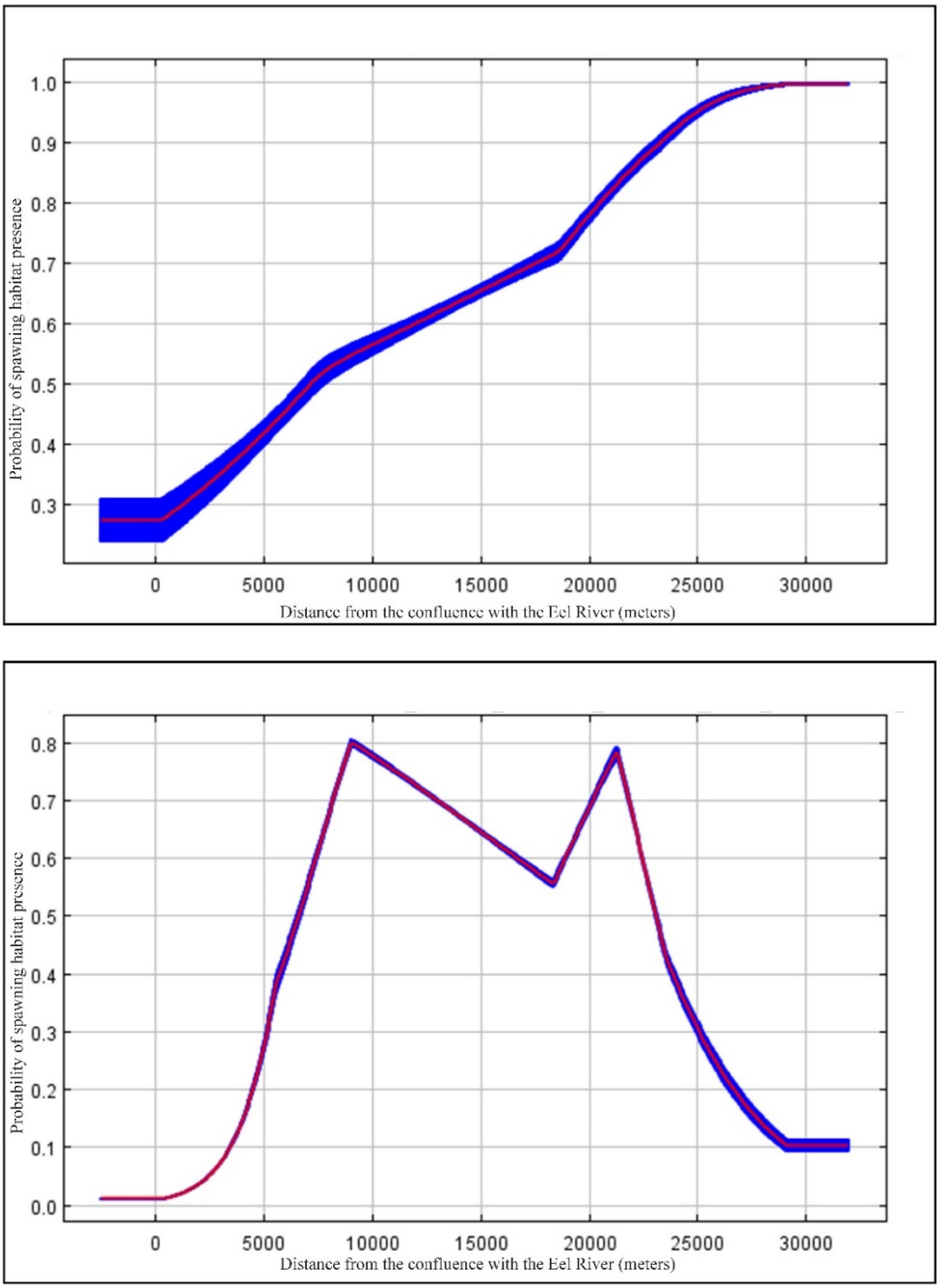

Figure 79. MaxEnt results - Steelhead spawning habitat, response curves for distance from the confluence of Indian Creek with the Eel River. Upper curve shows probability response while keeping all other environmental variables constant; lower curve represents response when MaxEnt probability model is derived using only the single variable. Red denotes average response over 100 replicated runs; blue denotes +/- 1 standard deviation.

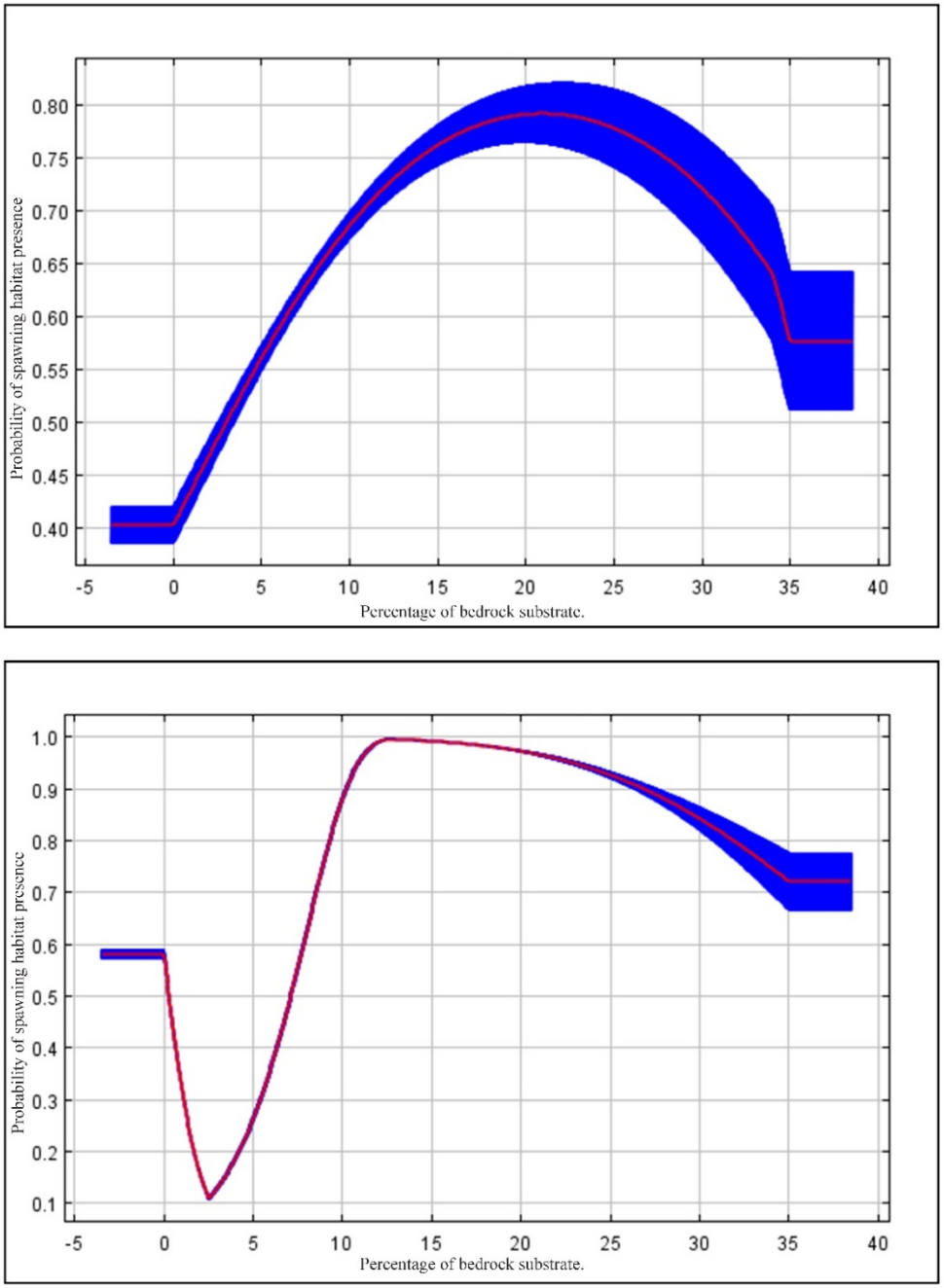

Figure 80. MaxEnt results - Steelhead spawning habitat, response curves for percentage of bedrock substrate. Upper curve shows probability response while keeping all other environmental variables constant; lower curve represents response when MaxEnt probability model is derived using only the single variable. Red denotes average response over 100 replicated runs; blue denotes +/- 1 standard deviation.

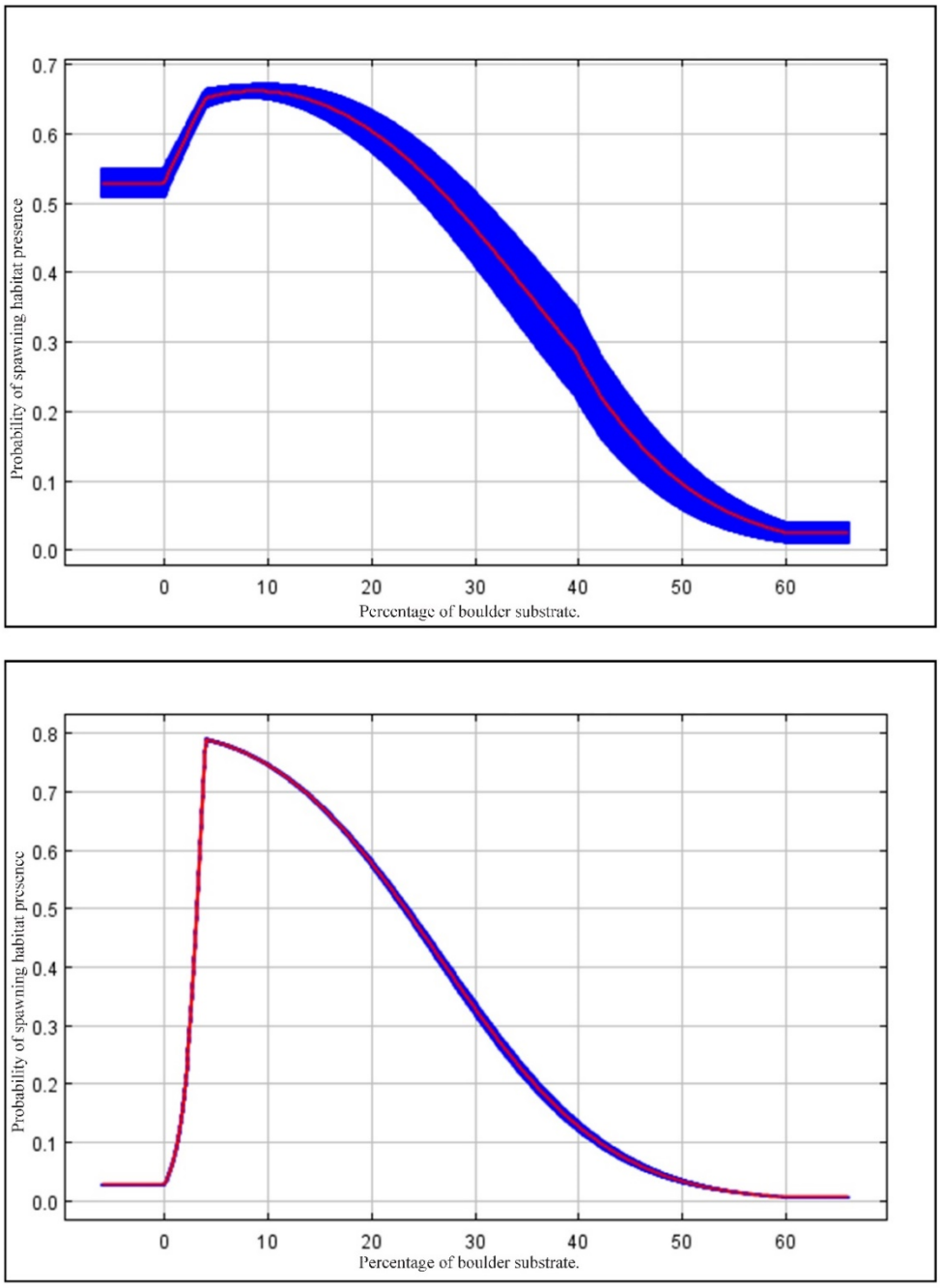

Figure 81. MaxEnt results - Steelhead spawning habitat, response curves for percentage of boulder substrate. Upper curve shows probability response while keeping all other environmental variables constant; lower curve represents response when MaxEnt probability model is derived using only the single variable. Red denotes average response over 100 replicated runs; blue denotes +/- 1 standard deviation.

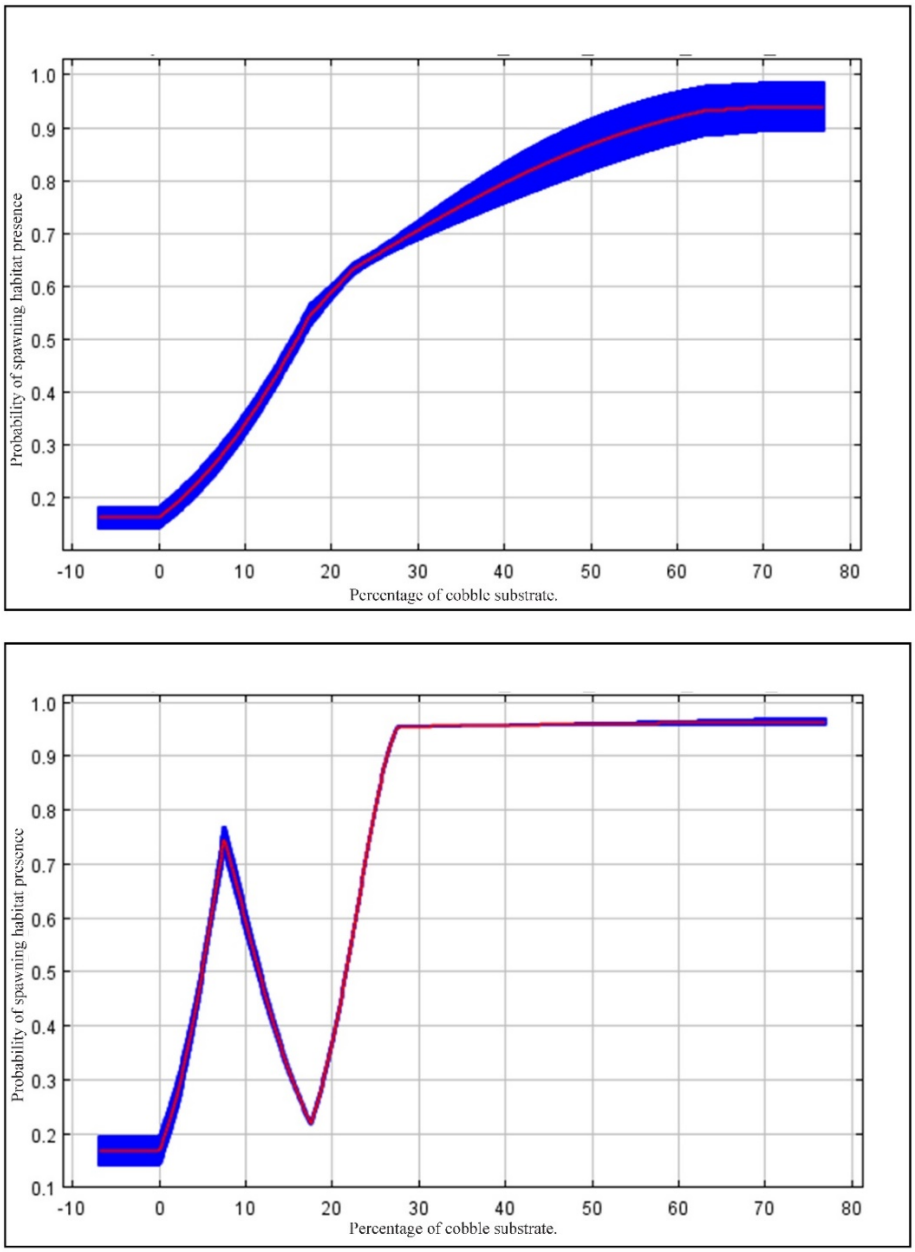

Figure 82. MaxEnt results - Steelhead spawning habitat, response curves for percentage of cobble substrate. Upper curve shows probability response while keeping all other environmental variables constant; lower curve represents response when MaxEnt probability model is derived using only the single variable. Red denotes average response over 100 replicated runs; blue denotes +/- 1 standard deviation.

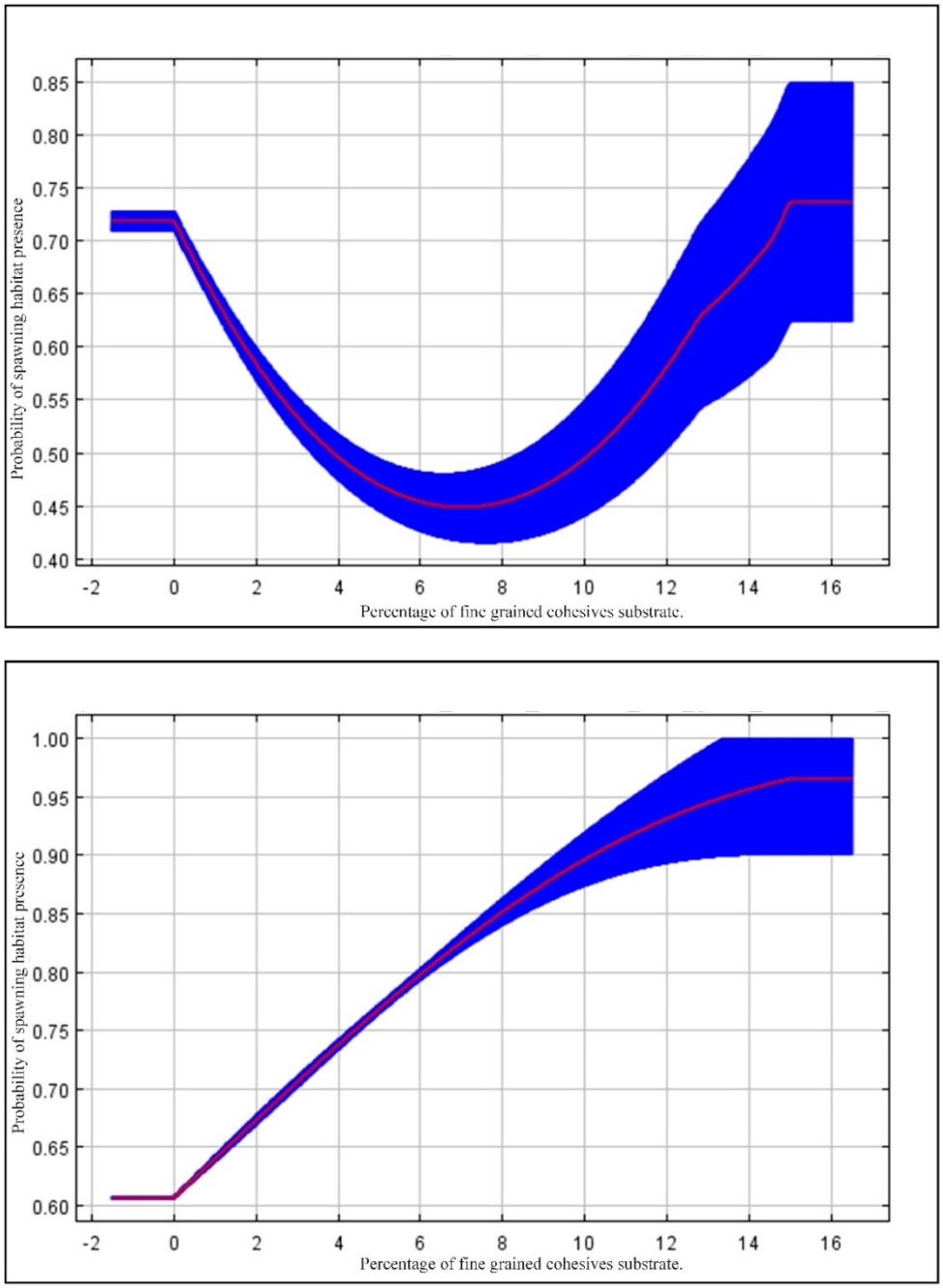

Figure 83. MaxEnt results - Steelhead spawning habitat, response curves for percentage of fine grained cohesives substrate. Upper curve shows probability response while keeping all other environmental variables constant; lower curve represents response when MaxEnt probability model is derived using only the single variable. Red denotes average response over 100 replicated runs; blue denotes +/- 1 standard deviation.

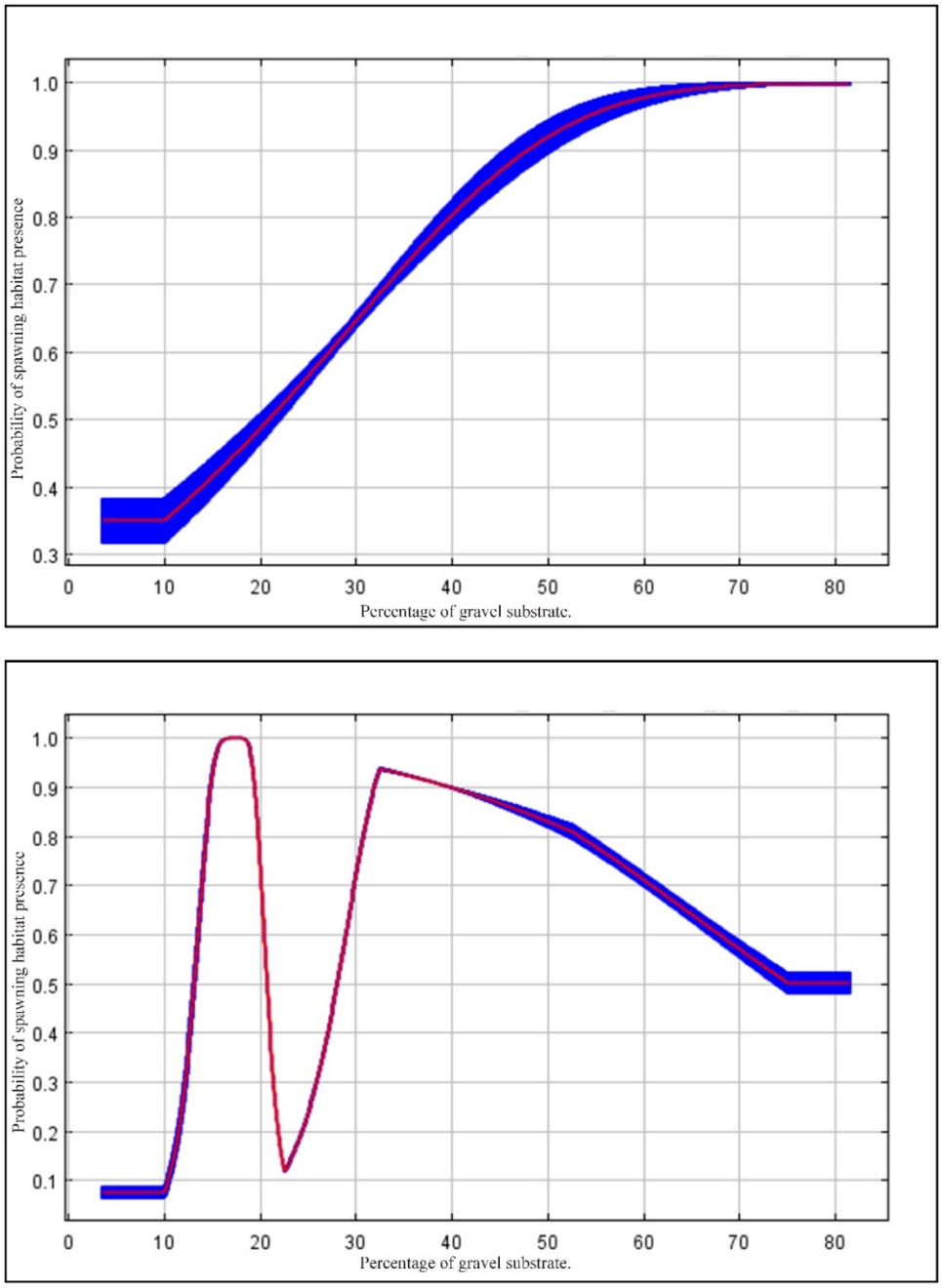

Figure 84. MaxEnt results - Steelhead spawning habitat, response curves for percentage of gravel substrate. Upper curve shows probability response while keeping all other environmental variables constant; lower curve represents response when MaxEnt probability model is derived using only the single variable. Red denotes average response over 100 replicated runs; blue denotes +/- 1 standard deviation.

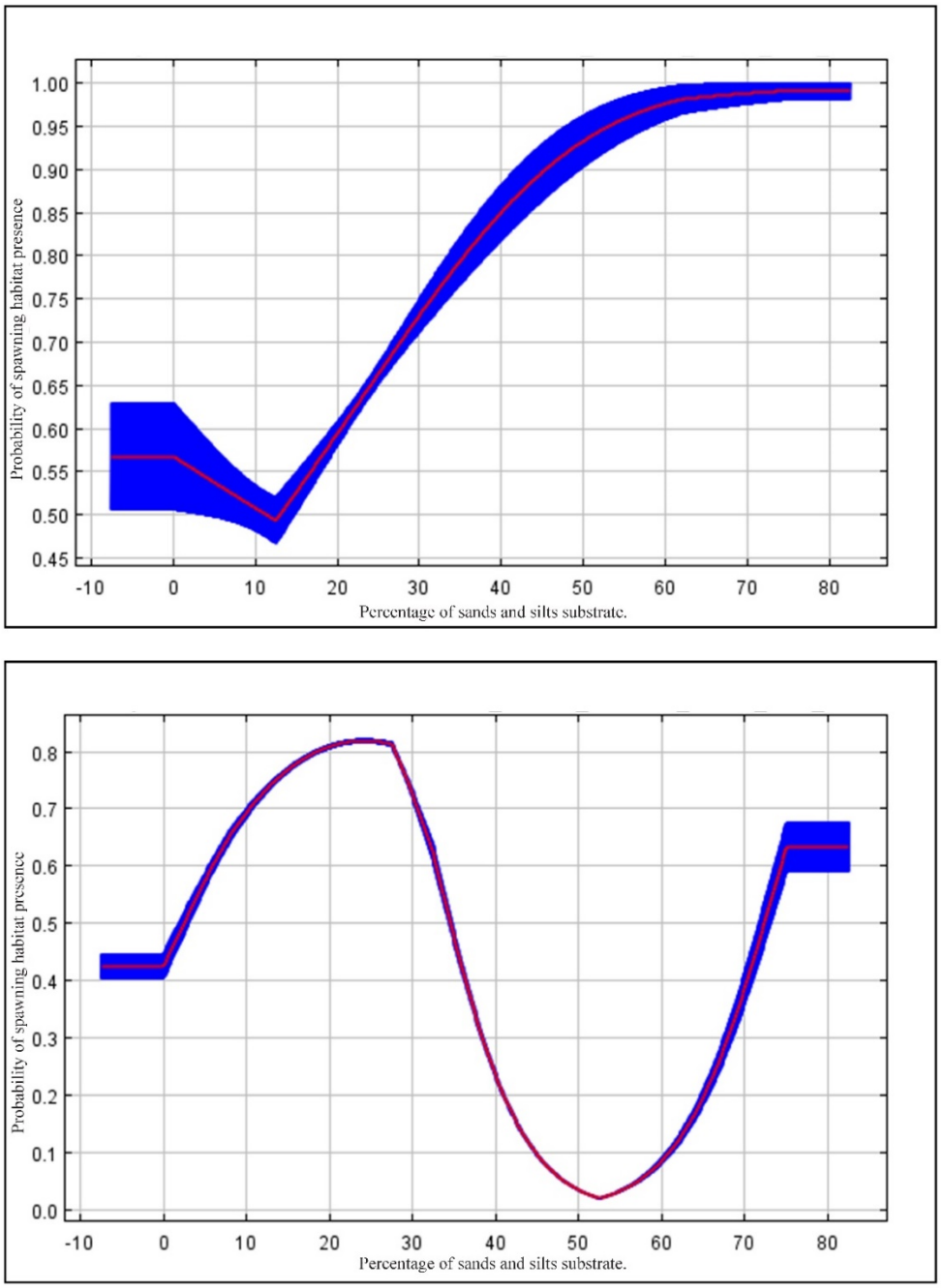

Figure 85. MaxEnt results - Steelhead spawning habitat, response curves for percentage of sands and silts substrate. Upper curve shows probability response while keeping all other environmental variables constant; lower curve represents response when MaxEnt probability model is derived using only the single variable. Red denotes average response over 100 replicated runs; blue denotes +/- 1 standard deviation.

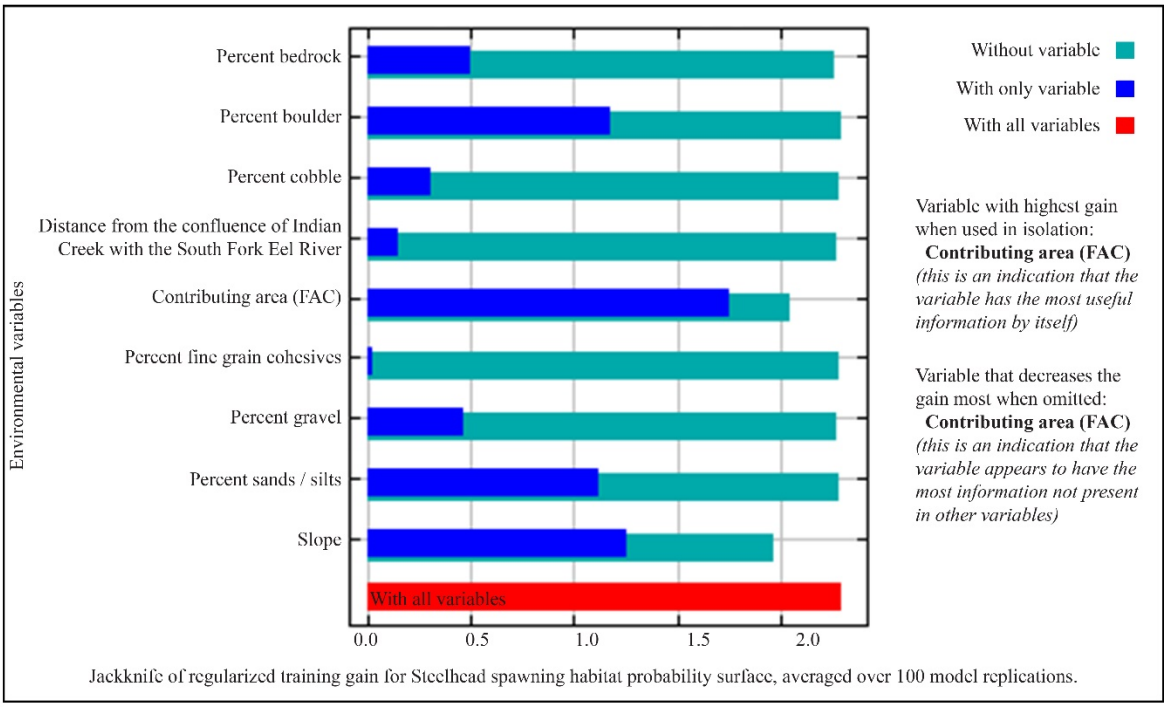

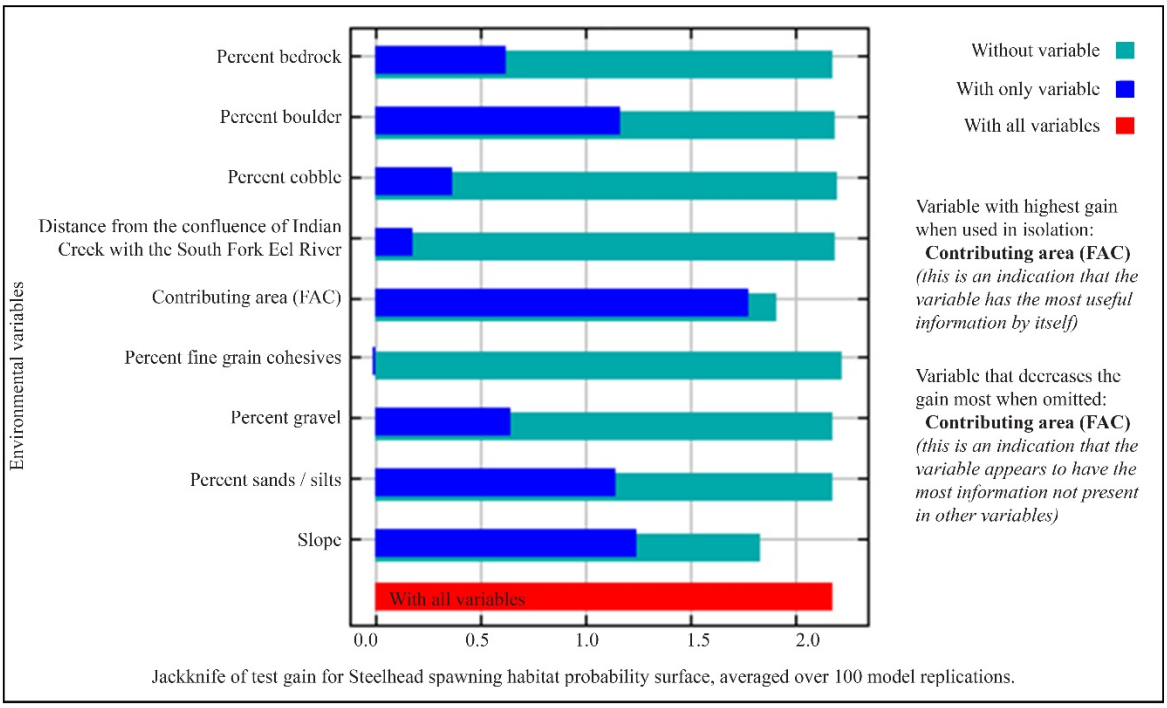

Figure 86. MaxEnt results - Steelhead spawning habitat, jackknife tests for environmental variable importance - regularized training gain (upper) and test gain (lower).

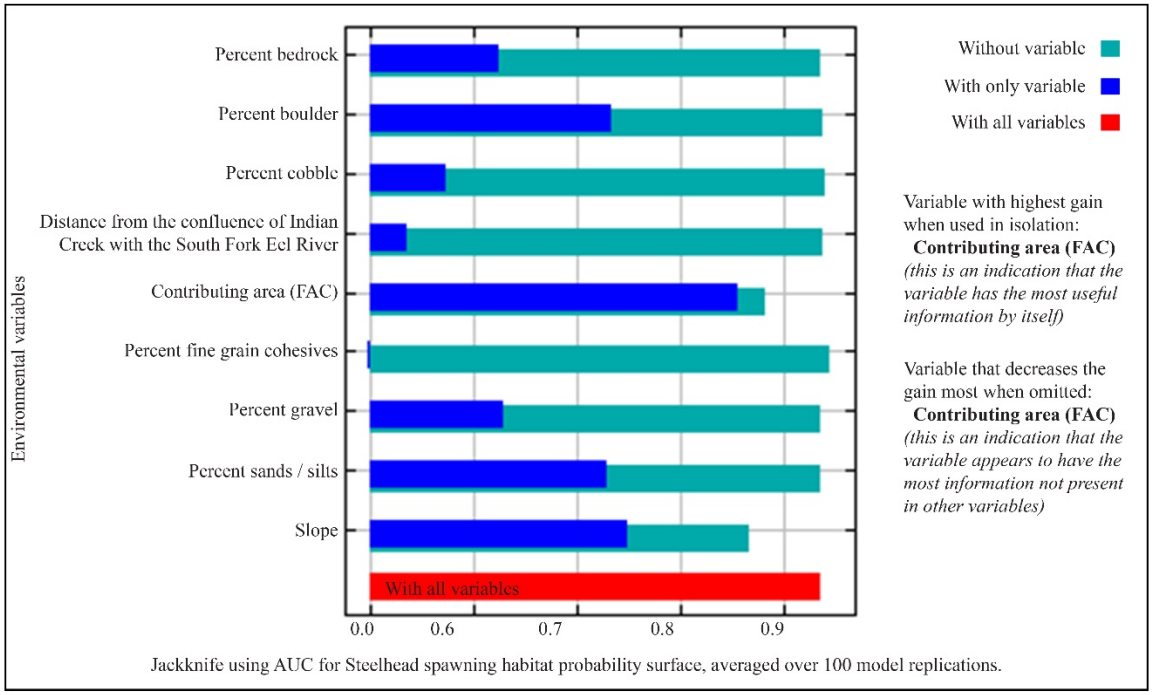

Environmental variable:	Percent contribution	Permutation importance
Contributing area (FAC)	74.1	76.2
Slope	16.3	16.8
Distance from the confluence of Indian Creek with the South Fork Eel River	3.3	1.7
Substrate: Percentage bedrock	2	1.2
Substrate: Percentage boulder	1.3	0.3
Substrate: Percentage cobble	0.5	0.9
Substrate: Percentage fine grain cohesives	1.1	0.7
Substrate: Percentage gravel	0.8	0.8
Substrate: Percentage sands/silts	0.6	1.4

Figure 87. MaxEnt results - Steelhead spawning habitat, jackknife test using AUC for environmental variable contributions.

APPENDIX F: PHOTO POINT LOCATIONS DURING SITE VISITS TO SELECTED LOCATIONS WITHIN THE ANDERSON CREEK SUBWATERSHED OF THE INDIAN CREEK WATERSHED PROJECT AREA, WITH CARTOGRAPHIC REPRESENTATIONS OF CORRESPONDING SPAWNING HABITAT MODEL RESULTS.

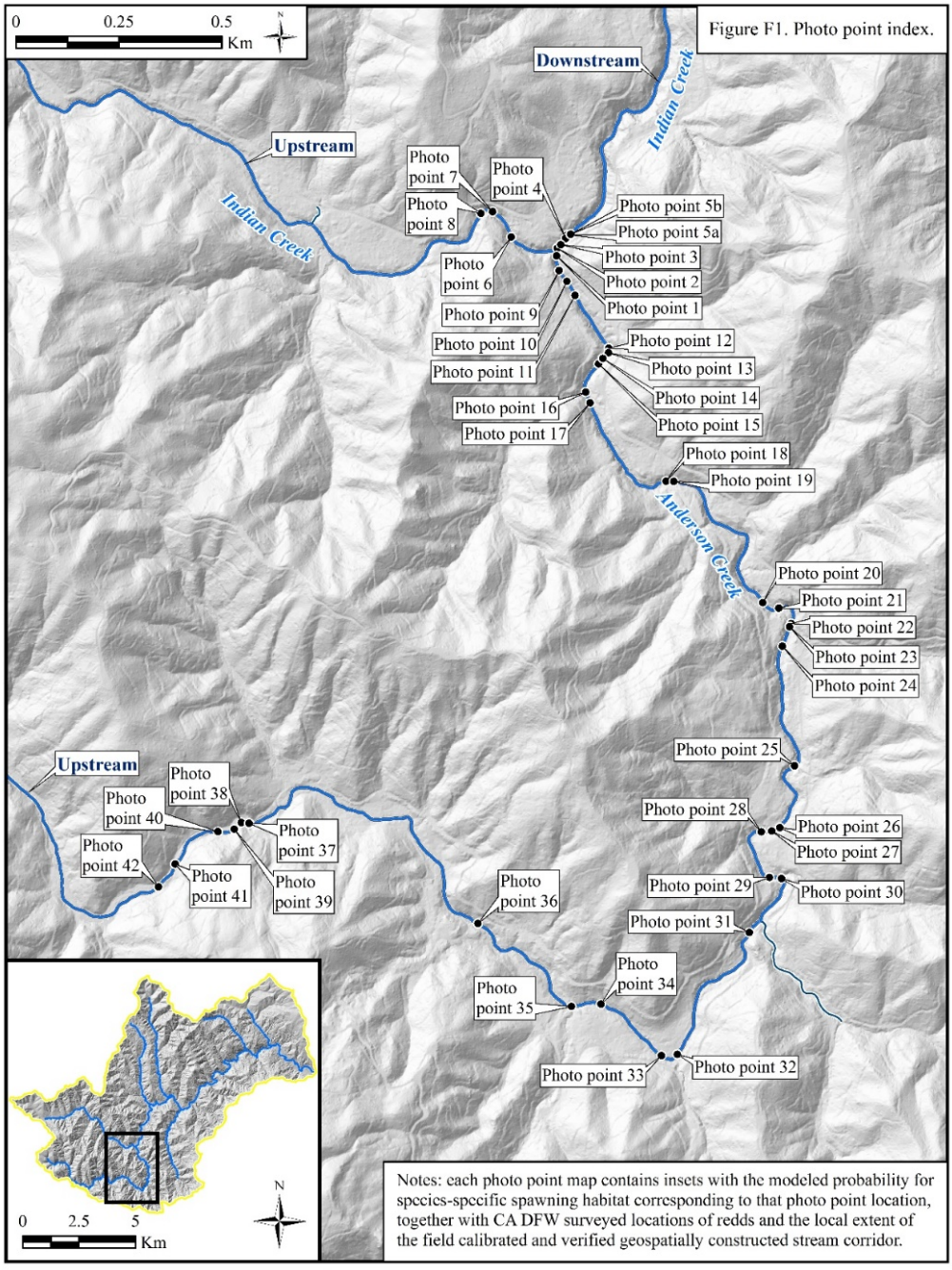

Figure 88. Photo point index for successful modeling field-verification visit, Anderson Creek subwatershed.

Photo point 1. Confluence of Anderson Creek with Indian Creek, facing North

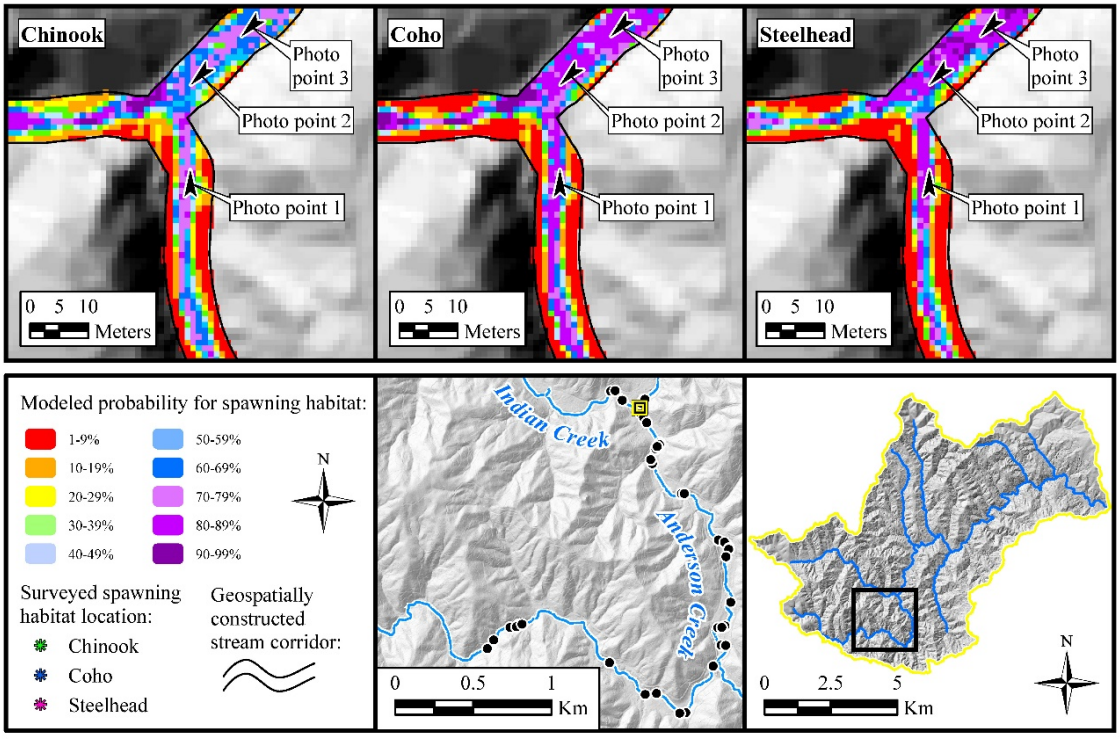

Figure 89. Photo point 1.

Photo point 2. Confluence of Anderson Creek with Indian Creek, facing Southwest

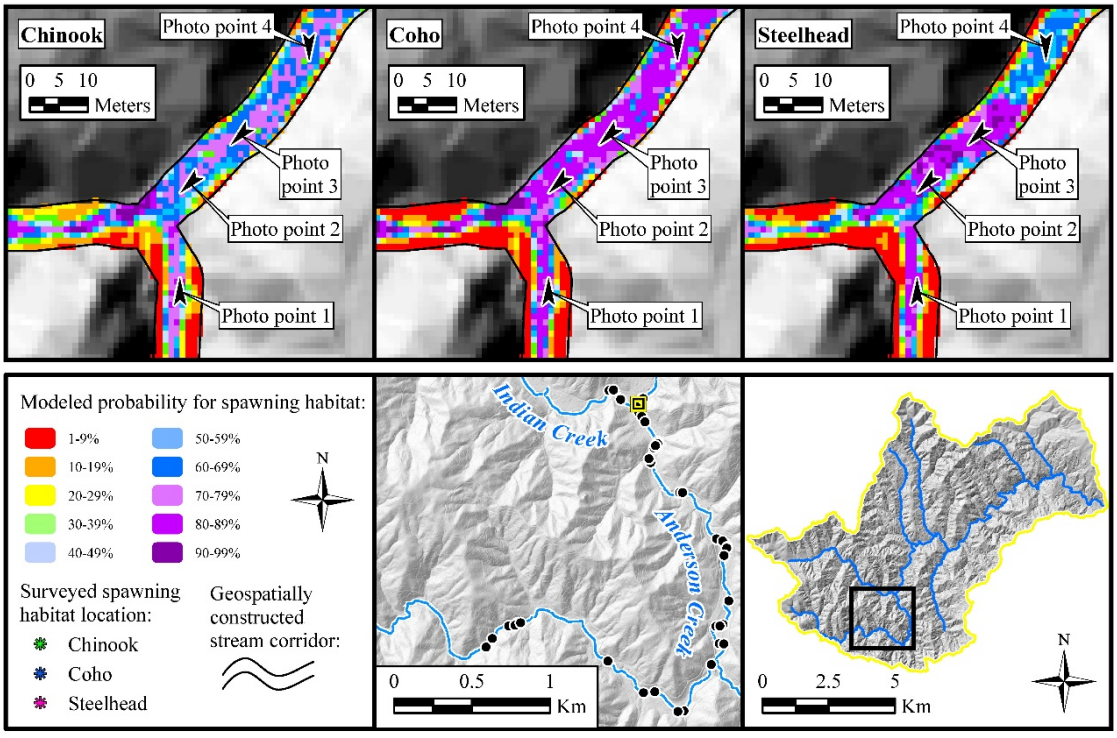

Figure 90. Photo point 2.

Photo point 3. Confluence of Anderson Creek with Indian Creek, facing Southwest

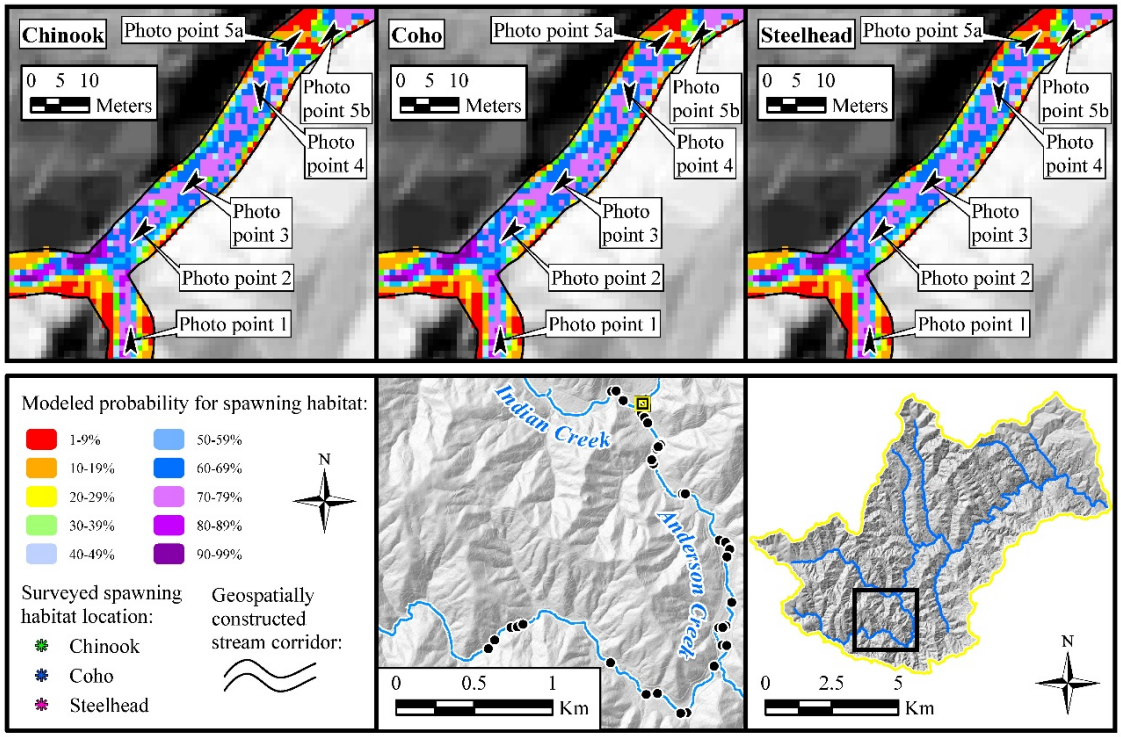

Figure 91. Photo point 3.

Photo point 4. Abrupt change in particle sizing percentages- gravel/cobble (right) to >80% bedrock near cascade area displayed in Photo points 5a-5b (upper left)

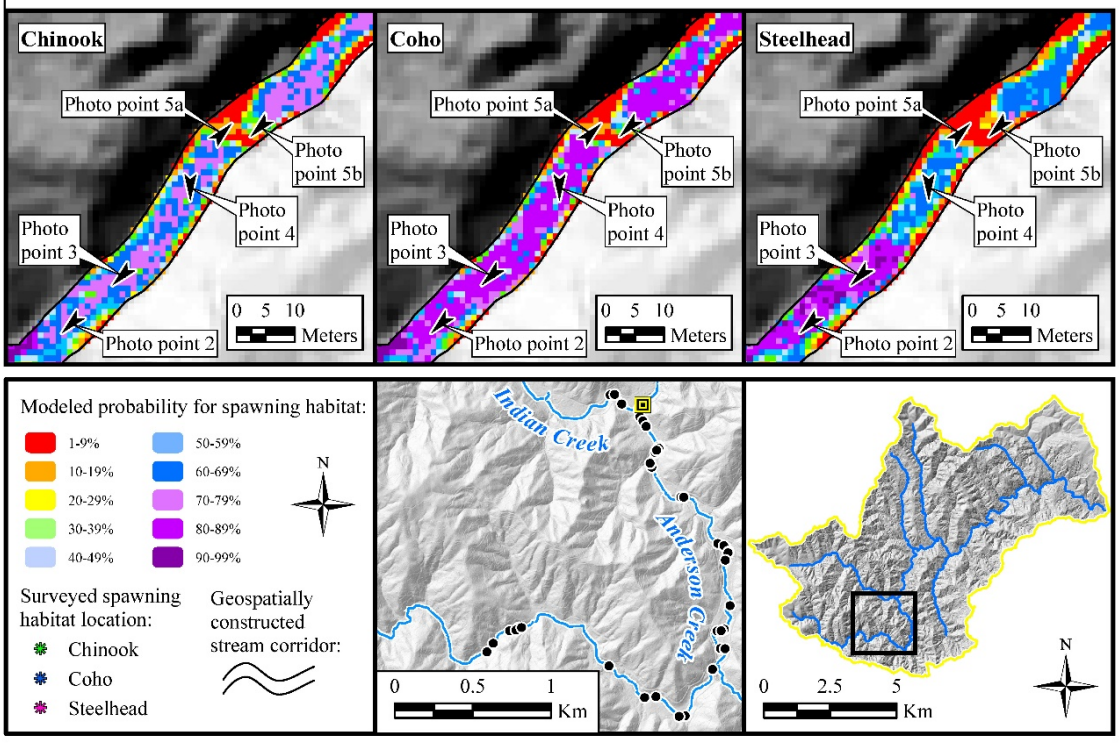

Figure 92. Photo point 4.

Photo point 5a. Cascade area with significant increase in slope, overlooking pool, facing Northeast downstream. Note significant decrease in spawning habitat probability at cascade bedrock/pour point.

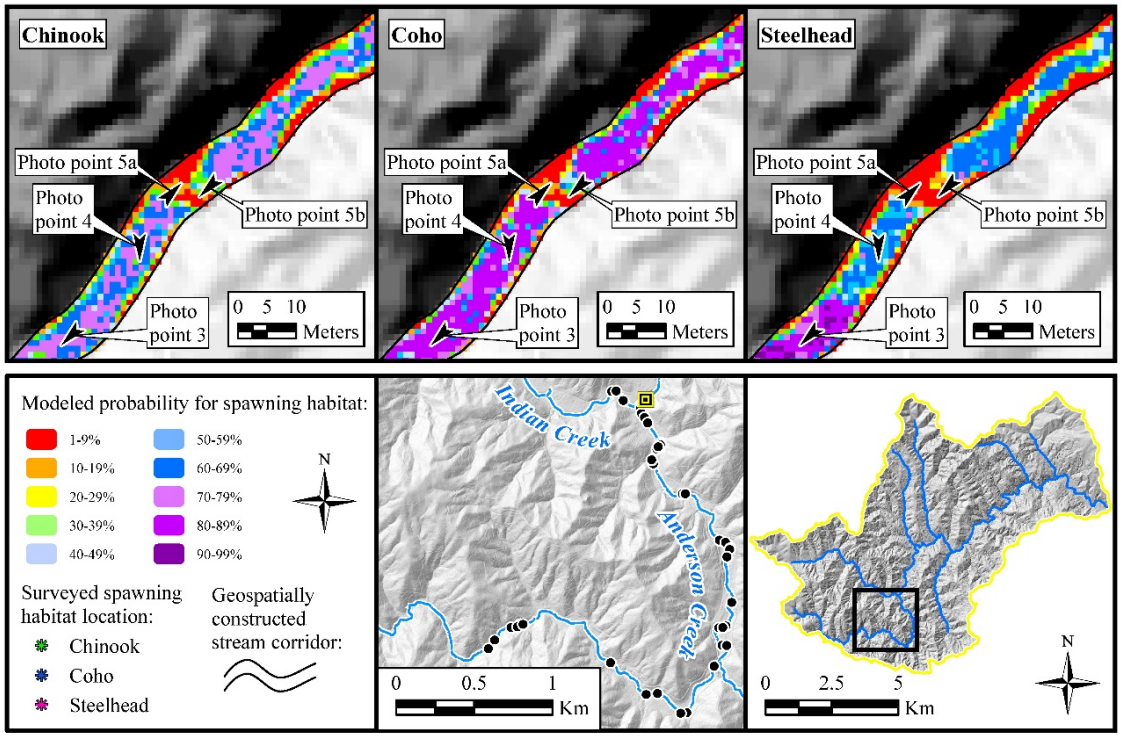

Figure 93. Photo point 5a.

Photo point 5b. Cascade area with significant increase in slope, facing Southwest upstream Indian Creek. Note increase in spawning habitat probability upstream from cascade area, transitioning at particle change noted in Photo point 4.

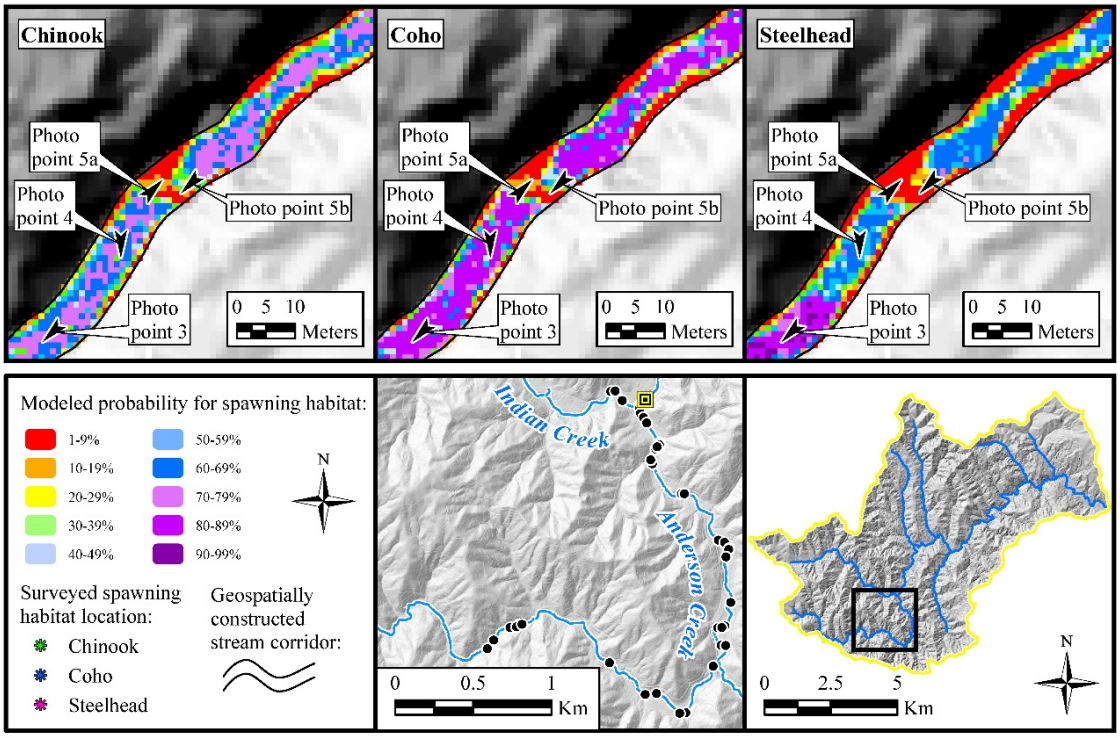

Figure 94. Photo point 5b.

Photo point 6. Facing upstream Indian Creek.

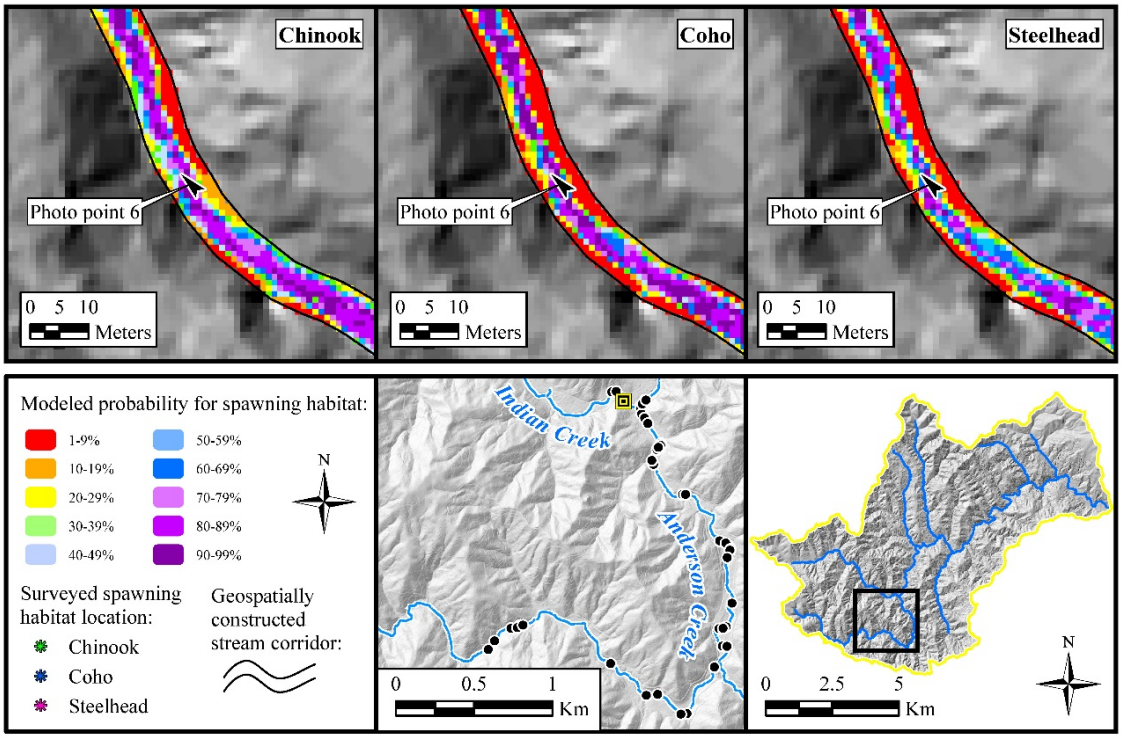

Figure 95. Photo point 6.

Photo point 7. Facing upstream Indian Creek.

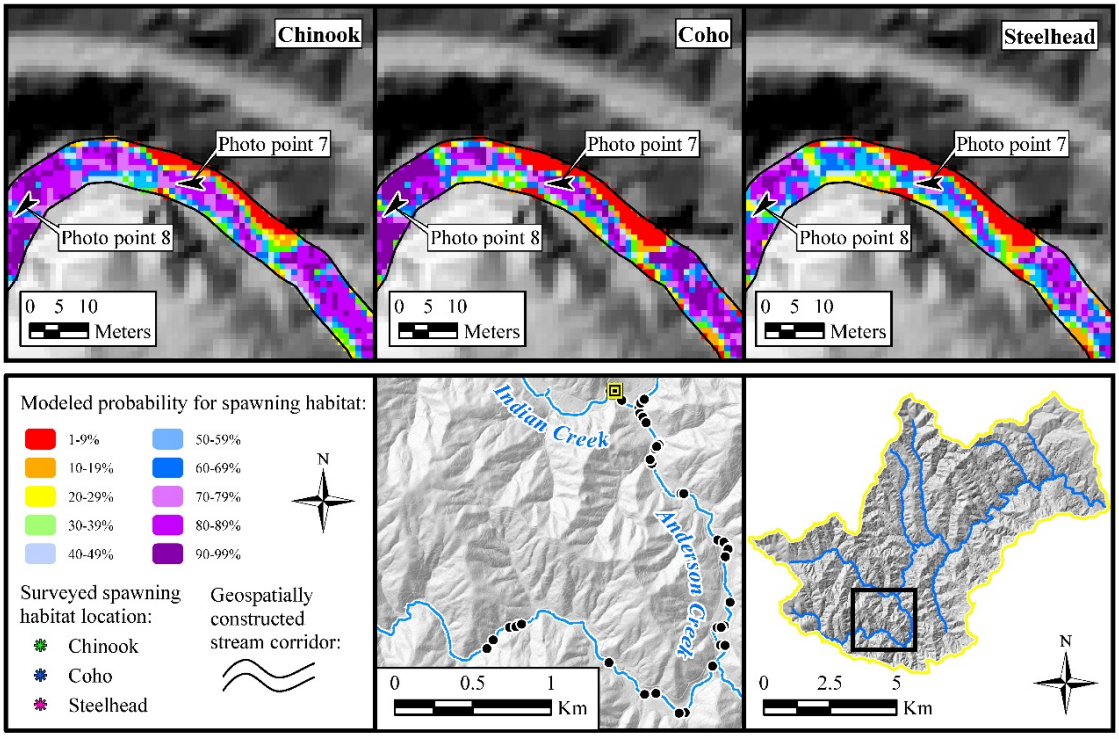

Figure 96. Photo point 7.

Photo point 8. Cascade area, facing upstream Indian Creek. Note sharp decrease in spawning habitat probability immediately opposite pool area at cascade.

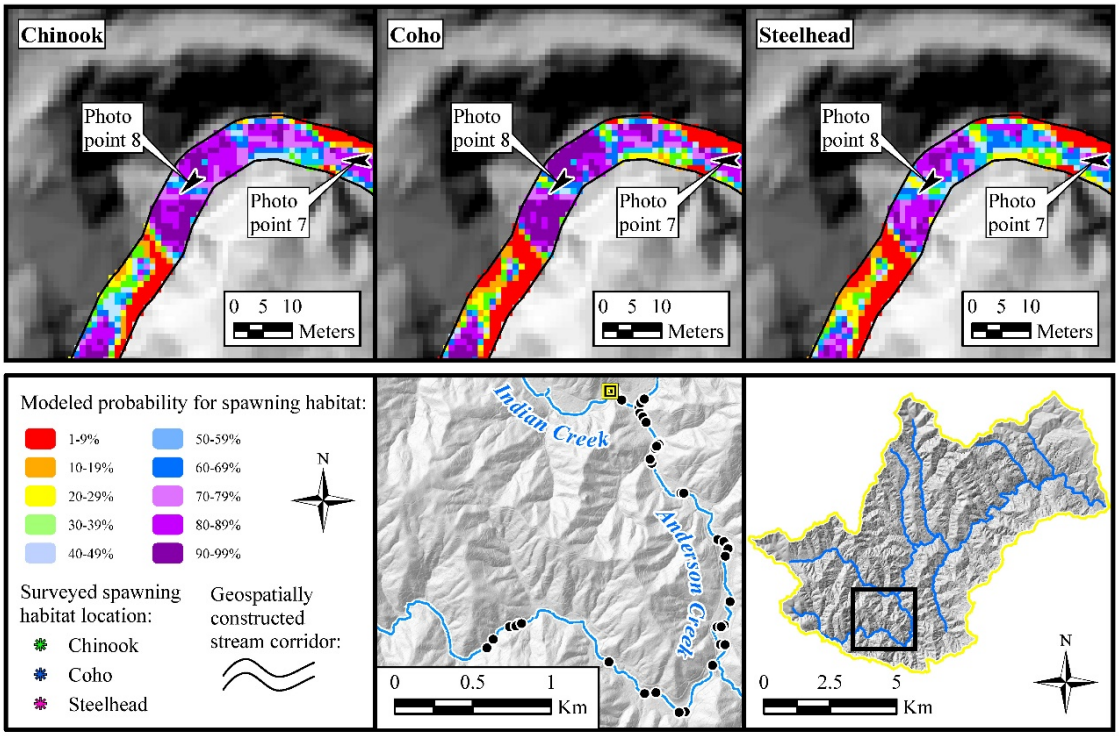

Figure 97. Photo point 8.

Photo point 9. Facing upstream Anderson Creek.

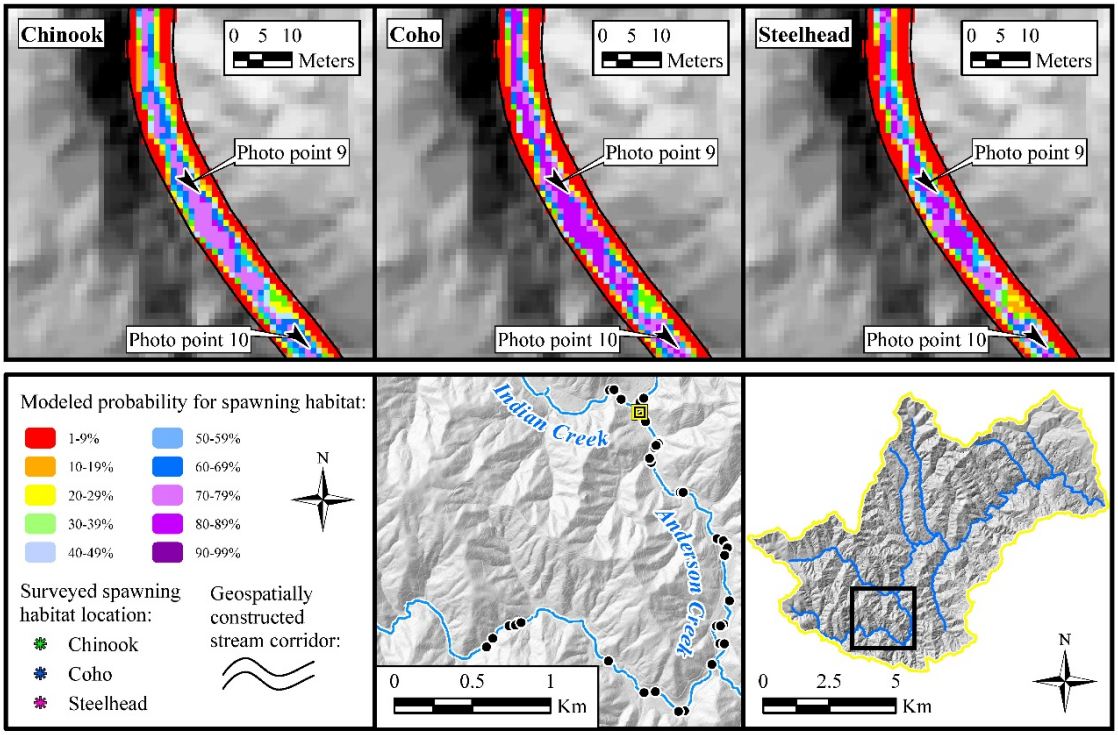

Figure 98. Photo point 9.

Photo point 10. Facing upstream Anderson Creek. Note constrained channel with high slope and decrease in spawning habitat probability on both sides of channel.

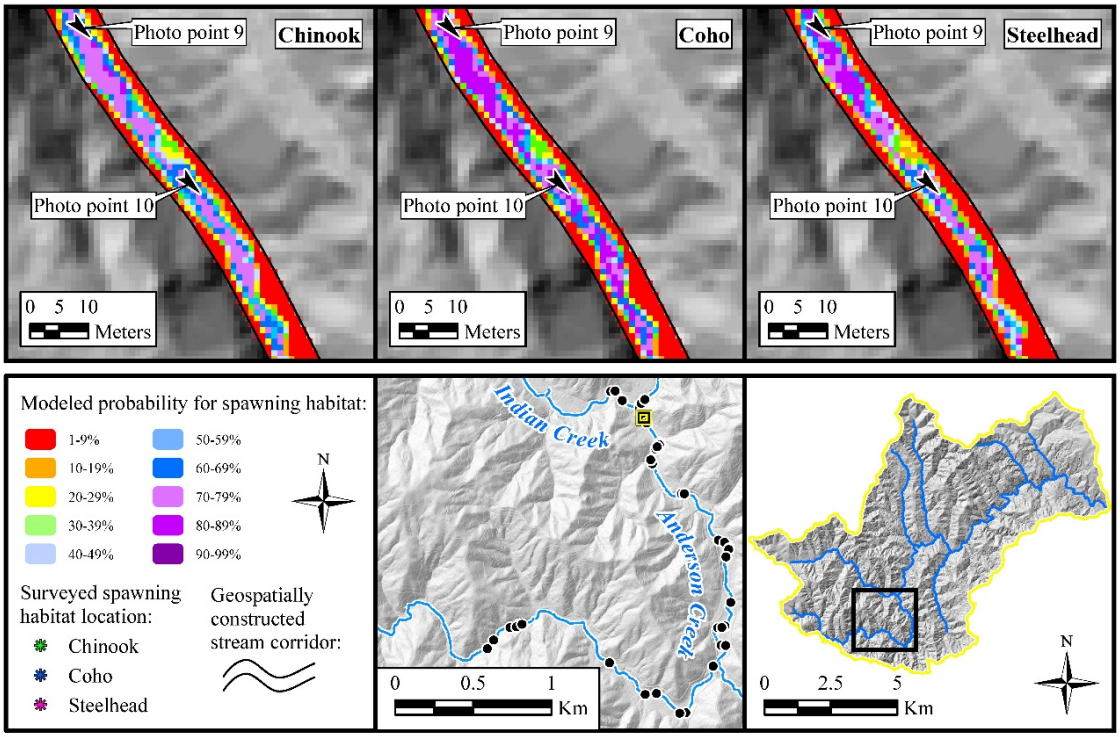

Figure 99. Photo point 10.

Photo point 11. Facing downstream Anderson Creek. Note emplacement of large woody debris structures on right side. LiDAR DEM information upon which habitat probability surface derived predates LWD structures.

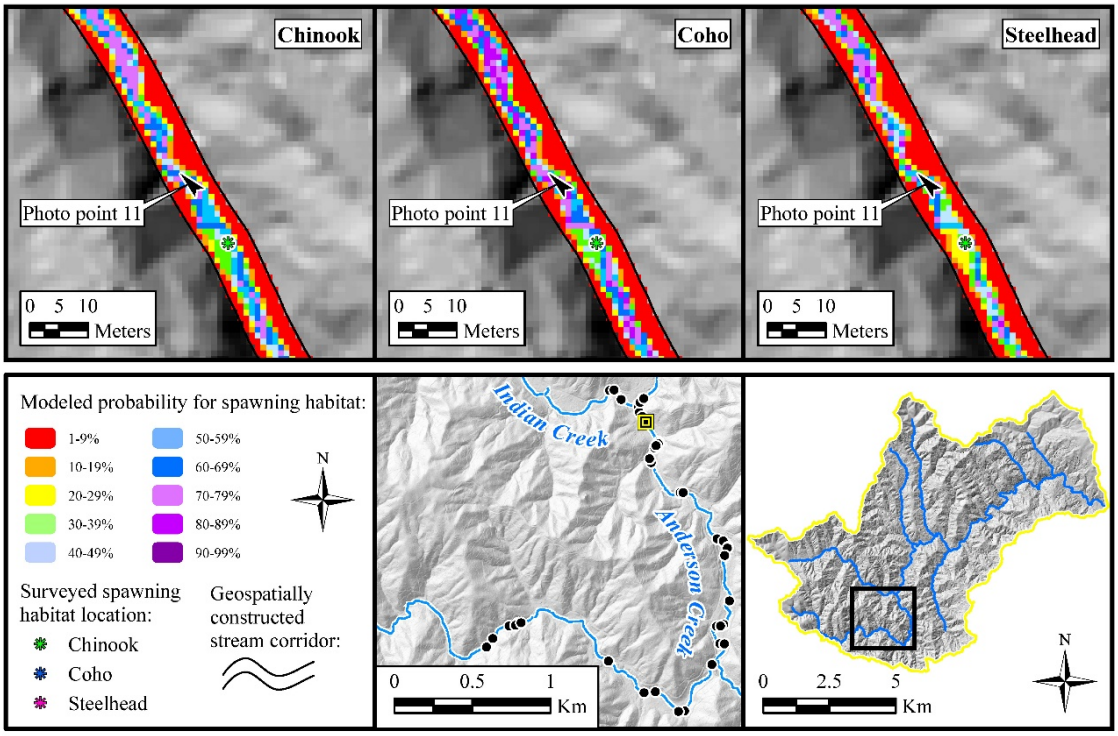

Figure 100. Photo point 11.

Photo point 12. Facing upstream Anderson Creek.

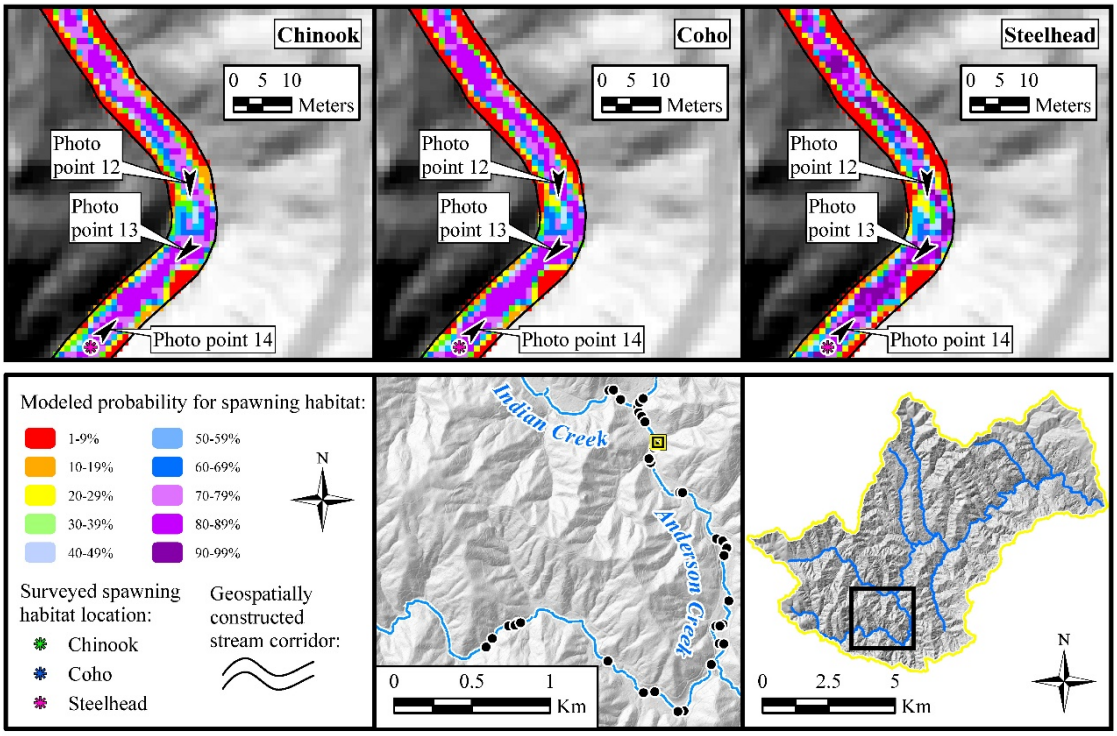

Figure 101. Photo point 12.

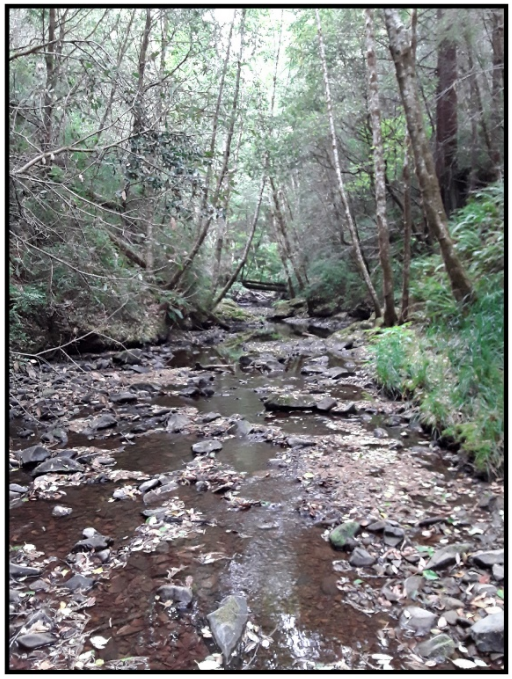

Photo point 13. Facing upstream Anderson Creek. Note bedrock extrusion into channel on left side as well decrease in spawning habitat probability.

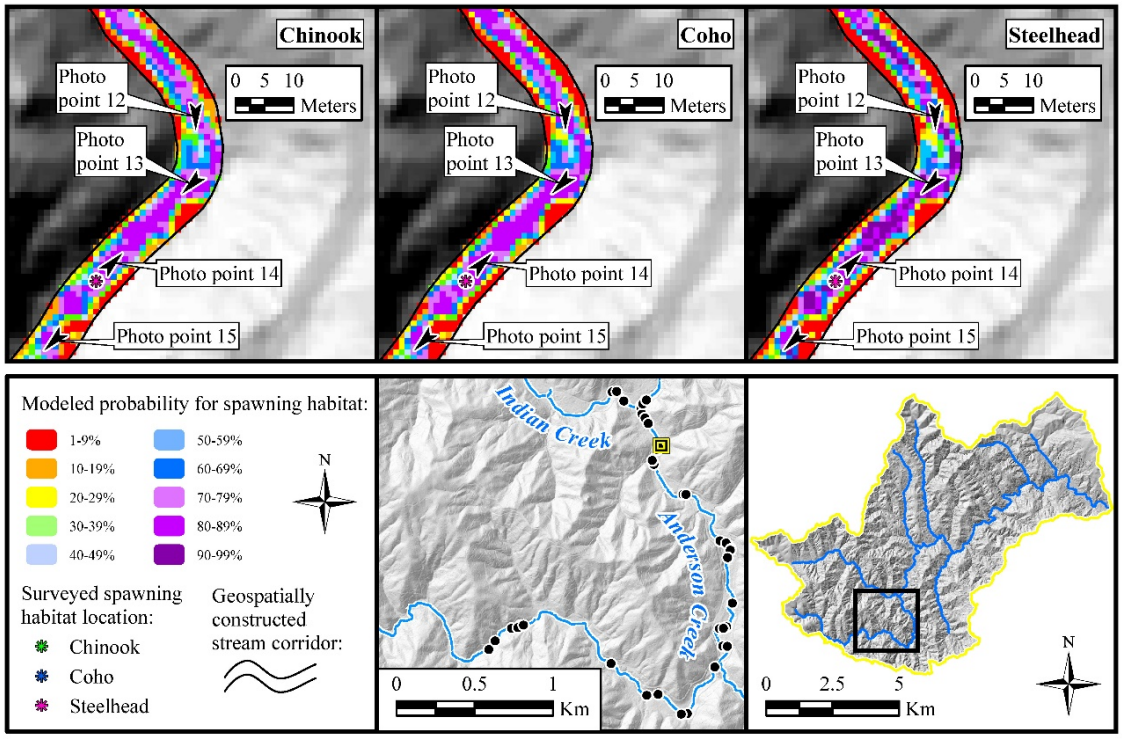

Figure 102. Photo point 13.

Photo point 14. Facing downstream Anderson Creek.

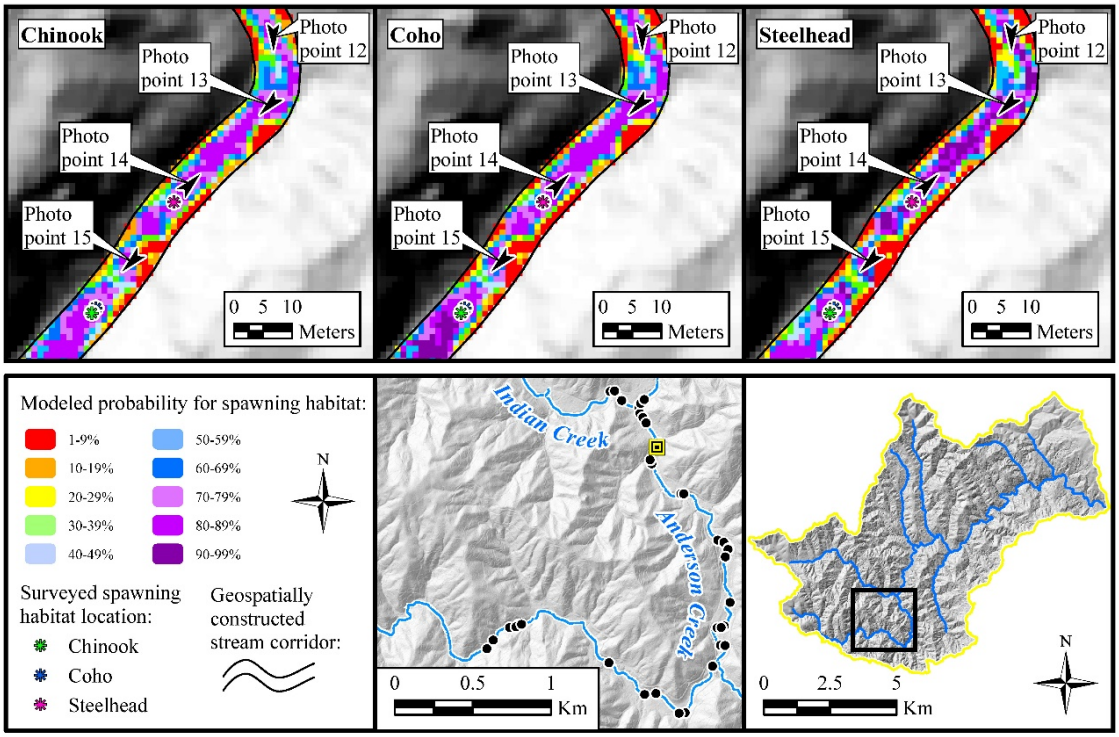

Figure 103. Photo point 14.

Photo point 15. Facing upstream Anderson Creek.

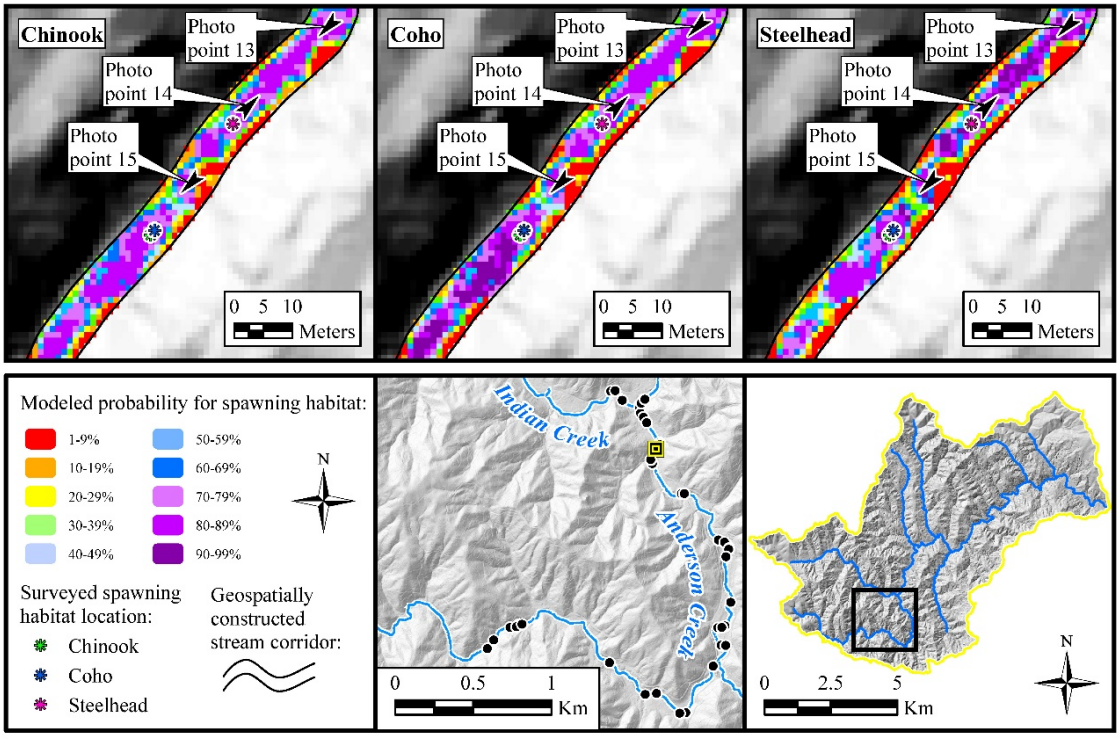

Figure 104. Photo point 15.

Photo point 16. Facing upstream Anderson Creek.

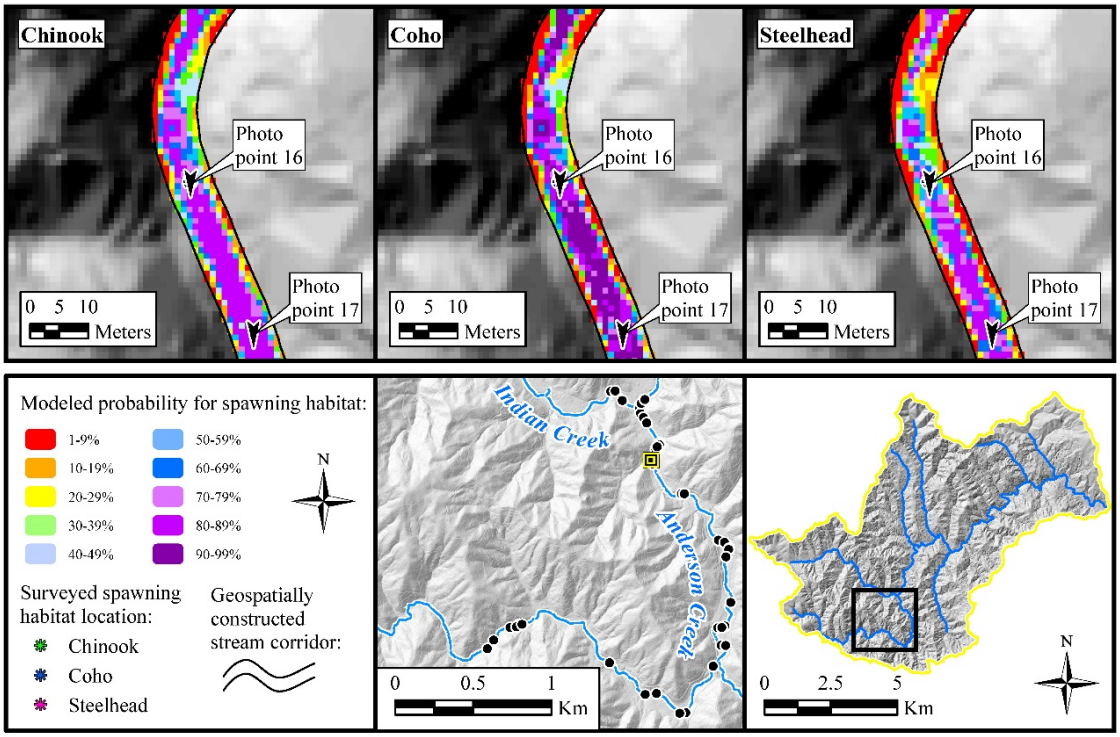

Figure 105. Photo point 16.

Photo point 17. Facing upstream Anderson Creek.

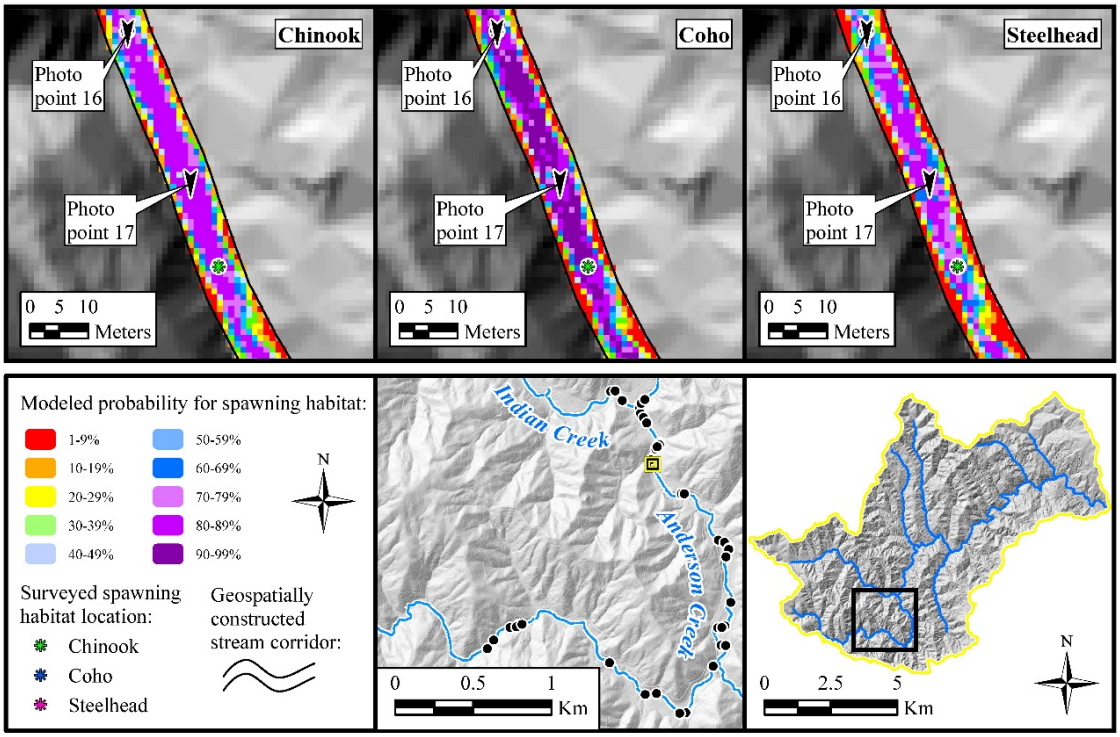

Figure 106. Photo point 17.

Photo point 18. Facing upstream Anderson Creek.

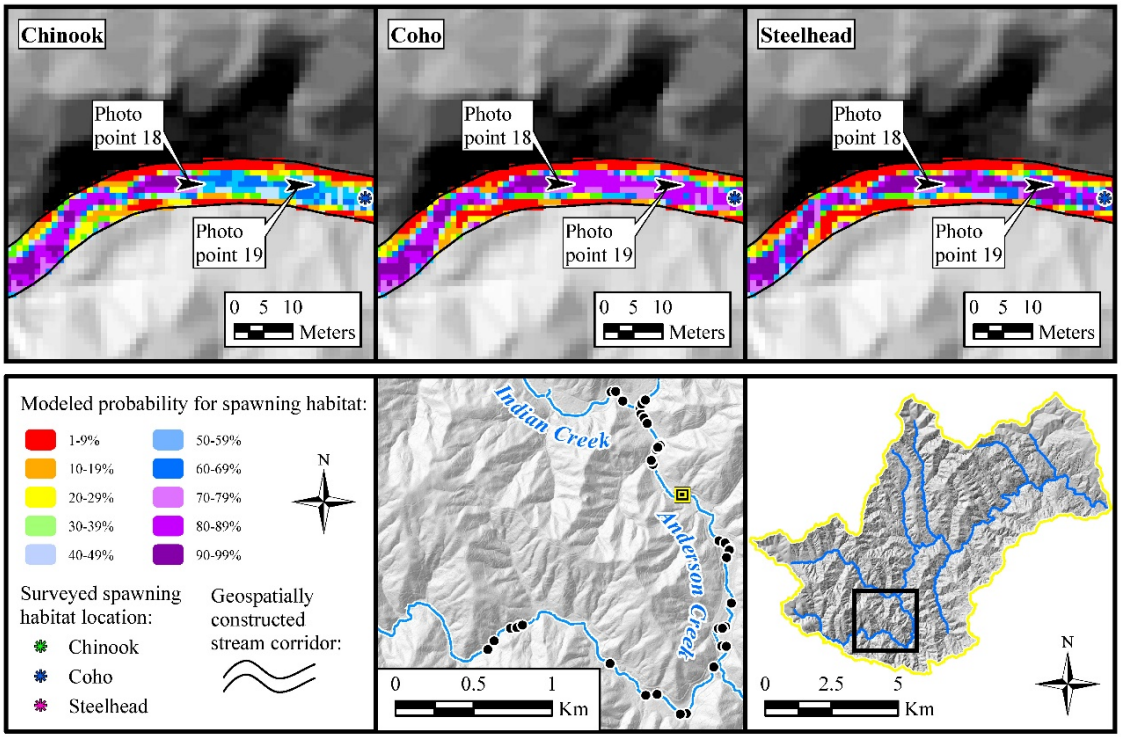

Figure 107. Photo point 18.

Photo point 19. Facing upstream Anderson Creek.

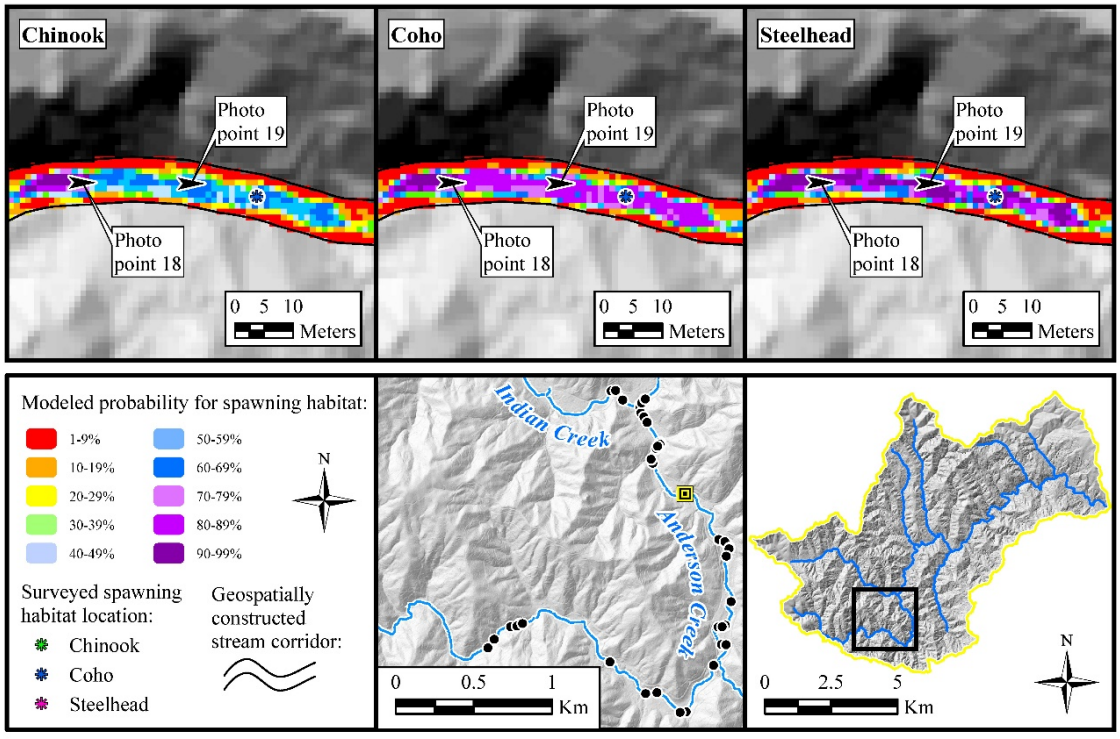

Figure 108. Photo point 19.

Photo point 20. Facing downstream Anderson Creek. Note the channel being constrained on both left and right bank with corresponding decrease in spawning habitat probability.

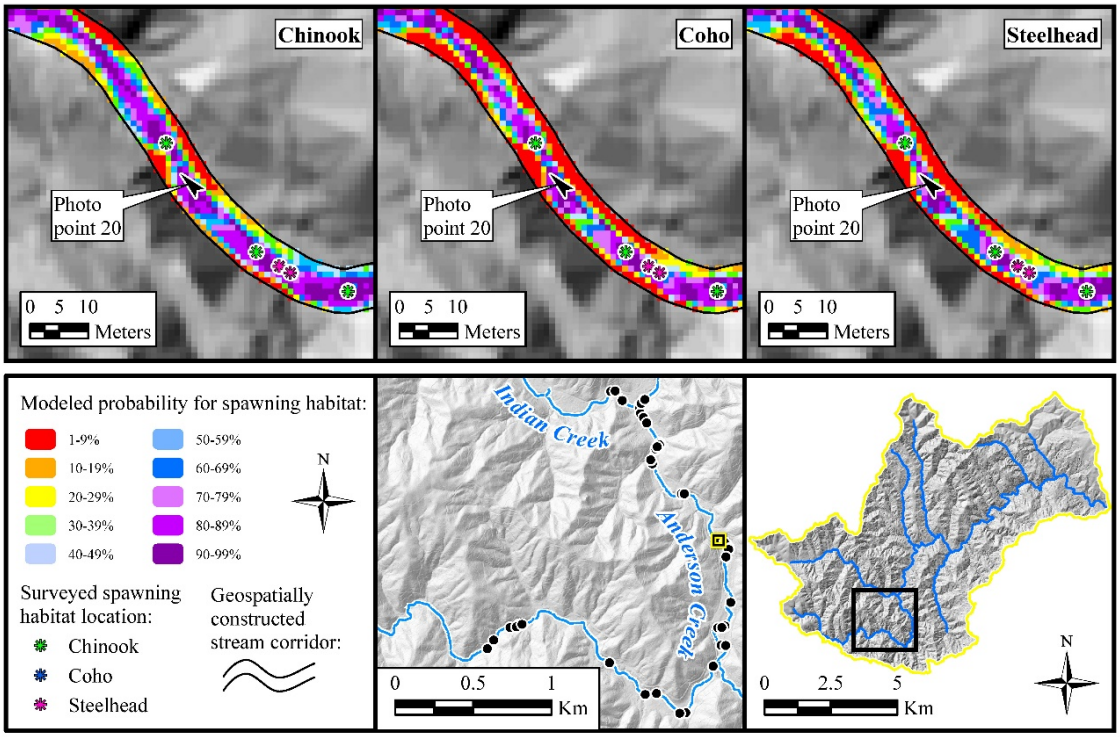

Figure 109. Photo point 20.

Photo point 21. Facing upstream Anderson Creek.

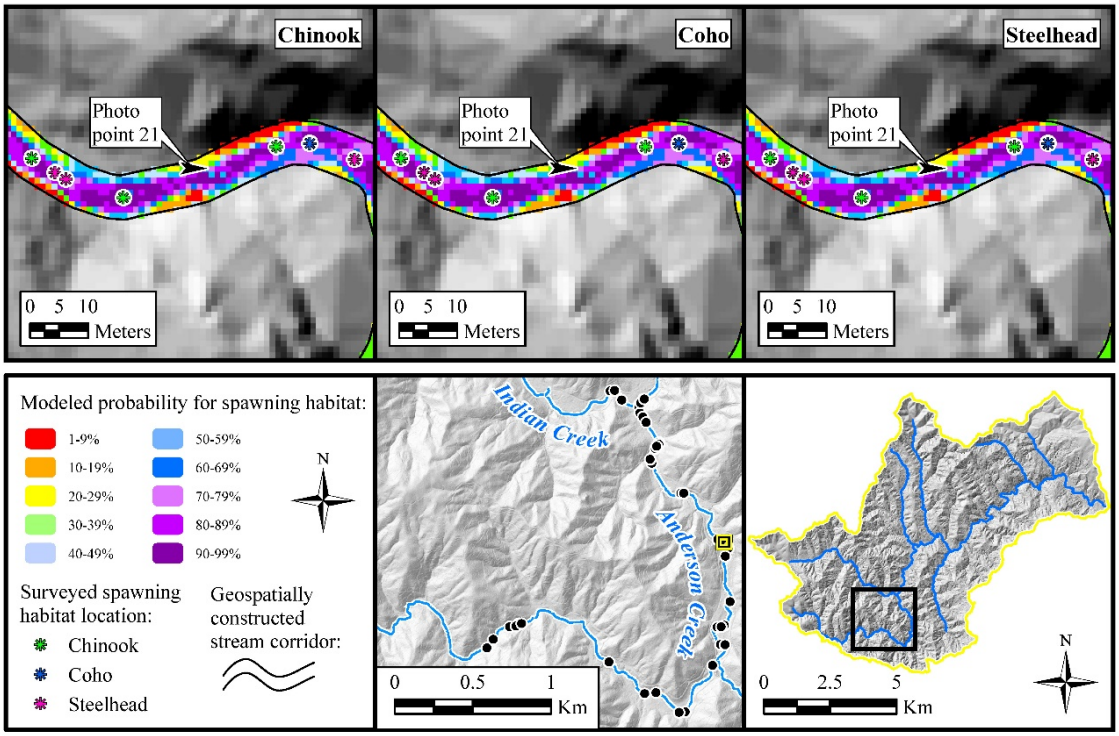

Figure 110. Photo point 21.

Photo point 22. Tributary stream to Anderson Creek, with Seth Ricker on left (CA DFW) and Tom Leroy on right (PWA). Tributary stream modeled at <<1% habitat probability, field checked and confirmed by SR (9/26/18).

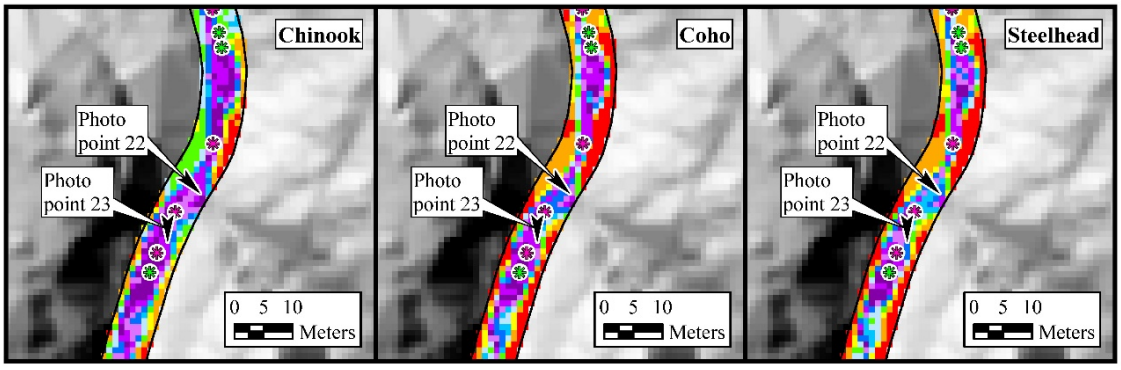

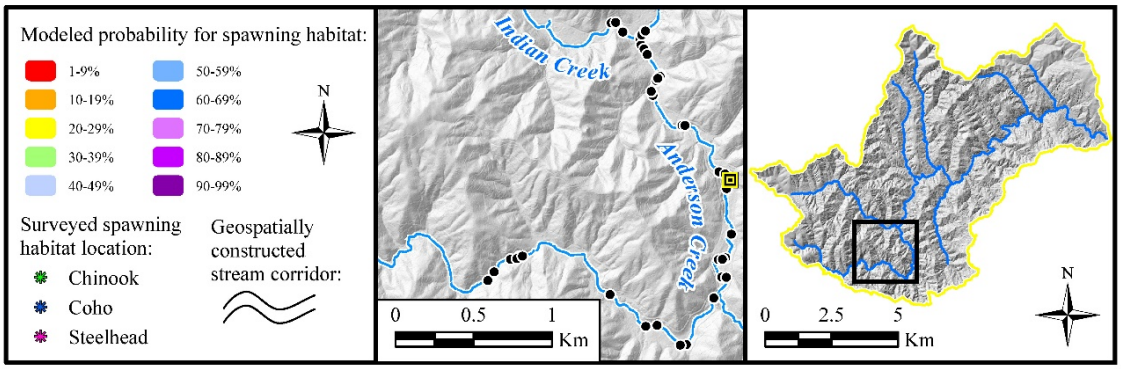

Figure 111. Photo point 22.

Photo point 23. Facing upstream Anderson Creek.

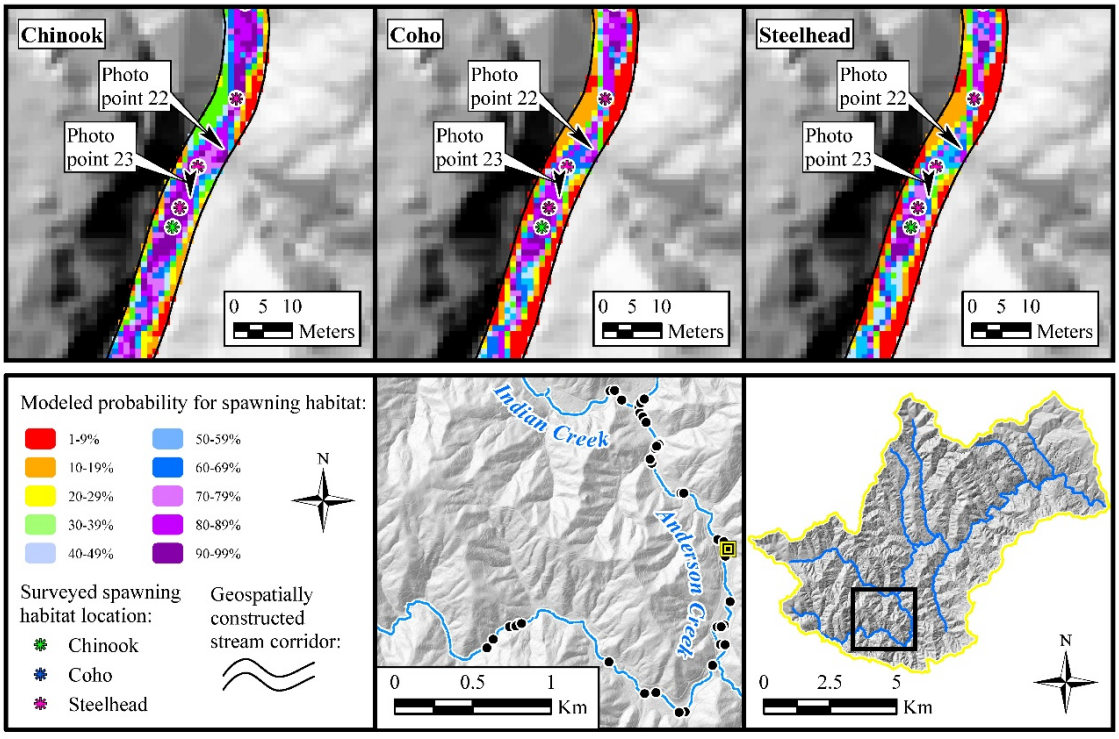

Figure 112. Photo point 23.

Photo point 24. Facing downstream Anderson Creek.

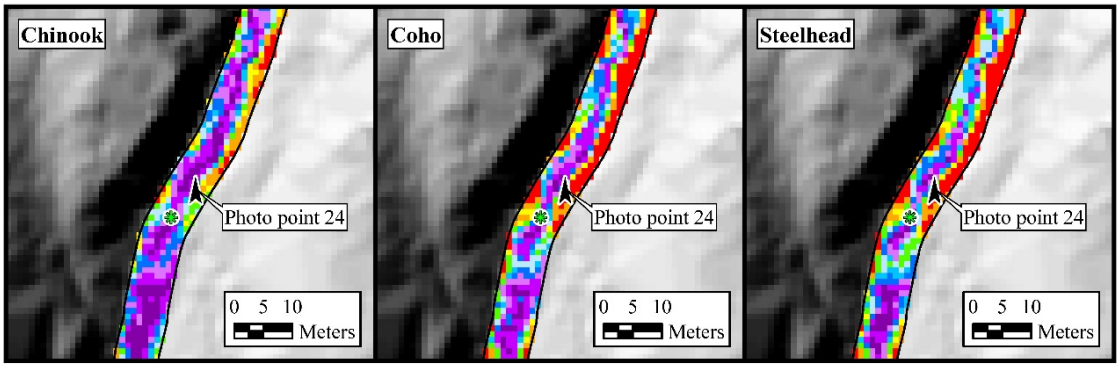

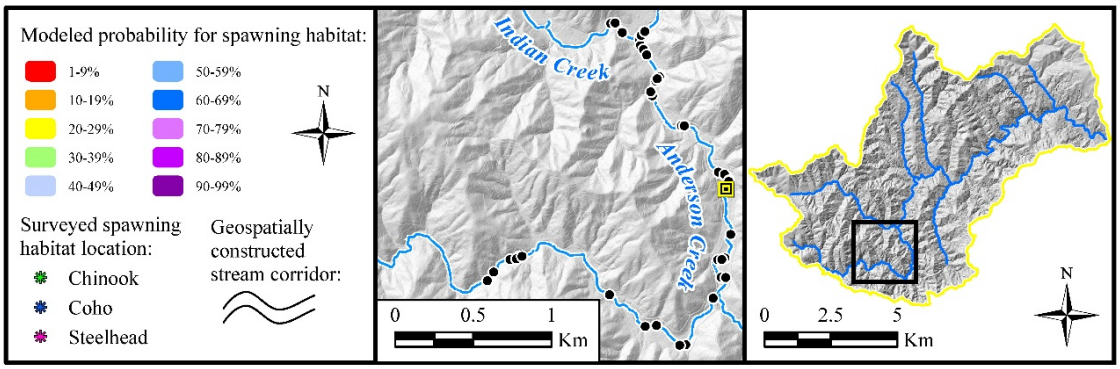

Figure 113. Photo point 24.

Photo point 25. Facing upstream Anderson Creek. Note historical railroad track (c. 1900) used to extract commercial timber.

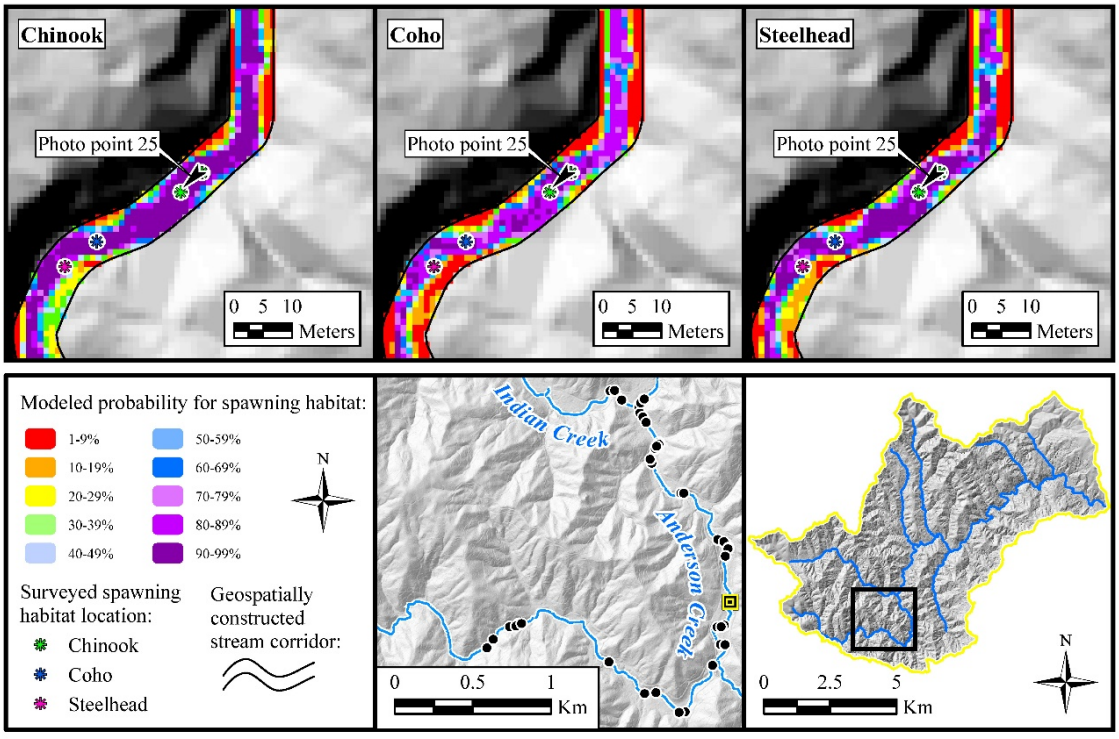

Figure 114. Photo point 25.

Photo point 26. Facing downstream Anderson Creek.

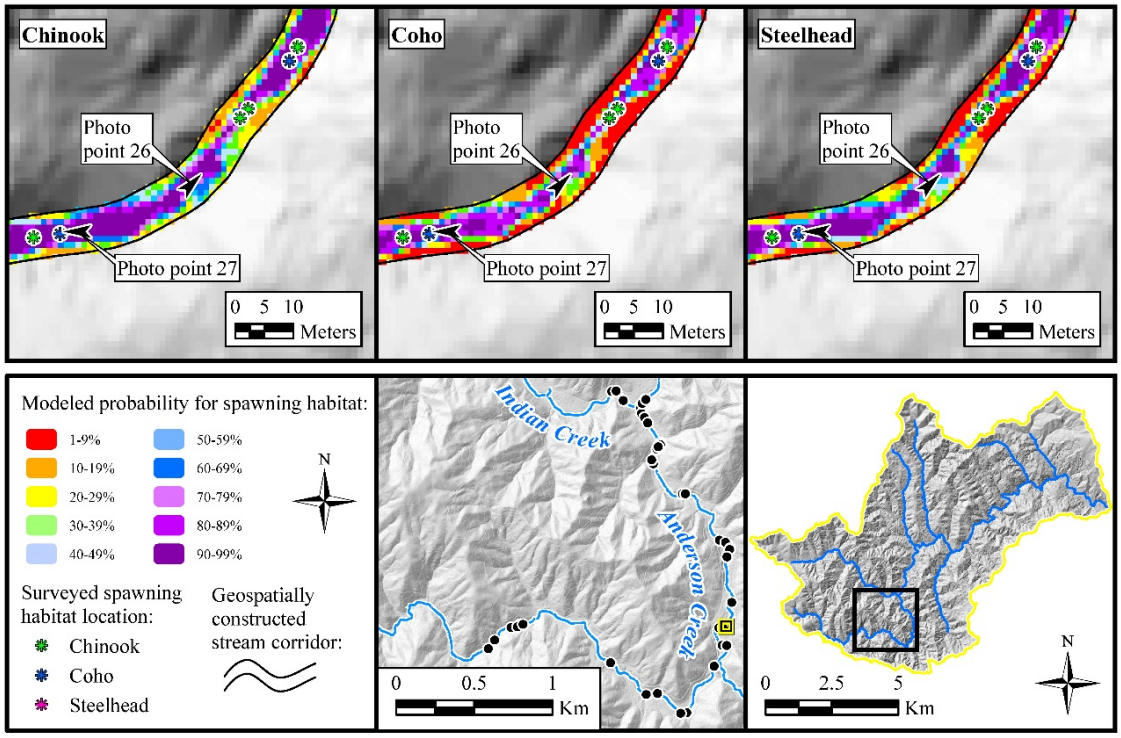

Figure 115. Photo point 26.

Photo point 27. Facing upstream Anderson Creek. Note historical railroad track (c. 1900) used to extract commercial timber extending across stream.

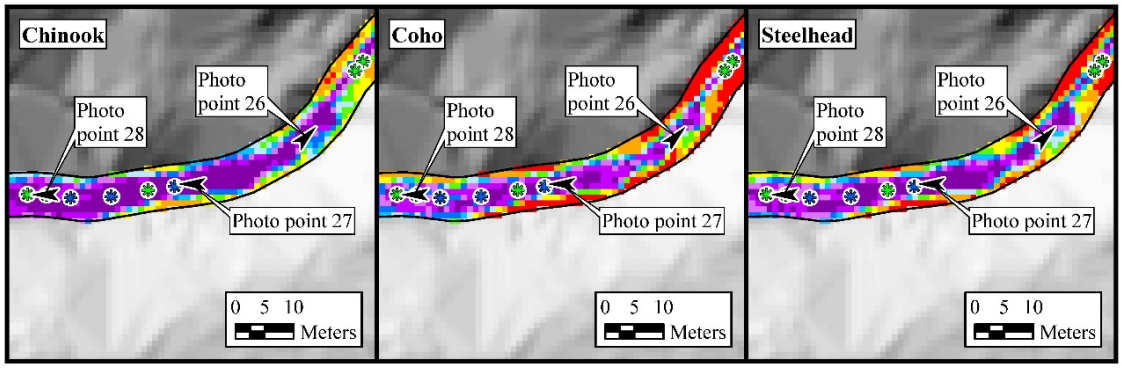

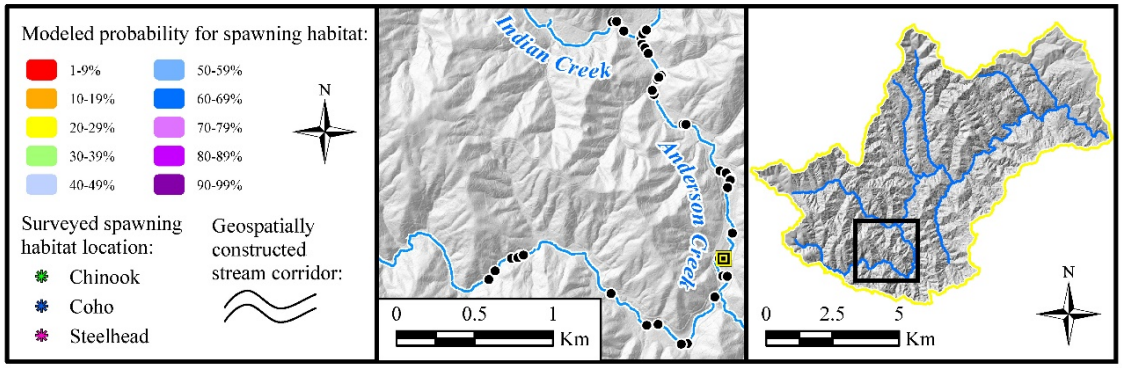

Figure 116. Photo point 27.

Photo point 28. Facing upstream Anderson Creek. Pictured are Seth Ricker (left) and Tom Leroy (right) on historical tree embedded in and extending across stream. Also note historic commercial railroad track (c. 1900).

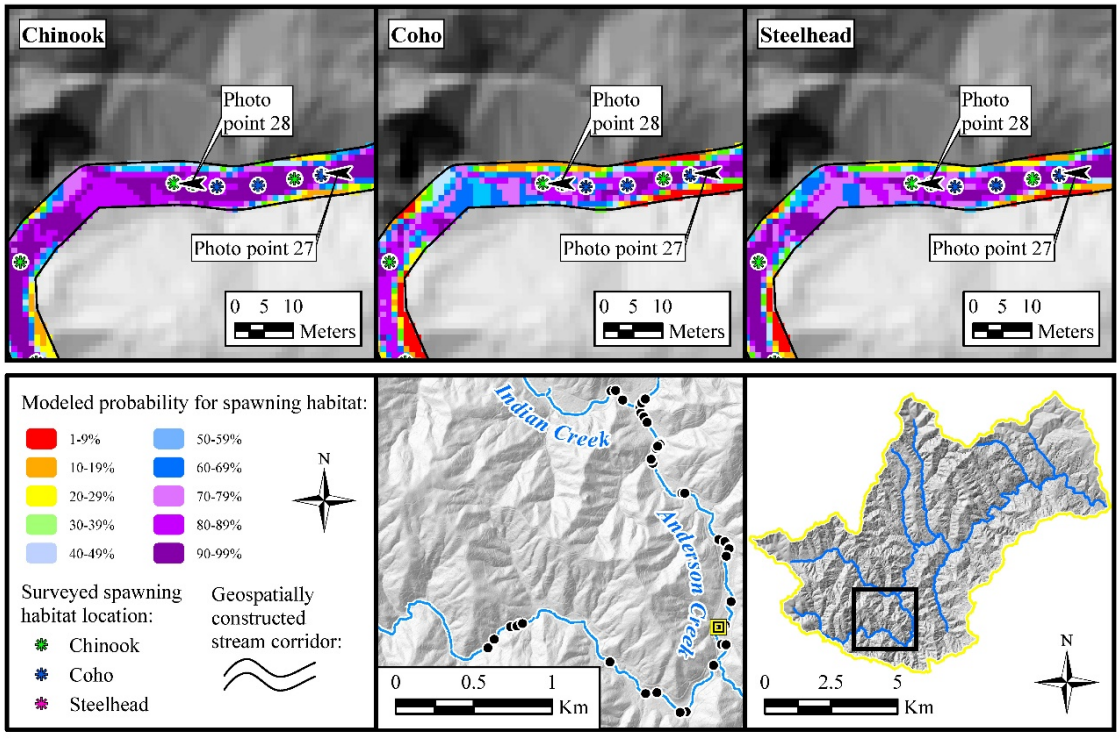

Figure 117. Photo point 28.

Photo point 29. Facing upstream Anderson Creek. Pictured are Tom Leroy (left) and Seth Ricker (right) underneath historic railroad track (c. 1900). Note pool morphology corresponding with high habitat probability.

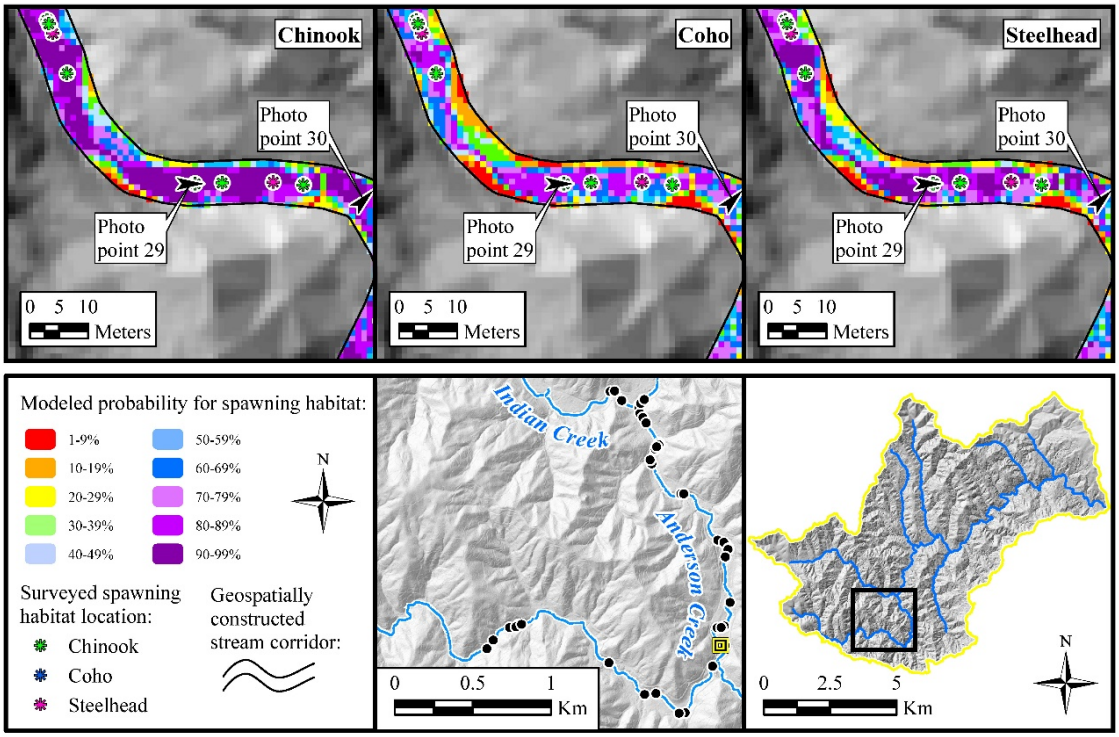

Figure 118. Photo point 29.

Photo point 30. Tributary stream to Anderson Creek, with Seth Ricker on left and Tom Leroy on right. Tributary stream modeled at <<1% habitat probability, field checked and confirmed by SR (9/26/18).

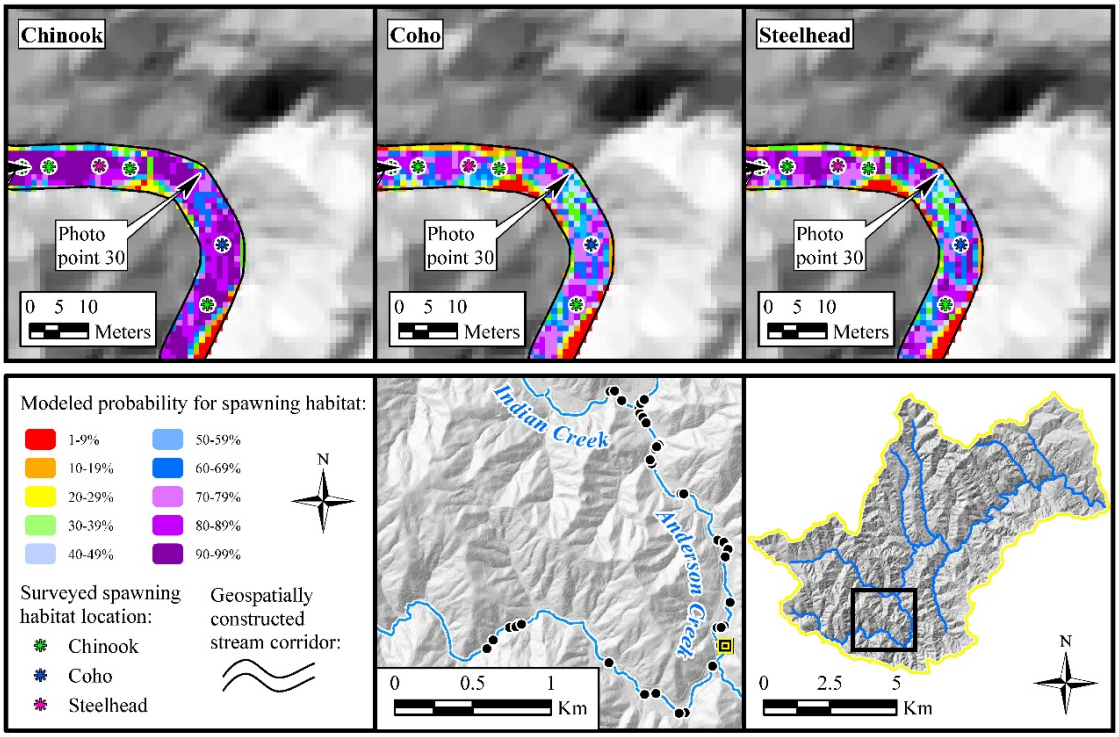

Figure 119. Photo point 30.

Photo point 31. Facing upstream Anderson Creek. Note channel slope reconstruction and recontouring from PWA road decommissioning project (2015), which postdates LiDAR DEM data acquisition.

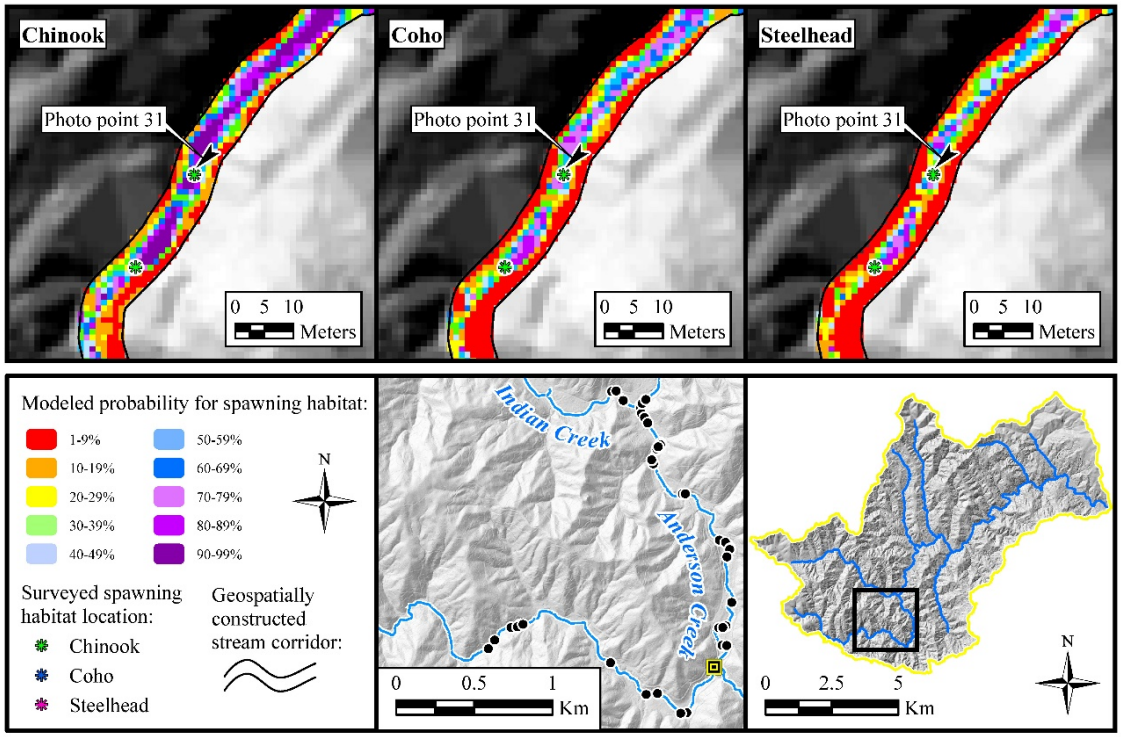

Figure 120. Photo point 31.

Photo point 32. Tributary stream to Anderson Creek; bankfull width for tributary predicted at < 1m ; flow accumulation to that point is 280,000 sq. meters. Stream modeled at <<1% habitat probability, field checked and confirmed (9/26/18).

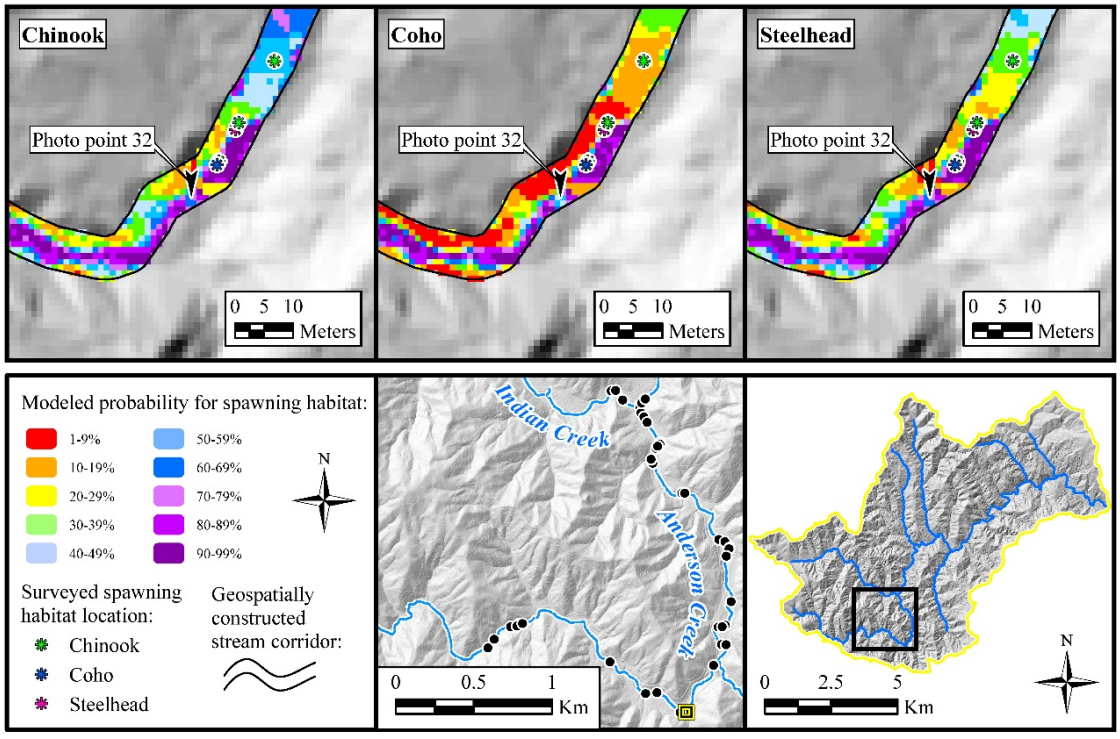

Figure 121. Photo point 32.

Photo point 33. Facing upstream Anderson Creek. Pictured are Seth Ricker (left) and Tom Leroy (right). Note channel constraint on right side with corresponding decrease in probability.

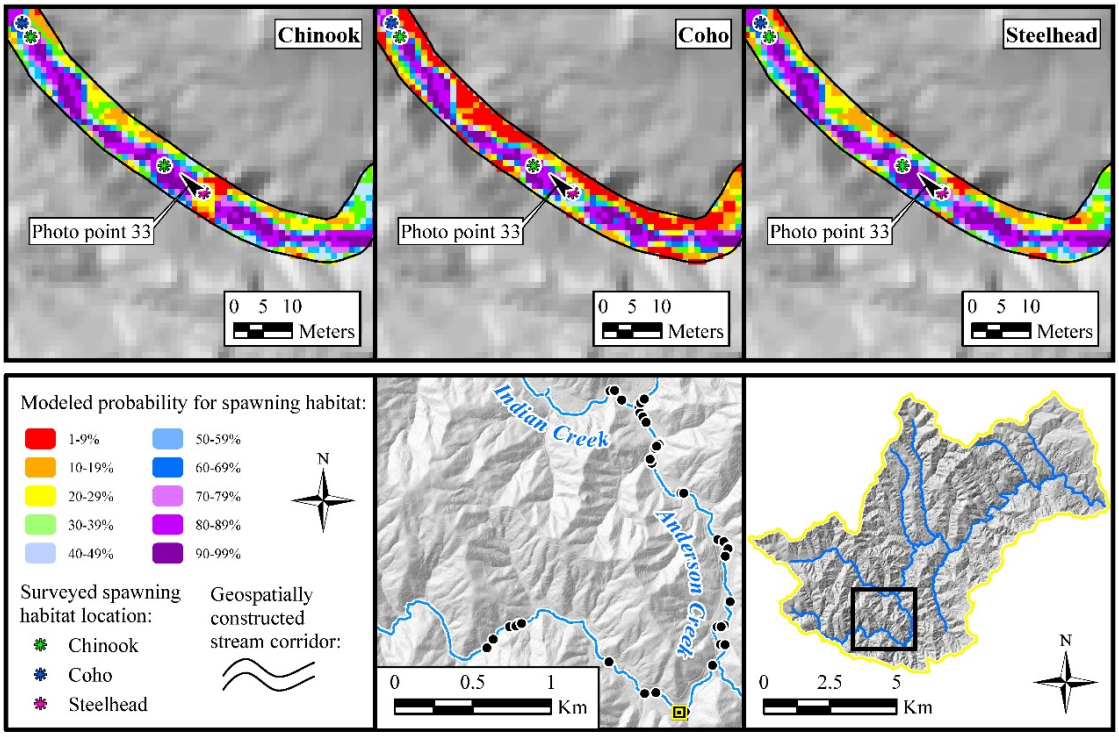

Figure 122. Photo point 33.

Photo point 34. Facing downstream Anderson Creek. Pictured are Seth Ricker (CA DFW) on left and Justin Bissell (author, PWA/HSU) on right, field checking model results.

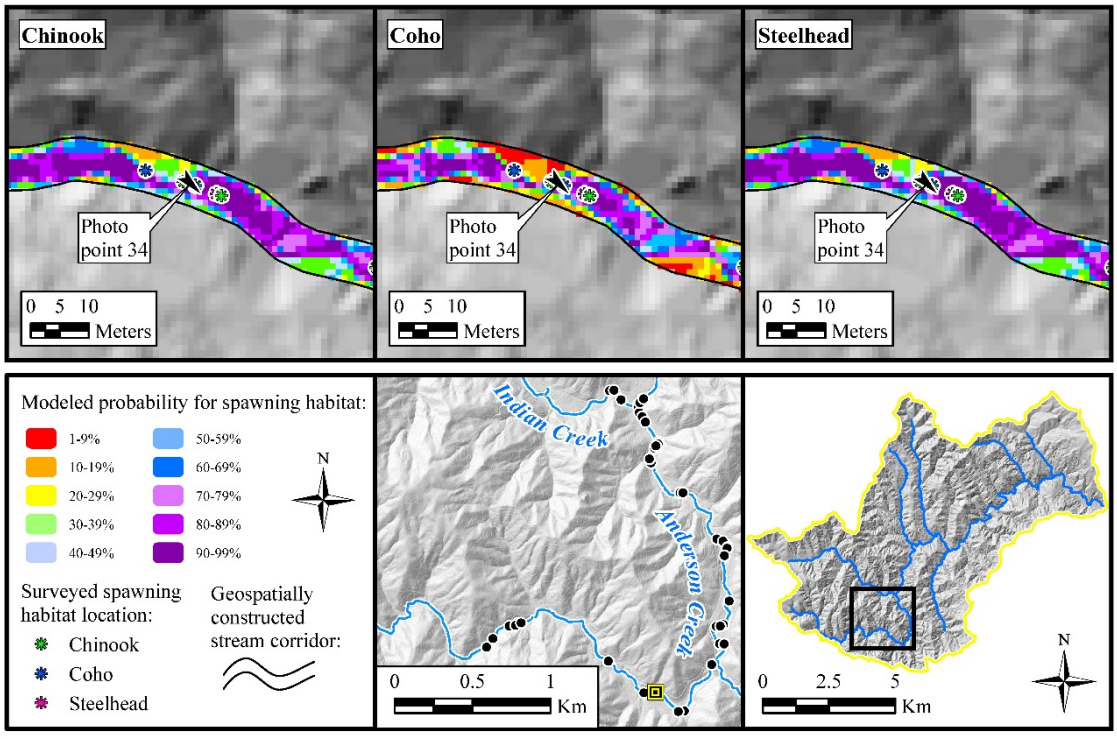

Figure 123. Photo point 34.

Photo point 35. Tributary stream to Anderson Creek; bankfull width for tributary predicted at < 1m ; flow accumulation to that point is 418,600 sq. meters. Stream modeled at <<1% habitat probability, field checked and confirmed (9/26/18).

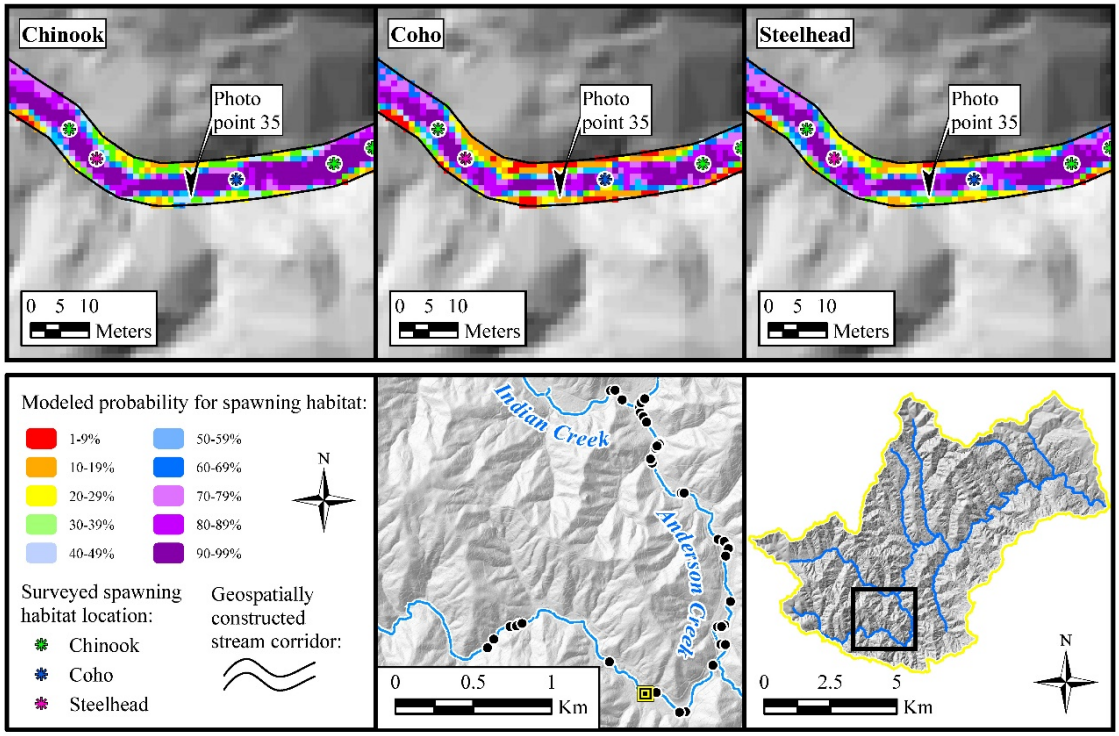

Figure 124. Photo point 35.

Photo point 36. Facing upstream Anderson Creek. Note high slopes and high anthropogenic disturbance on both sides of channel and extremely dense and extensive log jam immediately upstream from photo point position.

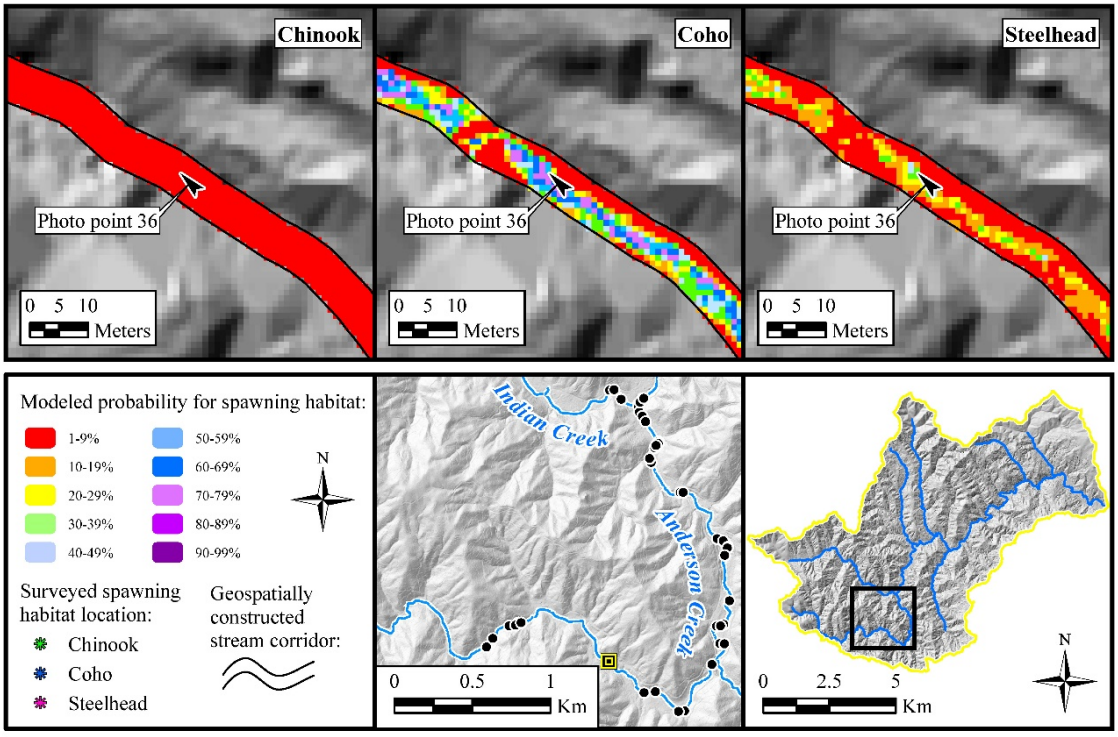

Figure 125. Photo point 36.

Photo point 37. Facing upstream Anderson Creek. High degree of historical anthropogenic influence in and around channel; buried stumps, high sedimentation prevelant.

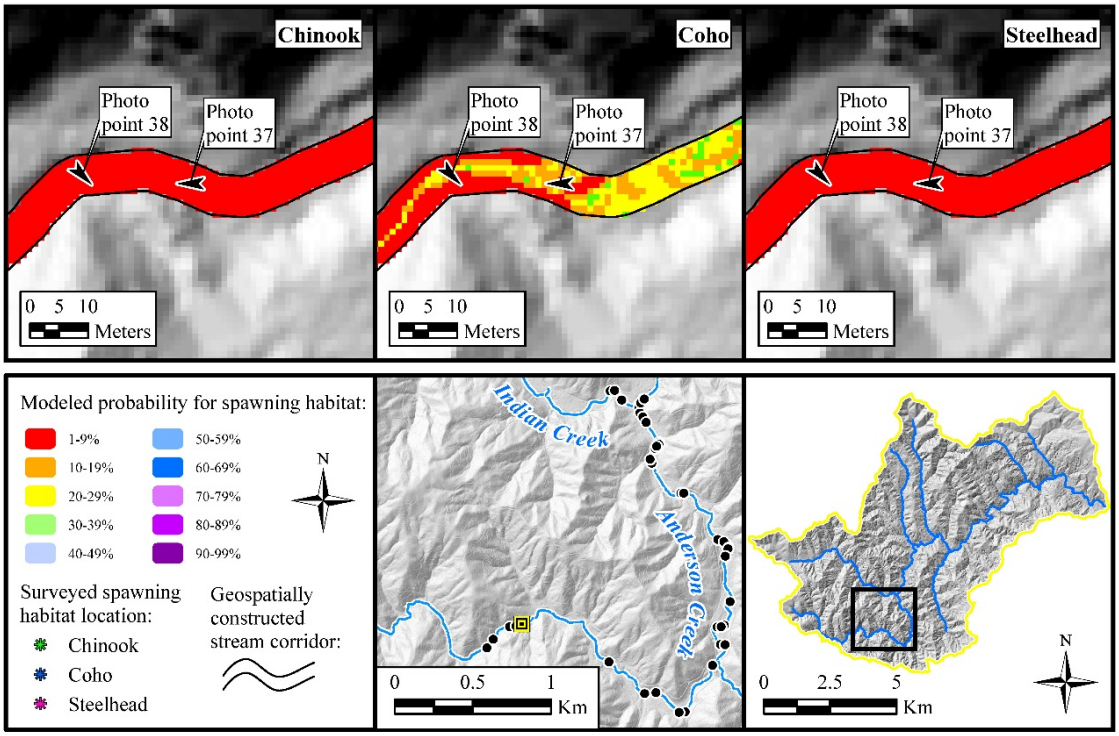

Figure 126. Photo point 37.

Photo point 38. Facing Anderson Creek channel - downstream (left) and upstream (right). High degree of historical anthropogenic influence in and around channel; buried stumps, high sedimentation prevelant.

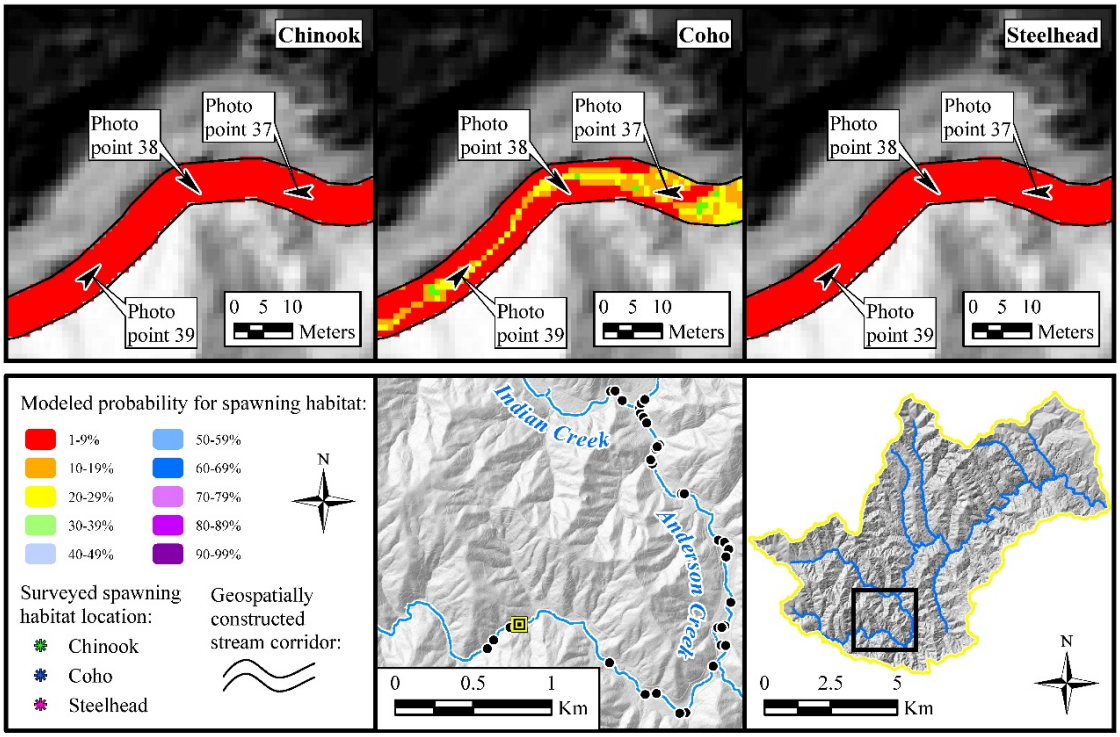

Figure 127. Photo point 38.

Photo point 39. Facing downstream Anderson Creek. Significant amounts of of historical anthropogenic influence on left; high slope area on right.

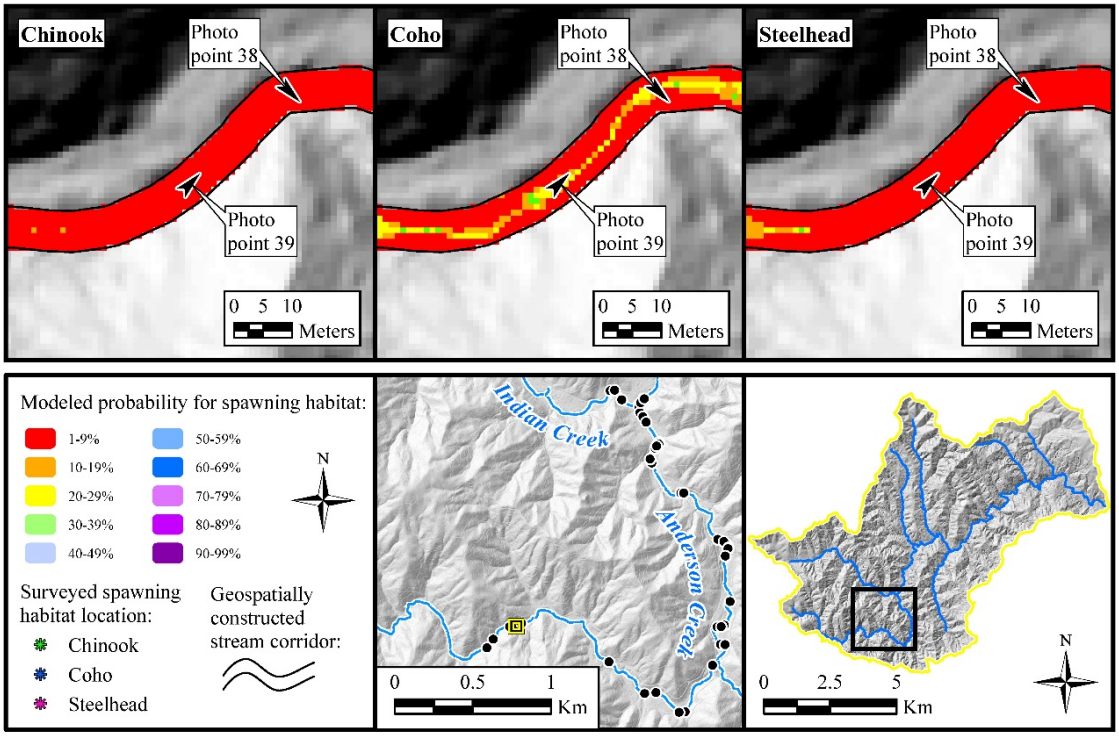

Figure 128. Photo point 39.

Photo point 40. Facing upstream Anderson Creek. High degree of historical anthropogenic influence in and around channel; buried stumps, high sedimentation prevelant.

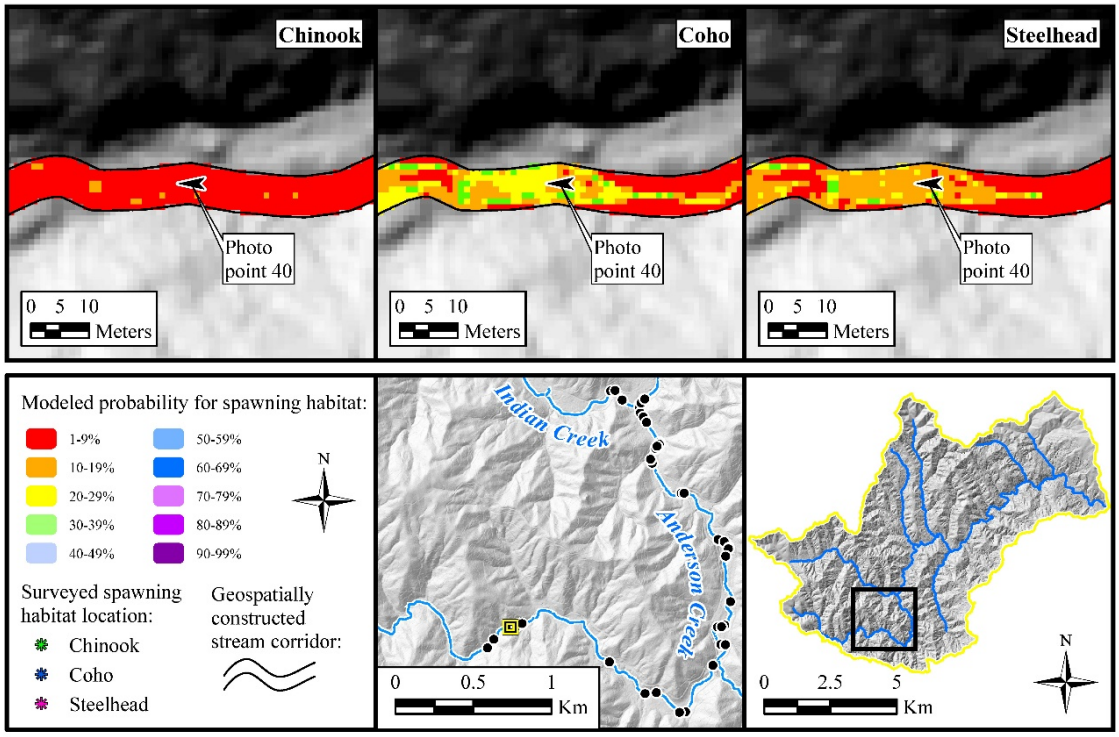

Figure 129. Photo point 40.

Photo point 41. Facing downstream Anderson Creek outside area of high historical anthropogenic disturbance.

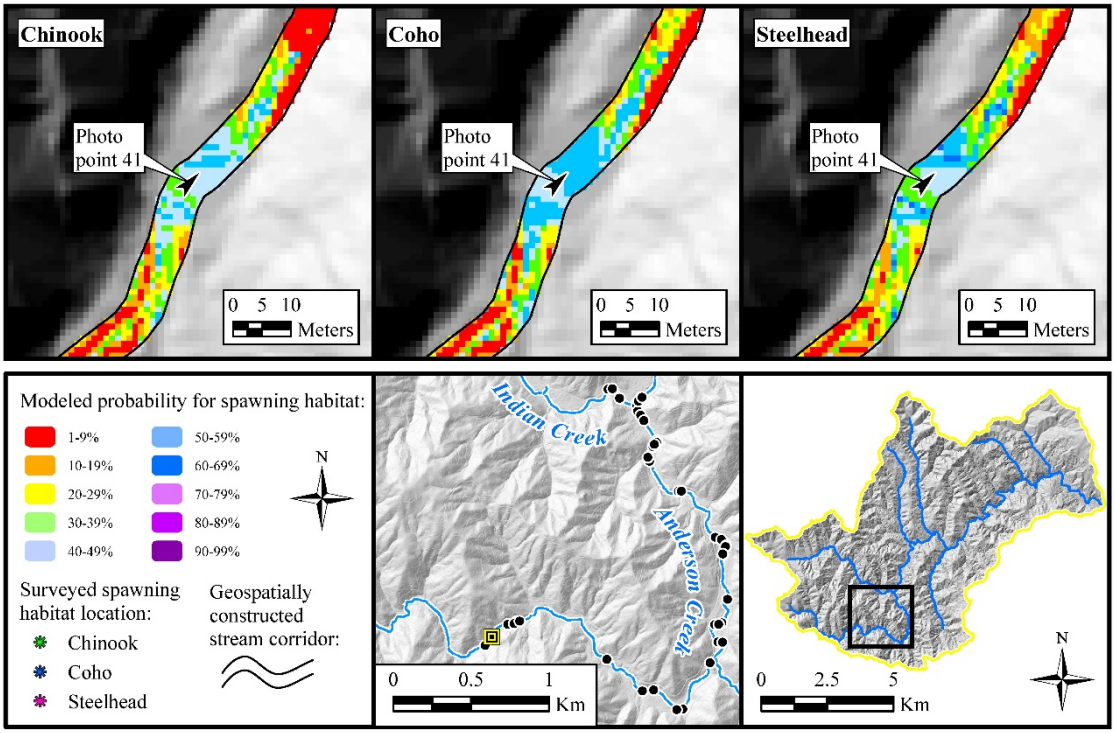

Figure 130. Photo point 41.

Photo point 42. Facing upstream Anderson Creek. End of field survey.

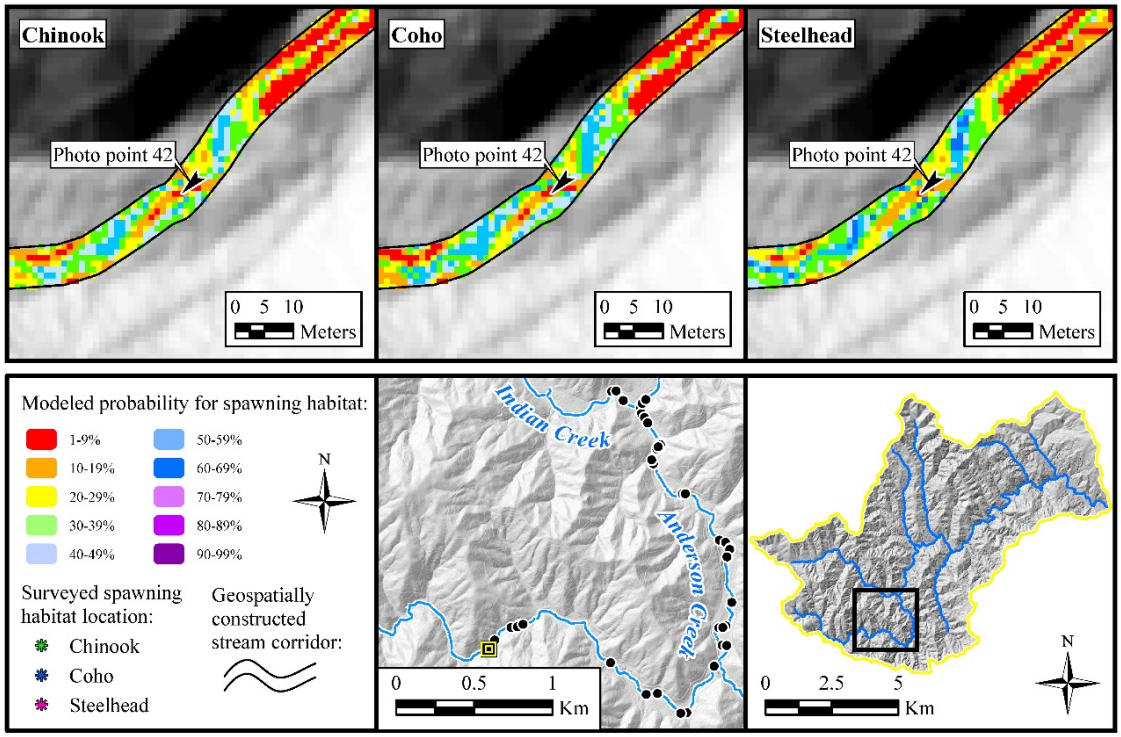

Figure 131. Photo point 42.

APPENDIX G: RASTER COVARIATE INPUTS USED IN MAXENT TO DEVELOP SPAWNING HABITAT PROBABILITY SURFACES – SELECTED AREAS AND STATISTICAL TABLES.

Table 11. Areas of modeled Indian Creek stream system used as raster covariate environmental variable assigned bedrock substrate classification.

Percentage of bedrock:	% of total area of modeled stream corridor assigned this percentage	Total area of modeled stream corridor assigned this percentage (m^2)
0% bedrock	12.89%	203,797
5% bedrock	79.43%	1,255,403
10% bedrock	3.25%	51,372
15% bedrock	1.48%	23,359
20% bedrock	1.61%	25,520
25% bedrock	1.09%	17,289
30% bedrock	0.13%	1,983
35% bedrock	0.11%	1,747
Total area (sq. meters):	100%	1,580,470

Table 12. Areas of modeled Indian Creek stream system used as raster covariate environmental variable assigned boulder substrate classification.

Percentage of boulders:	% of total area of modeled stream corridor assigned this percentage	Total area of modeled stream corridor assigned this percentage (m^2)
0% boulder	78.36%	1,238,519
3% boulder	0.21%	3,337
5% boulder	7.11%	112,410
10% boulder	6.28%	99,194
15% boulder	3.49%	55,208
20% boulder	1.93%	30,533
25% boulder	1.61%	25,495
30% boulder	0.50%	7,939
35% boulder	0.33%	5,190
45% boulder	0.10%	1,637
60% boulder	0.06%	1,008
Total area (sq. meters):	100%	1,580,470

Table 13. Areas of modeled Indian Creek stream system used as raster covariate environmental variable assigned cobble substrate classification.

Percentage of cobble:	% of total area of modeled stream corridor assigned this percentage	Total area of modeled stream corridor assigned this percentage (m^2)
0% cobble	0.10%	1,531
5% cobble	2.66%	42,019
10% cobble	2.38%	37,606
15% cobble	5.12%	80,893
20% cobble	77.09%	1,218,356
25% cobble	5.74%	90,642
30% cobble	2.70%	42,736
35% cobble	1.17%	18,525
40% cobble	1.36%	21,501
45% cobble	0.42%	6,635
47% cobble	0.21%	3,337
50% cobble	0.46%	7,325
55% cobble	0.14%	2,157
60% cobble	0.36%	5,672
70% cobble	0.10%	1,535
Total area (sq. meters):	100%	1,580,470

Table 14. Areas of modeled Indian Creek stream system used as raster covariate environmental variable assigned fine grain cohesive substrate classification.

Percentage of fine grain cohesives:	% of total area of modeled stream corridor assigned this percentage	Total area of modeled stream corridor assigned this percentage (m^2)
0% fine grain cohesives	91.75%	1,450,084
5% fine grain cohesives	7.74%	122,304
10% fine grain cohesives	0.37%	5,837
15% fine grain cohesives	0.14%	2,245
Total area (sq. meters):	100.00%	1,580,470

Table 15. Areas of modeled Indian Creek stream system used as raster covariate environmental variable assigned gravel substrate classification.

Percentage of gravels:	% of total area of modeled stream corridor assigned this percentage	Total area of modeled stream corridor assigned this percentage (m^2)
10% gravel	0.36%	5,667
15% gravel	0.81%	12,763
20% gravel	3.79%	59,962
25% gravel	77.01%	1,217,150
30% gravel	7.37%	116,403
35% gravel	3.48%	54,981
40% gravel	5.19%	82,070
45% gravel	0.60%	9,553
50% gravel	0.58%	9,113
55% gravel	0.39%	6,202
60% gravel	0.24%	3,783
65% gravel	0.15%	2,427
75% gravel	0.03%	396
Total area (sq. meters):	100%	1,580,470

Table 16. Areas of modeled Indian Creek stream system used as raster covariate environmental variable assigned sands / silts substrate classification.

Percentage of sands / silts:	% of total area of modeled stream corridor assigned this percentage	Total area of modeled stream corridor assigned this percentage (m^2)
0% sands / silts	0.21%	3,337
5% sands / silts	0.38%	6,076
10% sands / silts	3.04%	48,057
15% sands / silts	2.73%	43,162
20% sands / silts	3.97%	62,666
25% sands / silts	4.21%	66,465
30% sands / silts	3.10%	48,997
35% sands / silts	2.31%	36,548
40% sands / silts	3.31%	52,276
45% sands / silts	0.50%	7,929
50% sands / silts	72.77%	1,150,067
55% sands / silts	0.34%	5,372
60% sands / silts	2.72%	42,966
65% sands / silts	0.11%	1,732
70% sands / silts	0.05%	774
75% sands / silts	0.26%	4,046
Total area (sq. meters):	100%	1,580,470

ACRONYMS

CDFW - California Department of Fish and Wildlife

LiDAR / LIDAR / Lidar / lidar – Light Detection and Ranging

DEM – Digital elevation model

USGS – United States Geographic Survey

PWA – Pacific Watershed Associates

LCF – Lost Coast Forestlands, LLC

RFFI – Redwood Forest Foundation, Inc.

USDA – United States Department of Agriculture

NOAA – National Oceanic and Atmospheric Administration

ESRI – Environmental Systems Research Institute